FUNDACIÓN AQUAE

TESIS

Environmental and economic sustainability of submerged anaerobic membrane bioreactors treating urban wastewater

Ruth Pretel Jolis

Madrid 2014

Department of Hydraulic Engineering and Environment
Universitat Politècnica de València

AQUAE FUNDACIÓN

Department of Hydraulic Engineering and Environment

UNIVERSITAT POLITÈCNICA DE VALÈNCIA

Environmental and economic sustainability of submerged anaerobic membrane bioreactors treating urban wastewater

This thesis is submitted in partial fulfilment of the requirements for the Degree of Doctor of Philosophy

Ph.D. THESIS
RUTH PRETEL JOLIS

SUPERVISORS:
JOSÉ FERRER POLO
MARIA VICTORIA RUANO GARCÍA
ÁNGEL ROBLES MARTÍNEZ

NOVEMBER 2015

ACKNOWLEDGEMENTS

Quiero expresar mi agradecimiento a mi director de tesis el doctor José Ferrer y a la doctora Aurora Seco, por haberme brindado la oportunidad de formar parte de este grupo de investigación y por la confianza que en mí han depositado.

Me gustaría agradecer sinceramente a mis directores la doctora Mª Victoria Ruano y el doctor Ángel Robles, por su esfuerzo y dedicación. Sus conocimientos, sus orientaciones, su manera de trabajar, su persistencia, su paciencia y su motivación han sido fundamentales para mi formación como investigadora.

Al Ministerio de Educación, Cultura y Deporte, por la beca concedida durante estos cuatro años, dentro del programa de ayudas a la Formación de Personal Universitario (FPU) y al Departamento de Ingeniería Hidráulica y Medioambiente de la Universidad Politécnica de Valencia por el buen trato y ayuda que siempre he recibido.

I would like to thank Jeremy S. Guest for giving me the chance to learn with them and welcoming me into their research group during three months. Of course, I also want to thank the people I met at the University of Illinois at Urbana-Champaign: Kia, Diana, Lisa, Brian, Bernardo, Susy, Daniel, Anass, Camila, Jaime, Eva, Sunny, Sara and so on.

A Ramón y Daniel Aguado por la ayuda recibida en mis inicios en la docencia universitaria y por los buenos momentos vividos en el almuerzo. A mi "compi de la NASA" Freddy, que tanto me ha ayudado y tantos consejos me ha ofrecido en mi etapa como investigadora y por todos los buenos momentos vividos. Y también a Antonio y Joaquín, por los buenos ratos pasados en el almuerzo y por esos días de pádel que no se olvidan.

A Alex y Dani, por todas las risas que nos hemos echado tanto dentro como fuera del despacho, por esas minis escapadas que hacíamos en la merienda para despejar la mente y por las partidas de pádel que siempre recordaré, habéis sido más que amigos para mí. Todo esto sin olvidarme de Tao y Ana, por esa alegría que habéis dado al despacho.

A Moni y Joana, que habéis sido un apoyo incondicional durante mi etapa como investigadora y unas amigas como vosotras no se encuentra todos los días, así que quiero agradecer vuestra valiosa amistad.

A mis compañeras de planta, las “samberas”, Patri y Silvia, por todo lo que hemos tenido que luchar para mantener el SAnMBR operativo, sólo me llevo buenos recuerdos de vosotras.Y también agradecer al resto de compañeros de “burja”: Josep, Paqui, Alberto, Núria M., Luís, Juan, Emérita, Javier C., Rafa, Ana P., Javier E, Laura C., Laura S., Hector, Josué, Núria Z, Óscar… que tanta vida habéis dado al grupo.

A mis amigos, Amadeo, Carlos, Carmen, Emi, Fer, Patri, Pedro, Kitos, Narae, Miguel, Vicky, Victor…porque aunque nos vemos poco siempre vais a estar en mi vida.

A mi familia, por estar siempre conmigo, principalmente a mi madre, a mi padre y a mis hermanos, que os quiero mucho, y en especial a mi hermana gemela e incondicional mejor amiga Raquel, que en mi larga trayectoria como investigadora ha sabido escucharme, entenderme y aguantarme.

Y en último lugar a Luka por su compañía y a mi pareja Carlos, por estar siempre a mi lado y darme consejos en la realización de mi tesis. Sin ti no lo hubiera logrado, eres lo más grande, te quiero.

ABSTRACT

Anaerobic MBRs (AnMBRs) can provide the desired step towards sustainable wastewater treatment, broadening the range of application of anaerobic biotechnology to low-strength wastewaters (*e.g.* urban ones) or extreme environmental conditions (*e.g.* low operating temperatures). This alternative technology gathers the advantages of anaerobic treatment processes (*e.g.* low energy demand stemming from no aeration and energy recovery through methane production) jointly with the benefits of membrane technology (*e.g.* high quality effluent, and reduced space requirements). It is important to highlight that AnMBR may offer the possibility of operation in energy neutral or even being a net energy producer due to biogas generation. Other aspects that must be taken into account in AnMBR are the quality and nutrient recovery potential of the effluent and the low amount of sludge generated, which are of vital importance when assessing the environmental impact of a wastewater treatment plant (WWTP).

The main aim of this Ph.D. thesis is to assess the economic and environmental sustainability of AnMBR technology for urban wastewater treatment at ambient temperature. Specifically, this thesis focusses on the following aspects: (1) development of a detailed and comprehensive plant-wide energy model for assessing the energy demand of different wastewater treatment systems at both steady- and unsteady-state conditions; (2) proposal of a design methodology for AnMBR technology and identification of optimal AnMBR-based configurations by applying an overall life cycle cost (LCC) analysis; (3) life cycle assessment (LCA) of AnMBR-based technology at different temperatures; and (4) evaluation of the overall sustainability (economic and environmental) of AnMBR for urban wastewater treatment.

In this research work, a plant-wide energy model coupled to the extended version of the plant-wide mathematical model BNRM2 is proposed. The proposed energy model was used for assessing the energy performance of different wastewater treatment processes. In order to propose a guidelines for designing AnMBR at full-scale and to identify optimal AnMBR-based configurations, the proposed energy model and LCC were used. LCA was used to assess the environmental performance of AnMBR-based technology at different temperatures. An overall sustainability (economic and environmental) assessment was conducted for: (a) assessing the implications of design and operating decisions by including sensitivity and uncertainty analysis and navigating trade-offs across environmental and economic criteria.; and (b) comparing AnMBR to aerobic-based technologies for urban wastewater treatment.

This Ph.D. thesis is enclosed in a national research project funded by the Spanish Ministry of Science and Innovation entitled "*Using membrane technology for the energetic recovery of wastewater organic matter and the minimisation of the sludge produced*" (MICINN project CTM2008-06809-C02-01/02). To obtain representative results that could be extrapolated to full-scale plants, this research work was carried out in an AnMBR system featuring industrial-scale hollow-fibre membrane units that was operated using effluent from the pre-treatment of the Carraixet WWTP (Valencia, Spain).

RESUM

El reactor anaerobi de membranes submergides (AnMBR) pot proporcionar el pas desitjat cap a un tractament d'aigües residuals sostenible, i suposa una extensió en l'aplicabilitat de la biotecnologia anaeròbia al tractament d'aigües residuals amb baixa càrrega (*p.e.* aigua residual urbana) o a condicions mediambientals extremes (*p.e.* baixes temperatures d'operació). Aquesta tecnologia alternativa reuneix els avantatges dels processos de tractament anaerobi (baixa demanda d'energia per l'estalvi de l'aireig i possibilitat de recuperació energètica per la producció de metà), conjuntament amb els beneficis de l'ús de de la tecnologia de membranes (*p.e* efluent d'alta qualitat, i reduïdes necessitats d'espai). Cal destacar que la tecnologia AnMBR permet la possibilitat de l'autoabastiment energètic del sistema degut a la generació de biogàs. Altres aspectes que s'han de considerar en el sistema AnMBR són el potencial de recuperació de nutrients, la qualitat de l'efluent i la baixa quantitat de fang generat, tots ells de vital importància quan s'avalua l'impacte mediambiental d'una planta de tractament d'aigües residuals urbanes.

L'objectiu principal d'aquesta tesi doctoral és avaluar la sostenibilitat econòmica i mediambiental de la tecnologia AnMBR per al tractament d'aigües residuals urbanes a temperatura ambient. Concretament, aquesta tesi se centra en les tasques següents: (1) desenrotllament d'un detallat i complet model d'energia per al conjunt de la planta a fi d'avaluar la demanda d'energia de diferents sistemes de tractament d'aigües residuals tant en règim estacionari com en transitori; (2) proposta d'una metodologia de disseny i identificació de les configuracions òptimes de la tecnologia AnMBR mitjançant l'aplicació una anàlisi del cost de tot el cicle de vida (CCV) ; (3) anàlisi del cicle de vida (ACV) de la tecnologia AnMBR a diferents temperatures; i (4) avaluació global de la sostenibilitat (econòmica i mediambiental) de la tecnologia AnMBR per al tractament d'aigües residuals urbanes.

En aquest treball d'investigació es proposa un model d'energia a nivell de tota la planta acoblat a la versió estesa del model matemàtic BNRM2. El model d'energia proposat s'ha utilitzat per a avaluar l'eficiència energètica de diferents processos de tractament d'aigües residuals urbanes. A fi de proposar unes directrius per al disseny d'AnMBR a escala industrial i identificar les configuracions òptimes de la tecnologia AnMBR, s'ha aplicat tant el model d'energia proposat, com el cost del cicle de vida (CCV). L'anàlisi del cicle de vida (ACV) s'ha utilitzat per a avaluar el rendiment mediambiental de la tecnologia AnMBR a diferents temperatures. En aquest treball s'ha dut a terme una avaluació global de la sostenibilitat (econòmica i mediambiental) de la tecnologia AnMBR per a: (a) avaluar les implicacions de les decisions de disseny i operació per mitjà d'una anàlisi de sensibilitat i incertesa i examinar les

contrapartides en funció de criteris econòmics i mediambientals; i (b) comparar la tecnologia AnMBR amb tecnologies basades en processos aerobis per al tractament d'aigües residuals urbanes.

Aquesta tesi doctoral està integrada en un projecte nacional d'investigació, subvencionat pel Ministerio de Ciencia e Innovación (MICINN), amb títol "*Modelación de la aplicación de la tecnología de membranas para la valorización energética de la materia orgánica del agua residual y la minimización de los fangos producidos*" (MICINN, projecte CTM2008-06809-C02-01/02). Per a obtenir resultats representatius que puguen ser extrapolats a plantes reals, aquesta tesi doctoral s'ha dut a terme utilitzant un sistema AnMBR que incorpora mòduls comercials de membrana de fibra buida. A més, aquesta planta és alimentada amb l'efluent del pretractament de l'EDAR del Barranc del Carraixet (València, Espanya).

RESUMEN

El reactor anaerobio de membranas sumergidas (AnMBR) puede proporcionar el paso deseado hacia un tratamiento sostenible del agua residual, ampliando la aplicabilidad de la biotecnología anaerobia al tratamiento de aguas residuales de baja carga (*ej.* agua residual urbana) o a condiciones medioambientales extremas (*ej.* bajas temperaturas de operación). Esta tecnología combina las ventajas de los procesos de tratamiento anaerobio (baja demanda energética gracias a la ausencia de aireación y a la recuperación energética a través de la producción de metano) con los beneficios de la tecnología de membranas (*ej.* efluente de alta calidad y reducidas necesidades de espacio). Cabe destacar que la tecnología AnMBR permite la posibilidad del autoabastecimiento energético del sistema debido a la generación de biogás. Otros aspectos que se deben considerar en el sistema AnMBR son el potencial de recuperación de nutrientes, la calidad del efluente generado y la baja cantidad de fangos producidos, siendo todos ellos de vital importancia cuando se evalúa el impacto medioambiental de una planta de tratamiento de aguas residuales urbanas.

El objetivo principal de esta tesis doctoral es evaluar la sostenibilidad económica y medioambiental de la tecnología AnMBR para el tratamiento de aguas residuales urbanas a temperatura ambiente. Concretamente, esta tesis se centra en las siguientes tareas: (1) desarrollo de un modelo de energía detallado y completo que permita evaluar la demanda energética global de diferentes sistemas de tratamiento de aguas residuales tanto en régimen estacionario como en transitorio; (2) propuesta de una metodología de diseño e identificación de configuraciones óptimas para la implementación de la tecnología AnMBR, aplicando para ello un análisis del coste de ciclo de vida (CCV); (3) análisis del ciclo de vida (ACV) de la tecnología AnMBR a diferentes temperaturas; y (4) evaluación global de la sostenibilidad (económica y medioambiental) de la tecnología AnMBR para el tratamiento de aguas residuales urbanas.

En este trabajo de investigación se propone un modelo de energía acoplado a la versión extendida del modelo matemático BNRM2. El modelo de energía propuesto se usó para evaluar la eficiencia energía de diferentes procesos de tratamiento de aguas residuales urbanas. Con el fin de proponer unas directrices para el diseño de AnMBR a escala industrial e identificar las configuraciones óptimas para la implementación de dicha tecnología, se aplicaron tanto el modelo de energía propuesto como un análisis CCV. El ACV se usó para evaluar la viabilidad medioambiental de la tecnología AnMBR a diferentes temperaturas. En este trabajo se llevó a cabo una evaluación global de la sostenibilidad (económica y medioambiental) de la tecnología AnMBR para: (a) evaluar las implicaciones que

conllevan ciertas decisiones durante el diseño y operación de dicha tecnología mediante un análisis de sensibilidad e incertidumbre, y examinar las contrapartidas en función de criterios económicos y medioambientales; y (b) comparar la tecnología AnMBR con tecnologías basadas en procesos aerobios para el tratamiento de aguas residuales urbanas.

Esta tesis doctoral está integrada en un proyecto nacional de investigación, subvencionado por el Ministerio de Ciencia e Innovación (MICINN), con título *"Modelación de la aplicación de la tecnología de membranas para la valorización energética de la materia orgánica del agua residual y la minimización de los fangos producidos"* (MICINN, proyecto CTM2008-06809-C02-01/02). Para obtener resultados representativos que puedan ser extrapolados a plantas reales, esta tesis doctoral se ha llevado a cabo utilizando un sistema AnMBR que incorpora módulos comerciales de membrana de fibra hueca. Además, esta planta es alimentada con el efluente del pre-tratamiento de la EDAR del Barranco del Carraixet (Valencia, España).

TABLE OF CONTENTS

MAIN NOMENCLATURE AND ABBREVIATION

AD	*anaerobic digestion*
AeMBR	*aerobic MBR*
Alk	*carbonate alkalinity*
AnMBR	*anaerobic MBR*
AnR	*anaerobic reactor*
BNRM2	*biological nutrient removal model 2*
BVSS	*biodegradable volatile suspended solids*
CAS	*conventional activated sludge*
CAPEX	*capital expenses*
CHP	*combined heat and power*
CH_4	*methane*
CIP	*clean in place*
COD	*chemical oxygen demand*
COD_T	*total COD*
DESASS	*design and simulation of activated sludge systems*
EAAS	*extended aeration activated sludge*
EP	*eutrophication potential*
GWP	*global warming potential*
GHG	*greenhouse gases*
HF	*hollow fibre*
HRT	*hydraulic retention time*
HS-S	*total sulphide measured as sulphur*
J	*transmembrane flux*
J_{20}	*20 ºC-normalised J*
J_C	*critical J*
$J_{20, C}$	*20 ºC-normalised* J_C
K	*permeability*
LCA	*life cycle analysis*
LCI	*life cycle inventory*
LCIA	*life cycle impact assessment*
LCC	*life cycle cost*
LMH	*litre per square metre of membrane area per hour*
MA	*methanogenic Archaea*
MBR	*membrane bioreactor*
MLTS	*mixed liquor total solids*
MT	*membrane tank*

NVSS	*non volatile suspended solids*
NH_4-N	*ammonium measured as nitrogen*
NH_4	*total ammonium*
N_2O	*dinitrogen monoxide*
OLR	*organic loading rate*
OPEX	*operating expenses*
O&M	*operating and maintenance*
PS	*primary settler*
PO_4-P	*orthophosphate measured as phosphorous*
PO_4^{3-}	*total orthophosphate*
Q_G	*flow rate of biogas*
Qrec	*recycling sludge flow rate from the membrane tank to the anaerobic reactor*
Rrec	*sludge recycling ratio*
SGD_m	*specific gas demand per square metre of membrane area*
SGD_p	*specific gas demand per permeate volume*
SRB	*sulphate reducing bacteria*
SO_4-S	*sulphate measured as sulphur*
SRF	*sludge recycling flow*
SRT	*sludge retention time*
T	*temperature*
TAEC	*total annualised equivalent cost*
TS	*total solids*
TSS	*total suspended solids*
TMP	*transmembrane pressure*
UASB	*upflow Anaerobic Sludge Blanket*
UWW	*urban wastewater*
VFA	*volatile fatty acids*
VS	*volatile solids*
VSS	*volatile suspended solids*
WWT	*wastewater treatment*
WWTP	*wastewater treatment plant*

CHAPTER 1:

Introduction:
Anaerobic membrane bioreactors for treating urban wastewater

1.1 Wastewater treatment process for treating urban wastewater

A wastewater treatment plant (WWTP) is a complex facility where various physical, biological or chemical processes are applied to change the properties of the wastewater in order to turn it into an effluent that can be safety discharged into the environment or that is usable for a certain purpose.

Urban wastewater (UWW) treatment techniques have been used for over a century [1.1]. Hence, many different processes have been developed and many variations tested. The activated sludge process and the processes using biofilms are two of the biological processes most commonly used nowadays [1.1]. In the activated sludge process, a mixture of wastewater and activated sludge is stirred and aerated and subsequently separated from the treated wastewater by sedimentation and wasted or returned to the process as needed.

In 1990, technological advances in wastewater treatment were required for meeting stringent effluent standards in urban WWTPs. Therefore, alternative UWW treatment technologies were implemented including membranes, which offers several advantages over traditional processes such as high effluent quality, small footprint size of the treatment plant and reduced sludge production [1.2]. Moreover, in recent years, there has been increasing interest in the development of mainstream anaerobic treatment systems due to the sustainable advantages that presents this type of processes over the aerobic treatments ones (see, for instance,[1.3]).

1.1.1 Anaerobic vs. aerobic wastewater treatment

The complete anaerobic digestion of organic matter only takes place under strict anaerobic conditions. It requires specific adapted bio-solids and particular process conditions, which are considerably different from those needed for aerobic treatment. The anaerobic digestion (AD) process involves strict and facultative anaerobic microorganisms in anaerobic conditions and comprehends three overall biological steps (acidogenesis, acetogenesis and methanogenesis) and two extracellular solubilisation steps (disintegration and hydrolysis) (see Figure 1.1).

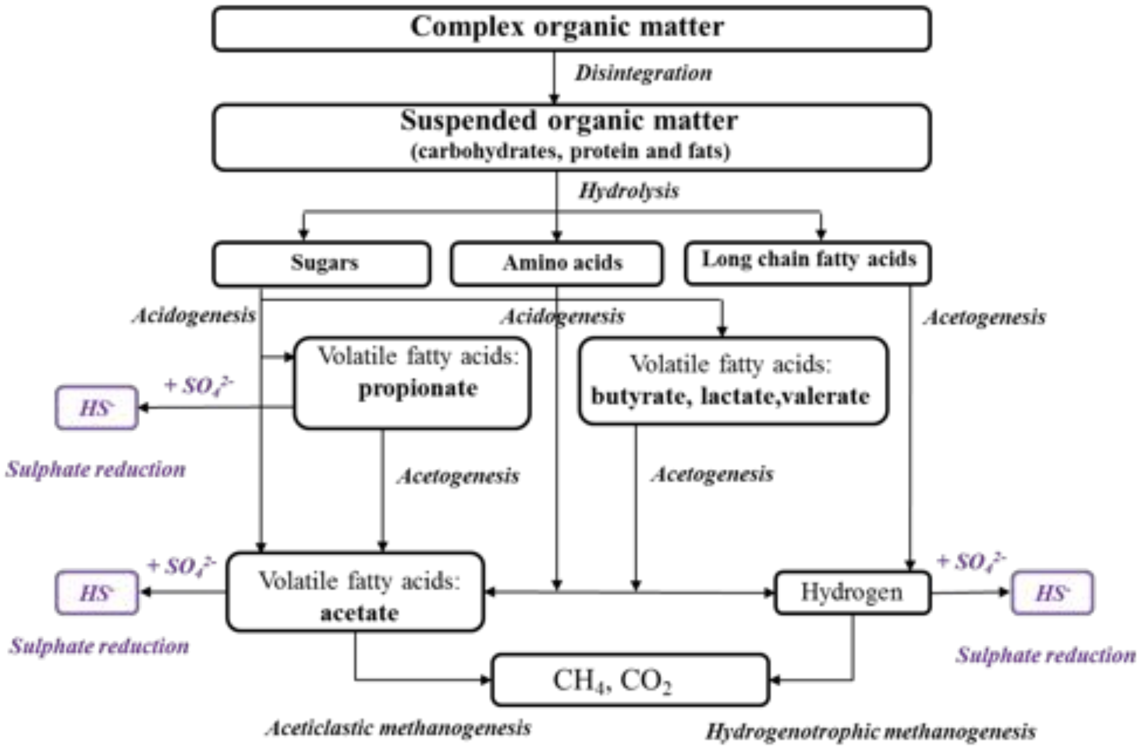

Figure 1.1 Key process steps in the anaerobic treatment of sulphate-loaded wastewater.

- *Extracellular solubilisation (disintegration and hydrolysis)*

The initial disintegration step is a largely non-biological step that converts composite particulate substrate to inerts, particulate carbohydrates, proteins and lipids. The initial hydrolysis step consists in the enzymatic hydrolysis of organic matter (particulate carbohydrates, proteins and lipids) in smaller organic chains (amino acids, long chain fatty acids, single carbohydrates), and used to be the slowest step in AD.

- *Acidogenesis*

In the second stage, known as acidogenesis, acidogenic bacteria transform the products of the hydrolysis reaction into short chain volatile acids, ketones, alcohols, hydrogen and carbon dioxide. The principal acidogenesis stage products are valeric acid ($CH_3(CH_2)_3COOH$), butyric acid ($CH_3(CH_2)_2COOH$), lactic acid ($C_3H_6O_3$), propionic acid (CH_3CH_2COOH), acetic acid (CH_3COOH), formic acid ($HCOOH$), ethanol (C_2H_5OH), methanol (CH_3OH), etc.

- *Acetogenesis*

  In the third stage, known as acetogenesis, the rest of acidogenesis products (i.e. the propionic acid, butyric acid and alcohols) are transformed by acetogenic bacteria into hydrogen, carbon dioxide and acetic acid.

- *Methanogenesis*

  The fourth and final stage is called methanogenesis. During this stage, Methanogenic Archaea (MA) converts the hydrogen and acetic acid formed by the acid formers to methane gas and carbon dioxide.

Moreover, sulphate reduction to sulphide from propionic acid, acetic acid and hydrogen by the sulphate reducing bacteria (SRB) can occur at the same time. In this respect, a competition between MA and SRB for the available substrate can occur when there is significant sulphate content in the influent, reducing therefore the available COD for methanisation [1.4]. Specifically, 2 kg of COD are consumed by SRB in order to reduce 1 kg of influent SO_4-S.

In comparison with conventional aerobic wastewater treatments, and in the light of the very much desirable development and implementation of more sustainable technologies, the anaerobic wastewater treatment concept offers the following sustainable benefits:

- Low energy demand since no aeration is required.
- Methane generation (a source for energy production) from organic matter. According to McCarty *et al*. [1.5], methane production from sewage sludge digestion in conventional aerobic treatment is half of the methane production achieved from full anaerobic treatment of the organic matter content in the wastewater (see Figure 1.2).
- Relatively small space requirements of the system. Up to 90% reduction when using expanded sludge beds systems [1.6].
- Low sludge production. According to McCarty *et al*. [1.5], sludge production in conventional aerobic treatment with sludge AD is two times the sludge production in full anaerobic treatment (see Figure 1.2).
- Wasted sludge generally well stabilised since anaerobic processes require high operating temperature and/or long sludge retention time (SRT).
- Anaerobic organisms unfed for long periods of time (exceeding one year) without any serious deterioration of their activity [1.7].

- Maximising nutrient recovery potential from wastewater (e.g. the effluent can be used for fertirrigation purposes.

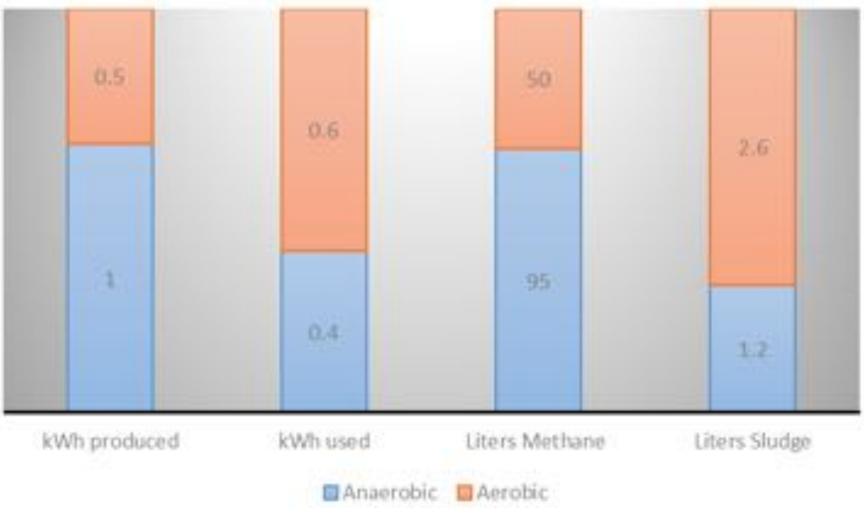

Figure 1.2 Comparison of energy, methane and sludge production per cubic meter of treated wastewater in full anaerobic treatment versus conventional aerobic treatment with sludge anaerobic digestion (based on McCarty *et al.* [1.5]).

At the present state of knowledge some drawbacks can be still brought up against anaerobic treatment:

- Several parameters need to be tightly controlled in order to achieve optimum performance, such as: pH, temperature, salts, alkalinity, heavy metals, ammonia and antibiotics. For instance, the low-growth rate of anaerobic bacteria requires considerable biomass concentrations and/or high temperatures in order to achieve suitable organic matter removal rates, especially for low-strength wastewaters like urban ones.
- The presence of sulphate in wastewater leads to the production of hydrogen sulphide during anaerobic digestion. H_2S will then form part of the generated biogas. Hydrogen sulphide is extremely corrosive and its presence requires the purchase of more robust and therefore expensive generators.
- The anaerobic sludge presents low sedimentation, which involves operating with high reaction volumes.

Historically, anaerobic processes have been mainly employed for industrial or high strength wastewater treatment [1.8]. Their application to low-strength WWT is mainly limited by difficulty in retaining slow-growth-rate anaerobic microorganisms when operating at short hydraulic retention times (HRTs), which are usually associated with low-strength WWTP.

1.1.2 Traditional urban wastewater treatment plant

The traditional activated sludge process (i.e. conventional activated sludge (CAS) and extended aeration activated sludge (EAAS)) are widely used for treating low-strength wastewaters (< 1000 mg COD/L) such as urban one. In the activated sludge process, a bacterial biomass suspension (the activated sludge) is responsible for the removal of pollutants. A review on the historical evolution of the activated sludge process can be found, for instance, in Orhon [1.9].

Depending on the design and the specific application, a WWTP based on activated sludge technology can achieve biological removal of both nitrogen and phosphorus (N and P, respectively), besides removal of organic carbon substances. Evidently, many different activated sludge process configurations have evolved over time [1.10]. Figure 1.3shows a traditional activated sludge process consisting of a University of Cape Town (UCT) configuration (extracted from Gernavey *et al*. [1.10]).

Activated sludge technology has been highly effective at achieving organic carbon and nutrient removal from UWW, but has resulted in energy-intensive treatment that has broad environmental consequences. Moreover, large quantities of sludge are produced, which need to be treated and disposed. According to Xing *et al*. [1.11], sludge production in activated sludge processes is generally in the range of 0.3-0.5 kg $TSS \cdot kg^{-1}$ $COD_{REMOVED}$. Therefore, the wastewater treatment needs to radically improve energy balance in order to progress towards energy self-sufficiency [1.12].

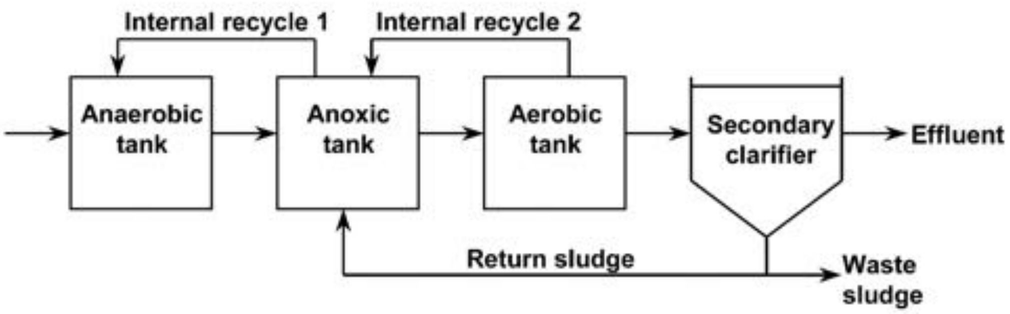

Figure 1.3 Scheme of a University of Cape Town (UCT) WWTP lay-out (extracted from Gernavey *et al*. [1.10]).

1.1.3 Technological advances in urban wastewater treatment

Nowadays, meeting key issues in UWW treatment (e.g. restrictions in effluent standards, rising treatment costs and spatial constraints) might require alternative UWW treatment technologies rather than traditional ones [1.13]. As commented before, recent technological advances in UWW treatment include membranes, which offers several advantages over traditional processes: high effluent quality, small footprint size of the treatment plant and reduced sludge production [1.2].

1.1.3.1 Aerobic membrane bioreactors in urban wastewater treatment

Aerobic membrane bioreactor (AeMBR) technology combines the biological degradation process by activated sludge with a direct solid–liquid separation by membrane filtration. By using micro or ultrafiltration membrane technology (with pore sizes usually ranging from 0.05 to 0.4 μm) [1.14], MBR technology allows the complete retention of the microorganisms inside the system. This complete retention of microorganisms allows high SRT to be obtained with reduced working volumes [1.15]. In this respect, MBR applied to UWW treatment is a promising alternative to obtain high biomass and COD concentrations in the system by decoupling both HRT and SRT.

Depending on the configuration of the filtration process, MBR can be classified in submerged /immersed MBRs and side-stream MBRs [1.16]. The concept of submerged membranes was conceived in early 1990s by independent teams in Japan and Canada. In the University of Tokyo (Japan), Professors Aya and Yamamoto conducted laboratory experiments with hollow-fibre membranes which were immersed in an activated sludge reactor. Yamamoto *et al.* [1.17] published a famous paper as the proof of concept of the submerged MBR process which revolutionised membrane-based UWW treatment. The concept was picked up by Japanese companies that continued the development and commercialisation of this technology. Specifically, Kubota Corporation developed flat-sheet membrane panels, while Mitsubishi Rayon Corporation focused their efforts on fine hollow-fibre membranes. Several MBR variants exist in the market nowadays, but they are all originally variants of the two membrane configurations mentioned before.

Studies on the treatment of UWW with MBRs mostly utilised submerged configurations [1.18], which can be divided in two types: internal submerged MBR (see Figure 1.4) and external submerged MBR system (see Figure 1.5).

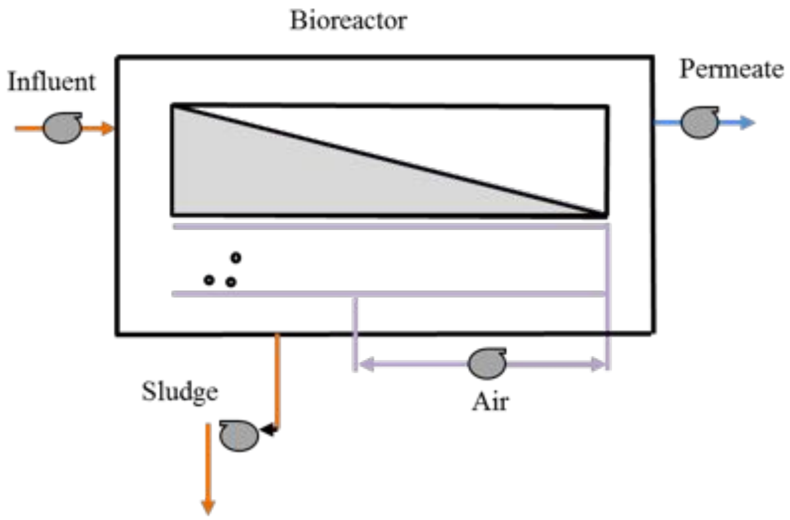

Figure 1.4 Internal submerged MBR system.

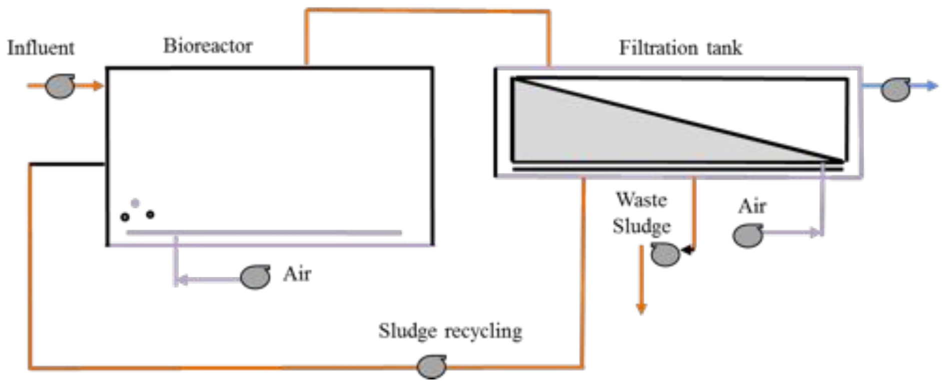

Figure 1.5 External submerged MBR system.

External MBRs were considered to be more suitable for wastewater streams characterised by high temperature, high organic strength, extreme pH, high toxicity and low filterability.

MBR has many advantages over traditional processes [1.15], such as:

- Secondary clarifiers and tertiary filtration processes are eliminated, thereby reducing plant footprint and reactor requirements. Unlike secondary clarifiers, the efficiency of the solid separation process is not dependent on the concentration or characteristics of the mixed liquor. Since elevated mixed liquor suspended solid concentrations are possible, the aeration basin volume can be reduced, reducing therefore the plant footprint.

- Good disinfection capability.
- High volumetric loading.
- High SRT, which allows achieving low sludge productions.
- Generation of a high-quality effluent that is suitable for reuse. Typical output quality of membrane systems includes suspended solid (SS) < 1 mg/L.

As a result, the MBR process has become an attractive option for the treatment and reuse of different types of wastewaters.

Although the MBR market has recently strongly risen, further research is required into the field due to membrane limitations. Figure 1.6 shows a survey conducted in 2010, 2012 and 2015 aimed at revealing the main technical issues and limitations of operating MBRs [1.19]. This study identified screening/pre-treatment and membrane surface fouling as the greater concern in MBR technology in 2015. Moreover, this survey revealed that membrane fouling, membrane chemical cleaning, energy demand and operator knowledge have increased their concern in the last years. With regard to energy demand, AeMBR is based on aerobic processes where a significant electricity demand is required for aeration and energy recovery from organic matter is not maximised [1.5; 1.20]. On the other hand, the competiveness of this technology is threatened by the low operational cost of CAS systems [1.21].

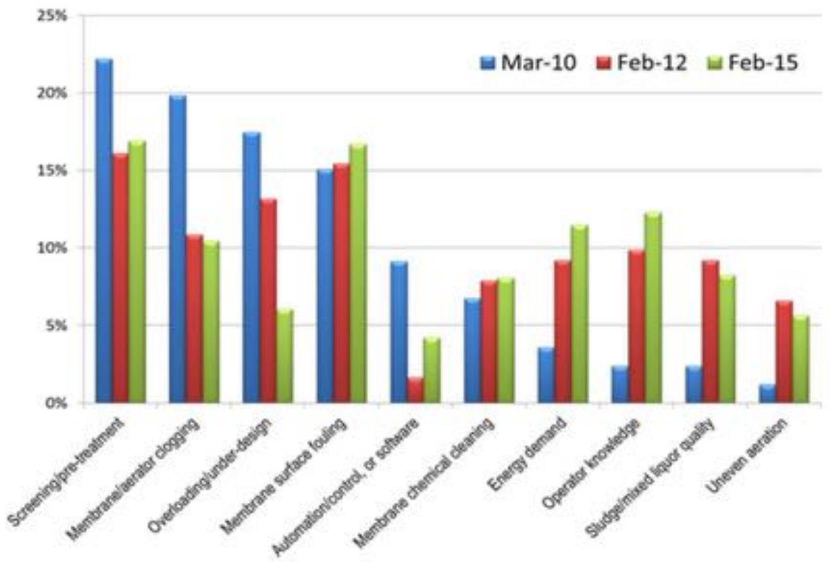

Figure 1.6 Responses to the survey Q1: “In your experience, what are the main technical issues or limitations that prevent MBRs working as they should?” [1.19].

1.1.3.2 Anaerobic membrane bioreactors in urban wastewater treatment

AD has been successfully used for the treatment of wastewaters during the last 30 years [1.22]. Nowadays, anaerobic WWT can be considered an established technology and it is successfully used for the treatment of many kinds of industrial wastewaters as well as sewage [1.23; 1.24; 1.25]. The success of anaerobic WWT can be attributed to an efficient uncoupling of the SRT from the HRT through biomass immobilisation, which can be accomplished through membrane assisted physical separations [1.26].

The first application of membranes in anaerobic WWT was reported by Grethlein in 1978. It consisted of an external cross-flow membrane applied to the treatment of a septic tank effluent. On the other hand, the first commercially-available anaerobic MBR (AnMBR) was developed by Dorr-Oliver in the early 1980s, which was known as membrane anaerobic reactor system (MARS).

Studies on the treatment of UWW with AnMBRs mostly utilised submerged configurations [1.18], either internal or external. A membrane externally connected to the anaerobic bioreactor is the configuration most commonly used. The bioreactor can be a continuously stirred tank reactor (CSTR), an upflow anaerobic sludge blanket (UASB) [1.27; 1.28] an expanded granular sludge bed (EGSB) [1.29], or a fluidised bed [1.30] reactor coupled to membrane filtration.

1.1.3.2.1 Advantages of AnMBR

AnMBR technology gathers the before-mentioned advantages of anaerobic treatment processes jointly with the before-mentioned benefits of using membranes instead of a secondary clarifier [1.31]. Although there is still some uncertainties around AnMBR performance, this technology is becoming increasingly popular for UWW treatment (e.g. [1.20; 1.32; 1.33; 1.34; 1.35]) Indeed, although AnMBR technology has not been applied to full-scale UWW treatment yet, recent literature has reported increasing interest by the scientific community on its applicability at ambient temperatures [1.8; 1.28; 1.30; 1.31; 1.36; 1.37; 1.38; 1.39; 1.40; 1.41].

As mentioned before, AnMBR technology allows a complete biomass retention, since it enables uncoupling both HRT and SRT, making biomass concentration independent of the low growth rates of anaerobic microorganisms [1.42]. Moreover, AnMBR presents added benefits when compared to aerobic WWTPs, such as: lower sludge production, possible net energy production, and no aeration costs for organic matter removal [1.43]. In particular, submerged AnMBRs have gained attention for their ability to produce methane-rich biogas during the treatment of UWW [1.33; 1.39; 1.44]. Biogas capture is a key operating opportunity of AnMBR technology which further improves its energy balance [1.33] and thereby reduces its operating costs. Jeison [1.45] reported reductions of up to 90% in the sludge produced when AnMBR technology was used.

Hence, AnMBRs can provide the desired step towards sustainable UWW treatment [1.35; 1.39; 1.46]. This alternative for WWTPs is more sustainable because it transforms wastewater into a renewable source of energy and nutrients, whilst providing a recyclable water resource. Indeed, AnMBR offers the possibility of operating in energy neutral or even positive net energy balance due to biogas generation [1.27; 1.29; 1.47; 1.48; 1.49].

1.1.3.2.2 Barriers of applying AnMBR

Given the early stage of development and uncertainties around AnMBR performance, it is unclear how detailed design and operational decisions influence the environmental and economic performance of AnMBR [1.20]. Therefore, it is needed to establish the basis of an economic framework aimed at designing AnMBRs for full-scale UWW treatment by considering the key parameters affecting process performance. Moreover, selecting appropriate layouts for wastewater treatment should take into account not only economic terms (i.e. investment, operation and maintenance) but also environmental terms (e.g. eutrophication, global warming potential (GWP), marine ecotoxicity, etc.). In this respect, several barriers can be found in AnMBRs, as follows:

- *Membrane fouling and cleaning:* Membrane fouling is the result of the interaction between membrane surface and sludge suspension. This phenomenon usually decrease system productivity, cause frequent membrane chemical cleaning which might reduce membrane lifespan whilst increasing replacement costs, and increase energy requirements for sludge recirculation or gas scouring [1.8; 1.35]. In this respect, membrane fouling and cleaning issues remain a critical obstacle limiting the widespread application of membrane systems in WWTP [1.34; 1.35; 1.45; 1.50].

- *Sulphide production:* When UWW containing sulphate is anaerobically treated, sulphate is reduced to sulphide. The production of this end product can cause some disadvantages. For instance, the amount of produced biogas is reduced because some of the influent COD (approx. 2 g COD per g SO_4-S) is consumed by SRB (see, for instance, [1.39]). Moreover, the presence of hydrogen sulphide in biogas and mixed liquor causes some technical problems such as: 1) toxicity to anaerobic microorganisms; 2) reduction of the quality of the produced biogas; 3) corrosion in pipes, engines and boilers, entailing higher maintenance and replacement costs; and 4) downstream oxygen demand for oxidising hydrogen sulphide.

- *Temperature*: Low ambient temperatures have been normally considered a barrier for anaerobic treatment because the energy requirements associated with heating large quantities of wastewater outweigh the energy recovery potential [1.22; 1.51]. As a result, anaerobic processes have not been widely applied for full-scale UWW treatment at low temperatures [1.27]. Despite anaerobic processes are most often operated at high/warm temperatures to increase microorganism growth rate, AnMBRs have recently been shown to perform adequately at lower temperatures (e.g. 15-20 °C) [1.20; 1.33; 1.39]. However, the lower the temperature the higher the proportion of the produced methane that is dissolved in the effluent [1.52]. This methane dissolved in the effluent could strip out thus being emitted to the atmosphere.

- *Lack of direct nutrient removal capability*: A post-treatment is required to produce an effluent suitable for being discharged directly into the aquatic environment [1.53]. However, some approaches can be applied according to McCarty *et al.* [1.5]: 1) chemical precipitation or its conversion into struvite for recovery as fertiliser; 2) anammox process, which oxidises ammonia with nitrite to produce harmless N_2 gas; 3) source-separation of urine so that it does not become part of the UWW; and 4) crop or landscape irrigation of the AnMBR effluent.

- *Mathematical models:* A critical issue for advancing on AnMBR development is using mathematical models capable of accurately predicting system performance under different design and operational scenarios. Some software in the field of wastewater engineering have already included the analysis of process water management and sludge treatment, (e.g. gPROMS, BioWin, Simba6 etc.). However, these modelling software do not include new promising technologies aimed at enhancing wastewater treatment, such as aerobic and anaerobic membrane bioreactor (MBR and AnMBR, respectively).

1.1.3.2.3 Biological and membrane performance in AnMBR

Figure 1.7 shows the process flow diagram of an external submerged AnMBR system including the key operating parameters in both biological and filtration process: T, HRT, SRT, mixed liquor suspended solids concentration in the anaerobic reactor ($MLSS_{RAN}$), sludge recycling ratio (r) defined as sludge recycling flow per influent flow, specific gas demand per square metre of membrane area (SGD_m), 20 ºC-standardised transmembrane flux (J_{20}) and mixed liquor suspended solids concentration in the membrane tank ($MLSS_{MT}$).

Both biological treatment performance and membrane performance in AnMBR are discussed in the following section.

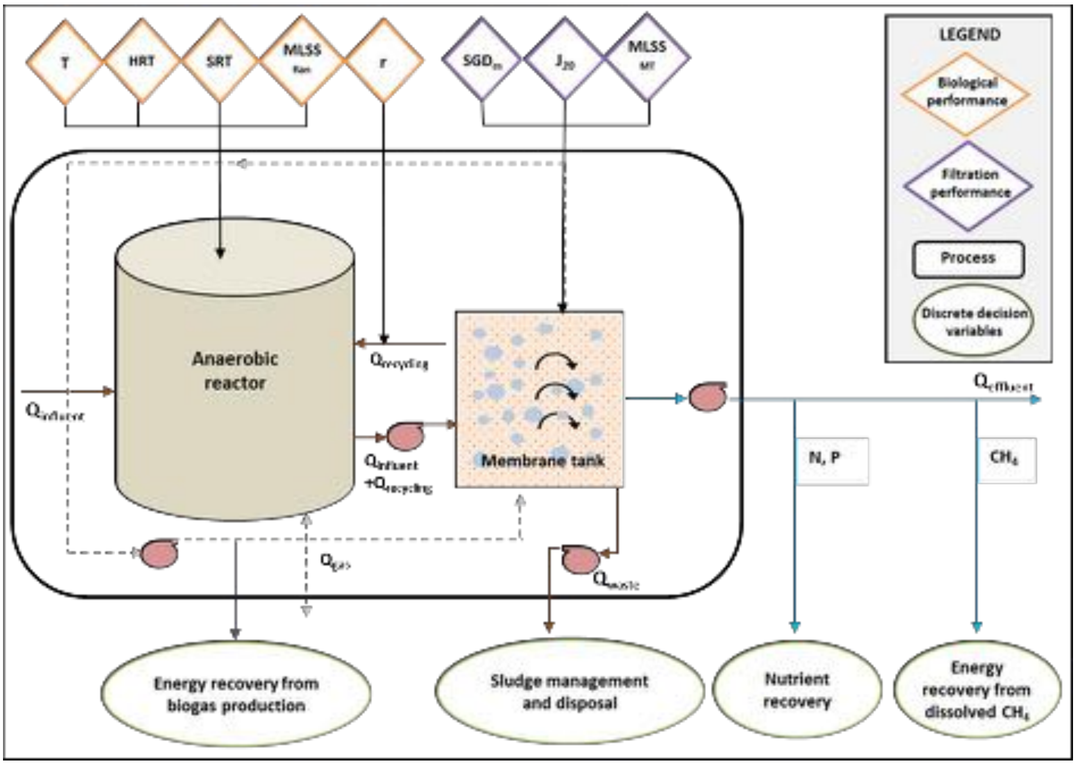

Figure 1.7 Process flow diagram of an AnMBR including the key operating parameters in the filtration and biological process. Nomenclature: **T**: operating temperature; **HRT**: hydraulic retention time; **SRT**: Sludge retention time; **r**: sludge recycling ratio; $\mathbf{SGD_m}$: specific gas demand per m^2 of membrane area; $\mathbf{J_{20}}$: 20 ºC-standardised transmembrane flux**;** $\mathbf{MLSS_{MT}}$: mixed liquor suspended solids concentration in the membrane tank; and $\mathbf{MLSS_{Ran}}$ mixed liquor suspended solids concentration in the anaerobic reactor.

1.1.3.2.3.1 Biological performance of AnMBR

Temperature

The temperature dependence of biological reaction rates gain a significant importance for the overall efficiency of the anaerobic treatment process. Generally, the activity of microorganisms in biological processes decreases when temperature decreases, which results in a decrease in organic matter removal efficiency [1.32]. Temperature effect studies have been focused on overall anaerobic degradation process or methanogenesis [1.54]. Lowering operational temperature generally leads to a decrease in the maximum specific growth rate and substrate utilisation rate. In this respect, due to the low growth rate of anaerobic bacteria, high temperatures are usually required in order to achieve suitable organic matter removal rates, especially for low-strength wastewaters like urban ones. In addition, MA yield has been shown to decrease with decreasing temperature, which consequently results in a decrease in biogas production. The production of biogas and its potential use as a source of energy is one of the most interesting benefits of anaerobic wastewater treatment [1.33; 1.40; 1.44]. On the other hand, it is clear that the solubility of methane increases with decreasing temperature [1.40].

SRT, HRT and OLR

As mentioned before, the growth rate of anaerobic microorganisms are greatly reduced at low temperatures. Therefore, long SRTs are commonly necessary not only to meet appropriate effluent and sludge standards and produce considerable amounts of biogas, but also to prevent biomass washout [1.22]. Therefore, the success of anaerobic treatment of UWW at low temperatures depends on the ability to detach SRT from HRT. Regarding HRT, this parameter is considered important from an economic perspective as it has a strong influence on capital cost (e.g. shorter HRTs allow smaller reactors). Moreover, biogas yield may increase linearly when deceasing HRT due to an increase in the organic loading rate (OLR) [1.32]. Nevertheless, decreasing HRT may increase COD concentration in both mixed liquor and permeate since OLR increases.

Sludge production and disposal

Jeison [1.45] reported reductions of up to 90% in sludge production when AnMBR technology was used. In addition, depending on the operating conditions, the produced sludge could be enough stabilised to be directly disposed on farmland with no further digestion step (no pathogens and low biological methane production).

Sewage sludge treatment is an environmentally sensitive problem in terms of both energy and pollutants. The fate of sewage sludge will continue to be an ongoing challenge as long as wasted sludge quantities continue increasing [1.55]. The main alternatives of sludge handling and disposal are: agriculture, composting, landfilling and incineration. However, new treatment processes are being introduced in the market such as energy valorisation and landscape.

Laws concerning agricultural spreading of sludge [1.56] are becoming more and more restrictive. The regulation on the use of sewage sludge in agriculture involved the creation of the "*Sludge National Register*", which includes information to be supplied by the water purification plants, sludge treatment facilities and managers who perform agricultural application. Updating the information contained in the

Register must conform to the provisions of the Spanish order: "*AAA / 1072/2013*", on the use of sewage sludge in agriculture. According to the Spanish national register of sludge, extracted from MAGRAMA [1.56], agricultural disposal has prevailed as the final destination of the sludge, which represents approximately 80% of total generated sludge. A reduction of the landfill has been achieved (about 8% currently), and incineration is growing (around 4%). Other lower quantitative importance destination is the use of sludge in non-agricultural soils.

On the other hand, different studies regarding sludge disposal have been reported in recent literature. Agricultural application is the most common scenario for the final disposal of the sludge, which takes into account the positive effects of the nutrient value of the sludge. Moreover, it expanded the system to include the avoided production of synthetic fertilisers (see, for instance, [1.55; 1.57]) as well as the negative consequences associated with the heavy metals also present in the sludge (see for instance, [1.58; 1.59]). Comparing the environmental impact on several sludge treatment scenarios such as agriculture spreading, incineration, and landfill, among others, Lundin *et al.* [1.60] reported that agricultural application had the lowest cost among the evaluated options, whereas incineration had the highest cost. Houillon and Jolliet [1.55] found that landfill was the least preferable option from an environmental point of view and Hong *et al.* [1.61] found that contribution of landfill had an important role on global warming potential (GWP).

1.1.3.2.3.2 Membrane performance of AnMBR

<u>*Membrane fouling*</u>

Fouling is the major drawback of any membrane-based system, affecting the operation and performance of the AnMBR system and therefore the well balanced behaviour of the whole system. In this respect, fouling mitigation (during operation) and membrane capital cost remain the dominant sources of costs, which are critical challenges to enable AnMBR to overtake activated sludge processes in practice [1.8].

Due to the application of negative pressure on the permeate side, a deposition of a strong matrix of fouling layer develops on the membrane, which results in more hydraulic resistance thus lower flux. In order to maintain the operating flux, the transmembrane pressure (TMP) may be significantly increased, leading to an inevitable final chemical cleaning of the membrane for restoration of a reasonable flux. Over a period of time, the flux is reduced to a point where membrane cannot be used and need to be replaced [1.62]. Membrane resistance represents the sum of the resistance of the membrane itself, plus the resistance due to fouling and stable cake formation, i.e. the one that cannot be easily reverted by back-flushing cycles [1.42].

Membrane fouling can be traditionally classified into reversible, irreversible and irremovable fouling based on the cleaning practice [1.35]:

- *Reversible fouling*: Refers to fouling that can be removed by physical cleaning from the membrane surface (membrane scouring by air/gas sparging, back-flushing, etc.). Removable fouling occurs due to deposition of material on the membrane surface. In general, deposition of biosolids (cake layer formation) is regarded as the major process causing reversible fouling. For long-term operation, the dominance of reversible fouling can be caused by a poor sludge filterability and/or low efficiency of physical cleaning [1.63].

- *Irreversible fouling*: Refers to permanent fouling which cannot be eliminated by physical cleaning approaches, thus it must be removed by chemical cleaning methods. Irremovable fouling is caused by the pore blocking and strongly attached foulants during membrane filtration. A deposition of solid layer on the membrane during a continuous filtration process will result in irremovable fouling layer. Considering the nature and the causes of irremovable fouling, many efforts have been performed to investigate cake layer [1.64; 1.65].

- *Irremovable fouling:* Refers to the ‘long-term irreversible fouling which is not readily removed by typical chemical cleaning. Once a membrane is irremovably fouled during long-term operation, the original virgin membrane permeability is never recovered [1.63].

According to Smith *et al*. [1.66], future research efforts should focus on optimising membrane operating in order to minimise any kind of membrane fouling and thereby decrease energy demand and increase membrane lifetime. Membrane fouling has been controlled through various strategies [1.16; 1.67; 1.68], which are linked to the membrane configuration. In external cross-flow configurations, a high cross-flow velocity is maintained to limit inorganic and organic foulant build-up on the membrane [1.53]. In submerged configurations, the main points of fouling control strategies as regards membrane operation are:

- Optimising the frequency and duration of the physical cleaning stages (back-flushing and relaxation) [1.69].
- Optimising different operating variables such as gas sparging intensity (usually measured as SGD_m [1.70].

- Operating membranes under sub-critical filtration conditions bounded by critical flux (J_C) [1.46; 1.71; 1.72].

SGD$_{m,}$ MLSS$_{MT}$ and critical flux (J_c)

Further research is required to determine which fouling mitigating strategy is most effective per energy input. For instance, Martin *et al.* [1.51] reported that gas sparging intensity in each operating range is a key operating parameter with a high variability. Moreover, lower permeate fluxes (J) are typically observed in AnMBRs than in AeMBR as a result of less flocculation and increased concentrations of fine particulates and colloidal solids in the mixed liquor [1.16; 1.51]. In addition, the necessity of working at high SRT for anaerobic treatment of low-strength wastewaters usually result in high MLSS concentrations, thus low membrane permeability are reached [1.46]. Therefore, the effect of SGD$_{m,}$ J and MLTS on membrane fouling must be further assessed and optimised.

On the other hand, it is important to mention that other studies comparing AeMBRs to AnMBRs for UWW treatment have indicated similar fouling propensities [1.73] or even less propensity for fouling in AnMBRs [1.74].

Several published studies provide the J_C of both aerobic and anaerobic MBRs on a laboratory scale [1.65; 1.75; 1.76]. J_C is defined as a quantitative filtration parameter defined as ''the flux below which a decline of flux with time does not occur; above it, fouling is observed'' [1.77; 1.78]. The flux-step method is commonly applied for determining Jc [1.14; 1.42]. This method enables Jc to be determined in a wide range of operating conditions, considering MLSS level and gas sparging intensity the factors that affect Jc most. However, further studies would be needed in order to determine J_C in AnMBR on a semi-industrial scale. Moreover, the effect of the main operating conditions on membrane fouling cannot be evaluated properly at the lab scale because they depend heavily on the membrane size. In particular, in hollow-fibre (HF) membranes the HF length is a critical parameter [1.46]. For instance, Robles *et al.* [1.46] determined J_C at different operating conditions in a HF-AnMBR system at semi-industrial scale. Figure 1.8 shows 20 ºC-standardised transmembrane critical flux ($J_{C,20}$) to be directly related to SGD_m when operating at high MLTS levels (at 23 and 28 g L^{-1}). The results indicated that it is theoretically possible to operate membranes sub-critically at high MLTS levels without applying prohibitive SGD_m levels (from 0.17 to 0.50 $Nm^3\ h^{-1}\ m^{-2}$) when working at J_{20} between 10 and 15 LMH. Indeed, a considerable increase in J_{20} could be achieved in sub-critical filtrations conditions by increasing SGD_m just slightly.

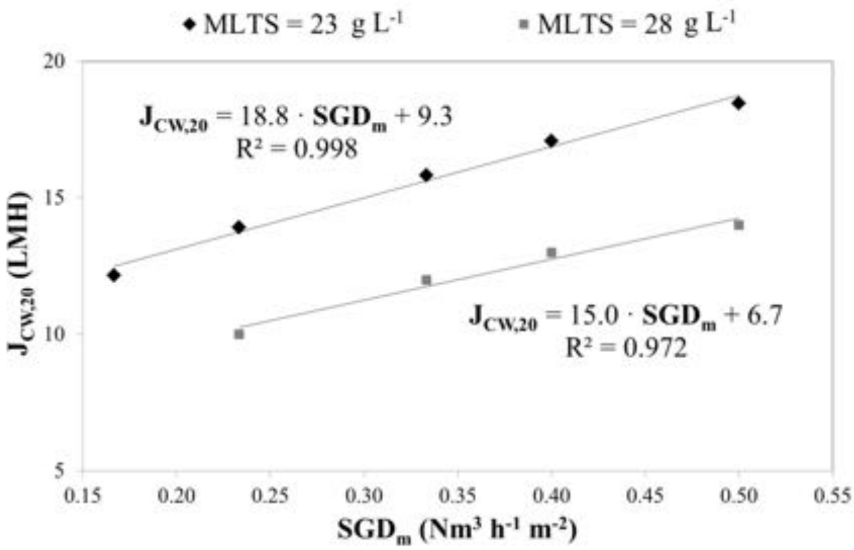

Figure 1.8 Effect of SGD_m on J_{CW20} at MLTS levels of 23 and 28 g L^{-1} [1.46]. $\mathbf{J_{CW,20}}$: 20 ºC-standardised transmembrane critical flux.

1.2 Plant-wide modelling in urban wastewater treatment

To date, the scientific community involved in the wastewater treatment field has been mainly focused on water quality and associated plant-wide modelling issues [1.79]. In this respect, the use of mathematical models for WWTP design and upgrading, process optimisation, operator training, and development of control strategies has become a standard engineering tool in the last decade (see, for instance, [1.10;1.80]). In this respect, it is necessary to model energy inputs and outputs in WWTP for evaluating the energy consumption and efficiency of different wastewater treatment alternatives, focusing furthermore in reducing the associated overall cost and the potential environmental impact (e.g. greenhouse gases (GHG) emissions).

Plant-wide modelling in wastewater treatment becomes attractive to many researchers as it provides a holistic view of the process and it allows for a more comprehensive understanding of the interactions between unit processes. Nonetheless, sensitivity and uncertainty analysis need to be carried out, since model predictions are not free from uncertainty (e.g. approximation of reality, assumptions…).

1.2.1 Energy modelling in urban wastewater treatment

Different studies can be found in literature dealing with energy modelling in WWTP. Jeppsson *et al.* [1.81] proposed an extension of the Benchmark Simulation Model no 1 (BSM1) aimed at facilitating control strategy development and process performance evaluation at a plant-wide level, including

therefore a complete energy balance. Gomez *et al.* [U. Jeppsson, C. Rosen, J. Alex, J. Copp, K.V. Gernaey, M.-N. Pons, P.A. Vanrolleghem, Towards a benchmark simulation model for plant-wide control strategy performance evaluation of WWTPs. Water Sci. Technol. 53 (2006), 287–295.
1.82] presented a new biochemical model for aerobic digestion that introduced an energy balance to dynamically predict the temporary evolution of temperature in an autothermal thermophilic aerobic digester. Righi *et al.* [1.83] assessed the environmental profile and energy balance of different waste treatment systems. Another representative study was conducted by Lemos *et al.* [1.84], who assessed the environmental performance and the electricity consumption of an entire urban water system; whilst Nowak *et al.* [1.85] considered several ways of ensuring positive energy balance of wastewater treatment.

Plant-wide energy models are expected to be a promising tool for selection of the best among the alternatives aimed to meet the desired criteria in the WWTP network (e.g. low energy consumption) [1.86]. Process variables can be both tuned and optimised, and technologies can be compared in a rigorous way, especially by including energy aspects in the computations [1.79]. However, scarce literature has been found dealing with the development of a plant-wide energy model including new technologies for treating UWW at full-scale, such as membrane ones.

Some software in the field of wastewater engineering have included the analysis of process water management and sludge treatment, (e.g. BioWin, gPROMS, Simba6 etc.). For instance, BioWin is a wastewater treatment process simulator that ties together biological, chemical, and physical process models. BioWin is used world-wide to design, upgrade, and optimise wastewater treatment plants of all types. The core of BioWin is the proprietary biological model which is supplemented with other process models (e.g. water chemistry models for calculation of pH, mass transfer models for oxygen modelling and other gas-liquid interactions). Descoins *et al.* [1.79] developed a plant-wide model, implemented in the modelling software gPROMS, including the main biochemical transformations. Pijájová and Derco [1.87] assessed the performance of UWW treatment systems using the simulator SIMBA 6. These softwares have already included not only the analysis of process water management and sludge treatment, but also the assessment of energy consumption and efficiency.

However, these modelling softwares do not include new promising technologies aimed at enhancing wastewater treatment, such as aerobic and anaerobic membrane bioreactor (MBR and AnMBR, respectively). In this respect, Ferrer *et al.* [1.80] proposed a computational software called DESASS for designing, simulating and optimising both aerobic and anaerobic UWW treatment technologies, which was later updated for including new technologies such as SHARON, BABE, MBR and AnMBR. The updated-version of this software incorporates the biological nutrient removal model 2 (BNRM2) [1.88]. Durán [1.89] calibrated and validated this mathematical model across a wide range of operating conditions in an AnMBR system featuring industrial-scale membranes. However, a detailed and comprehensive plant-wide model for assessing the energy demand, economic and environmental impact of different wastewater treatment systems (beyond CAS system) needs to be developed.

1.2.2 Sensitivity and uncertainty analysis in urban wastewater treatment modelling

As mentioned before, WWTP models are used for many applications/purposes including plant design, optimisation and control. However, the model predictions are not free from uncertainty as these models are an approximation of reality (abstraction), and are typically built on a considerable number of assumptions [1.90].

Uncertainty analysis can be defined as a random variability in some parameter or measurable quantity and it is performed to estimate the uncertainty in the final results. The identification, evaluation and comparison of uncertainties are important since they provide a deeper insight into the risk analysis, add credibility in the results, and aid in the decision making process. Monte-Carlo procedure is commonly used for uncertainty analysis, by using randomised variables and analysing the trends in the output data [1.91]. A widely used example of Monte Carlo simulation is Latin hypercube sampling (LHS). The stratified sampling approach of LHS ensures that the resulting sample designs are non-collapsing and generally more space-filling than simple random sampling [1.92].

Sensitivity analysis determine which input parameters are found to have significantly high effects on the outputs and therefore are mainly responsible for their variance. The Morris screening method is commonly used for the sensitivity analysis. The Morris screening method [1.93] consists in obtaining a given number of representative matrixes of input combinations using an efficient random sampling strategy. This method is characterised by being a reliable alternative method for factors prioritisation purposes, which is also computationally efficient [1.93; 1.94; 1.95]

1.3 Energy balance in urban wastewater treatment

Nowadays, wastewater treatment is an energy-intensive activity whose energy costs vary considerably from one WWTP to another depending on the type of influent, treatment technology and required effluent quality. Specifically, some studies indicate that bioreactor aeration could account for up to 60%

of total WWTP energy consumption [1.96; 1.97]. Therefore, it is particularly important to implement new energy-saving technologies that reduce the overall WWTP carbon footprint and improve environmental sustainability [1.98; 1.99]. According to previous studies [1.58; 1.100; 1.101], optimising the energy balance of a WWTP is a key point in its overall environmental performance.

Figure 1.9 shows the energy consumption of the major elements involved in the urban water cycle and treatment processes [1.102]. As Figure 1.9 shows, wastewater treatment is estimated to represent roughly 1% of total electricity demand. With an estimated electricity consumption of 0.9-3.9 kWh per m^3 of wastewater treated [1.2], this energy demand equates to roughly 6-25 tonnes of CO_2 emitted per day by a WWTP treating 50000 $m^3 \cdot d^{-1}$ (assuming the 2012 Spanish electricity mix). In addition, these high levels of electricity consumption inflate operating costs and incur a diverse set of life cycle environmental impacts stemming from electricity production processes.

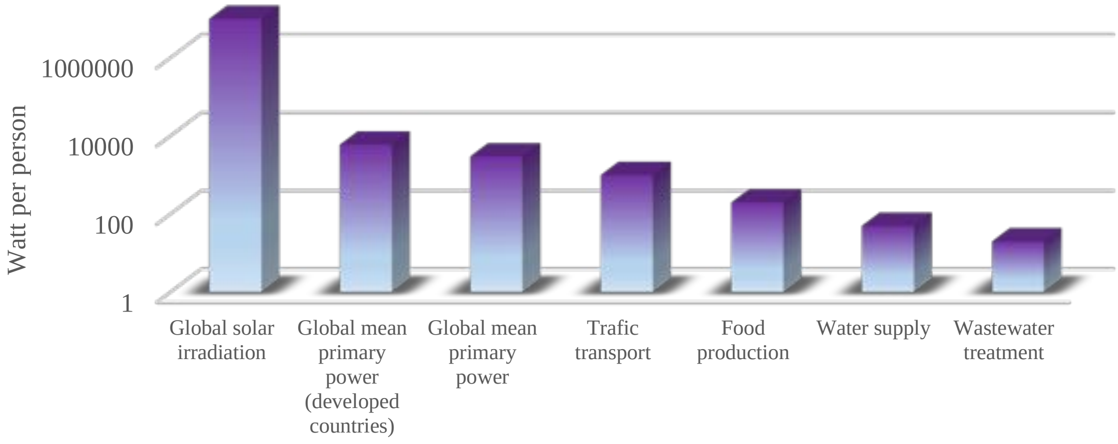

Figure 1.9 Global primary power consumption of the major elements involved in the urban water cycle and treatment processes.

Therefore, it is important to point out that energy self-sufficiency wastewater treatment should be taken into account as a component of a global water management strategy. In this respect, one primary objective should be improving wastewater treatment performance, followed by choosing the best available technologies for enhanced the best use of sludge for energy production and recovery. To be more attractive, efficient energy recovery technologies must be cost-effective, reliable, easy to operate, and should have no adverse impacts on water quality or environment.

There is an increasing need for large WWTPs to generate as much electricity as possible from biogas, which not only ensures significant operational cost savings, but also improves the environmental profile of the plant [1.103]. The expansion of renewable energies is viewed to be an important factor for a secure energy future [1.104]. Furthermore, biogas offers greater energy and environmental benefits when generating both power and heat simultaneously using combined heat and power (CHP) technology than when generating both separately [1.105].

Figure 1.10 illustrates two examples of energy balance [1.106; 1.107]. In both cases the treatment processes are the same, including primary settling, conventional activated sludge process (nitrification/ denitrification), anaerobic sludge stabilisation, and use of biogas for energy purposes. The main assumptions are the following: COD loads of 48 and 42 kg·(cap.yr)$^{-1}$, methane production of 0.35 L_{CH4}·g^{-1} COD, and methane energy potential of 10 kWh·m^{-3}. Despite the slightly more concentrated wastewater used in the first example, the energy balance is quite similar: 57% is transferred to the digester and only 26% is transferred into methane. Using the same conversion efficiency of 32 %, only 9% of the embodied chemical energy is recovered as electricity.

The most promising technology for recovering the chemically-bound energy in wastewater is AD. Maximising the energy gain from each of the potential sources of energy saving and generation would allow WWTPs (particularly the largest ones) to recover and eventually to generate all the energy needed for plant operation, and even yield and energy surplus at times. Hence, the unlocking and enhanced reuse of energy contained in wastewater is a key tool in solving the water-energy nexus.

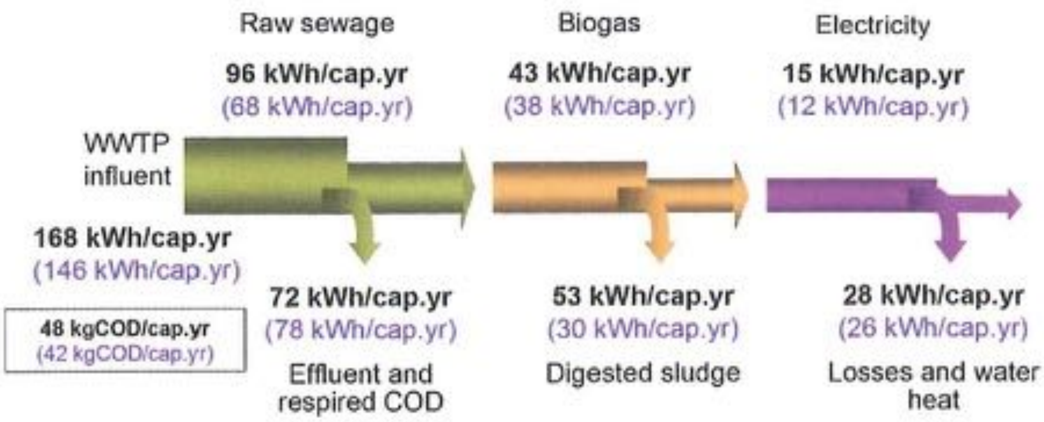

Figure 1.10 Energy COD balance for typical WWTPs (extracted by Cornel *et al.* [1.106] and Lazarova *et al.*, [1.107]).

In compliance with GWRC [1.108], WWTPs have the potential to become environmental platforms, and provide an energy source for tomorrow's eco-cities as part of a system characterised by the smallest possible ecological footprint.

1.3.1 Typical energy consumption and associated cost of the main technologies involved in urban wastewater treatment

Table 1.1 shows the typical energy consumption of different technologies involved in the UWW treatment, considering preliminary treatment, CAS, high rate activated sludge (HRAS), MBR and AnMBR technologies. According to Judd and Judd [1.2], the full-scale aerobic MBR in Nordkanal (Germany) and Immingham Docks (United Kingdom) had a specific energy demand of 0.9 and 3.9 kWh·m^{-3}, respectively. On the other hand, CAS and MBR in Schilde (Belgium) consumed 0.19 and 0.64 kWh·m^{-3}, respectively [1.21]. AnMBR and high rate activated sludge (HRAS) system consumed from -0.15 to 0.21 kWh·m^{-3} and from -0.08 to 0.13 kWh·m^{-3}, respectively [1.20]. Nevertheless, it is important to note that AnMBR energy demand does not include the energy needed to remove nutrients unlike the rest of wastewater treatment systems. Moreover, the results obtained in each case study strongly depend on influent wastewater characteristics and evaluated operating conditions.

Table 1.1 Typical energy consumption of different technologies involved in the UWW treatment.

Operation	Energy consumption (kWh m^{-3})	References
Preliminary treatment	0.16 – 0.30	[1.102]
CAS	0.19	[1.21]
	0.3 – 1.4	[1.102]
HRAS	-0.079 – 0.13	[1.20]
MBR	0.9 – 3.9	[1.2]
	0.5 – 2.5	[1.102]
	0.64	[1.21]
	0.438	[1.109]
	0.9	[1.110]
	0.7 – 1.070	[1.72]
	6.06	[1.111]
AnMBR	-0.15 – 0.21	[1.20]

Table **1.2** shows the energy consumption of different MBRs for UWW treatment. As shown in

Table **1.2**, most of the energy consumed in aerobic MBR systems is due to air scouring of the membrane module (up to 75%).

Table 1.2 Energy consumption of different MBR involved in the UWW treatment: *MBRs of Schilde* [1.21], *Immingham Docks* [1.2], *Nordkanal* [1.2], *BSM-MBR* [1.110]; *MBR optimised* [1.109]; *two MBR from Verrecht et al.* [1.72]; *and Kubota MBR pilot* [1.111].

Energy Consumption kWh m^{-3}	Schilde	Immingham Docks	Nordkanal	BSM-MBR	Optimised MBR	1º MBR [1.72]	2º MBR [1.72]	Kubota MBR pilot
Mixing	0.047	---	0.104	0.030	0.040	0.021	0.043	1.350
Sludge recycling pumping	0.102	---	0.001	0.050	0.016	0.077	0.182	0.650
Pumping effluent	0.074	---	0.024	0.070	0.010	0.007	0.021	0.500
Bioreactor aeration	0.067	1.000	0.109	0.210	0.006	0.077	0.246	0.500
Membrane aeration	0.225	2.900	0.441	0.530	0.320	0.518	0.578	2.450
Rest *(sludge dewatering, pre-treatment, pumping station...)*	0.124	---	0.221	---	0.046	---	---	0.610
Total	0.640	3.900	0.900	0.900	0.438	0.700	1.070	6.060

Figure 1.11 shows the energy flow diagram of an aerobic MBR process extracted from Krause & Dickerson [1.109]. As shown in Figure 1.11, in particular, 73% of the energy is consumed in air sparging for membrane scouring and 10% of the energy is consumed by the mixing system energy.

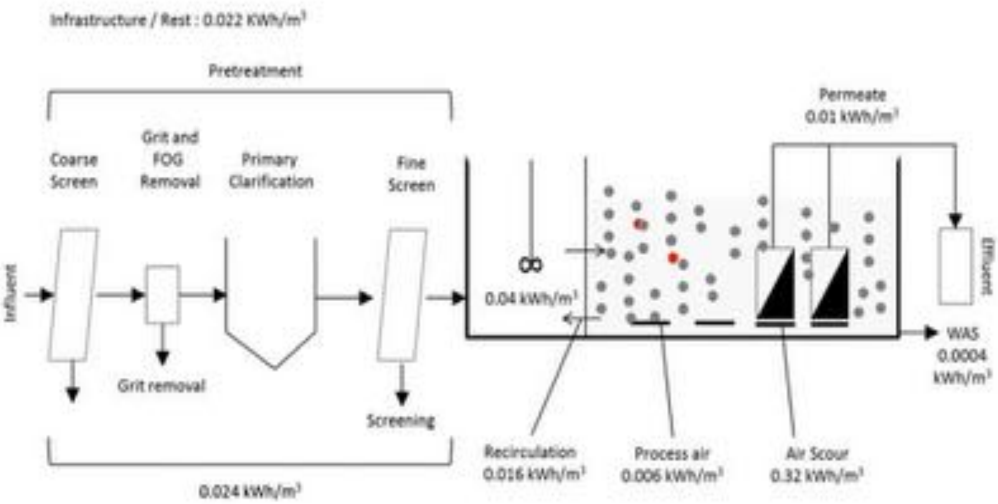

Figure 1.11 Energy demand for an aerobic MBR process (extracted from Krause & Dickerson, [1.109]).

As mentioned before, given the early stage of development and uncertainties around AnMBR performance, further research is needed for improving the net energy balance and the energy cost of AnMBR technology.

In order to determine the life cycle cost (LCC) of any wastewater treatment system, all costs should be converted to uniform annual cost. Capital costs are normally calculated assuming a given discount rate and project lifetime [1.20; 1.112]. Annual operating and maintenance (O&M) costs are estimated based on energy and reagent consumption, energy recovery from methane capture, sludge handling and disposal, and replacement of the required equipment [1.8; 1.20]. Table 1.3 shows the operating costs of two different AnMBR systems extracted from Lin *et al.* [1.8] and Smith *et al.* [1.20]. Lin *et al.* [1.8] assessed the total cost in a laboratory-scale AnMBR system and showed that membrane costs and membrane scouring energy accounted for the largest fraction of total life cycle capital costs and operational costs, respectively. It is important to highlight that energy recovery was not included in this study. Nevertheless, it was stated that the operating costs can be totally offset by the benefits from biogas recovery. On the other hand, Smith *et al.* [1.20] assessed the total cost in an AnMBR system when treating medium and high strength wastewater and accounted for a total of €0.124 per m^3. In addition, energy recovery increased by 60% and 130% of the total energy consumption for AnMBR system in medium and high strength wastewater.

Table 1.3 Operating cost of two AnMBR systems.

Operating cost, €·m^{-3}	Energy consumption	Sludge disposal/chemical consumption and others	Total
Lin *et al.,* 2011	0.015	0.010	0.025
Smith *et al.,* 2014	----	----	0.124

1.3.2 Bernoulli principle and hydraulic equations

Bernoulli principle can be derived from the principle of conservation of energy. This states that, in a steady flow, the sum of all forms of energy in a fluid along a streamline is the same at all points on that streamline. This requires that the sum of kinetic energy, potential energy and internal energy remains constant. The Bernoulli principle is therefore expressed by the following equation (Eq. 1.1):

$$\frac{P_1}{\gamma} + \frac{V_1}{2g} + Z_1 + H_m = \frac{P_2}{\gamma} + \frac{V_2}{2g} + Z_2 + \Delta h \qquad \textbf{(Eq. 1.1)}$$

where $\frac{P}{\gamma}$ (m) is the pressure term, $\frac{v}{2g}$ (m) is the kinetic energy term, *Z* (m) is the height term, *Hm* (m) is the pump impulsion height and Δh (m) is the linear and accidental pressure drops.

If kinetic energy terms are considered negligible and the pressure term in both sides is equal, Eq. 1.1 can be expressed as follows (Eq. 1.2):

$$H_m = \Delta Z + \Delta h \qquad \textbf{(Eq. 1.2)}$$

where *Hm* (m) is the pump impulsion height, ΔZ (m) is the difference in height and Δh (m) is the linear and accidental pressure drops.

For calculating the linear pressure drops (*Hf*), the equation of Darcy Weisbach can be employed (Eq. 1.3):

$$Hf = \frac{L \cdot f \cdot V^2}{2 \cdot g \cdot D} \qquad \textbf{(Eq. 1.3)}$$

where H_f (m) is the linear pressure drops, *L* (m) is the pipe length, f is the friction factor, *V* ($m \cdot s^{-1}$) is the fluid velocity, *D* (m) is the pipe diameter and *g* ($m \cdot s^{-1}$) is the acceleration of gravity.

The friction factor (*f*) can be calculated by means of Colebrook equation (Eq. 1.4):

$$\frac{1}{\sqrt{f}} = -2 \cdot \log\left(\frac{\varepsilon/1000}{3.7 \cdot D(m)} + \frac{2.51}{Re \cdot \sqrt{f}}\right) \qquad \textbf{(Eq. 1.4)}$$

where *f* is the friction factor, *Re* is the Reynolds number, μ ($m^2 \cdot s^{-1}$) is the fluid viscosity, $\mathcal{E}$ (mm) is the pipe roughness and *D* (m) is the pipe diameter.

For calculating the accidental pressure drops (*Hp*), the following equation can be employed Eq. 1.5:

$$Hp = k\,\frac{V^2}{2\cdot g} \tag{Eq. 1.5}$$

where *Hp* (m) is the accidental pressure drops, *K* is coefficient of friction pressure, *V* ($m\cdot s^{-1}$) is the velocity flow and *g* ($m\cdot s^{-1}$) is the acceleration of gravity.

Judd and Judd [1.2] proposed the following equations in order to calculate the energy requirements of pumps and blowers in MBR technology (see Eq. 1.6; Eq. 1.7; Eq. 1.8):

Blower power requirements:

$$P_B = \frac{(\mathrm{M}\cdot\mathrm{R}\cdot\mathrm{T_{gas}})}{(\alpha-1)\cdot\eta_{blower}}\left[\left(\frac{p_2}{p_1}\right)^{\frac{\alpha-1}{\alpha}}-1\right] \tag{Eq. 1.6}$$

where P_B ($J\cdot s^{-1}$) is the blower power requirement (adiabatic compression), *M* ($mol\cdot s^{-1}$) is the molar flow rate of biogas, *R* ($J\cdot mol^{-1}\cdot K^{-1}$) is the gas constant for biogas, P_1 (atm) is the absolute inlet pressure, P_2 (atm) is the absolute outlet pressure, T_{gas} (K) is the biogas temperature, α is the adiabatic index and η_{blower} is the blower efficiency.

Sludge pumping power requirements:

$$P_s = \frac{\rho\cdot g\cdot Q\cdot \mathrm{Hm}}{\eta_{pump}} \tag{Eq. 1.7}$$

where P_s ($J\cdot s^{-1}$) is the sludge pumping power requirement, *Q* ($m^3\cdot s^{-1}$) is the volumetric flow rate, *ρ* ($kg\cdot m^{-3}$) is the liquor density, *g* ($m\cdot s^{-1}$) is the acceleration of gravity, Hm (m) is the pump height impulsion and pump efficiency (η_{pump}).

Permeate pumping power requirements:

$$P_{permeate} = \frac{\mathrm{q_{stage}}\cdot \mathrm{TMP_{stage}}}{\eta_{pump}} \tag{Eq. 1.8}$$

where $P_{permeate}$ ($J\cdot s^{-1}$) is the power requirement during filtration, degasification or back-flushing calculated from transmembrane pressure (TMP_{stage} in Pa), pump volumetric flow rate (q_{stage} in $m^3\cdot s^{-1}$) and pump efficiency (η_{pump}).

1.3.3 CHP system for energy production

According to EPA [1.105], CHP is the sequential or simultaneous generation of multiple forms of useful energy (usually mechanical and thermal) in a single, integrated system. CHP systems consist of a number of individual components (prime mover (heat engine), generator, heat recovery, and electrical interconnection) configured into an integrated whole. Prime movers for CHP systems include steam turbines, gas turbines (also called combustion turbines), spark ignition engines, diesel engines, microturbines and fuel cells. These prime movers are capable of burning a variety of fuels, including biomass/biogas, natural gas, or coal to produce shaft power or mechanical energy.

CHP offers energy and environmental benefits over electric-only and thermal-only energy generation systems in both central and distributed power generation applications. CHP systems can be potentially used in a wide range of applications and their high energy generation efficiencies result in lower emissions than separate heat and power generation systems (SHP). The advantages of CHP broadly include the following [1.105]:

- The simultaneous production of useful thermal and electrical energy in CHP systems lead to increased fuel efficiency.
- CHP units can be strategically located at the point of energy use. Such onsite generation avoids the transmission and distribution losses associated with electricity purchased via the grid from central stations.
- CHP is versatile and can be coupled with existing and planned technologies for many different applications in the industrial, commercial, and residential sectors.

Figure 1.12 shows the efficiency advantage of CHP compared with conventional central station power generation and onsite boilers. When considering both thermal and electrical processes together, CHP typically requires only three quarters the primary energy SHP systems require. CHP systems utilise less fuel than separate heat and power generation, resulting for same level of output in fewer GHG emissions [1.105].

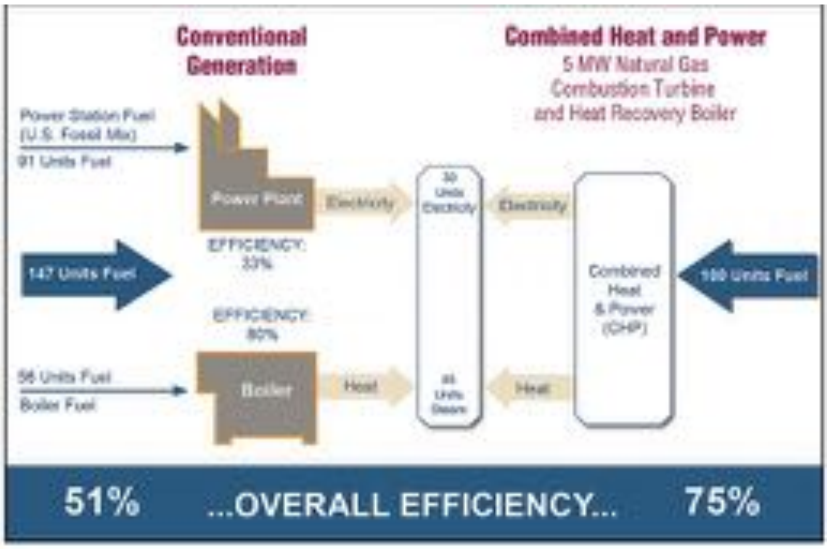

Figure 1.12 Overall efficiency of combined heat and power (CHP) versus separate heat and power (SHP) production [1.105].

Table 1.4 shows the efficiency of different CHP technologies according to the catalogue of CHP biomass provided by the EPA, [1.113].

Table 1.4 Efficiency of different CHP system [1.113].

	Power efficiency, %	Heat efficiency, %	Overall efficiency, %
Steam turbine	26.5	53.5	80
Reciprocating IC Engine	33.4	40.2	73.6
Gas/combustion Turbine	30.4	39.6	70
Microturbine	27	33.5	60.5

A synopsis of the key characteristics of each CHP systems (steam turbines, gas turbines/combustion, microturbines, reciprocating internal combustion (IC) engines, fuel cells and stirling engines) is shown in Table 1.5, including their ability to run on biomass or biogas.

Table 1.5 Comparison of Prime Mover Technologies Applicable to Biomass [1.113]

	Prime Mover					
Characteristic	**Steam Turbine**	**Gas/ Combustion Turbine**	**Microturbine**	**Reciprocating IC Engine**	**Fuel Cell**	**Stirling Engine**
Size	50 kW to 250 MW	500 kW to 40 MW	30 kW to 250 kW	Smaller than 5 MW	Smaller than 1 MW	Smaller than 200 kW
Fuels	Biomass/ Biogas fuelled boiler for steam	Biogas	Biogas	Biogas	Biogas	Biomass or Biogas
Fuel preparation	None	PM filter needed	PM filter needed	PM filter needed	Sulphur, CO, methane can be issues	None
Sensitivity to fuel moisture	N/A	yes	yes	YES	yes	No
Electric efficiency (electric, HHV)*	5 to 30%	22 to 36%	22 to 30%	22 to 45%	30 to 63%	5 to 45%
Turn-down ratio	Fair, responds within minutes	Good, responds within a minute	Good, responds quickly	Wide range, responds within seconds	Wide range, slow to respond (minutes)	Wide range, responds within a minute
Operating issues	High reliability, slow start-up, long life, maintenance infrastructure readily available,	High reliability, high-grade heat available, no cooling required, requires gas compressor, maintenance infrastructure readily available	Fast start-up, requires fuel gas compressor	Fast start-up, good load following, must be cooled when CHP heat is not used, maintenance infrastructure readily available, noisy	Low durability, low noise	Low noise
Field experience	Extensive	Extensive	Extensive	Extensive	Some	Limited
Commercialisation status	Numerous models available	Numerous models available	Limited models available	Numerous models available	Commercial introduction and demonstration	Commercial introduction and demonstration
Installed cost (as CHP system)	$350 to $750/kW (without boiler)	~ $700 to $2,000/kW	$1,100 to $2,000/kW	$800 to $1,500/kW	$3,000 to $5,000 /kW	Variable $1,000 to $10,000 /kW
Operations and maintenance (O&M) costs	Less than 0.4 ¢/kWh	0.6 to 1.1 ¢/kWh	0.8 to 2.0 ¢/kWh	0.8 to 2.5 ¢/kWh	1 to 4 ¢/kWh	Around 1 ¢/kWh

**Efficiency calculations are based on the higher heating value (HHV) of the fuel, which includes the heat of vaporisation of the water in the reaction products.*

1.3.4 Technologies for capturing dissolved methane

Scarce research can be found related to methane solubility in AnMBRs [1.38; 1.39; 1.114] and even fewer regarding the quantification of methane dissolved in AnMBR effluent [1.30; 1.52; 1.115]. Some studies reported that around 50 and 54% of the methane generated in an AnMBR system remained in the liquid phase when operating at 15 ºC [1.115] and 20 ºC [1.52], respectively. On the other hand, Kim *et al.* [1.30] observed that 30% of the generated methane left the system through the liquid phase when operating at 35 ºC. This highlights the important role that temperature has in methane solubility and direct methane recovery [1.53].

Future research efforts should focus on increasing the likelihood of net energy recovery through the development of efficient methods for dissolved methane recovery. Different processes have been reported in recent literature aimed at preventing methane emission:

Stripping of AnMBR effluent through post-treatment aeration:

Methane stripping with air is the process by which dissolved methane is removed from a liquid by physical transfer of methane into air by bubbling air through leachate containing dissolved methane [1.66]. According to McCarty *et al.* [1.5], the energy consumption for stripping the methane contained in an AnMBR effluent through post-treatment aeration is estimated to be less than 0.05 kWh·m^{-3} [1.5]. However, according to Smith [1.66], energy recovery from the resulting mixture of methane and air has not been attempted yet. Foreseeable complications with this practice include the dilution of methane with air and potential explosion hazards resulting from a methane and oxygen rich off-gas. Furthermore, the efficiency of this practice for removing dissolved methane from AnMBR effluent is not well established.

Degassing membrane (DM) for methane recovery:

According to Smith *et al.* [1.66], the use of degassing membranes represents a more controlled approach by which methane is recovered from AnMBR effluent but not diluted with air. In a recent study by Bandara *et al*. [1.116], the dissolved methane in the effluent from an UASB reactor was recovered using a hollow-fibre degassing membrane (DM) module and quantified at 35, 25 and 15 ºC. The system was particularly effective when operating at low temperature (15 ºC), reaching a methane recovery efficiency of 90%. Therefore, DM can be a promising technology for improving methane recovery in low-strength wastewater treatment at low temperature. However, this technology needs further investigation since from an economic point of view, energy requirements associated to DM technology must be substantially reduced.

According to DIC Corporation [1.117], DM removes gases dissolved in liquids through a tube-shaped gas permeable membrane made of polytetrafluoroethylene (PTFE). Specifically, gases dissolved in the liquid flowing through the tube are removed by the pressure difference between the gases inside and outside the tube, which is created by a vacuum on the outside of the tube as shown in Figure 1.13.

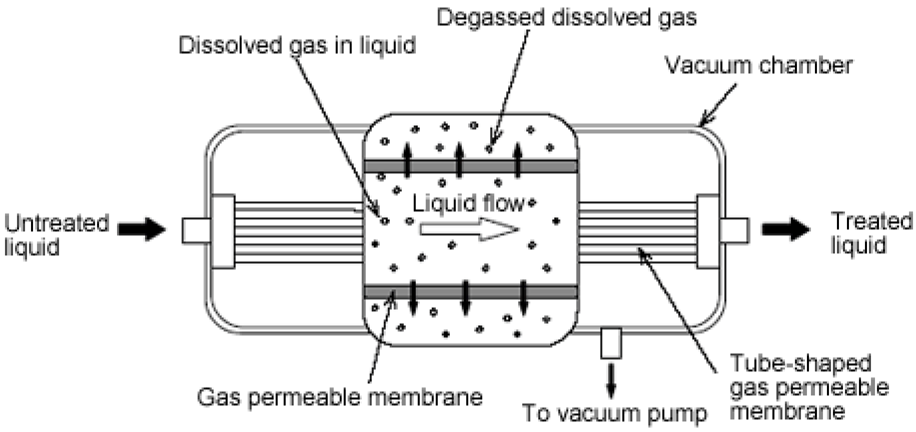

Figure 1.13 Schematic diagram of a degassing membrane [1.117].

<u>*Down-flow hanging sponge (DHS) reactor:*</u>

Hatamoto *et al.* [1.118] evaluated a down-flow hanging sponge (DHS) reactor in order to oxidise dissolved methane biologically (see Figure 1.14). Methane-oxidising bacterial communities such as Methanotrophs species are considered important species for dissolved methane oxidation, since they are able to oxidise up to 95% of the dissolved methane in the effluent. However, as the dissolved methane is oxidised, methane cannot be recovered for energy production. Moreover, further studies are needed to determine the appropriate configuration and operating conditions in DHS reactors to achieve reductions in GHG emissions.

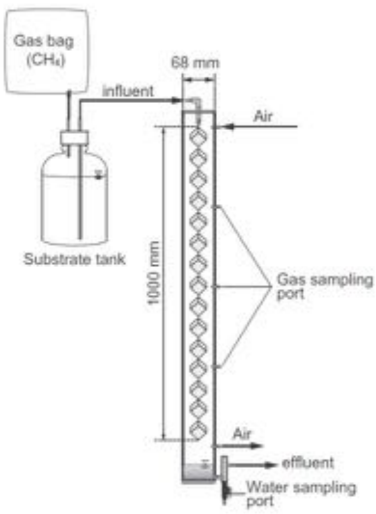

Figure 1.14 Schematic diagram of a closed DHS reactor [1.118].

1.4 Life cycle assessment (LCA)

1.4.1 Background

Life cycle assessment (LCA) is a core topic in the field of environmental management. Its history goes back to the early seventies, known by different names such as resource and environmental profile analysis (REPA), energy analysis or product eco balance. The first examples of environmental assessments of products were carried out on packaging, which were published at the end of the 1960s and the beginning 1970s in the USA. These studies primarily focussed on energy and resource requirements of waste [1.119]. In the 1980s, several European countries used LCA to compare beverage packagings [1.120]. Since then, interest in LCA has strongly grown, and a growing number of different and increasingly complex products and systems have been successfully assessed.

Three international bodies have been concerned with the development and application of LCA: SETAC (the society of environmental toxicology and chemistry), ISO (International organisation for standardisation) and UNEP (United Nations Environment Program).

- SETAC was the first international body to act as an organisation for the development of LCA. SETAC's involvement with LCA dates from 1989.
- ISO is a world-wide federation of national standards bodies from both industrialised and developing countries, which aims to standardise a wide range of products and activities. ISO has standardised this framework within the series ISO 14040 on LCA. This second edition of ISO 14040, together with ISO 14011:2006, cancels and replaces ISO 14040:1997, ISO 14041:1998, ISO 14042:2000 and ISO 14043:2000, which have been technically revised (ISO 14040,2006).
- UNEP is the third international body in the field of LCA, represented by its department of technology, industry and economics in Paris.

In 2002, the UNEP and SETAC launched an International Life Cycle Partnership (known as the Life Cycle Initiative) in order to enable users around the world to put life cycle thinking into effective practice.

Different definitions of LCA have been stablished according with the three international bodies mentioned before (i.e. SETAC, ISO and UNEP):

- *Objective process to evaluate the environmental burdens associated with a product, process, or activity by identifying energy and materials used and wastes and emissions released to the environment, and to evaluate opportunities to achieve environmental improvements* [1.121].
- *Compilation and evaluation of inputs, outputs and the potential environmental impacts of a product (good or service) system throughout its life cycle, from the extraction of raw material to product disposal* [1.122].
- *Tool for the systematic evaluation of the environmental aspects of a product or service system through all stages of its life cycle. LCA provides an adequate instrument for environmental decision support. Reliable LCA performance is crucial to achieve a life-cycle economy* [1.123].

According to SETAC [1.124] the prime objectives of carrying out a LCA are:

- Providing a picture as complete as possible of the interactions of an activity with the environment.
- Contributing to the understanding of the overall and interdependent nature of the environmental consequences of human activities.
- Providing decision-makers with information which defines the environmental effects of these activities and identifies opportunities for environmental improvements.

1.4.2 Phases in an LCA study

There are four phases in an LCA study (ISO 14040, [1.122]) (see Figure 1.15):

a) Goal and scope definition phase (described in ISO 14041)
b) Inventory analysis phase (described in ISO 14041)
c) Impact assessment phase (described in ISO 14042)
d) Interpretation phase (described in ISO 14043)

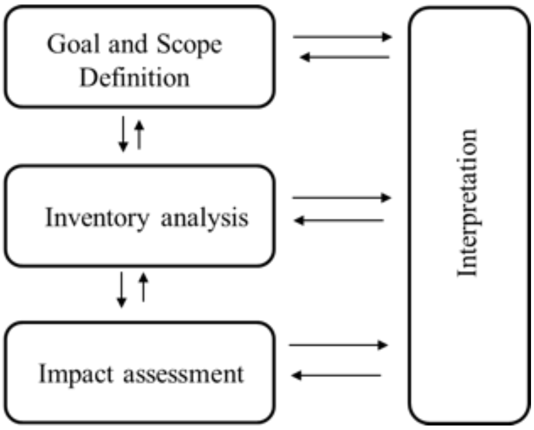

Figure 1.15 The four phases in an LCA study.

a) Goal and scope definition phase

The definition of the activity, purpose of the study, functional unit, boundaries system and methodology are established in this phase. The scope of an LCA depends on the subject and the intended use of the study. The depth and the breadth of LCA can differ considerably depending on the goal of a particular LCA.

- Functional unit (FU): Quantified performance of a product system for use as a reference unit (ISO 14044: 2006E).
- Reference flow: measure of the outputs from processes in a given product system required to fulfil the function expressed by the functional unit.
- System boundaries: All the unit processes that should be accounted for and for which data should be collected. The complete life cycle of a product should be included in the system boundaries, from cradle to grave (cradle-to-grave LCA). However, often only a part of the chain is covered, mostly the life cycle phases up until the factory gate (cradle-to-gate LCA) in which the use and disposal phases (end-of-life) are not included.
- Life cycle impact assessment (LCIA) Methodology: Researchers have discussed the most appropriate number and representation of impact categories and the best available methodologies in various public and literature forums [1.125; 1.126]. Recent methodologies include stressors and impact categories that were not included within environmental regulations but were assumed to be of interest to society. Despite the number of existing LCIA methodologies, there is no worldwide consensus nowadays on either the list of impact categories for inclusion or the associated methodologies for use in LCIA [1.126]. The ISO standard allows the use of impact categories indicators that are somewhere between the inventory result (i.e. emission) and the "endpoint". Indicators that are chosen between the inventory results and the "endpoints" are

sometimes referred to as indicators at “midpoint level”. Some of the methodologies used in LCA are shown in Table 1.6.

Table 1.6 LCA methodologies [1.127]

Method	Characteristics
Impact 2002+	Damage approach; many similarities with Eco-indicator 99, but completely recalculated toxicity factors
TRACI 2002	Midpoint method developed by US EPA
CML 2 baseline 2000	Update of the 1992 method, more advanced models, and inclusion of fate analysis
EPS 2000	Damage approach; using monetarisation (willingness to pay) instead of weighting by a panel
Eco-indicator 99	Damage approach, uses category indicators at endpoint level. Three versions are included using different assumptions
Ecopoints 97 (UBP)	Distance to target based on Swiss policy targets (also referred to as Ecoscarcity method or UBP
EDIP/UMIP 97	Characterisation and Normalisation method developed for the Danish EPA

b) Inventory analysis phase

The life cycle inventory (LCI) phase is the second phase of LCA. It is an inventory of inputs (such as materials and energy) and outputs (such as (by) products, wastes and emissions) that occurs and are used during the life cycle. It involves the collection of the data necessary to meet the goals of the defined study.

Depending on the available time and budget, there are a number of strategies to collect such data. It is useful to distinguish two types of data:

- Foreground data: refers to very specific data. It typically includes data that describes a particular product system and production system.
- Background data: refers to generic data of materials, energy, transport and waste management systems. It typically includes data found in database and literature.

c) Impact assessment phase

The life cycle impact assessment (LCIA) phase is the third phase of the LCA. The purpose of LCIA is to provide additional information to help assessing a product system's LCI results so as to better understand their environmental significance. This phase is aimed at evaluating the environmental impacts of the environmental resources and releases identified during the LCI, comprising obligatory elements (such as selection, classification, and characterisation) and optional elements (such as normalisation, ranking, grouping and weighting).

- *Selection*

An adequate selection of appropriate impact categories must be conducted. The choice is guided by the goal of the study. An important help in the process of selecting impact categories is the definition of the so-called endpoints. According to ISO, endpoint is understood as issues of environmental concern, like human health, extinction of species, availability of resources for future generation, etc. Depending on the methodology used (i.e. tool for the reduction and assessment of chemical and other environmental impacts such as TRACI, CML 2 baseline 2000 or Ecoindicator 99), different impact categories are selected:

- TRACI is a midpoint oriented LCIA method including the following impact categories: Global Warming Potential (GWP) (CO_2-eq), Acidification (H^+-eq), Photochemical Oxidation (smog) NOx-eq), Human Health: Carcinogenics (benzene-eq), Human Health: Non Carcinogenics (toluene eq), Human Health: criteria air pollutants (PM 2,5-eq), Eutrophication (N-eq), Ozone Depletion (CFC^{-11}-eq), Ecotoxicity and Smog (NOx-eq), Fossil Fuel Depletion, Land Use and Water Use.
- CML 2 baseline 2000 is a midpoint oriented LCIA method including the following impact categories: Ozone Layer Depletion (kgCFC^{-11}-eq), Abiotic Depletion (kg Sb-eq), Global Warming Potential (kg CO_2-eq), Acidification (kgSO_2 eq), Eutrophication (kgPO_4-eq), Human Toxicity (Kg 1,4 DB-eq), Marine Aquatic Ecotoxicity (Kg 1,4 DB-eq), Terrestrial Ecotoxicity (Kg 1,4 DB-eq), Photochemical Oxidation (kg C_2H_4-eq) and Fresh Water Aquatic Ecotoxicity (Kg 1,4 DB-eq).
- Eco-indicator 99 is a endpoint oriented LCIA method including the following impact categories: Human Health (expressed as DALY: disability adjusted life years): Climate Change, Ozone Layer Depletion, Carcinogenic Substances, Respiratory Effects (organic and inorganic) and ionizing radiation; Ecosystem Quality (expressed as PDF: potential disappeared fraction): Land Use, Acidification/ Eutrophication, and Ecotoxicity; Resources (expressed as MJ surplus energy): Depletion of Fossil Fuel and Depletion of Minerals.

- Classification

The inventory results of an LCA contain hundreds of different emissions and resource extraction parameters. Once the relevant impact categories are determined, the resources and emissions determined during the inventory process (LCI) are classified into environmental impact categories.

- Characterisation

Once the impact categories are defined and the LCI are assigned to these impact categories, it is necessary to define characterisation factors. These factors should reflect the effect of an input or output in a respective environmental impact category.

- Normalisation:

Normalisation is conducted in order to express all category indicators in a single unit. For each baseline indicator, normalisation scores are calculated for the reference situations: the world in 1990, Europe in 1995 or the Netherlands in 1997. The normalised result for a given impact category and region is obtained by multiplying the characterisation factors by their respective emissions. The sum of these products in every impact category gives the normalisation factor.

- Grouping and ranking

In order to avoid weighting whilst making results easier to interpret, impact category indicators may be grouped and ranked.

- Weighting

Weighting quantifies the relative significance of each indicator within the goal and scope of the assessment so that the environmental impact categories of highest importance receive higher attention. An interesting method was developed by Hofstetter, *et al.* [1.128], which used a missing triangle (see Figure 1.16).

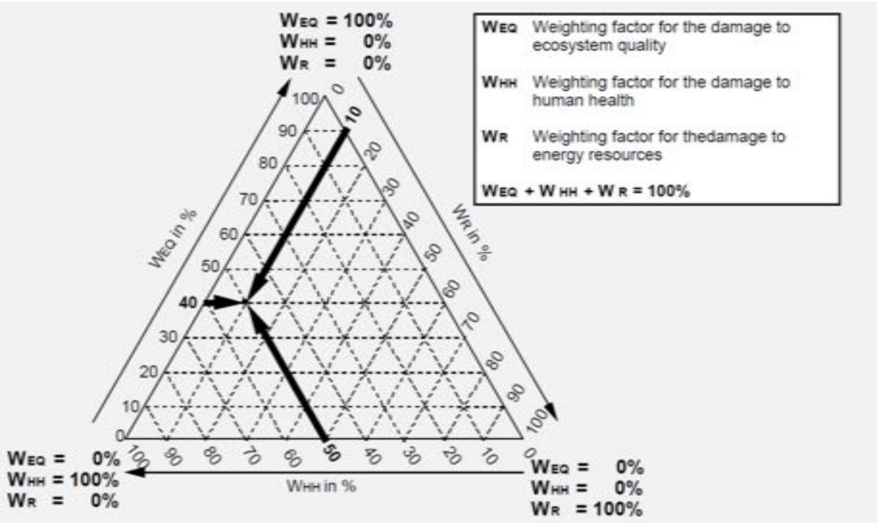

Figure 1.16 The mixing triangle (based on Hofstetter *et al.* [1.128]).

d) Interpretation phase

The fourth phase in life cycle assessment is to interpret the results of LCIA as a basis for conclusions, recommendations and decision-making in accordance with the goal and scope definition.

1.4.3 Software tools for general LCA studies

Due to the large amount of data required to perform an LCA it is recommended to use a software tool which facilitates the efficient undertaking of a study. Currently, there are different softwares available in the market which allow conducting LCA studies in different degrees of detail (see Table 1.7).

As regards Table 1.7, SimaPro can be considered the leading LCA tool, which includes many LCI datasets, including the renowned Ecoinvent v3.1 database, the new industry-specific agri-footprint database, and the ELCD database. The methodology of SimaPro is consistent and transparent across the different stages of your LCA. SimaPro is a LCA software used by industry, consultancies, universities and research institutes in more than 80 countries. The characteristics of the software are the following (in compliance with Pré consultants, [1.129]):

- Wide applicability like carbon and water footprint.
- All-in-one package. Various LCI data libraries included at no additional cost.
- Updated frequently with new data.
- Mid-point and end-point impact assessment methods available for various purposes.
- Highly transparent results due to interactive results analysis.
- Accurate and fast calculation engine.
- Flexible and easy to model complex life cycles.
- Multi-user versions available.
- Easily connection with other tools through the COM interface.

Table 1.7 Software programs for general LCA studies [1.127]

Software	Development Company	Comments
Boustead	Boustead Consulting (UK)	Very complete tool suitable for LCA studies in the Steel, Chemical and Plastics Industry
Eco-it	Pré Consultants (NL)	Especially suitable for designers of products and containers. It uses Ecoindicator '99. It is easy to use
Ecopro	Sinum Ag.- EcoPerformance Systems (CH)	It allows simple life cycle studies of products to be realised. It uses BUWAL database
Ecoscan	TNO Industrial Technology (NL)	Can be used by technicians and those in charge of implementing eco-design of products. It has several database and is easy to use
Euklid	Frauhofer-Institut (DE)	Program directed at LCA studies of industrial products
KCL Eco	Finnish Pulp and Paper Research Institute (FI)	Possesses a very complete user interface. Uses Ecoindicator 95 or DAIA 98 and has good data for the paper industry
GaBi 4	PE INTERNATIONAL GmbH and LBP, University of Stuttgart (DE)	Apart from conventional uses of LCA this program also includes the possibility of performing an economic analysis through the inclusion of the Life Cycle Cost (LCC) and social impacts through Life Cycle Working Environment (LCWE)
LCAit	Chalmers Industritenik (SE)	Mainly applied in the area of containers and paper products
Miet	Leiden University (NL)	Works with MS excel and is based on environmental data from USA. It is a free distribution programme
Pems	Pira International (UK)	Can be used by experts or novices in the field. Possesses a flexible user interface
Simapro	Pré Consultants (NL)	Allows LCAs to be carried out using multiple impact evaluation methodologies. Comes with several complete databases. Suitable for design or R&D departments
Team	Ecobilan (FR)	Very complete tool flexible and powerful although more complicated to use. Allows cost information to be entered
Wisard	Pricewaterhouse Coopers (FR)	Suitable for economic and environmental impact analysis for municipal solid waste
Umberto	Ifeu-Institut (DE)	Gives high quality data and transparent results. Data libraries are complete and flexible. Suitable for performing business eco-balances

1.4.4 Environmental performance in urban wastewater treatment

The first reference in the implementation of LCA in WWTP dates back to 1995 [1.130], where LCA was used to assess the sustainability of different small WWT technologies. Aferwards, a more sotphisticated LCA methodology was used to evaluate the societal sustainability of municipal WWT in the Netherlands [1.131], highlighting the importance of reducing effluent pollution and minimizing the sludge production.

LCA approach has become a useful tool for assessing the sustainability of different UWW treatment schemes (see e.g. [1.58; 1.100; 1.132; 1.133]). As commented before, it evaluates the environmental load linked to a process, product or service by collecting all the related inputs and outputs through the whole life cycle and the quantification of the environmental impacts associated.

Several studies have been published dealing with LCA applied to WWTPs. Indeed, Corominas *et al.* [1.101] reviewed 45 studies on LCA and wastewater, highlighting key aspects and going deep into the characterisation of the studies. Moreover, Corominas *et al.* [1.101] reported that eutrophication (EP) impact category has been considered the most compelling environmental issue in the majority of published LCAs on WWTPs. GWP, although is not among the most relevant impact categories for WWTPs, is one of the most well investigated categories since this category impact was included in 91% of the documents reviewed.

The emission of GHGs by anthropogenic activities has been widely acknowledged to be the main cause of global warming [1.132; 1.135; 1.136]. The accumulation of emitted GHGs has increased rapidly and now threatens not only human beings but also entire ecosystems on the Earth. WWTPs have been recognised as one of the largest of minor GHG generators due to the production of three primary GHGs (i.e., carbon dioxide (CO_2), methane (CH_4), and nitrous oxide (N_2O)) both on-site and off-site [1.135; 1.137; 1.138; 1.139; 1.140]

Because of an increased interest in sustainability within water management, UWW treatment practices are being revaluated with a focus on reducing energy demands and environmental impacts, while recovering resources in the form of water, materials, and energy [1.36]. Therefore, UWW treatment can be accomplished in an energy neutral or even positive net energy balance ([1.5; 1.36], mitigating GHG emissions.

Some of the LCA studies associated with WWTPs are briefly described in the following paragraphs.

Lundin et al. [1.57]: LCA was used to compare the environmental loads including the whole urban wastewater system to evaluate the environmental consequences of changing from existing centralized WWTPs to more decentralized systems. Eco indictor 99 methodology and one p.e (population equivalent) per year as functional unit were used to perform the analysis. The study concluded that the impact associated with construction was minor, relative to the associated operation. The separation systems outperformed the conventional systems by showing lower emissions to water and more efficient recycling of nutrients to agriculture, especially of nitrogen but also of phosphorus.

Lassaux et al. [1.141]: The goal of this study was to determine the environmental impact of using one cubic metre of water in the Walloon Region (Belgium) from the pumping station to the WWTP. The function was production, distribution and treatment of water in the Walloon Region. The functional unit was defined as one cubic metre of water measured at the tap of the consumer. Eco indictor 99 methodology was used to perform the analysis. Results showed that acidification and eutrophication were the most important impact categories. It was mainly attributed to the wastewater discharge without any treatment, but also by the effluent of the WWTP. GWP was not among the most relevant impact category for WWTPs.

Gallego et al. [1.58]: LCA was applied to analyse the environmental impact of different technologies for wastewater treatment in small populations. In this study, 13 WWTPs of less than 20000 p.e located in Galicia (NW Spain) were inventoried and SimaPro was used to determine the environmental loads, based in IDEMAT and Ecoinvent database and CML 2 baseline 2000 methodology. Results showed that eutrophication (mainly due to PO_4^{3-}, NH_4 and COD) and terrestrial ecotoxicity (due to the content of heavy metals in the sludge) were the most significant categories for all WWTPs. Moreover, energy consumption was a key element in the overall environmental performance of the evaluated WWTPs.

Foley et al. [1.132]: This paper defines the LCI of resources consumed and emissions produced in 10 different wastewater treatment scenarios. The used functional unit was influent quality. The results showed that infrastructure resources, operational energy, direct GHG emissions and chemical consumption generally increase with increased nutrient removal.

Rodriguez-Garcia et al. [1.100]: The performance of 24 WWTPs was evaluated using a streamlined LCA with Eutrophication and GWP as environmental indicators, and operational costs as economic indicators. WWTPs were further classified in six typologies by their quality requirements according to their final discharge point or water reuse. Moreover, two different functional units, one based on volume (m^3) and other based on eutrophication reduction (kg PO_4 removed) were applied. SimaPro was used to determine the environmental loads, based in Ecoinvent database and CML 2 baseline 2000 methodology. Results showed that the functional unit "kg PO_4 removed" better reflected the objectives of a WWTP.

Hospido et al. [1.142]: LCA was applied for the evaluation of four membrane bioreactor configurations of increasing complexity. The selected functional unit was cubic meter of produced permeate. SimaPro was used to determine the environmental loads, based in IDEMAT, Ecoinvent database, and CML 2 baseline 2000 methodology. The main contributors to the evaluated environmental impacts were identical for all the alternatives. Hence, electricity use played an important role in all the impact categories. Agricultural application of sewage sludge was also a relevant contribution on toxicity-related categories and acidification potential. The comparison among the different configurations revealed an inverse relationship between the environmental cost associated to the wastewater treatment and the complexity of the applied process.

Garrido-Baserba et al. [1.133]: LCA was implemented in a knowledge-based Decision support system (DSS) for WWTP selection. Hence, the environmental criteria to the decision making process when selecting the most appropriate process flow diagrams for specific scenarios was included. A sample group of 22 actual operating facilities in Spain (corresponding to five different typologies) were assessed by two relevant impact categories within the system: Eutrophication and GWP. Ecoinvent database and CML 2 baseline 2000 methodology were used to perform the analysis. Results demonstrated that combined LCA and DSS implementation is a suitable tool to assess WWTP design during the decision-making process.

Nevertheless, few works have been conducted on LCA (as well as into LCC) applied to AnMBR for UWW treatment due to the lack of knowledge in this field. For instance, Smith et al. [1.20] used an environmental and economic criteria to evaluate submerged AnMBRs relative to alternative aerobic technologies. The objective of this study was to compare AnMBR technology to conventional wastewater energy recovery technologies: high rate activated sludge with anaerobic digestion (HRAS+AD), conventional activated sludge with anaerobic digestion (CAS+AD), and aerobic membrane bioreactor with anaerobic digestion (AeMBR+AD). Wastewater treatment process modelling and system analyses were combined to evaluate the conditions under which AnMBR may produce more net energy thus presenting lower life cycle environmental emissions. For medium strength domestic wastewater treatment under baseline assumptions at 15°C, AnMBR recovered 49% more energy as biogas than HRAS+AD. However, global warming impact associated with AnMBR was high due to emissions of methane dissolved in the effluent.

1.5 Scope and outline of this thesis

On the basis of current research found in literature it is expected that combining membrane filtration and anaerobic biological process will represent a sustainable and cost-effective technology for the anaerobic treatment of UWW at ambient temperature conditions. In this respect, the main objective of this Ph.D. thesis is to investigate the environmental and economic feasibility of AnMBR technology for UWW treatment at ambient temperature. To obtain representative results that could be extrapolated to full-scale plants, this research work is based on data obtained in an AnMBR system featuring industrial-scale HF membrane units that was operated using effluent from the pre-treatment of the Carraixet WWTP (Valencia, Spain).

This Ph.D. thesis is enclosed in a national research project funded by the Spanish Ministry of Science and Innovation entitled “Using membrane technology for the energetic recovery of wastewater organic matter and the minimisation of the sludge produced” (MICINN project CTM2008-06809-C02-01/02).

This Ph.D. thesis is presented as a series of chapters that represent journal papers (compendium of papers). According to the aim of the thesis, the following series of objectives were defined:

a) Implementation and validation of a detailed and comprehensive plant-wide energy model for WWTPs (*Chapter 2*). This objective involves the following:

- Developing a plant-wide energy model for WWTPs.
- Implementing the developed model in the simulating software DESASS.
- Modelling the energy demand of different urban WWTPs entailing different technologies at steady-state conditions to assess the model performance.
- Modelling the dynamics in reactor temperature and heat energy requirements in an AnMBR plant at unsteady-state conditions to assess the model performance.

b) Proposal of a design methodology for AnMBR technology and identification of optimal AnMBR-based configurations by applying an overall life cycle cost (LCC) analysis (developed in *Chapters 3, 4, 5 and 6*). This objective involves the following:

- Assessing the effect of SRT (from 30 to 70 days) and ambient temperature (from 17 to 33 ºC) in the operating cost (i.e. energy consumption, methane production and sludge handling and disposal) of an AnMBR plant treating sulphate-rich UWW.
- Proposing a guideline for minimising LCC during the design of full-scale submerged AnMBRs operating at 15 and 30 ºC with both sulphate-rich and low-sulphate UWW.
- Identifying and assessing the effect of the main factors affecting the cost of the filtration process in submerged AnMBRs for UWW treatment.
- Identifying optimal AnMBR-based configurations for different operating scenarios: sulphate-rich and low-sulphate UWW treatment at 15 and 30 ºC. Three different AnMBR-based configurations were considered: AnMBR, AnMBR + anaerobic digester (AD), primary settler (PS) + AnMBR + AD

c) Life cycle assessment (LCA) of AnMBR-based technology (*Chapter 7*).

- Assessing the environmental impact of a submerged AnMBR for UWW treatment at different temperatures: ambient temperature of 20 and 33 ºC, and controlled temperature of 33 ºC.

d) Sustainability (economic and environmental) evaluation of AnMBR-based technology (*Chapters 8 and 9).* This objective involves the following:

- Leveraging a quantitative sustainable design framework and navigating trade-offs across environmental, economic, and technological criteria.
- Applying sensitivity and uncertainty analyses to characterise the relative importance of individual design decisions.
- Assessing the economic and environmental sustainability of submerged AnMBRs in comparison with aerobic-based technologies for UWW treatment, focusing on the removal of organic matter, nitrogen and phosphorus at ambient temperature.

1.6 References

1.1 U. Jeppsson, Modelling aspects of wastewater treatment processes. Ph.D. Thesis, Lund Institute of Technology, Sweden, 1996. Available on: http://www.iea.lth.se/publications.

1.2 S. Judd, C. Judd, The MBR Book: Principles and Applications of Membrane Bioreactors for Water and Wastewater Treatment, 2nd edition, Elsevier, ISBN: 978–0–08–096682–3, 2011.

1.3 B. Demirel, O. Yenigun, T.T. Onay. Anaerobic treatment of dairy wastewaters: a review. Process Biochemistry 40 (2005) 2583–2595

1.4 L.W. Hulshoff Pol, Treatment of sulphate-rich wastewaters: microbial and process technological aspects TMR Summer School Programme, The Biological Sulfur Cycle: Environ.Sci. Technol., April, Wageningen, The Netherlands, 1998.

1.5 P.L. McCarty, J. Bae, J. Kim, Domestic wastewater treatment as a net energy producer–can this be achieved? Environ. Sci. Technol. 45 (2011) 7100–7106.

1.6 J.B. Van Lier, Biological wastewater treatment: principles modelling and design. Published by IWA publishing, London, UK. Chapter 16, 2008.

1.7 G. Lettinga. Anaerobic digestion and wastewater treatment systems. Department ofEnvironmental Technology, WageningenAgricultural University, Bomenweg 2, 6703 HD Wageningen, The Netherlands. Antonie van Leeuwenhoek 67: 3-28, 1995.

1.8 H. Lin, B.-Q. Liao, J. Chen, W. Gao, L. Wang, F. Wang, X. Lu, New insights into membrane fouling in a submerged anaerobic membrane bioreactor based on characterization of cake sludge and bulk sludge, Bioresour. Technol. 102 (2011) 2373–2379.

1.9 D. Orhon. Evolution of the activated sludge process: the first 50 years. J Chem. Technol. Biotechnol. 90 (2015) 608-640.

1.10 K.V. Gernaey, M.C.M. van Loosdrecht, M. Henze, M. Lind, S. B. Jørgensen, Activated sludge wastewater treatment plant modelling and simulation: state of the art. Environ. Modell. Softw. 19 (2004) 763–783.

1.11 C.-H. Xing, W.-Z. Wu, Y. Quian, E. Tardieu, Excess sludge production in membrane bioreactors: a theoretical investigation, J. Environ. Eng. ASCE, 129 (2003) 291–297.

1.12 F. A. Meerburg, N. Boon, T. Van Winckel, J. A.R. Vercamera, I.Nopens, S.E. Vlaeminck. To ward energy-neutral wastewater treatment: A high-rate contact stabilization process to maximally recover sewage organics. Bioresour. Technol. 179 (2015), 373–381.

1.13 S. Gabarrón, M. Dalmaua, J. Porroa, I. Rodriguez-Rodaa, J. Comasa, Optimization of full-scale membrane bioreactors for wastewater treatment through a model-based approach. J. Chem. Eng. 267 (2015), 34-42

1.14 P. Le-Clech, V. Chen, T. A.G. Fane, Fouling in membrane bioreactors used in wastewater treatment J. Membrane Sci. 284 (2006) 17–53 Review.

1.15 S. Judd, The status of membrane bioreactor technology, Trends Biotechnol. 26 (2008), 109–116.

1.16 B.Q. Liao, J.T. Kraemer, D.M. Bagley, Anaerobic membrane bioreactors: Applications and research directions, Crit. Rev. Env. Sci. Tec. 36 (2006), 489–530.

1.17 K. Yamamoto, H. Hiasa, M. Talat, T. Matsuo, Direct solid liquid separations using hollow fiber membranes in activated sludge aeration tank, Water Sci. Technol. 21 (1989) 43–54.Wenbo Yang, Nazim Cicek, John Ilg, State-of-the-art of membrane bioreactors: Worldwide research and commercial applications in North America J. Membrane Sci. 270 (2006) 201–211.

1.18 W. Yang, N. Cicek, J. Ilg, State-of-the-art of membrane bioreactors: Worldwide research and commercial applications in North America. J. Membrane Sci. 270 (2006) 201–211.

1.19 S. Judd and C. Judd, The 2015 MBR Survey results. The MBR Site, March 2015. Available on: http://www.thembrsite.com/features/2015-mbr-survey-results/ (acceded 6 April 2015).

1.20 A. L, Smith, L.B. Stadler, L. Cao, N.G, Love, L. Raskin, S.J. Skerlos, Navigating Wastewater Energy Recovery 1 Strategies: A Life Cycle Comparison of Anaerobic Membrane Bioreactor and Conventional Treatment Systems with Anaerobic Digestion. Environ. Sci. Technol. 48 (2014), 5972-5981

1.21 A. Fenu, J. Roels, T. Wambecq, K. De Gussem., C. Thoeye, G. De Gueldre, B. Vand De Steene, Energy audit of a full scale MBR system. Desalination 262 (2010), 121-128.

1.22 G. Lettinga, S. Rebac and G. Zeeman, Challenge of psychrophilic anaerobic wastewater treatment, Trends Biotechnol. 19 (2001a), 363–370.

1.23 G. Zeeman, G. Lettinga, The role of anaerobic digestion of domestic sewage in closing the water and nutrient cycle at community level, Water Sci. Technol. 39 (1999), 187–194.

1.24 G. Lettinga, J.B. Van Lier, J.C.L. Van Buuren, G. Zeeman, Sustainable development in pollution control and the role of anaerobic treatment, Water Sci. Technol. 44 (2001b), 181–188.

1.25 W. Verstraete, P. Van de Caveye, V. Diamantis, Maximum use of resources present in domestic "used water", Bioresour. Technol. 100 (2009), 5537–5545.

1.26 D. Jeison, J.B. van Lier, Feasibility of thermophilic anaerobic submerged membrane bioreactors (AnSMBR) for wastewater treatment Desalination 231 (2008) 227–235.

1.27 S. Aiyuk, J. Amoako, L. Raskin, A. van Haandel, W. Verstraete, Removal of carbon and nutrients from domestic wastewater using a low investment, integrated treatment concept. Water Res. 38(2004), 3031-3042.

1.28 J.H. Ho, S.W. Sung, Methanogenic activities in anaerobic membrane bioreactors (AnMBR) treating synthetic municipal wastewater, Bioresour. Technol. 101 (2010), 2191–2196.

1.29 L.B. Chu, F.L Yang, X.W. Zhang, Anaerobic treatment of domestic wastewater in a membrane-coupled expended granular sludge bed (EGSB) reactor under moderate to low temperature. Process Biochemistry 40(2005), 1063-1070.

1.30 J. Kim, K. Kim, H. Ye, E. Lee, C. Shin, P.L. McCarty, J. Bae, Anaerobic fluidised bed membrane bioreactor for wastewater treatment, Environ. Sci. Technol. 45 (2011), 576–581.

1.31 Z. Huang, S.L. Ong, H.Y. Ng, Feasibility of submerged anaerobic membrane bioreactor (SAMBR) for treatment of low-strength wastewater, Water Sci. Technol. 58 (2008), 1925–1931.

1.32 H. Ozgun, R.K. Dereli, M.E. Ersahin, C. Kinaci, H. Spanjers, J.B. van Lier, A review of anaerobic membrane bioreactors for municipal wastewater treatment: Integration options, limitations and expectations, Sep. Purif. Technol. 118 (2013) 89-104.

1.33 L. Raskin, 2012. Anaerobic Membrane Bioreactors for Sustainable Wastewater Treatment. WERF Report U4R08, June 2012.

1.34 D.C. Stuckey, Recent developments in anaerobic membrane reactors, Bioresour.Technol. 122 (2012) 137–148.

1.35 H. Lin, W. Peng, M. Zhang, J. Chen, H. Huachang, Y. Zhang, A review on anaerobic membrane bioreactors: Applications, membrane fouling and future perspectives, Desalination 314 (2013) 169–188.

1.36 J.S. Guest, S.J. Skerlos, J.L Barnard, M.B. Beck, G.T. Daigger, H. Hilger, S.J. Jackson, K. Karvazy, L. Kelly, L. Macpherson, J.R. Mihelcic, A. Promanik, L. Raskin, M.C.M. Van Loosdrecht, D. Yeh, N.G. Love, A new planning and design paradigm to achieve sustainable resource recovery from wastewater. Environ. Sci. Technol. 43(2009), 6126-6130.

1.37 D.W. Gao, T. Zhang, C.Y.Y. Tang, W.M. Wu, C.Y. Wong, Y.H. Lee, D.H. Yeh, C.S. Criddle, Membrane fouling in an anaerobic membrane bioreactor: differences in relative abundance of bacterial species in the membrane foulant layer and in suspension, J. Membr. Sci. 364 (2010), 331–338.

1.38 M. Dagnew, W. Parker, P. Seto, K. Waldner, Y. Hong, R. Bayly, J. Cumin, Pilot testing of an AnMBR for municipal wastewater treatment. 84th Annual Water Environment Federation Technical Exhibition and Conference, Los Angeles, CA, 2011.

1.39 J.B. Giménez, A. Robles, L. Carretero, F. Durán, M.V. Ruano, M.N. Gatti, J. Ribes, J. Ferrer, A. Seco, Experimental study of the anaerobic urban wastewater treatment in a submerged hollow-fibre membrane bioreactor at pilot scale, Bioresour.Technol. 102 (2011), 8799–8806.

1.40 D. Martinez-Sosa, B. Helmreich, T. Netter, S. Paris, F. Bischof, H. Horn, Anaerobic submerged membrane bioreactor (AnSMBR) for municipal wastewater treatment under mesophilic and psychrophilic temperature conditions, Bioresour.Technol. 102 (2011) 10377–10385.

1.41 M.L Salazar-Pelaez, J.M. Morgan-Sagastume, A. Noyola, Influence of hydraulic retention time on fouling in a UASB coupled with an external ultrafiltration membrane treating synthetic municipal wastewater. Desalination 277(2011), 164-170.

1.42 D. Jeison, J.B. van Lier, Cake formation and consolidation: Main factors governing the applicable flux in anaerobic submerged membrane bioreactors (AnSMBR) treating acidified wastewaters, Sep. Purif. Technol. 56 (2007), 71–78.

1.43 B. Lew, S. Tarre, M. Beliavski, C. Dosoretz, M. Green, Anaerobic membrane bioreactor (AnMBR) for domestic wastewater treatment, Desalination 243 (2009) 251–257.

1.44 A.L. Smith, S.J. Skerlos, L. Raskin, Psychrophilic anaerobic membrane bioreactor treatment of domestic wastewater. Water Res. 47 (2013), 1655-1665.

1.45 D. Jeison, Anaerobic membrane bioreactors for wastewater treatment: feasibility and potential applications, PhD Thesis, Universidad de Wageningen, Holanda, 2007.

1.46 A. Robles, M.V. Ruano, J. Ribes, J. Ferrer, Sub-critical long-term operation of industrial scale hollow-fibre membranes in a submerged anaerobic MBR (HF-AnMBR) system, Sep. Purif. Technol. 100 (2012) 88–96.

1.47 J.B Van Lier, G. Lettinga, Appropriate technologies for effective management of industrial and domestic waste waters: The decentralised approach. Water Sci. Technol. 40(1999), 171-183.

1.48 G. Zeeman, G. Lettinga, The role of anaerobic digestion of domestic sewage in closing the water and nutrient cycle at community level, Water Sci. Technol. 39 (1999), 187–194.

1.49 A. van Haandel., M.T. Kato, P.F.F. Cavalcanti and L. Florencio, Anaerobic reactor design concepts for the treatment of domestic wastewater. Reviews in Environ. Sci. Biotechnol. 5(2006), 21-38.

1.50 S. Judd, The MBR site, July 2011, Available on: http://www.thembrsite.com (acceded 6 March 2013).

1.51 I. Martin, M. Pidou, A. Soares, S. Judd, B. Jefferson, Modelling the energy demands of aerobic and anaerobic membrane bioreactors for wastewater treatment, Environ. Technol. 32 (2011), 921–932.

1.52 J.B. Giménez, N. Martí, J. Ferrer, A. Seco, Methane recovery efficiency in a submerged anaerobic membrane bioreactor (AnMBR) treating sulphate-rich urban wastewater: Evaluation of methane losses with the effluent, Bioresour. Technol. 118 (2012) 67–72.

1.53 A.L. Smith, Low-Temperature Anaerobic Membrane Bioreactor for Energy Recovery from Domestic Wastewater. A dissertation submitted in partial fulfillment of the requirements for the degree of Doctor of Philosophy (Environmental Engineering) in the University of Michigan 2014.

1.54 H.Q.Yu, H. H.P, Fang. Acidogenesis of gelatin-rich wastewater in an upflow anaerobic reactor: influence of pH and temperature. Water Res. 37 (2003) 55–66.

1.55 G. Houillon, O. Jolliet, Life cycle assessment of processes for the treatment of wastewater urban sludge: energy and global warming analysis. J. Clean. Prod. 13 (2005), 287e299.

1.56 MAGRAMA. Official website of the Ministry of Agriculture, Food and Environment. Spanish government, Madrid. Available on: http://www.magrama.gob.es/es/calidad-y-evaluacion-ambiental/temas/prevencion-y-gestion-residuos/flujos/lodos-depuradora/ (Acceded 5 April 2014).

1.57 M. Lundin, M. Bengtsson, S. Molander, Life Cycle Assessment of Wastewater Systems: Influence of System Boundaries and Scale on Calculated Environmental Loads. Environ. Sci. Technol. 34 (2000), 180-186.

1.58 A. Gallego, A. Hospido, M.T. Moreira, G. Feijoo, Environmental performance of wastewater treatment plants for small populations, Resour. Conser. Recy. 52 (2008) 931–940.

1.59 A. Hospido, M. Carballa, M. Moreira, F. Omil, J.M. Lema, G. Feijoo, Environmental assessment of anaerobically digested sludge reuse in agriculture: Potential impacts of emerging micropollutants. Water Res. 44 (2010), 3225-3233.

1.60 M. Lundin, M. Olofsson, G.J. Pettersson, H. Zetterlund, Environmental and economic assessment of sewage sludge handling options. Resour. Conserv. Recy. 41 (2004), 255–278.

1.61 J. Hong, J. Hong, M. Otaki, O. Jolliet, Environmental and economic life cycle assessment for sewage sludge treatment processes in Japan. Waste Manage. 29 (2009), 696-703.

1.62 .I. Hai, K. Yamamoto and C-H. Lee. Membrane biological reactors. Theory, Modeling, Design, Management and Applications to wastewater Reuse. Faisal IWA publishing. 2014.

1.63 Z. Wang, J. Ma, C.Y. Tang, K. Kimura, Q. Wang, X. Han, Membrane cleaning in membrane bioreactors: A review. J. Membrane Sci. 468 (2014), 276-307.

1.64 W.J. Gao, H.J. Lin, K.T. Lin, H. Schraft, B.Q. Liao, Structure of cake layer in submerged anaerobic membrane bioreactor, J. Membrane. Sci. 374 (2011), 110–120.

1.65 D. Jeison, J.B. van Lier, On-line cake-layer management by trans-membrane pressure steady state assessment in Anaerobic Membrane Bioreactors for wastewater treatment, Biochem. Eng. J. 29 (2006), 204–209.

1.66 A.L. Smith, L.B. Stadler, N.G. Love, S.J. Skerlos, L. Raskin, Perspectives on anaerobic membrane bioreactor treatment of domestic wastewater: A critical review, Bioresour. Technol. 122 (2012), 149–159.

1.67 M.V.G. Vallero, G. Lettinga, P.N.L, Lens, High rate sulfate reduction in a submerged anaerobic membrane bioreactor (SAMBaR) at high salinity. J. Membrane Sci. 253 (2005), 217–232.

1.68 L. Dvorák, M. Gómez, M. Dvoraková, I. Ruzicková, J. Wanner, The impact of different operating conditions on membrane fouling and EPS production. Bioresour. Technol. 102 (2011), 6870–6875

1.69 A. Robles, M.V Ruano, J. Ribes, A. Seco, J. Ferrer, Model-based automatic tuning of a filtration control system for submerged anaerobic membrane bioreactors (AnMBR), J. Membrane Sci. 465 (2014) 14 – 26.

1.70 A. Robles, M.V. Ruano, J. Ribes, J. Ferrer, Factors that affect the permeability of commercial hollow-fibre membranes in a submerged anaerobic MBR (HF-AnMBR) system, Water Res. 47 (2013) 1277-1288.

1.71 R.W. Field, D. Wu, J.A. Howell, B.B. Gupta, Critical flux concept for microfiltration fouling, J. Membrane Sci. 100 (1995) 259 – 272.

1.72 Verrecht, T. Maere, I. Nopens, C. Brepols, S. Judd, The cost of a large-scale hollow fibre MBR, Water Res. 44 (2010) 5274 – 5283.

1.73 A. Achilli, E.A. Marchand, A. E. Childress, A performance evaluation of three membrane bioreactor systems: aerobic, anaerobic, and attached-growth. Water Sci. Technol. 63(2011), 2999-3005.

1.74 S.H. Baek, and K.R. Pagilla, Aerobic and anaerobic membrane bioreactors for municipal wastewater treatment. Water Environ. Res. 78(2006), 133-140.

1.75 G. Guglielmi, Membrane bioreactors for municipal wastewater treatment, Ph.D. thesis, Universita' di Trento, Italy, 2002.

1.76 S. Delgado, R. Villaroel, E. González, Effect of shear intensity on fouling in submerged membrane bioreactor for wastewater treatment, J. Membr. Sci. 311 (2008), 173–181.

1.77 P. Bachin, P. Aimar, V. Sanchez, Model for colloidal fouling of membranes, AIChE J. 41 (1995), 368–377.

1.78 A. Robles, M.V Ruano, F. García-Usach, J. Ferrer, Sub-critical filtration conditions of commercial hollow-fibre membranes in a submerged anaerobic MBR (HF-AnMBR) system: The effect of gas sparging intensity. Bioresour. Technol. 114 (2012), 247–254.

1.79 N. Descoins, S. Deleris, R. Lestienne, E. Trouvé, F. Maréchal, Energy efficiency in waste water treatments plants: Optimization of activated sludge process coupled with anaerobic digestion. Energy (2011) 1-12.

1.80 J. Ferrer, A. Seco, J. Serralta, J. Ribes, J. Manga, E. Asensi, J.J. Morenilla, F. Llavador, DESASS: a software tool for designing, simulating and optimising WWTPs, Environ. Modell. Softw. 23(2008), 19–26.

1.81 U. Jeppsson, C. Rosen, J. Alex, J. Copp, K.V. Gernaey, M.-N. Pons, P.A. Vanrolleghem, Towards a benchmark simulation model for plant-wide control strategy performance evaluation of WWTPs. Water Sci. Technol. 53 (2006), 287–295.

1.82 J. Gómez, M. de Gracia, E. Ayesa, J.L. Garcia-Heras, 2007. Mathematical modelling of autothermal thermophilic aerobic digesters. Wat. Res. 41 (2007), 959–968.

1.83 S. Righi, L. Oliviero, M. Pedrini, A. Buscaroli, C.D. Casa, Life Cycle Assessment of management systems for sewage sludge and food waste: centralized and decentralized approaches. J. Clean Prod. 44 (2013) 8-17.

1.84.D. Lemos, D.C Dias, X. Gabarrell, L. Arroja, Environmental assessment of an urban water system. J. Clean Prod. 54 (2013) 157-165.

1.85 O. Nowak, P. Enderle, P. Varbanov, Ways to optimize the energy balance of municipal wastewater systems: lessons learned from Austrian applications. J. Clean. Prod. 88 (2015) 125-131.

1.86 H. Bozkurt, A. Quaglia, K.V. Gernaey, G. Sin, A mathematical programming framework for early stage design of wastewater treatment plants. Environ. Modell. Softw. 64 (2015), 164-176.

1.87 I. Pijákovà, J. Derco, Application of Dynamic Simulations for Assessment of Urban Wastewater Systems Operation. Chem. Biochem. Eng. Q. 29 (2015) 55-62.

1.88 R. Barat, J. Serralta, M.V. Ruano, E. Jiménez, J. Ribes, A. Seco, J. Ferrer, Biological Nutrient Removal Model Nº 2 (BNRM2): A general model for Wastewater Treatment Plants, Water Sci. Technol. 67 (2013), 1481–1489.

1.89 F. Durán, 2013. Mathematical modelling of the anaerobic urban wastewater treatment including sulphate-reducing bacteria. Application to an anaerobic membrane bioreactor (Modelación matemática del tratamiento anaerobio de aguas residuales urbanas incluyendo las bacterias sulfatorreductoras. Aplicación a un biorreactor anaerobio de membranas). Ph.D. thesis. Dept. of Hydraulic Engineering and Environment. Universitat Politècnica de València, Spain.

1.90 A. Robles, 2013. Modelling, simulation and control of the filtration process in a submerged anaerobic membrane bioreactor treating urban wastewater. Ph.D. thesis. Dept. of Hydraulic Engineering and Environment. Universitat Politècnica de València, Spain.

1.91 G. Sin, K.V. Gernaey, M.B. Neumann, M.C.M. van Loosdrecht, W. Gujer. Uncertainty analysis in WWTP model applications: A critical discussion using an example from design. Water Res. 43 (2009) 2894-2906.

1.92 M.M. Rajabi, B. Ataie-Ashtiani, H. Janssen. Efficiency enhancement of optimized Latin hypercube sampling strategies: Application to Monte Carlo uncertainty analysis and meta-modeling. Adv. Water Resour. 76 (2015) 127-139.

1.93 M.D. Morris. Factorial sampling plans for preliminary computational experiments, Technometrics 33(1991), 161–174.

1.94 A. Saltelli, M. Ratto, S. Tarantola, F. Campologno. Sensitivity Analysis for Chemical Models, Chemical Rev. 108 (2005), 2811–2827.

1.95 G. Sin, K.V. Gernaey, M.B. Neumann, M.C.M. van Loosdrecht, W. Gujer. Global sensitivity analysis in wastewater treatment plant model applications: Prioritizing sources of uncertainty. Water Res. 45 (2011) 639-651.

1.96 G. Tchobanoglous, F.L Burton, H.D. Stensel, Metcalf & Eddy, Inc. Wastewater Engineering. Treatment and Reuse. 4th ed. New York: McGraw-Hill, Fourth edition. pp. 1704 (2003) 15-5.

1.97 F. Hernandez-Sancho, M. Molinos-Senante, R. Sala-Garrido, Energy efficiency in Spanish wastewater treatment plants: A non-radial DEA approach. Sci. Total Environ. 409 (2011), 2693-2699.

1.98 G. Olsson, B. Carlsson, J. Comas, J. Copp, K.V. Gernaey, P. Ingildsen, U. Jeppsson, C. Kim, L. Rieger, I. Rodríguez-Roda, J.-P. Steyer, I. Takács, P.A Vanrolleghem, A. Vargas Casillas, Z. Yuan, L. Åmand, L, Instrumentation, Control and Automation in Wastewater- from London 1973 to Narbonne 2013. Water Sci. Technol. 69 (2014), 1373-85.

1.99 B. Nicolae, B. George-VladbaDunarea, Life cycle analysis in refurbishment of the buildings as intervention practices in energy saving. Energ. Buildings 86 (2015) 74–85.

1.100 G. Rodriguez-Garcia, M. Molinos-Senante, A. Hospido, F. Hernández-Sancho, M.T. Moreira, G. Feijoo, Environmental and economic profile of six typologies of wastewater treatment plants. Water Res. 45 (2011), 5997-6010.

1.101 L. Corominas, J. Foley, J.S. Guest, A. Hospido, H.F. Larsen, S. Morera, A. Shaw, Life cycle assessment applied to wastewater treatment: State of the art. Water Res. 47 (2013), 5480-5495.

1.102 A. Meda, P. Cornel, Energy and water: relationships and recovery potential, IWA Water and Energy conference, Amsterdam, The Netherlands, 10–12 November 2010.

1.103 N. Gurieff, J. Bruus, B. Nielsen, D. Nawawi-Lansade and M. Cantegril Moving towards an energy neutral WWTP – the positive impact of ExelysTM continuous thermal hydrolysis in achieving this goal. Water Pract. Tech. Vol 7 No 2 (2012).

1.104 A. Bauer, P. Böschb, A. Friedl, T. Amona, Analysis of methane potentials of steam-exploded wheat straw and estimation of energy yields of combined ethanol and methane production. J. Biotechnol.142 (2009), 50-55.

1.105 EPA. Environmental Protection Agency. Combined Heat and Power Partnership. Agency of the United States federal government, 2015.

1.106 P. Cornel, A. Meda, and S. Bieker, wastewater as a source of energy, nutrients and service water. Treatise on Water Science. Editor: Petzr Wilderer, Elsevier Verlag., 2011.

1.107 V. Lazarova, K.H Choo and P. Cornel, Water-energy interactions in water reuse. IWA Publishing, London, UK.

1.108 GWRC. Water and energy in the urban water cycle; improving energy efficiency in municipal wastewater treatment. Report prepared by the nanyang Environment and water research institute (NEWRI), PUB Signapore and Global Water research Coalition (GWRC), Signapore, 2012.

1.109 S. Krause and D. Dickerson, Energy efficient MBR process. In Membrane Bioreactor Technology, Volume 1, water Treatment Academy, Bangkok, Thailand, 2011.

1.110 T. Maere, B. Verrecht, S. Moerenhout, S. Judd, I. Nopens, BSM-MBR: A benchmark simulation model to compare control and operational strategies for membrane bioreactors. Water Res. 45 (2011) 2181-2190.

1.111 J.A. Gil, L. Túa, A. Rueda, B. Montaño, M. Rodríguez, D. Prats, Monitoring and analysis of the energy cost of an MBR. Desalination 250 (2010) 997–1001.

1.112 M. Molinos-Senante, F. Hernández-Sancho, R. Sala-Garrido, M .Garrido-Baserba, Economic feasibility study for wastewater treatment: a cost-benefit analysis. Sci. Total Environ. 408 (2011), 953-957.

1.113 EPA. Catalog of Biomass Combined Heat and Power Catalog of Technologies, 2007. Available on: http://www.epa.gov/chp/documents/biomass_chp_catalog.pdf (Acceded 5 May 2015).

1.114 A.Y. Hu, D.C. Stuckey, Treatment of dilute wastewaters using a novel submerged anaerobic membrane bioreactor, J. Environ. Eng.-ASCE 132 (2006), 190–198.

1.115 A.L. Smith, H. Dorer, N.G. Love, S.J. Skerlos, L. Raskin, Role of membrane biofilm in psychrophilic anaerobic membrane bioreactor for domestic wastewater treatment, In: 84th Annual Water Environment Federation Technical Exhibition and Conference (WEFTEC), Los Angeles, California, October 15–19, 2011.

1.116 W.M.K.R.T.W. Bandara, H. Satoh, M. Sasakawa, Y. Nakahara, M. Takahashi, S. Okabe, Removal of residual dissolved methane gas in an upflow anaerobic sludge blanket reactor treating low-strength wastewater at low temperature with degassing membrane, Water Res. 45 (2011) 3533–3540.

1.117 DIC Corporation. Available on: http://www.dicglobal.com/us/en/products/membrane/separel/solvent.html (Acceded 10 May 2014).

1.118 M. Hatamoto, H. Yamamoto, T. Kindaichi, N. Ozaki, A. Ohashi, Biological oxidation of dissolved methane in effluents from anaerobic reactors using a down-flow hanging sponge reactor, Water Res. 44 (2010) 1409–1418.

1.119 H. Wenzel, M. Hauschild and L. Alting , Environmental Assessment of Products – Volume 1, Methodology, tools and case studies in product development, London, Weinheim, New York: Chapman & Hall, 1997.

1.120 M.P. Lundholm, G. Sundström, Resource and environmental impact of Tetra Brik carton and refillable and non−refillable glass bottles, Tetra Brik Aseptic environmental profile, AB Tetra Pak, Malmö, 1985.

1.121 Society of Environmental Toxicology and Chemistry (SETAC), 'Life−cycle Assessment', Workshop Report, Brussels: SETAC, 1992.

1.122 ISO. International Organization for Standardization (ISO) 14040: Environmental Management - Life Cycle Assessment e Principles and Framework (Geneva), 2006.

1.123 UNEP. United Nations Environment Programme Available on: http://www.unep.org/resourceefficiency/Consumption/StandardsandLabels/MeasuringSustainability/LifeCycleAssessment/tabid/101348/Default.aspx (Acceded 2 February 2015).

1.124 Society of Environmental Toxicology and Chemistry (SETAC), 'Guidelines for Life−cycle Assessment: A "Code of Practice"', SETAC workshop in Sesimbra, Portugal 31 March−3 April, Brussels: SETAC, 1993.

1.125 H.A. Udo de Haes, O. Jolliet, G. Finnveden, M. Hauschild, W. Krewitt, and R. Mueller-Wenk, Best available practice regarding impact categories and category indicators in life cycle impact assessment, Part 1. Int J Life Cycle Assess 4(1999): 66–74.

1.126 J. C. Bare, G. A. Norris, D. W. Pennington, T. McKone, TRACI The Tool for the Reduction and Assessment of Chemical and Other Environmental Impacts. J. Ind. Ecol. Volume 6, (2003) Number 3–4.

1.127 B. Peuportier, S. Scarpellini, M. Glaumann, , T. Malmqvist, G. Krigsvol, C. Wetzel, H. Staller, Z. Szalay, V. Degiovanni, E.Stoykova, ENSLIC_BUILDING: Energy Saving through Promotion of Life Cycle Assessment in Buildings Deliverable D2.1 State of the art report and Deliverable D2.2 Collection of published material, , 2007. Acceded on 10 march 2015: http://ec.europa.eu/energy/intelligent/projects/sites/iee-projects/files/projects/documents/enslic_building_lca_state_of_the_art_report_en.pdf.

1.128 P. Hofstetter, A. Braunschweig M. Mettier, R. Müller-Wenk, O. Tietje, Dominance, Analysis in the Mixing Triangle, A graphical decision support tool for product comparisons, submitted to the J. Ind. Ecol. 1999.

1.129 Pré consultants. SimaPro. World's Leading LCA Software, 2015. Available on: http://www.pre-sustainability.com/simapro (Acceded 10 march 2015).

1.130 R.H.C. Emmerson, G.K. Morse, J.N. Lester, D.R. Edge. The life-Cycle Analysis of Small scale Sewage-Treatment Processes. J. CIWEM (1995) 317-325.

1.131 P.J. Roeleveld, A. Klapwijk, P.G. Eggels, W.H. Rulkens, W. van Starkenburg. Sustainability of municipal waste water treatment. Water Science and Technology. Volume 35, Issue 10, 1997, Pages 221–228.

1.132 J. Foley, D. de Hass, K. Hartley, P. Lant, Comprehensive life cycle inventories of alternative wastewater treatment systems. Water Res. 44 (2010a), 1654-1666.

1.133 M. Garrido-Baserba, A. Hospido, R. Reif, M. Molinos-Senante, J. Comas, M. Poch, Including the environmental criteria when selecting a wastewater treatment plant. Environ. Modell. Softw. (2013) 1-9.

1.134 J. Foley D. de Haas Z. Yuan, P. Lant, Nitrous oxide generation in full-scale biological nutrient removal wastewater treatment plants. Water Res. (2010b); 44:831–44.

1.135 G. Rodriguez-Garcia, A. Hospido, D.M. Bagley, M.T. Moreira, G. Feijoo. A methodology to estimate greenhouse gases emissions in Life Cycle Inventories of wastewater treatment plants. Environ. Impact Asses. 37 (2012) 37–46.

1.136 D. Kyung, M. Kim, J. Chang, W. Lee, Estimation of greenhouse gas (GHG) emissions from a hybrid wastewater treatment plant. J. Clean Prod. Available online 19 February 2015. In Press, Accepted Manuscript.

1.137 H.R. Sahely, H.L. MacLean, H.D. Monteith, D.M. Bagley. Comparison of on-site and upstream greenhouse gas emissions from Canadian municipal wastewater treatment facilities. J. Environ. Eng. Sci., 5 (2006), pp. 405–415.

1.138 M. Bani Shahabadi, L. Yerushalmi, F. Haghighat. Impact of process design on greenhouse gas (GHG) generation by wastewater treatment plants. Water Res. 43 (2009) 2679–2687.

1.139 L. Corominas, X. Flores-Alsina, L. Snip, P.A. Vanrolleghem, Comparison of different modeling approaches to better evaluate greenhouse gas emissions from whole wastewater treatment plants. Biotechnol. Bioeng. 109 (2012), 2854-2863.

1.140 L. Yerushalmi, O. Ashrafi, F. Haghighat. Reductions in greenhouse gas (GHG) generation and energy consumption in wastewater treatment plants. Water Sci. Technol, 67 (5) (2013), pp. 1159–1164.

1.141 S. Lassaux, R. Renzoni, A. Germain, Life Cycle Assessment of Water from the Pumping Station to the Wastewater Treatment Plant. Int. J. Life Cycle Ass. 12 (2007) 118 – 126.

1.142 A. Hospido, I. Sanchez, G. Rodriguez-Garcia, A.Iglesias, D. Buntner, R. Reif, M.T. Moreira, G. Feijoo. Are all membrane reactors equal from an environmental point of view? Desalination 285 (2012) 263–270.

CHAPTER 2:

A plant-wide energy model for WWTPs: application to AnMBR technology

Abstract

The aim of this study is to propose a detailed and comprehensive plant-wide model for assessing the energy demand of different wastewater treatment systems (beyond the traditional activated sludge) at both steady- and unsteady-state conditions. The proposed model enables calculating power and heat energy requirements (W and Q, respectively), and energy recovery (power and heat) from methane and hydrogen capture. In order to account for the effect of biological processes on heat energy requirements, the model has been coupled to the extended version of the plant-wide mathematical model BNRM2, which is implemented in the simulation software DESASS. Two case studies have been evaluated to assess the model performance: (1) modelling the energy demand of two urban WWTPs based on conventional activated sludge (CAS) and submerged anaerobic MBR (AnMBR) technologies at steady-state conditions; and (2) modelling the dynamics in reactor temperature and heat energy requirements in an AnMBR plant at unsteady-state conditions. The results indicated that the proposed model can be used for assessing the energy performance of different wastewater treatment processes, thus being useful for different purposes, e.g. WWTP design or upgrading, or development of new control strategies for energy savings.

Keywords

Anaerobic MBR; BNRM2; DESASS; plant-wide energy model; wastewater treatment

Highlights

A plant-wide energy model for WWTPs is proposed.
The model considers power, heat and cogenerated energy.
Simulation results were validated with experimental data from an AnMBR system.
The model reproduced the experimental temperature and heat energy demand adequately.

R. Pretel, A. Robles, M.V. Ruano, A.Seco, J. Ferrer
A plant-wide energy model for WWTPs: application to AnMBR technology
Submitted to Water Res.

2.1 Introduction

Wastewater treatment is an energy-intensive activity whose energy costs vary considerably from one wastewater treatment plant (WWTP) to another, depending on the type of influent, treatment technology and required effluent quality. Different environmental concerns (e.g. global warming and greenhouse gases (GHG) emissions) are some of the driving factors promoting changes in the wastewater treatment field [2.1]. Indeed, sustainable water management is increasingly important for utilities and is driving efforts to reduce energy consumption in WWTPs without compromising effluent quality. Specially, energy saving is the fastest, highest impacting and most cost-effective way of reducing GHG emissions [2.2]. Therefore, energy saving in WWTPs is a key point for improving overall environmental performance in wastewater treatment domain [2.3].

Besides actions focussed on saving energy and increase energy efficiency, the expansion of renewable energies is viewed to be an important factor for a secure energy future [2.4]. In this respect, since the water-energy-carbon nexus is gaining increasing importance as a field of research, biogas production from sewage sludge digestion is a subject of interest in both energy and wastewater domains [2.5]. Part of the energy recovered from wastewater in the form of biogas is usually used for heating purposes, whilst the rest can be employed for meeting WWTP power requirements after conversion to electrical power. Hence, the possibility of energy recovery from wastewater is a key operating opportunity in the wastewater treatment field in order to find energy savings thus reducing operating costs. Furthermore, biogas offers greater energy and environmental benefits when generating power and heat simultaneously using CHP (combined heat and power) technology than when generating both separately [2.6].

To date, the interest of the scientific community involved in the wastewater treatment field has been mainly focused on water quality and associated plant-wide modelling issues [2.7]. In this respect, the use of mathematical models for WWTP design and upgrading, process optimisation, operator training, and development of control strategies has become a standard engineering tool in the last decade (see, for instance, [2.8; 2.9]). Indeed, model-based analysis seems to be a promising method for improving energy efficiency in wastewater treatment [2.10]. Process variables can be both tuned and optimised, and technologies can be compared in a rigorous way, especially by including energy aspects in the computations [2.7]. Hence, plant-wide energy models are expected to be a promising tool for selection of the best among the alternatives aimed to meet the desired criteria in the WWTP network (e.g. low energy consumption) [2.10].

Different studies can be found in literature dealing with energy modelling in wastewater treatment. Jeppsson et al. [2.11] proposed an extension of the Benchmark Simulation Model no 1 (BSM1) aimed at facilitating control strategy development and process performance evaluation at a plant-wide level, including therefore a complete energy balance. Gómez et al. [2.12] presented a new biochemical model for aerobic digestion that introduced an energy balance to dynamically predict the temporary evolution of temperature in an autothermal thermophilic aerobic digester. Righi et al. [2.13] assessed the environmental profile and energy balance of different waste treatment systems. Another representative study was conducted by Lemos et al. [2.14], who assessed the environmental performance and the electricity consumption of an entire urban water system; whilst Nowak et al. [2.15] considered several ways of ensuring positive net energy balance in wastewater treatment. However, scarce literature has been found dealing with the development of a plant-wide energy model including new technologies for treating urban wastewater at full-scale, such as membrane-based ones.

On the other hand, some software in the field of wastewater engineering already included not only the analysis of process water management and sludge treatment, but also the assessment of energy consumption and efficiency (e.g gPROMS, Simba 6, W2E, WWTP/check, etc.). For instance, Tous et al. [2.16] applied the simulation program W2E for calculating the energy and mass balance of different sewage sludge treatments; Descoins et al. [2.7] developed a plant-wide model, implemented in the modelling software gPROMS, including not only the main biochemical transformations but also the energy consumption for each involved physical unit operation; and Pijájová and Derco [2.17] assessed the performance of urban wastewater treatment systems using the simulator SIMBA 6. However, these modelling softwares do not include new promising technologies aimed at enhancing wastewater treatment, such as aerobic and anaerobic membrane bioreactor (MBR and AnMBR, respectively).

The aim of this study is to propose a detailed and comprehensive plant-wide model for assessing the energy demand of different wastewater treatment systems (beyond the conventional activated sludge (CAS) system) at both steady- and unsteady-state conditions. The proposed model has been coupled to the extended version of the plant-wide mathematical model BNRM2 [2.18] proposed by Durán [2.19], which is implemented in the new version of the simulation software DESASS [2.9]. DESASS allows the design, upgrading, simulation and optimisation of municipal and industrial WWTPs, including, among others, MBR and AnMBR technologies. In this respect, the proposed energy model allows calculating the overall energy demand of different WWTPs, enabling therefore their analysis and improvement from an environmental point of view (e.g. reduction of GHG emissions associated with energy consumption). Specifically, the model enables calculating power and heat energy requirements (W and Q, respectively), and energy recovery (power and heat) from methane and hydrogen capture during the anaerobic treatment of organic matter. The *W* term (power energy) entails the main equipment employed in WWTPs (e.g. blowers, pumps, diffusers, stirrers, dewatering systems, etc.). The *Q* term (heat energy) considers heat transfer through pipe and reactor walls, heat transfer due to gas decompression, external heat required when temperature is controlled, and enthalpy of the biological reactions included in the extended version of the plant-wide model BNRM2.

2.2 Materials and methods

2.2.1 Energy model description

The proposed model, which is coupled to the extended version of the plant-wide mathematical model BNRM2 [2.19], consists of a set of energy equations that could be solved for both steady and dynamic conditions. The model represents the total energy demand of the evaluated treatment scheme using Eq. 2.1. This equation symbolises the sum of potential energy (E_p), kinetic energy (E_k), and internal (molecular) forms of energy (h) such as electrical and chemical energy, being equal to the heat transferred to the system (Q) and the work applied by the system on its surroundings (W) during a given time interval.

$$\Delta E_p + \Delta E_k + \Delta h = W + Q \qquad \textbf{(Eq. 2.1)}$$

2.2.1.1 Power energy (W)

The equipment considered for calculating the *W* term (power energy) consists of the following: pumping equipment (pumps and blowers), diffusers, stirrers, circular suction scraper bridges (for primary and secondary settlers and sludge thickeners), rotofilters and sludge dewatering systems.

Table 2.1 shows the equations employed for calculating *W*. The energy consumption of blowers (Eq. 2.2 and Eq.2.3), general pumps (feeding and recycling) (Eq.2.4) and permeate pumps (Eq.2.5) is calculated as proposed by Judd and Judd [2.20]. To calculate the net power energy required by the permeate pump ($P_{permeate}$), the sum of the power energy consumed in the following four membrane operating stages was considered: filtration ($P_{filtration}$), back-flushing ($P_{back\text{-}flushing}$), degasification ($P_{degasification}$) and ventilation ($P_{ventilation}$). Eq.2.5 is used to calculate the power energy consumed in filtration, back-flushing and degasification stages, whilst Eq.2.4 is used to calculate the power energy consumed in ventilation stage since the fluid does not pass through the membrane [2.21].

Table 2.1 Equations used for determining power energy requirements in WWTPs.

Power Energy	Equation	
Power energy consumed by the blower, P_B in J·s^{-1}	$\frac{(M \cdot R \cdot T_{gas})}{(\alpha-1)\cdot\eta_{blower}}\left[\left(\frac{p_2}{p_1}\right)^{\frac{\alpha-1}{\alpha}}-1\right]$	**Eq. 2.2**
Absolute outlet pressure, P_2 in atm	$\left\{p_1\cdot 10^5+\Delta h_{difussers}+Y_{reactor}\cdot\rho_{liquor}\cdot g+\left[\left(\frac{2\cdot(L+Leq)\cdot f\cdot V^2\cdot\rho}{D}\right)inlet.+\left(\frac{2\cdot(L+Leq)\cdot f\cdot V^2\cdot\rho}{D}\right)outlet.\right]\right\}x10^{-5}$	**Eq.2.3**
Power energy consumed by the general pump, P_g in J·s^{-1}	$q_{imp}\cdot\rho\cdot g\cdot\frac{\left\{\left[\left(\frac{(L+Leq)\cdot\cdot f\cdot V^2}{D\cdot 2\cdot g}\right)inlet+\left(\frac{(L+Leq)\cdot f\cdot V^2}{D\cdot 2\cdot g}\right)outlet\right]+[Z_1-Z_2]\right\}}{\eta_{pump}}$	**Eq.2.4**
Power energy consumed during filtration, degasification or back-flushing, P_{stage} in J·s^{-1}	$\frac{q_{stage}\cdot TMP_{stage}}{\eta_{pump}}$	**Eq.2.5**
Power energy consumed by the stirrer, $P_{stirrer}$ in J·s^{-1}	$\frac{E_{stirrer}\cdot V_{reactor}}{\eta_{engine}}$	**Eq.2.6**
Power energy consumed by the sludge dewatering system,$P_{dewatering}$ in kWh·d^{-1}	$\frac{E_{dewatering}\cdot M_{MLSS}}{\eta_{engine}}$	**Eq.2.7**
Symbols		
M	Molar flow rate of gas, mol·s^{-1}	
R	Gas constant for gas, J·mol^{-1}·K^{-1}	
P_1	Absolute inlet pressure, atm	
P_2	Absolute outlet pressure, atm	
T_{gas}	Gas temperature, K	
α	Adiabatic index	
η_{blower}	Blower efficiency	
$Ah_{difussers}$	Diffusers pressure drops, Pa	
$Y_{reactor}$	Sludge level in the reactor, m	
ρ	Sludge density, kg·m^{-3}	
g	Acceleration of gravity, m·s^{-1}	
$\frac{2\cdot(L+L_{eq})\cdot f\cdot V^2\cdot\rho}{D}$	Linear and accidental pressure drops, Pa	
$q_{imp.}$	Impulsion volumetric flow rate, m^3·s^{-1}	
L	Pipe length, m	
L_{eq}	Equivalent pipe length of accidental pressure drops, m	
V	Velocity, m·s^{-1}	
f	Friction factor	
d	Diameter, m,	
Z_1-Z_2	Height difference, m	
η_{pump}	Pump efficiency	
TMP_{stage}	Transmembrane pressure, Pa	
q_{stage}	Pump volumetric flow rate, m^3·s^{-1}	

$E_{Stirrer}$	Specific power energy of the stirrer, $w \cdot m^{-3}$
η_{engine}	Engine efficiency
$E_{dewatering}$	Specific energy consumption of the dewatering system, $kWh \cdot tSS^{-1}$
M_{MLSS}	Mass flow, $tSS \cdot d^{-1}$

Power energy for stirring and dewatering systems is calculated by Eq.2.6 and Eq.2.7, respectively. The default values included in DESASS for the specific energy consumption ($E_{dewatering}$) of the different types of dewatering systems considered in the model are 5-20, 15-40, 30-60 and 50-150 $kWh \cdot tSS^{-1}$ for band filter, press filter, centrifuge and vacuum filter, respectively.

2.2.1.2 Heat energy (Q)

Table 2.2 shows the equations employed for calculating Q. Q was assumed to be the sum of the following terms: external heat energy (input or output) required when temperature is controlled ($Q_{EXTERNAL}$, Eq.2.8); heat energy dissipated through pipes and reactor walls ($Q_{DISSIPATED}$, Eq.2.9); heat energy released or absorbed by the gas decompression process ($Q_{DECOMPRESSION}$, Eq.2.13); and heat energy released or absorbed by the biological reactions taking place in the treatment unit ($Q_{ENTHALPY}$, Eq.2.20). Figure 2.1 illustrates an example of the process flow diagram related to temperature and heat energy requirements in a closed-air reactor.

Table 2.2 Equations used for determining heat energy requirements in WWTPs.

Heat Energy	Equation	
External heat energy required, $Q_{EXTERNAL}$ in $kcal \cdot h^{-1}$	$C_{P\,water} \cdot q \cdot \rho \cdot \left(T_{fixed} - T_{inflow}\right)$	**Eq.2.8**
Heat energy dissipated through walls, $Q_{DISSIPATED}$ in $kcal \cdot h^{-1}$	$\Sigma U \cdot S \cdot \Delta T$	**Eq.2.9**
Heat transfer coefficient in the non-buried section of the reactor, $U_{non\text{-}baried}$ in $kcal \cdot h^{-1} \cdot m^{-2} \cdot k^{-1}$	$\dfrac{1}{\Sigma \dfrac{\delta_{reactor}}{K_{reactor}} + \dfrac{1}{h_{air}}}$	**Eq.2.10**
Heat transfer coefficient in the buried section of the reactor, U_{buried} in $kcal \cdot h^{-1} \cdot m^{-2} \cdot k^{-1}$	$\dfrac{1}{\Sigma \dfrac{\delta_{reactor}}{K_{reactor}} + \dfrac{\delta_{soil}}{K_{soil}}}$	**Eq.2.11**
Soil conductivity, Ks in $kcal \cdot m^{-1} \cdot h^{-1} \cdot °C^{-1}$	$0.025 \cdot$ % humidity + 1.2	**Eq.2.12**

Heat energy released/absorbed after gas decompression, $Q_{DESCOMPRESSION}$ in kcal·h^{-1}	$\frac{R \cdot T}{\alpha - 1}\left[\left(\frac{P_1}{P_2}\right)^{\frac{\alpha-1}{\alpha}} - 1\right] \cdot \frac{M}{\Sigma(MW \cdot \%)_i \cdot 4.187}$	**Eq.2.13**
Gas temperature (considering heat dissipated through the pipe), $T_{GAS,PIPES}$ in K	$\frac{\Sigma(Cp_i \cdot (T) \cdot \%_i) \cdot [\frac{\mathrm{M}}{\Sigma(MW \cdot \%)_i \cdot 4.187}] \cdot \mathrm{T} - \Sigma \frac{K_{pipe}}{\delta_{pipe}} \cdot S_{pipe} \cdot (\Delta T)}{\Sigma(Cp_i \cdot (T) \cdot \%_i) \cdot [\frac{\mathrm{M}}{\Sigma(MW \cdot \%)_i \cdot 4.187}]}$	**Eq.2.14**
Gas temperature increase during compression, $T_{GAS,COMPRESSION}$ in K	$(\frac{P_2}{P_1})^{\alpha-1/\alpha} \cdot T$	**Eq.2.15**
Molar enthalpy of the reaction at a given temperature, ΔH_T in kcal·mol^{-1}	$\left(\eta \Delta H^{\circ}{}_F\right)_{PRODUCTS} - \left(\eta \Delta H^{\circ}{}_F\right)_{REACTANTS} + \int_{298.15}^{T} \Sigma \eta \cdot C_P$	**Eq.2.16**
Specific heat for solids and liquids, $Cp_{solids\text{-}liquids}$ in kcal·kmol^{-1}·K^{-1}	$\left(A + BT + CT^2 + DT^3 + ET^4\right) \cdot 2.39 \cdot 10^{-7}$	**Eq.2.17**
Specific heat for gases, Cp_{gases} in kcal·kmol^{-1}·K^{-1}	$\left(A + B\left[\left(\frac{\frac{C}{T}}{\sinh\left(\frac{C}{T}\right)}\right)\right]^2 + D\left[\left(\frac{\frac{E}{T}}{\sinh\left(\frac{E}{T}\right)}\right)\right]^2\right) \cdot 2.39 \cdot 10^{-7}$	**Eq.2.18**
Specific heat for dissolved methane, $Cp_{methane}$ in kcal·kmol^{-1}·K^{-1}	$\left(\frac{A^2}{1-\frac{T}{Tc}} + B - 2AC\,(1-\frac{T}{Tc}) - AD\,(1-\frac{T}{Tc})^2 - \frac{C^2\,(1-\frac{T}{Tc})^3}{3} - \frac{CD\,(1-\frac{T}{Tc})^4}{2} - \frac{D^2\,(1-\frac{T}{Tc})^5}{5}\right) \cdot 2.39 \cdot 10^{-7}$	**Eq.2.19**
Heat released/absorbed by biological reactions in the treatment unit, $Q_{ENTHALPY}$ in kcal·h^{-1}	$\Sigma(\frac{r_x \cdot v_{x,y}}{MW} x \Delta H_T)_i\, Vx \frac{1}{24}$	**Eq.2.20**

Symbols

C_{Pwater}	Specific heat, 1 Kcal·Kg^{-1}·K^{-1} for water
q	Inlet flow rate, m^3·h^{-1}
ρ	Sludge density, kg·m^{-3}
T_{fixed}-T_{inflow}	Difference between the intake temperature and the temperature set-point, K
U	Overall heat transfer coefficient, Kcal·h^{-1}·m^{-2}·K^{-1}
$S_{reactor}$	Surface of the reactor/pipe, m^2
ΔT	Temperature difference between the inside and the outside of the reactor/pipe, K
$\delta_{reactor}$	Reactor thickness, m
δ_{soil}	Thickness of the soil in contact with the reactor wall, m
$k_{reactor}$	Conductivity of the reactor material, Kcal·h^{-1}·m^{-1}·K^{-1}
h_{air}	Convective heat transfer coefficient of the air, 12 Kcal·h^{-1}·m^{-2}·K^{-1}
k_{soil}	Soil conductivity, Kcal·h^{-1}·m^{-1}·K^{-1}
M	Mass flow rate of gas, Kg·h^{-1}
T	Compound temperature, K
K_{pipe}	Conductivity of the pipe material, Kcal·h^{-1}·m^{-1}·K^{-1}
δ_{pipe}	Pipe thickness, m
MW	Molecular weight, g·mol^{-1}
P_1	Absolute inlet pressure, atm

P_2	Absolute outlet pressure, atm
α	Adiabatic index
$\Delta H^o_{F,\ PRODUCTS}$	Enthalpy of the products at 298.15 K, Kcal·mol^{-1}
$\Delta H^o_{F,\ REACTANTS}$	Enthalpy of the reactants at 298.15 K, Kcal·mol^{-1}
η	Stoichiometric number
C_P	Specific heat of each component of the reaction, Kcal·mol^{-1}·K^{-1}
A, B, C, D, E	Specifics constants for the compounds (listed in Table 2.1)
Tc	Critic temperature of the dissolved methane, 190.3K
$R_x \cdot v_{x,y}$	Generation/degradation speed of the main compound of the reaction, mg·l^{-1}·d^{-1}
ΔH_T	Enthalpy of the reaction at a given temperature, Kcal·mol^{-1}
V	Volume of the biological reaction, m^3

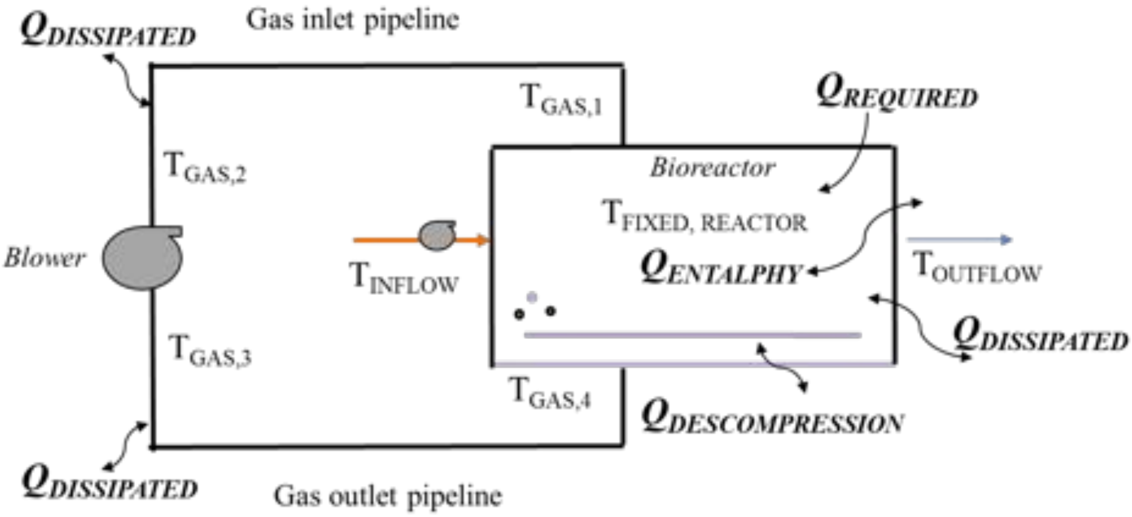

Figure 2.1 Flow diagram related to temperature and heat energy requirements in a closed-air treatment unit.

For calculating the heat energy dissipated (or gain) through the walls of the reactor ($Q_{DISSIPATED}$), the heat transfer coefficient in both surface and buried section of the reactor (see Eq.2.10 and Eq.2.11, respectively) and the soil conductivity (see Eq.2.12) are taken into account. As Eq.2.12 shows, the relationship between soil conductivity and moisture is obtained by linear interpolation, assuming that moist soil is completely saturated on water (100 % humidity and Ks of 3.7 kcal· m^{-1}·h^{-1}·°C^{-1}) and dry soil is completely dried (0% humidity and Ks of 1.2 kcal· m^{-1}·h^{-1}·°C^{-1}).

As Figure 2.1 illustrates, temperature variations occurring through the gas recirculation system have been also estimated in order to calculate the heat absorbed or released in the reactor during the gas decompression process ($Q_{DESCOMPRESSION}$). To this aim, it has been assumed that the gas presents a temperature T_1 in the inlet of the recirculation system equal to the temperature of the mixed liquor inside the reactor. Then, the gas moves through the pipe from the reactor to the blower inlet causing heat loss or gain until reaching a temperature T_2 (Eq.2.14). In the blower the temperature is increased from T_2 to T_3 due to the gas compression process (Eq.2.15). Finally, the gas moves through the pipe from the blower output to the reactor causing heat loss or gain until reaching a temperature T_4 (Eq.2.14).

As the proposed energy model was coupled to the plant-wide model BNRM2, the enthalpy of some key biological reactions involved in wastewater treatment can be calculated. Specifically, from a total of 67 equations from the model BNRM2, 27 equations were employed for calculating molar enthalpy at a given temperature by means of Kirchhoff equation (see Eq.2.16). Hydrolysis, fermentation, precipitation, re-dissolution, bacterial lysis and gas stripping (see [2.18; 2.19] were not included in the model since the heat absorbed or released in these reactions was considered negligible. The empiric formulas used to determine the specific heat of solids and liquids, gases and dissolved methane are shown in Eq.2.17, Eq.2.18 and Eq.2.19, respectively (see Table 2.2). The standard molar enthalpy of formation at 298K and the coefficients of the molar heat capacity at constant pressure (A, B, C, D and E) for each substance are shown in Table 2.3. Table 2.4 shows the biological reactions (including its corresponding molar enthalpy) considered in the proposed energy model. To convert the molar enthalpy of the reactions (kcal·mol^{-1}) to heat units ($Q_{ENTHALPY}$, kcal·h^{-1}), the stoichiometric matrix and kinetics of the biological reactions included in the BNRM2 are used (see Eq.2.20 in Table 2.2).

Table 2.3 Standard molar enthalpy of formation ($\Delta H°_F$) at 298K in Kcal·mol^{-1} and coefficients (A, B, C, D y E) of the molar heat capacity at constant pressure [see 2.22] for solids, liquids and gaseous substances in BNRM2.

Solids and liquids substances	**$\Delta H°_F$, Kcal·mol^{-1}**	**A**	**B**	**C**	**D**	**E**
CH_4(l)	-17.79	6.5708x10^1	3.8883x10^4	-2.5795x10^2	6.1407x10^2	---
$C_2H_4O_2$(l)	-103.37	1.3964x10^5	-3.2080x10^2	8.9850x10^{-1}	---	---
$C_3H_6O_2$(l)	-108.31	2.1366x10^5	-7.0270x10^2	1.6605	---	---
$C_4H_6O_2$(s)	-54.21	1.1600x10^5	---	---	---	---
$C_6H_{10}O_5$(s)	-244.09	2.08x10^5	---	---	---	---
$C_{12}H_{22}O_{11}$(l)	-530.62	2.6565x10^5	6.9779x10^2	---	---	---
CO_2(l)	-94.05	-8.3043x10^6	1.0437x10^5	-4.3333x10^2	6.0052x10^{-1}	
HNO_3(l)	-32.07	1.3125x105	-1.2190x10^2	1.7040x10^{-1}	---	---
H_2CO_3(l)	-146.64	5.5x10^2	4.27x10^2	---	---	---
H2(l)	---	2.256x10^4	-1.9859x10^3	1.1547x10^2	-1.2598	
H_2O(l)	-57.8	2.7637x10^5	-2.0901x10^3	8.1250	-1.4116x10^{-2}	9.3701x10^{-6}
H_2SO_4(l)	-175.57	5.983x10^4	3.9520x10^2	-5.2067x10^{-1}	3.1220x10^{-4}	-7.0570x10^{-8}

$H_2S(l)$	-4.92	$-3.749x10^6$	$-5.5411x10^4$	$2.7765x10^2$	$-4.631x10^{-1}$	---
$H_3PO_4(l)$	-299.54	$5.5228x10^4$	$3.0125x10^2$	---	---	---
$HPO_3(s)$	8.3532	41.727	0.3925	-0.0003	---	---
$NH_4(l)$	-10.96	$3.0094x10^6$	$-4.3692x10^4$	$2.4114x10^2$	$-5.8560x10^{-1}$	$5.2953x10^{-4}$
$NO_2(l)$	4.924	9.1934x104	1.7086x102	$-4.3000x10^{-3}$	---	---
N2(l)	---	$-3.34x10^4$	$3.507x10^3$	$-4.67x10^1$	$2.127x10^{-1}$	---
$O_2(l)$	---	$6.8337x10^4$	$-6.1354x10^2$	7.928	$-3.168x10^{-2}$	---
Gaseous substances						
$H_2S(g)$	-4.92	$3.3288x10^4$	$2.6086x10^4$	$9.1340x10^2$	$-1.7979x10^4$	$9.4940x10^2$
$N_2(g)$	---	$2.9105x10^4$	$8.6149x10^3$	$1.7016x10^3$	$1.0347x10^2$	$9.0979x10^2$
$CO_2(g)$	-94.05	$2.937x10^4$	$3.454x10^4$	$-1.428x10^3$	$2.6400x10^4$	$5.88x10^2$
$CH_4(g)$	-17.79	$3.3298x10^4$	$7.9933x10^4$	$2.0869x10^3$	$4.1602x10^4$	$9.9196x10^2$
$H_2(g)$	---	$2.7617x10^4$	$9.5600x10^3$	$2.466x10^3$	$3.7600x10^3$	$5.6760x10^2$
$NH_3(g)$	-10.96	$3.3480x10^4$	$4.8200x10^4$	$9.5189x10^2$	$-3.0100x10^4$	$1.0560x10^3$
$O_2(g)$	---	$2.9103x10^4$	$1.0040x10^4$	$2.5265x10^3$	$9.356x10^3$	$1.1538x10^3$

Table 2.4 Molar enthalpy at the operating temperature of the biological reactions in wastewater treatment system. **X_{OHO}**: heterotrophic organisms; **X_{PAO}**: polyphosphate accumulating organism; **$X_{PAO,PP}$**: poly-phosphate stored by X_{PAO}; **$X_{PAO,stor}$**: poly-hydroxy-alkanoates stored by X_{PAO}; **X_{AOO}**: ammonium oxidizing organisms; **X_{NOO}**: nitrite oxidizing organisms; **X_{AO}**: acidogenic bacteria; **X_{PRO}**: acetogenic bacteria; **X_{ACO}**: methanogenic acetoclastic organisms; **X_{HMO}**: methanogenic hydrogenotrophic organisms; **S_F**: sucrose; **S_{Ac}**: acetate; **S_{VFA}**: propionate; **S_{NO3}**: nitrate; and **S_{NO2}**: total nitrite concentration.

Aerobic growth of X_{OHO} over S_F	$C_{12}H_{22}O_{11}+ 12O_2 \rightarrow 12CO_2+11H_20$	$\Delta H^o_{T,1=} (12x\ \Delta H^o_{CO2}+11x\Delta H^o_{H2O}) - (\Delta H^o_{C12H12O6}) + \int_{298.15}^{T}[12x\ CpCO2 + 11xCpH2O - CpC12H12O6 - 12xCpO2]\ x(T\text{-}298.15)$
Aerobic growth of X_{OHO} over S_{Ac}	$CH_3COOH+ 2O_2 \rightarrow 2CO_2+2H_20$	$\Delta H^o_{T,2=} (2x\ \Delta H^o_{CO2}+2x\Delta H^o_{H2O})\text{-} (\Delta H^o_{CH3COOH} + \int_{298.15}^{T}[2x\ CpCO2 + 2xCpH2O - CpCH3COOH - 2xCpO2]\ x(T\text{-}298.15)$
Aerobic growth of X_{OHO} over S_{VFA}	$CH_3CH_2COOH+ \frac{7}{2}O_2 \rightarrow 3CO_2+3H_20$	$\Delta H^o_{T,3=}(3x\ \Delta H^o_{CO2}+3x\Delta H^o_{H2O})\text{-} (\Delta H^o_{CH3CH2COOH})+\int_{298.15}^{T}[3x\ CpCO2 + 3xCpH2O) - CpCH3CH2COOH - \frac{7}{2}xCpO2]\ x(T\text{-}298.15)$
Anoxic growth of X_{OHO} over S_F and S_{NO3}	$C_{12}H_{22}O_{11}+ 8NO_3 \rightarrow 12CO_2+11H_20+4N_2$	$\Delta H^o_{T,4=}(12x\ \Delta H^o_{CO2}+11x\Delta H^o_{H2O})\text{-} (\Delta H^o_{C12H22O11}+ 8x\Delta H^o_{NO3}) +\int_{298.15}^{T}[12x\ CpCO2 + 11xCpH2O + 4xCpN2 - CpC12H22O11 - 8xCpNO3]\ \cdot(T\text{-}298.15)$
Anoxic growth of X_{OHO} over S_{Ac} and S_{NO3}	$CH_3COOH + \frac{4}{3}NO_3 \rightarrow 2CO_2+2H_20+\frac{4}{6}N_2$	$\Delta H^o_{T,5=} (2x\ \Delta H^o_{CO2}+2x\Delta H^o_{H2O})\text{-} (\Delta H^o_{CH3COOH} + \frac{4}{3}x\Delta H^o_{NO2}) + \int_{298.15}^{T}[2x\ CpCO2 + 2xCpH2O + \frac{4}{6}xCpN2 - CpCH3COOH - \frac{4}{3}xCpNO2]\ x(T\text{-}298.15)$
Anoxic growth of X_{OHO} over S_{VFA} and S_{NO3}	$CH_3CH_2COOH+\frac{7}{3}NO_3 \rightarrow 6CO_2+6H_20+2N_2$	$\Delta H^o_{T,6=} (6x\ \Delta H^o_{CO2}+6x\Delta H^o_{H2O}\text{-}(\frac{7}{3}X\Delta H^o_{NO3}+ \Delta H^o_{CH3CH2COOH}) +\int_{298.15}^{T}[6x\ CpCO2 + 6xCpH2O + 2xCpN2 - CpCH3CH2COOH - \frac{7}{3}xCpNO3]\ x(T\text{-}298.15)$

Anoxic growth of X_{OHO} over S_F and S_{NO2}	$C_{12}H_{22}O_{11}$+ 12NO_2 → 12CO_2+11H_20+6N_2	$\Delta H^o_{T,7}$= (12x ΔH^o_{CO2}+11xΔH^o_{H2O})- ($\Delta H^o_{sucrose}$+ 12xΔH^o_{NO2}) $+\int_{298.15}^{T}[12x\ CpCO2+11xCpH2O+6xCpN2-Cpsucrose-12xCpNO2]$x(T-298.15)
Anoxic growth of X_{OHO} over S_{Ac} and S_{NO2}	CH_3COOH + 2NO_2 → 2CO_2+2H_20+2N_2	$\Delta H^o_{T,8}$=(2x ΔH^o_{CO2}+2xΔH^o_{H2O})- ($\Delta H^o_{CH3COOH}$ + 2xΔH^o_{NO2}) $+\int_{298.15}^{T}[2x\ CpCO2+2xCpH2O+2xCpN2-CpCH3COOH-2xCpNO2]$x(T-298.15)
Anoxic growth of X_{OHO} over S_{VFA} and S_{NO2}	$CH_3CH_2COOH+\frac{7}{2}NO_2$ → 3CO_2+3H_20+$\frac{7}{4}$N2	$\Delta H^o_{T,9}$= (3x ΔH^o_{CO2}+3xΔH^o_{H2O})- ($\Delta H^o_{CH3CH2COOH}$ + $\frac{7}{2}$xΔH^o_{NO2}) $+\int_{298.15}^{T}[3x\ CpCO2+3xCpH2O+\frac{7}{4}xCpN2-CpCH3CH2COOH-\frac{7}{2}xCpNO2]$x(T-298.15)
Storage of $X_{PAO,\ Stor}$ over S_{Ac}	$(CH_3COOH)1/2$ + 0.5$(C_6H_{10}O_5)1/6$ + 0.44HPO_3 →1.33$(C_4H_6O_2)1/4$ + 0.44H_3PO_4 +0.17CO_2 + 0.023H_2O	$\Delta H^o_{T,10}$= (1.33xΔH^o_{PHA}+0.17xΔH^o_{CO2}+0.44x$\Delta H^o_{phosphoric}$+0.023xΔH^o_{H2O})- ($\Delta H^o_{CH3COOH}$ + 0.5x$\Delta H^o_{glycogen}$ +0.44ΔH^o_{PP}) $+\int_{298.15}^{T}[1.33xCpPHA+0.17xCpCO2+0.44xCpphosphoric+0.023xCpH2O-CpCH3COOH-0.5xCpglycogen-CpPP-p]$x(T-298.15)
Storage of $X_{PAO,\ Stor}$ over S_{VFA}	$(CH_3CH_2COOH)1/3$ +0.5$(C_6H_{10}O_5)1/6$ + 0.44HPO_3 → 1.23$(C_4H_6O_2)$ 1/4 + 0.44H_3PO_4 +0.27CO_2 + 0.023H_2O	$\Delta H^o_{T,11}$= (1.23xΔH^o_{PHA}+0.27xΔH^o_{CO2}+0.44x$\Delta H^o_{phosphoric}$+0.023xΔH^o_{H2O})- ($\Delta H^o_{CH3CH2COOH}$ + 0.5x$\Delta H^o_{glycogen}$+0.44ΔH^o_{PP}) $+\int_{298.15}^{T}[1.23xCpPHA+0.27xCpCO2+0.44xCpphosphoric+0.023xCpH2O-CpCH3CH2COOH-0.5xCpglycogen-0.44CpPP-p]$ x(T-298.15)
Aerobic storage of $X_{PAO,\ PP}$	$C_4H_6O_2$+ H3PO4 +$\frac{9}{2}O_2$ → H PO_3 + 4CO_2+4H_2O	$\Delta H^o_{T,12}$= (4x ΔH^o_{CO2}+4xΔH^o_{H2O}+ΔH^o_{PP})- (ΔH_{PHA}+ ΔH_{H3PO4}) $+\int_{298.15}^{T}[4xCpCO2+4xCpH2O+CpPP-p-CpPHA-CpH3PO4-\frac{9}{2}xCpO2]$x(T-298.15)
Anoxic storage of $X_{PAO,\ PP}$ over S_{NO3}	$C_4H_6O_2$+ H_3PO_4+$\frac{9}{3}NO_3$ → H PO_3 + 4CO_2+4H_2O+$\frac{9}{6}N_2$	$\Delta H^o_{T,13}$= (4xΔH^o_{CO2}+4xΔH^o_{H2O}+ΔH^o_{PP})- (ΔH^o_{PHA}+ ΔH^o_{H3PO4} +$\frac{9}{3}$xΔH^o_{NO3}) $+\int_{298.15}^{T}[4xCpCO2+4xCpH2O+CpPP-p+\frac{9}{6}xCpN2-CpPHA-CpH3PO4-\frac{9}{3}xCpNO3]$ x(T-298.15)
Anoxic storage of $X_{PAO,\ PP}$ over S_{NO2}	$C_4H_6O_2$+ H_3PO_4 +$\frac{9}{2}NO_2$ → H PO_3+ 4CO_2+4H_2O +$\frac{9}{4}N_2$	$\Delta H^o_{T,14}$=(4xΔH^o_{CO2}+4xΔH^o_{H2O}+ΔH^o_{PP})- (ΔH^o_{PHA}+ ΔH^o_{H3PO4} +$\frac{9}{2}$xΔH^o_{NO2}) $+\int_{298.15}^{T}[4xCpCO2+4xCpH2O+CpPP-p+\frac{9}{4}xCpN2-CpPHA-CpH3PO4-\frac{9}{2}xCpNO2]$x(T-298.15
Aerobic growth on X_{PAO}	$C_4H_6O_2$ + $\frac{9}{2}O_2$ → 4CO_2+3H_2O	$\Delta H^o_{T,15}$= (4x ΔH^o_{CO2}+3xΔH^o_{H2O})- (ΔH^o_{PHA}) $+\int_{298.15}^{T}[4x\ CpCO2+3xCpH2O-CpPHA-\frac{9}{2}xCpO2]$ x(T-298.15)
Anoxic growth on X_{PAO} over S_{NO3}	$C_4H_6O_2$ + $\frac{9}{3}NO_3$ → $\frac{9}{6}N_2$+4CO_2+3H_2O	$\Delta H^o_{T,16}$= (4x ΔH^o_{CO2}+3xΔH^o_{H2O})- (ΔH^o_{PHA}+ $\frac{9}{3}$xΔH^o_{NO2}) $+\int_{298.15}^{T}[4x\ CpCO2+3x\ CpH2O+\frac{9}{6}x\ CpN2-CpPHA-\frac{9}{3}xCpNO2]$x(T-298.15)
Anoxic growth on X_{PAO} over S_{NO2}	$C_4H_6O_2$ + $\frac{9}{2}NO_2$ → $\frac{9}{4}N_2$+4CO_2+3H_2O	$\Delta H^o_{T,17}$= (4x ΔH^o_{CO2}+4xΔH^o_{H2O})- (ΔH^o_{PHA}+ $\frac{9}{2}$xΔH^o_{NO2}) $+\int_{298.15}^{T}[4x\ CpCO2+4xCpH2O+\frac{9}{4}xCpN2-CpPHA-\frac{9}{2}xCpNO2]$x(T-298.15)
Total nitrification	NH_4^+ +2 O_2 → NO_3^- +2H^++ H_20	$\Delta H^o_{T,18}$= (ΔH^o_{H2O}+ΔH^o_{NO3})- (ΔH^o_{NH4}) $+\int_{298.15}^{T}[CpH2O+CpNO3-CpNH4-2xCpO2]$ x(T-298.15)
Ammonium anaerobic oxidation (Sharon-Anammox process)	$NH4^+$ + $NO2^-$ → N2 + 2H20	$\Delta H^o_{T,18}$= (2xΔH^o_{H2O}-(ΔH^o_{NO2}+ΔH^o_{NH4}) $+\int_{298.15}^{T}[2xCpH2O+CpN2-CpNH4-CpNO2]$x(T-298.15)
Aerobic growth of X_{AOO}	NH_4^+ +$\frac{3}{2}$ O_2 → NO_2^- +2H^++ H_20	$\Delta H^o_{T,19}$= (ΔH^o_{H2O}+ΔH^o_{NO2})- (ΔH^o_{NH4}) $+\int_{298.15}^{T}[CpH2O+CpNO2-CpNH4-\frac{3}{2}xCpO2]$ x(T-298.15)

Aerobic growth of X_{NOO}	$NO_2^- + \frac{1}{2}O_2 \rightarrow NO_3^-$	$\Delta H^o_{T,20} = (\Delta H^o_{NO3}) - (\Delta H^o_{NO2}) + \int_{298.15}^{T}[CpNO3 - CpNO2 - \frac{1}{2}xCpO2]x(T\text{-}298.15)$
Anaerobic growth of X_{AO} (Acidogenesis)	$C_{12}H_{22}O_{11}+3H_2O \rightarrow 2CH_3COO^- + 2CH_3CH_2COO^- + 2HCO_3^- + 6H^+ + 2H_2$	$\Delta H^o_{T,21} = (2x\ \Delta H^o_{CH3COOH} + 2x\Delta H^o_{CH3CH2COOH} + 2x\Delta H^o_{HCO3}) - (\Delta H^o_{C12H22O11} + 3x\Delta H^o_{H2O}) + \int_{298.15}^{T}[2xCpH2 + 2xCpCH3COOH + 2xCpCH3CH2COOH + 2xCpHCO3 - 3xCpH2O - CpC12H22O11]x(T\text{-}298.15)$
Anaerobic growth of X_{PRO} (Acetogenesis)	$CH_3CH_2COO^- + 3H_2O \rightarrow CH_3COO^- + HCO_3^- + H^+ + 3H_2$	$\Delta H^o_{T,22} = (\Delta H^o_{CH3COOH} + \Delta H^o_{HCO3}) - (\Delta H^o_{CH3CH2COOH} + 3x\Delta H^o_{H2O}) + \int_{298.15}^{T}[CpCH3COOH + CpHCO3 + 3xCpH2 - CpCH3CH2COOH - 3xCpH2O]x(T\text{-}298.15)$
Anaerobic growth of X_{ACO} (Acetoclastic methanogenesis)	$CH_3\text{-}COO^- + H_2O \rightarrow CH_4 + HCO_3^-$	$\Delta H^o_{T,23} = (\Delta H^o_{CH4} + \Delta H^o_{HCO3}) - (\Delta H^o_{CH3COOH} + \Delta H^o_{H2O}) + \int_{298.15}^{T}[CpCH4 + CpHCO3 - CpCH3COOH - CpH2O]x(T\text{-}298.15)$
Anaerobic growth of X_{HMO} (Hydrogenotrophic methanogenesis)	$CO_2 + 4H_2 \rightarrow CH_4 + 2H_2O$	$\Delta H^o_{T,24} = (\Delta H^o_{CH4} + 2x\Delta H^o_{H2O}) - (\Delta H^o_{CO2}) + \int_{298.15}^{T}[CpCH4 + 2xCpH2O - CpCO2 - 4xCpH2]x(T\text{-}298.15)$
Sulphate reduction to sulphide from acetic acid	$CH_3COO^- + SO_4^{2-} \rightarrow HS^- + 2HCO_3^-$	$\Delta H^o_{T,25} = (\Delta H^o_{HS} + 2x\Delta H^o_{carbonic}) - (\Delta H^o_{CH3COOH} + \Delta H^o\ SO_4) + \int_{298.15}^{T}[CpHS + 2xCpcarbonic - CpCH3COOH - CpSO4]x(T\text{-}298.15)$
Sulphate reduction to sulphide from propionic acid	$CH_3CH_2COO^- + 0.75\ SO_4^{2-} \rightarrow CH_3COO^- + 0.75\ S^{2-} + CO_2$	$\Delta H^o_{T,26} = (\Delta H^o_{CH3COOH} + 0.75x\Delta H^o_{HS} + \Delta H^o_{CO2}) - (0.75x\Delta H^o\ SO_4 + \Delta H^o_{CH3CH2COOH}) + \int_{298.15}^{T}[CpCH3COOH + 0.75x\ CpHS + CpCO2 - 0.75xCpSO4 - CpCH3CH2COOH]x(T\text{-}298.15)$
Sulphate reduction to sulphide from H_2	$H_2 + 0.25\ SO_4^{2-} + 0.25\ H^+ \rightarrow 0.25\ HS^- + H_2O$	$\Delta H^o_{T,27} = (0.25x\Delta H^o_{HS} + \Delta H^o_{H2O}) - (0.25\Delta H^o\ SO_4) + \int_{298.15}^{T}[0.25XCpHS + CpH2O - 0.25xCpSO4 - CpH2]\ x(T\text{-}298.15)$

2.2.1.3 Energy recovery from methane capture

CHP technology is used as alternative to conventional energy generation systems. CHP consists of cogeneration through which electrical and heat energy production occurs simultaneously, obtaining an overall efficiency of up to 70-80%.

In WWTPs, CHP technology transforms the hydrogen and methane obtained during the anaerobic digestion of organic matter into heat and power energy, considering the efficiency of the different CHP technologies according to EPA [2.23].

Table 2.5 shows the equations employed in the model for calculating the energy recovery from methane and hydrogen capture in terms of heat ($Q_{methane}$, Eq.2.21) and power ($W_{methane}$, Eq.2.22). The maximum allowable concentration of H_2S (see Eq.2.23 in Table 2.5) in the biogas entering CHP motors (e.g microturbine for cogeneration) was set to 70 mg·MJ^{-1} biogas [2.24].

Table 2.5 Equations used for determining the energy recovery from methane and hydrogen capture in WWTPs.

Energy recovery from methane and hydrogen capture in terms of heat, $Q_{methane}$ in kcal·h^{-1}	$\frac{V_{biogas}\cdot(\%CH_4\cdot CV_{CH4}+\%H_2\cdot CV_{H2})\cdot\%_{heat effciency CHP}}{1000\cdot 24\cdot 4.187}\cdot\%_{Heat\ exchanger}$	**Eq.2.21**
Energy recovery from methane and hydrogen capture in terms of power, $W_{methane}$ in kW	$\frac{V_{biogas}\cdot(\%CH_4\cdot CV_{CH4}+\%H_2\cdot CV_{H2})\cdot\%_{power effciency CHP}}{1000\cdot 24\cdot 3600}$	**Eq.2.22**
Allowable value of H_2S in $mg_{H20}\cdot Mj^{-1}{}_{biogas}$	$\frac{\%_{H2S}\cdot MW_{H2S}}{(\%_{CH4}\cdot CV_{CH4}+\%H_2\cdot CV_{H2}\cdot 22.4)\cdot 10^{-3}}$	**Eq.2.23**

Symbols

V_{biogas}	Biogas volume, l·d^{-1}
$\%CH_4$	Methane richness, %
CV_{CH4}	Methane calorific power, KJ·m^{-3}
$\%H_2$	Hydrogen richness, %
CV_{H2}	Hydrogen calorific power, KJ·m^{-3}
$\%_{\text{heat efficiency CHP}}$	Heat efficiency of the CHP system, %
$\%_{\text{heat exchanger}}$	Heat exchanger efficiency, %
$\%_{\text{power efficiency CHP}}$	Power efficiency of the CHP system, %
$\%H_2S$	Hydrogen sulphur percentage, %
MW_{H2S}	Hydrogen sulphur molecular weight, mg·m^{-3}

2.2.2 Implementation of the energy model in the simulation software DESASS

Ferrer et al. [2.9] developed a computational software called DESASS for designing, simulating and optimising both aerobic and anaerobic wastewater treatment technologies, considering the most important physical, chemical and biological processes taking place in a traditional WWTP. Afterwards, DESASS was extended and updated for including new technologies such as SHARON, BABE, MBR and AnMBR. Moreover, DESASS incorporates a tool for designing the whole aeration system (i.e. blowers, piping and valve system, diffusers and their supports). As commented before, the simulation software incorporates an extended version of the plant-wide model BNRM2 [2.18], including the competition between both acetogenic and methanogenic microorganisms and sulphate-reducing microorganisms [2.19]. This mathematical model was validated beforehand using experimental data obtained from different wastewater treatment processes (see, for instance, [2.25; 2.26; 2.27; 2.28], including AnMBR likewise [2.19].

Apart from being useful for designing, simulating and optimising WWTPs in terms of process performance, DESASS has been updated for incorporating an energy model toolbox entailing the proposed plant-wide energy model. The principles guiding the development of this toolbox are user friendliness and flexibility to incorporate several elements involving power and heat energy demand in different WWTPs.

Figure 2.2 shows some of the windows that can be generated in DESASS by using the developed toolbox. In particular, this figure shows the design parameters related to the power energy requirements of a blower (Figure 2.2a); and the heat energy requirements in an AnMBR (Figure 2.2b).

In order to calculate the energy demand of a WWTP through the proposed tool, the following steps must be trailed:

(1) Creating a wastewater treatment layout incorporating both treatment units (e.g. settler, reactor, digester, thickener, dewatering system, etc…) and mechanical elements (e.g. pumps, blowers, diffusers, rotofilter, mechanical stirrers, circular suction scraper bridges, and sludge dewatering system).

(2) Defining all the necessary design parameters related to power and heat energy requirements (see Figure 2.2).

(3) Simulating the defined layout in order to obtain the results from the applied model.

Once the simulations have been finished, DESASS provides the energy model results of the evaluated system, including the before-mentioned terms: power requirements, heat energy requirements, cogenerated energy, and net energy demand. Moreover, the power energy requirements of each mechanical element and the heat energy requirements of each treatment unit can be shown independently clicking on the elements included in the designed layout.

Design parameters related to power energy requirements

Regarding the design of pumps and liquid pipelines, the toolbox allows the user editing the following terms: height difference in fluid level between two treatment units connected by a pumping system; engine and pump efficiency; and inlet and outlet pipe characteristics. As regards pipe characteristics, the following terms can be edited: material in order to establish the roughness and conductivity; either nominal diameter and fluid velocity for calculating the number of pipes or number of pipes and fluid velocity for calculating the nominal diameter; thickness; length; and equivalent length of accessories.

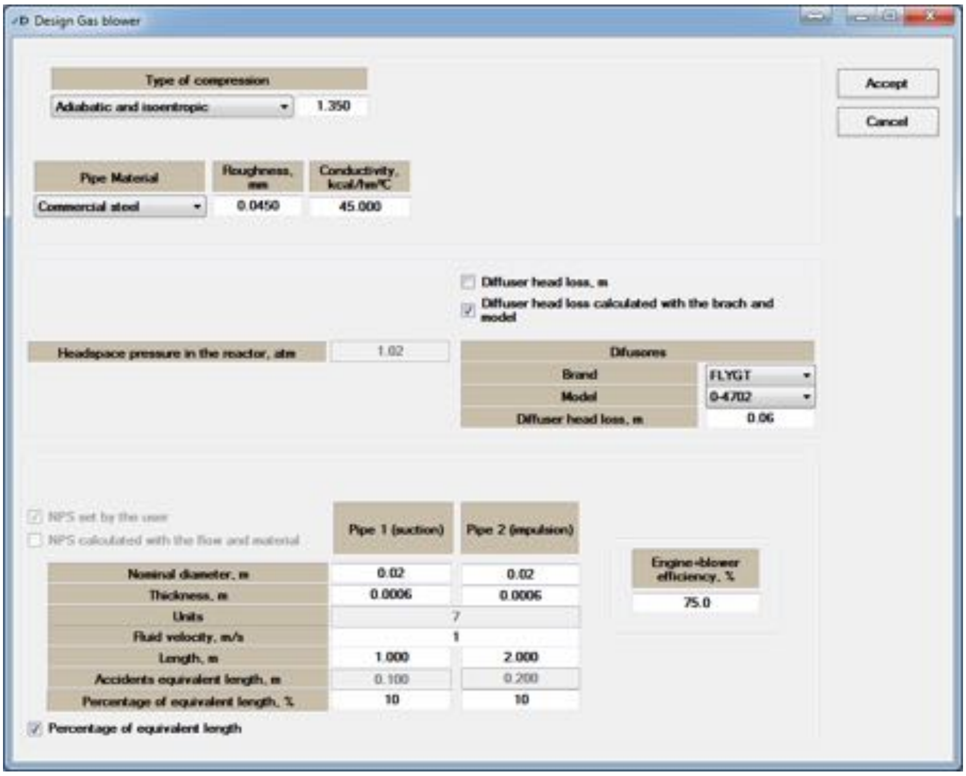

(a)

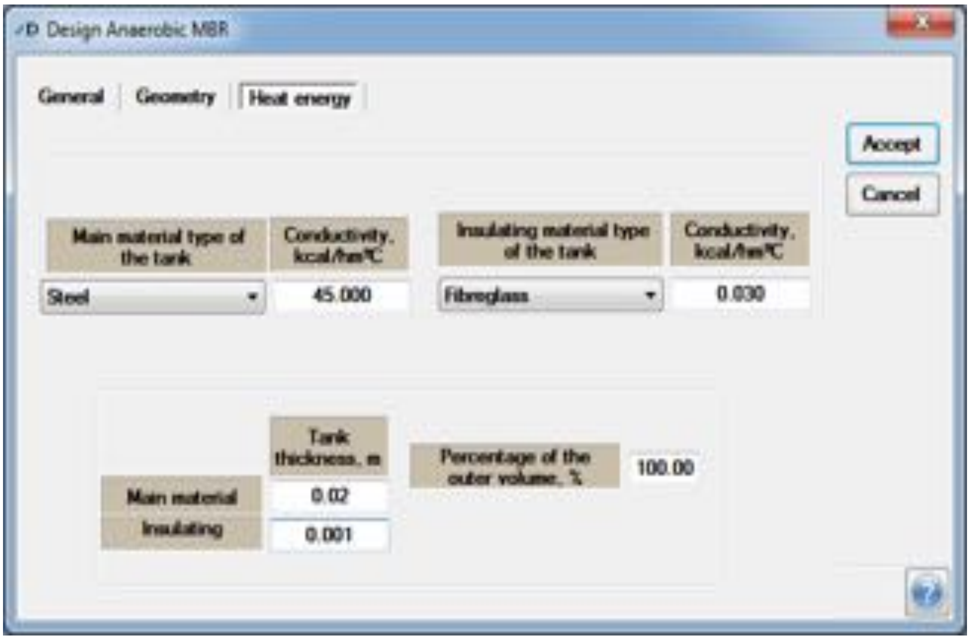

(b)

Figure 2.2 Example of a window extracted from the energy tool included in DESASS: **(a)** design properties of the gas blower; and **(b)** design properties of the anaerobic MBR.

Regarding the design of blowers and gas pipelines, the toolbox allows the user editing the following terms: headspace pressure in closed-air reactors; type of compression (adiabatic and isentropic, isothermal or polytropic); branch and model of the diffusers in order to calculate the head loss; inlet and outlet pipe characteristics (same terms as liquid pipelines); and engine and blower efficiency.

In order to calculate the real power energy requirements of pumps and blowers, the toolbox allows selecting commercial equipment extracted from an editable database including the following specifications: model, branch, flow, pressure and motor power. Flow, pressure and theoretical power consumption are calculated using Equations 2.2- 2.5, and are compared to those included in the database in order to propose a list of equipment fitting the requirements of the evaluated layout.

Regarding the design of stirrers, the user is able to edit power energy consumption in terms of $W \cdot m^{-3}$ and efficiency. Therefore, the toolbox compares the theoretical power requirements of the stirrer (calculated using the corresponding tank volume) to the power requirements from commercial equipment included in the editable database in order to propose a list of equipment fitting the design specifications. Concerning the dewatering system, the user is able to edit type (e.g. band filter, press filter, centrifuge and vacuum filter) and efficiency, thus the toolbox automatically selects power energy consumption in terms of $kWh \cdot tSS^{-1}$ in order to calculate the power requirements of the selected item. As regards rotofilter, the user is able to edit the motor power in terms of W; whilst for circular suction scraper bridges, the toolbox provides a list of models from the database that fit the corresponding motor power by selecting the unit branch.

Hence, the toolbox includes a database for selecting commercial equipment fitting the design criteria. This database can be edited by the user in order to incorporate new equipment.

Design parameters related to heat energy requirements

In order to calculate the heat energy dissipated through the walls of the reactor, the toolbox allows the user editing the temperature inside and outside the reactor, the temperature of the inflow, the type and thickness of reactor material (in order to calculate the conductivity), the type and thickness of insulating material (in order to calculate the conductivity), the reactor geometry and dimensions, the % of the outer reactor, the % of soil humidity and the thickness of the soil in contact with the reactor.

As previously mentioned, the toolbox allows the user editing the design parameters of the blower (e.g. headspace reactor pressure, type of compression, inlet and outlet pipe characteristics, etc.) in order to calculate the heat energy released or absorbed by the gas decompression process.
Moreover, the user is able to choice one of the two following options for heat energy calculation: (1) operating at fixed temperature thus simulating total heat energy requirements; or (2) operating at fixed heat energy requirements thus simulating system temperature.

Design parameters of cogeneration energy

For the cogeneration system, it is possible to select the type of CHP system to be used (e.g. steam turbine, reciprocating internal combustion engine, gas/combustion turbine and microturbine) in order to calculate power and heat energy production efficiency and also the efficiency of the heat exchanger. Therefore, the tool calculates the power and heat energy recovery from hydrogen and methane capture (biogas and dissolved methane in the effluent).

2.3 Case study

2.3.1 Modelling energy demand in a CAS and AnMBR urban WWTP at steady-state conditions

2.3.1.1 Design and operating parameters

The performance of the proposed plant-wide energy model at steady-state conditions is illustrated in this study by two case-specific examples of urban WWTP, including as main treatment technology: 1) CAS, and 2) AnMBR coupled to an aerobic-based post-treatment for nutrient removal. These treatment schemes were designed for meeting the European discharge quality standards (sensitive areas and population of more than 100000 p-e) as regards solids (<35 $mg \cdot L^{-1}$ of tSS), organic matter (<125 and 25 $mg \cdot L^{-1}$ of COD and BOD, respectively) and nutrients (<10 and 1 $mg \cdot L^{-1}$ of N and P, respectively). It is worth to point out that chemical removal of phosphorus was assumed in both cases for meeting phosphorous effluent standards. In addition, a maximum value of 35% of biodegradable volatile suspended solids (BVSS) was considered as sludge stabilisation criteria.

The classical AO (anoxic – oxic) configuration was selected for designing the aerobic-based treatment units (CAS-based WWTP and post-treatment unit in the AnMBR-based WWTP). The volume of anoxic and oxic tanks was 40 and 60% of total reactor volume, respectively.

Figure 2.3 shows the main window of DESASS with the layout of the CAS- and AnMBR-based WWTPs evaluated in this study. These treatment schemes were designed and simulated for a treatment flow rate of 50000 $m^3 \cdot day^{-1}$ and ambient temperature of 20 ºC. The full characterisation of the urban wastewater (UWW) used in this study is shown in Table 2.6. This characterisation corresponds with the effluent from the pre-treatment of the Carraixet WWTP (Valencia, Spain). Two simulation scenarios were evaluated: the treatment of sulphate-rich UWW (9.45 mg $COD \cdot mg^{-1}$ SO_4-S, corresponding with an influent sulphate concentration of 100 mg SO_4-$S \cdot L^{-1}$); and the treatment of low-sulphate UWW (94.5 mg $COD \cdot mg^{-1}$ SO_4-S, corresponding with an influent sulphate concentration of 10 mg SO_4-$S \cdot L^{-1}$). Methane capture efficiency was set to 100% in this case study.

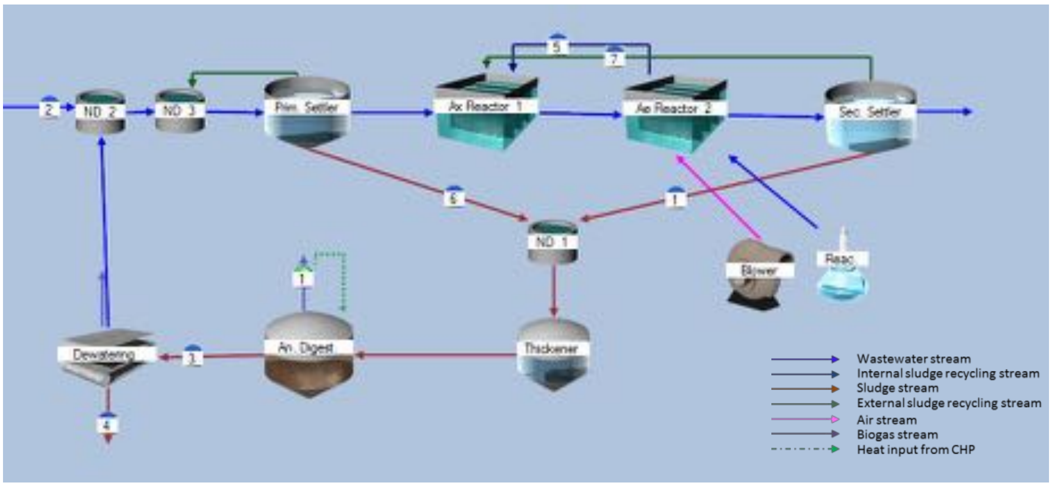

(a)

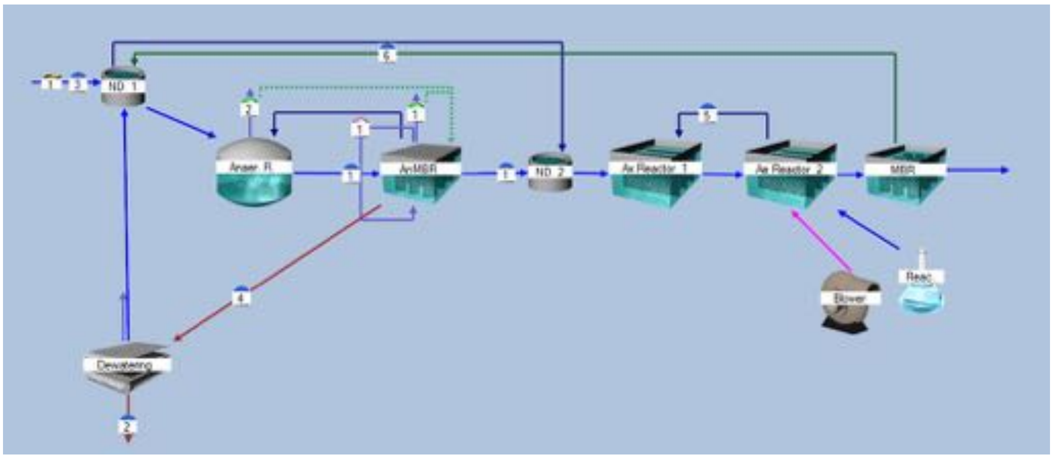

(b)

Figure 2.3 Main window of DESASS including the layout of the **(a)** CAS- and **(b)** AnMBR-based WWTPs (coupled to AeMBR-based post-treatment) evaluated in this study. Nomenclature: **ND**: Chamber; **Prim. Settler:** Primary Settler; **Sec. Settler:** Secondary Settler; **Ax Reactor:** Anoxic tank; **Ae Reactor:** Aerobic tank; **Reac.**: Reactant: (FeCl for P removal); **An. Digest.:** Anaerobic Digester; **MBR:** Membrane Bioreactor; **Anaer. R.**: Anaerobic Reactor; **AnMBR**: Anaerobic Membrane Bioreactor.

CAS technology: As commented before, the CAS unit consisted of an AO (anoxic – oxic) configuration, which was operated at hydraulic retention time (HRT) of 24 hours, sludge retention time (SRT) of 10 days and mixed liquor suspended solids (MLSS) concentration of 2.3 $g \cdot L^{-1}$. An anaerobic digester (operating at 35 ºC) was also included as main element of the CAS-based WWTP to meet the sludge stabilisation criteria. Heat energy input was needed to maintain a temperature of 35 ºC in the anaerobic digester unit. Biogas was considered to be captured from the anaerobic digester unit and used to generate energy.

Table 2.6 Characteristics of the wastewater entering the designed WWTPs (**sulphate-rich municipal wastewater; **low-sulphate municipal wastewater*).

Parameter	Unit	Value
T-COD	mg COD $\cdot L^{-1}$	945
T-BOD	mg COD$\cdot L^{-1}$	715
S-COD	mg COD $\cdot L^{-1}$	285
S-BOD	mg COD$\cdot L^{-1}$	255
TN	mg N$\cdot L^{-1}$	47
NH_4-N	mg N$\cdot L^{-1}$	16
TP	mg P$\cdot L^{-1}$	13
PO_4-P	mg P$\cdot L^{-1}$	4
SO_4-S	mg S$\cdot L^{-1}$	100*/10**
TSS	mg TSS$\cdot L^{-1}$	429
NVSS	mg NVSS$\cdot L^{-1}$	100

AnMBR technology: The AnMBR unit was operated at HRT of 18 hours, SRT of 40 days, 20 ºC-standardised transmembrane flux (J_{20}) of 20 LMH, specific gas demand per square metre of membrane area (SGD_m) of 0.1 $m^3 \cdot m^{-2} \cdot h^{-1}$ and MLSS in the membrane tank of 14 $g \cdot L^{-1}$. This operating mode resulted in minimum filtration costs in previous studies [2.29; 2.30]. Further digestion of the sludge was not required since the AnMBR unit was already designed for meeting the sludge stabilisation criteria. Biogas and methane dissolved in the effluent were both considered to be captured and used to generate energy. A post-treatment step based on AO (anoxic – oxic) configuration with chemical addition for phosphorous removal was included in the AnMBR-based treatment scheme in order to meet nutrient effluent standards. This step contemplated two possibilities: AeMBR- and CAS-based post-treatment. The AeMBR-based post-treatment was operated at SRT of 10 days, J_{20} of 29 LMH, specific air demand per square metre of membrane area (SAD_m) of 0.3 $m^3 \cdot m^{-2} \cdot h^{-1}$ and MLSS in the membrane tank of 2.6 $g \cdot L^{-1}$; whilst the CAS-based post-treatment was operated at SRT of 10 days and MLSS concentration of 2.3 $g \cdot L^{-1}$. A fraction of the influent wastewater was bypassed anyhow to the post-treatment unit in order to meet effluent quality standards (further organic matter was required for denitrification rather than the contained in the effluent from the AnMBR unit). Specifically, around 27% of the wastewater entering the AnMBR-based WWTP was derived directly to the post-treatment unit (see Figure 2.3).

2.3.1.2 Simulation results

Figure 2.4 shows the weighted average distribution of the simulated energy input and output for the CAS- and AnMBR-based WWTPs. As Figure 2.4 shows, the main term contributing the energy demand of the CAS-based WWTP was the power energy input (about 62.3%). In absolute terms, power requirements resulted in 0.48 $kWh \cdot m^{-3}$, heat energy requirements (to maintain a temperature of 35 ºC in the anaerobic digester) resulted in 245 $kcal \cdot m^{-3}$ and power and heat energy recovery from the produced biogas was 0.30 $kWh \cdot m^{-3}$ and 222 $kcal \cdot m^{-3}$, respectively. As regards the simulated AnMBR-based WWTP, energy demand was completely related to power energy input, since heat energy requirements were null due to operating at ambient temperature conditions. In absolute terms, power requirements resulted in 0.66 and 0.48 $kWh \cdot m^{-3}$ in AeMBR- and CAS-based post-treatment configurations, respectively. Power recovery from methane in both AeMBR- and CAS-based post-treatment configurations was 0.27 and 0.45 $kWh \cdot m^{-3}$ when treating sulphate-rich (100 mg SO_4-$S \cdot L^{-1}$) and low-sulphate (10 mg SO_4-$S \cdot L^{-1}$) urban wastewater, respectively. Therefore, the energy demand of CAS technology resulted in approx. 0.21 $kWh \cdot m^{-3}$ whilst for AnMBR coupled to an AeMBR- and CAS-based post-treatment resulted in approx. 0.38 and 0.21 $kWh \cdot m^{-3}$, respectively, when treating sulphate-rich UWW. Nevertheless, this energy demand could be reduced to 0.21 and 0.04 $kWh \cdot m^{-3}$ in AnMBR coupled to an AeMBR- and CAS-based post-treatment, respectively, when treating low-sulphate UWW. Hence, it can be concluded that from an energy perspective, AnMBR coupled to a CAS-based post-treatment may be a sustainable approach for UWW treatment in comparison with other existing technologies under the operating conditions and UWW characteristics evaluated in this case study.

2.3.2 Modelling temperature and heat energy requirements in an AnMBR system at unsteady-state conditions.

2.3.2.1 Design and operating parameters

The performance of the proposed plant-wide energy model at unsteady-state conditions was assessed by comparing the model results to experimental data obtained from an AnMBR plant that treated effluent from the pre-treatment of a full-scale WWTP (Valencia, Spain) (see Table 2.6).

The AnMBR plant consists of an anaerobic reactor with a total volume of 1.3 m^3 (0.4 m^3 head-space volume) connected to two membrane tanks each one with a total volume of 0.8 m^3 (0.2 m^3 head-space volume). Each membrane tank includes one ultrafiltration hollow-fibre membrane commercial system (PURON®, Koch Membrane Systems, 0.05 µm pore size, 30 m^2 total filtering area). A rotofilter of 0.5 mm screen size has been installed as pre-treatment system. One equalisation tank (0.3 m^3) and one CIP tank (0.2 m^3) are also included as main elements of the pilot plant. In order to control the temperature when necessary, the anaerobic reactor is jacketed and connected to a water heating/cooling system. Further details on this AnMBR can be found in Giménez et al. [2.31] and Robles et al. [2.32].

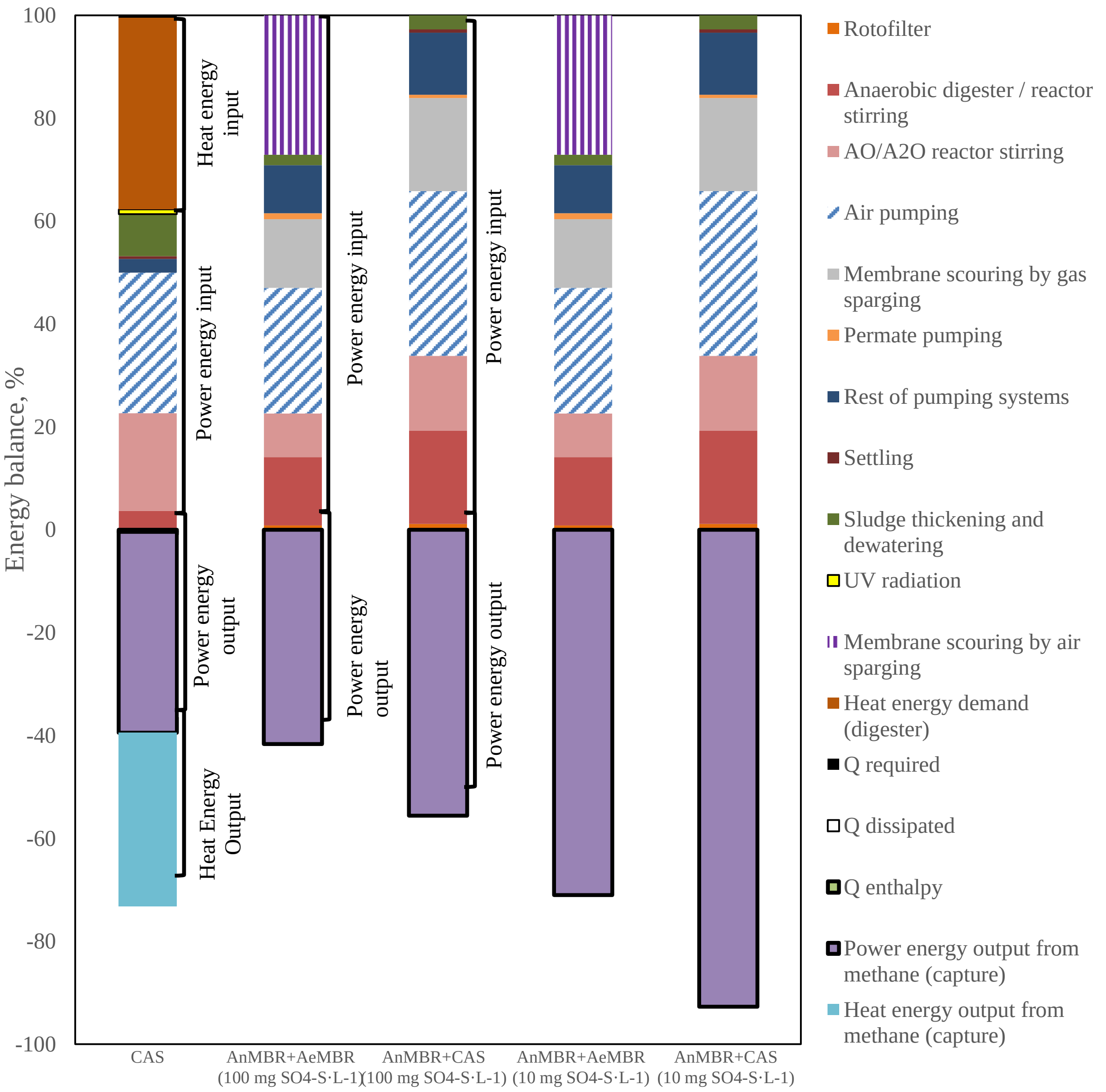

Figure 2.4 Weighted average distribution of the energy input and output in CAS and AnMBR (coupled to an AeMBR- or CAS-based post-treatment and treating 100 and 10 mg SO_4-S·L^{-1}) for UWW treatment.

Numerous on-line sensors and items of automatic equipment were installed in order to automate and control plant operations and provide on-line information about the state of the process [2.32]. The on-line sensors employed in this study consist of the following: two pH-temperature transmitters used to measure the temperature in both inflow and AnMBR; one flow indicator transmitter used for calculating the amount of mixed liquor to be heat; and one automatic valve that allows to pass water through the reactor jacket for controlling the temperature in the system. Besides the on-line process monitoring, grab samples of anaerobic sludge were taken for measuring sludge density.

As commented above, the temperature of the wastewater entering the AnMBR plant and the temperature inside the reactor were continuously recorded. Ambient temperature was obtained from a weather station located near the position of the plant. Hourly and daily average ambient temperature data was facilitated by the Spanish State Meteorological Agency [2.33].

According to the structure of the AnMBR plant, the following heat energy design parameters were considered for simulating the heat energy dissipated though the reactor walls: steel as reactor material, 3-cm reactor wall thickness, fiberglass as insulating material, 2-cm fiberglass thickness, cylinder and rectangular geometry for reactor and membrane tanks, respectively, 0.7-m diameter and 2.1-m height for reactor dimensions, 3-m height, 1.1-m width and 0.3-m depth for membrane tank dimensions, and 100% of outer volume.

The energy model was validated for both short-term and long-term operation. The short-term validation comprised an operating period of 24 hours, whilst the long-term validation comprised an operating period of 30 days. Both validations aimed at demonstrating the capability of the proposed model to reproduce energy variations in AnMBRs even when operating under dynamic conditions (i.e. ambient temperature and/or inflow temperature suffered different variations).

2.3.2.2 Simulation results

Figure 2.5 illustrates the variations in both experimental and simulated reactor temperature during a 24-hour operating period (Figure 2.5a and Figure 2.5b) and during a 30-day operating period (Figure 2.5c). External heat energy requirements were null ($Q_{EXTERNAL}$=0, Eq.2.8) since the temperature in the system was not controlled (reactor free temperature). As Figure 2.5 shows, the reactor temperature variations were mainly related to variations in the inflow temperature and ambient temperature, affecting therefore $Q_{DISSIPATED}$ (Eq.2.9); $Q_{DECOMPRESSION}$ (Eq.2.13) and $Q_{ENTHALPY}$ (Eq.2.20). Overall, the proposed model was able to correctly reproduce temperature dynamics in the evaluated AnMBR system.

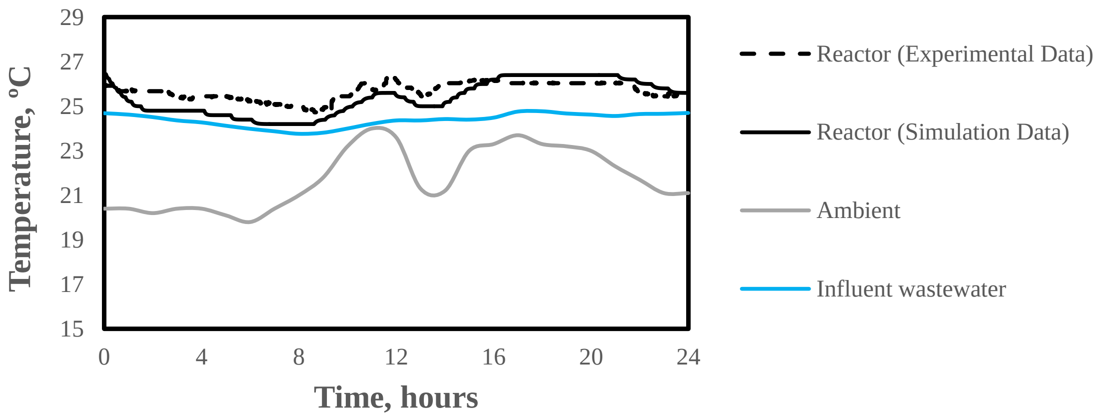

(a)

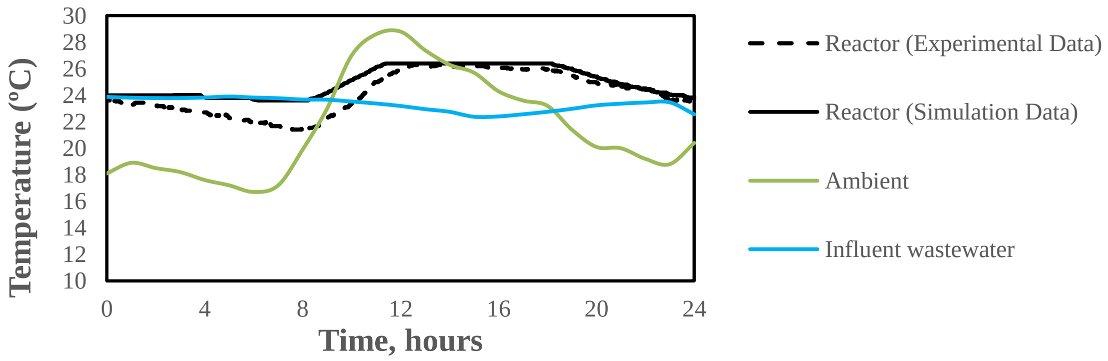

(b)

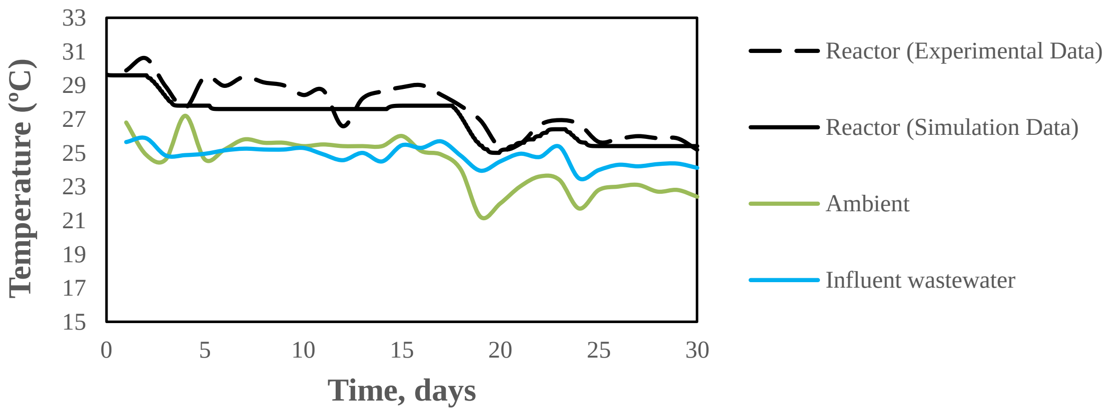

(c)

Figure 2.5 Experimental and simulated temperature considering null heat energy requirements in the AnMBR plant during a: **(a)** 24-hour operating period; **(b)** 24-hour operating period; and **(c)** 30-day operating period.

Figure 2.6 shows the experimental and simulated heat energy requirements in the AnMBR plant during a 24-hour period (Figure 2.6a and Figure 2.6b) and during a 30-day operating period (Figure 2.6c). All cases were run at controlled temperature of around 20ºC. Experimental heat energy requirements in Figure 2.6 were estimated according to the time interval during which the heating (Figure 2.6a and Figure 2.6c) or cooling (Figure 2.6b) valve opened. The heating/cooling time was expressed in minutes per hours in short-term operation (Figure 2.6a and Figure 2.6b) and hours per day in long-term operation (Figure 2.6c).

For the 24-hour period operating with heating system (see Figure 2.6a), the time interval (minutes/hour) during which the heating valve remained open decreased and increased according to variations in heat energy requirements for temperature control (see hours from 0 to 12 and from 12 to 24, respectively). Indeed, ambient temperature increased throughout the first 12 hours of operation and decreased during the last 12 hours, affecting therefore heat energy requirements. Comparing the tendency on the experimental data regarding heating time with the simulation results, it can be said that the proposed model was able to predict variations in heat energy requirements in the evaluated AnMBR system.

For the 24-hour period operating with cooling system (see Figure 2.6b), the cooling valve remained continuously opened from hours 8 to 18 (cooling time up to 60 minutes/hour). During this period, the ambient temperature increased (see hours from 8 to 14). Hence, higher external output of heat energy was required for controlling the temperature around the established set-point. As Figure 2.6a, the model was capable to predict the heat energy demand required for controlling the reactor temperature.

As regards the long-term validation, Figure 2.6c illustrates a decrease in the heating time (hours/day) during the 30-day period operating with heating system. Specifically, the time during which the heating valve remained open decreased during the first 18 days of operation due to an increase recorded in ambient temperature. From days 18 to 23 both ambient and inflow temperature decreased, resulting therefore in increased heating time. From days 23 to 28, the time interval during which the heating valve open decreased due to a new increase recorded in inflow and ambient temperature (see days from 23 to 28). As Figure 2.6s shows, the simulated heat energy requirements follow a similar pattern than the experimental heating time.

Hence, the experimental and model results shown in Figure 2.5 and Figure 2.6 indicate that the proposed model is capable to reproduce temperature and/or heat energy requirements versus variations in operating and environmental conditions.

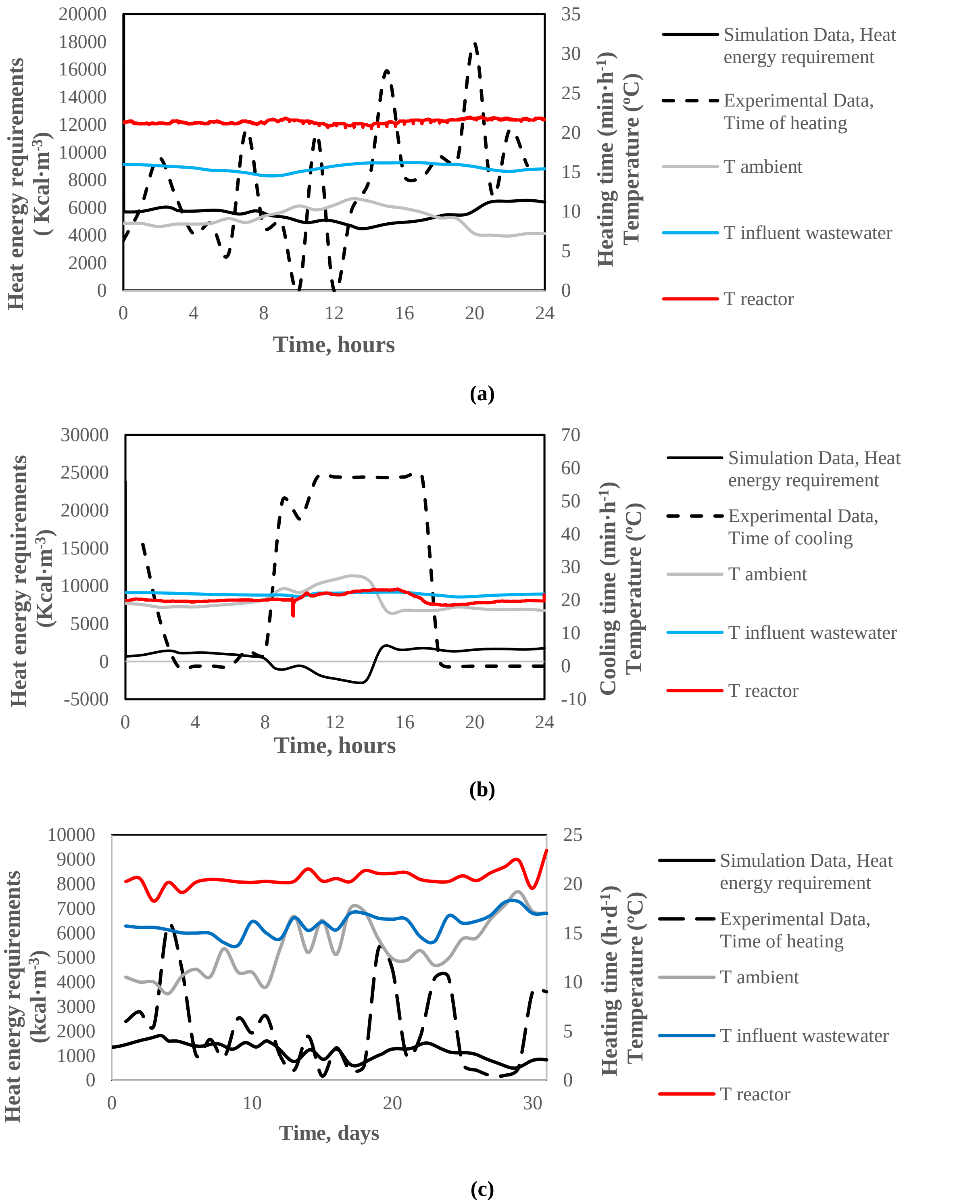

Figure 2.6 Experimental (time of heating/cooling, min·h^{-1}/ h·day^{-1}) and simulated (heat energy requirements, kcal·m^{-3}) heat energy requirements at controlled temperature of 20ºC in the AnMBR plant during a: **(a)** 24-hour operating period (heating requirements); **(b)** 24-hour operating period (cooling requirements); and **(c)** 30-day operating period.

2.4 The possible role of the proposed tool in the achievement of the carbon neutral WWTP

As previously commented, plant-wide modelling in the wastewater treatment field is attractive to many researchers as it provides a holistic view of the process and it allows for a more comprehensive understanding of the interactions between unit processes. Therefore, the proposed plant-wide energy modelling tool could represent a useful application for evaluating the energy consumption and efficiency of different wastewater treatment alternatives, focussing furthermore in reducing the associated potential environmental impact (e.g. GHG emissions). Different layouts can be easily evaluated under different influent, environmental and operating conditions, allowing to assess sustainability in the WWT field.

Therefore, this tool might be useful for supporting complex decisions for a particular problem under reduced time frames. Specifically, the tool could be helpful on determining for each specific case (i.e. implementation, upgrading and operation) whether one technology is the best available option or not. The tool could be therefore useful to justify multi-criteria decisions and provide end-users a tool to explore "what-if" scenarios.

Hence, the proposed plant-wide energy model can be used for different purposes such as WWTP design or upgrading, and development of new control strategies for energy savings and thus contributing to the pursuit of carbon neutral wastewater treatment.

2.5 Conclusions

This paper presents a detailed and comprehensive plant-wide model for assessing the energy demand of different wastewater treatment systems at both steady- and unsteady-state conditions. Two case studies have been evaluated: (1) modelling the energy demand of two possible urban WWTPs based on CAS and AnMBR technologies at steady-state conditions; and (2) modelling variations in reactor temperature and heat energy requirements in an AnMBR plant at unsteady-state conditions. The model was able to reproduce energy variations in AnMBRs even when operating under dynamic conditions (i.e. ambient temperature and/or inflow temperature suffered different variations). The proposed plant-wide energy model could be useful for different purposes such as WWTP design or upgrading, and development of new control strategies for energy savings.

2.6 Acknowledgements

This research work has been supported by the Spanish Ministry of Science and Innovation (MICINN, Project CTM2011-28595-C02-01/02) jointly with the European Regional Development Fund (ERDF) which are gratefully acknowledged. Ambient temperature data was facilitated by the Spanish State Meteorological Agency (AEMET), which is gratefully acknowledged.

2.7 References

2.1 G. Olsson, B. Carlsson, J. Comas, J. Copp, K.V. Gernaey, P. Ingildsen, U. Jeppsson, C.Kim, L. Rieger, I. Rodríguez-Roda, J.P. Steyer, I. Takács, P.A. Vanrolleghem, A. Vargas Casillas, Z. Yuan, L. Åmand, Instrumentation, Control and Automation in Wastewater- from London 1973 to Narbonne 2013. Water Sci. Technol. 69 (2014), 1373-85.

2.2 B. Nicolae, B. George-Vlad, Life cycle analysis in refurbishment of the buildings as intervention practices in energy saving Energ. Buildings 86 (2015), 74–85.

2.3 L. Corominas, J. Foley, J.S. Guest, A. Hospido, H.F. Larsen, S. Morera, A. Shaw, Life cycle assessment applied to wastewater treatment: State of the art. Water Res. 47 (2013), 5480-5495.

2.4 A. Bauer, P. Böschb, A. Friedl, T. Amona, Analysis of methane potentials of steam-exploded wheat straw and estimation of energy yields of combined ethanol and methane production. J. Biotechnol.142 (2009), 50-55.

2.5 G. Venkatesh, R.A. Elmi, Economic-environmental analysis of handling biogas from sewage sludge digesters in WWTPs (wastewater treatment plants) for energy recovery: Case study of Bekkelaget WWTP in Oslo (Norway). Energy 58 (2013), 220-235.

2.6 EPA, Environmental Protection Agency, Combined Heat and Power Partnership, Agency of the United States federal government, 2015.

2.7 N. Descoins, S. Deleris, R. Lestienne, E. Trouvé, F. Maréchal, Energy efficiency in waste water treatments plants: Optimization of activated sludge process coupled with anaerobic digestion. Energy (2011) 1-12.

2.8 K.V. Gernaey, M.C.M. van Loosdrecht, M. Henze, M. Lind, S.B. Jørgensen, Activated sludge wastewater treatment plant modelling and simulation: state of the art. Environ. Modell. Softw.19 (2004), 763-783.

2.9 J. Ferrer, A. Seco, J. Serralta, J. Ribes, J. Manga, E. Asensi, J.J. Morenilla, F. Llavador, DESASS: A software tool for designing, simulating and optimising WWTPs, Environ. Modell. Softw. 23 (2008) 19–26.

2.10 H. Bozkurt, A. Quaglia, K.V. Gernaey, G. Sin, A mathematical programming framework for early stage design of wastewater treatment plants. Environ. Modell. Softw. 64 (2015), 164-176.

2.11 U. Jeppsson, C. Rosen, J. Alex, J. Copp, K.V. Gernaey, M.N. Pons, P.A. Vanrolleghem, Towards a benchmark simulation model for plant-wide control strategy performance evaluation of WWTPs. Water Sci. Technol. 53 (2006), 287-295.

2.12 J. Gómez, M. de Gracia, E.Ayesa, J.L Garcia-Heras, Mathematical modelling of autothermal thermophilic aerobic digesters. Water Res. 41 (2007), 959-968.

2.13 S. Righi, L. Oliviero, M. Pedrini, A. Buscaroli, C.D. Casa, Life Cycle Assessment of management systems for sewage sludge and food waste: centralized and decentralized approaches. J. Clean. Prod. 44 (2013), 8-17.

2.14 D. Lemos, D.C. Dias, X. Gabarrell, L. Arroja, Environmental assessment of an urban water system. J. Clean. Prod. 54 (2013), 157-165.

2.15 O.Nowak, P. Enderle, P. Varbanov, Ways to optimize the energy balance of municipal wastewater systems: lessons learned from Austrian applications. J. Clean. Prod. 88 (2015), 125-131.

2.16 M. Tous, B. Ladislav, L. Houdková, M. Pavlas, P. Stehlík, Waste-to energy (W2E) software- a support tool for decision making process. Brno University of Technology, Institute of Process and Environmental Engineering, Chemical Engineering Transactions volume 18 (2009).

2.17 I. Pijákovà, J. Derco, Application of Dynamic Simulations for Assessment of Urban Wastewater Systems Operation. Chem. Biochem. Eng. Q. 29 (2015) 55-62.

2.18 R. Barat, J. Serralta, M.V. Ruano, E. Jiménez, J. Ribes, A. Seco, J. Ferrer, Biological Nutrient Removal Model Nº 2 (BNRM2): A general model for Wastewater Treatment Plants, Water Sci. Technol. 67 (2013), 1481–1489.

2.19 F. Durán, 2013, Mathematical modelling of the anaerobic urban wastewater treatment including sulphate-reducing bacteria. Application to an anaerobic membrane bioreactor (Modelación matemática del tratamiento anaerobio de aguas residuales urbanas incluyendo las bacterias sulfatorreductoras, Aplicación a un biorreactor anaerobio de membranas), Ph.D. thesis, Dept. of Hydraulic Engineering and Environment, Universitat Politècnica de València, Spain.

2.20 S. Judd, C. Judd, The MBR Book: Principles and Applications of Membrane Bioreactors for Water and Wastewater Treatment, 2nd edition, Elsevier, ISBN: 978–0–08–096682–3, 2011.

2.21 R. Pretel, A. Robles M.V. Ruano, A. Seco, J. Ferrer, Environmental impact of submerged anaerobic MBR (AnMBR) technology used to treat urban wastewater at different temperatures, Bioresour. Technol. 149 (2013) 532 – 540.

2.22 T.E. Daubert, R.P Danner, H.M. Sibul, C.C. Stebbins, Physical and thermodynamic properties of Pure Compounds: Data compilation, Taylor & Francis, Bristol, PA, 1994.

2.23 EPA. Catalog of Biomass Combined Heat and Power Catalog of Technologies, 2007.
http://www.epa.gov/chp/documents/biomass_chp_catalog.pdf

2.24 PSE Probiogas, Development of sustainable systems of biogas production and use in Spain. Funded by the Ministry of science and innovation. Spanish government, Madrid, 2010.
http://213.229.136.11/bases/ainia_probiogas.nsf/0/F9F832A77BF0CA25C125753F0058C4B2/$FILE/Cap2.pdf

2.25 J. Serralta, J. Ferrer, L. Borrás, A. Seco, An extension of ASM2d including pH calculation. Water Res. 38 (2004), 4029-4038.

2.26 J. Chanona, J. Ribes, A. Seco, J. Ferrer, Optimum design and operation of primary sludge fermentation schemes for volatile fatty acids production. Water Res. 40 (2006), 53-60.

2.27 M.N. Gatti, Characterization of wastewaters and calibration of the mathematical model BNRM1 for simulation of the biological removal process of organic matter and nutrients (Caracterización de las aguas residuales y calibración del modelo matemático BNRM1 para la simulación de los procesos de eliminación biológica de materia orgánica y nutrientes). Ph.D. thesis, Dept. of Hydraulic Engineering and Environment, Universitat de València, Spain, 2009.

2.28 M.V. Ruano, J. Serralta, J. Ribes, F. Garcia-Usach, A. Bouzas, R. Barat, A. Seco, J. Ferrer, Application of the General Model "Biological Nutrient Removal Model No.1" to upgrade two full-scale WWTPs. Environ.Technol. 33 (2011), 1005-1012.

2.29 J. Ferrer, R. Pretel, F. Durán, J.B Giménez, A. Robles, M.V. Ruano, J. Serralta, J. Ribes, A. Seco, Design methodology for anaerobic membrane bioreactors (AnMBR): A case study, Sep. Purif. Technol. 141 (2015), 378-386.

2.30 R. Pretel, A. Robles M.V. Ruano, A. Seco, J. Ferrer, Filtration process cost in anaerobic membrane bioreactors (AnMBRs) for urban wastewater treatment, Sent to Sep. Sci. Technol.

2.31 J.B. Giménez, A. Robles, L. Carretero, F. Durán, M.V. Ruano, M.N. Gattib, J. Ribes, J. Ferrer, A. Seco, Experimental study of the anaerobic urban wastewater treatment in a submerged hollow-fiber membrane bioreactor at semi-industrial scale, Bioresour. Technol. 102 (2011) 8799–8806.

2.32 A.Robles, F. Durán, M.V. Ruano, J. Ribes, A. Rosado, A. Seco, J. Ferrer, Instrumentation, control, and automation for submerged anaerobic membrane bioreactors. Environ. Technol. 25 (2015), 1-12.

2.33 AEMET, State Meteorological Agency (Agencia Estatal de Meteorología). Register of hourly and daily average ambient temperature from 2010 to 2014 located in Valencia.

CHAPTER 3:

The operating cost of an anaerobic membrane bioreactor (AnMBR) treating sulphate-rich urban wastewater

Abstract

The objective of this study was to evaluate the operating cost of an anaerobic membrane bioreactor (AnMBR) treating sulphate-rich urban wastewater (UWW) at ambient temperature (ranging from 17 to 33°C). To this aim, energy consumption, methane production, and sludge handling and recycling to land were evaluated. The results revealed that optimising specific gas demand with respect to permeate volume (SGD_P) and sludge retention time (for given ambient temperature conditions) is essential to maximise energy savings (minimum energy demand: 0.07 kWh·m^{-3}). Moreover, low/moderate sludge productions were obtained (minimum value: 0.16 kg TSS·kg^{-1} $COD_{removed}$), which further enhanced the overall operating cost of the plant (minimum value: €0.011 per m^3 of treated water). The sulphate content in the influent UWW significantly affected the final production of methane and thereby the overall operating cost. Indeed, the evaluated AnMBR system presented energy surplus potential when treating low-sulphate UWW.

Keywords

Energy consumption; industrial-scale hollow-fibre membranes; operating cost; anaerobic membrane bioreactor (AnMBR); sulphate-rich urban wastewater.

Highlights

The operating cost of an AnMBR treating sulphate-rich urban wastewater was evaluated.
Energy demand, methane and sludge production were studied in an AnMBR.
Low gas sparging intensities resulted in low energy demands: 0.07 kWh m^{-3}.
Low sludge production was obtained, enhancing the overall operating cost (€0.011 per m^3).
AnMBR could be net energy producer when treating low-sulphate urban wastewater.

R. Pretel, A. Robles, M.V. Ruano, A.Seco, J. Ferrer
The operating cost of an anaerobic membrane bioreactor (AnMBR) treating sulphate-rich urban wastewater
Sep. Purif. Technol. 126 (2014) 30–38

3.1 Introduction

Nowadays, a key issue in global sustainable development is the dependency on fossil fuels for electricity production, which represents up to the 80% of the global energy consumption [3.1]. In this respect, electricity consumption is a key element in the overall environmental performance of a wastewater treatment plant (WWTP) [3.2]. Hence, it is particularly important to implement new energy-saving technologies that reduce the overall energy balance of the WWTP, such as anaerobic membrane bioreactors (AnMBRs). This technology focuses on the sustainability benefits of anaerobic processes compared to aerobic processes, such as: minimum sludge production due to low biomass yield of anaerobic organisms; low energy demand since no aeration is required; and methane production that can be used to fulfil process energy requirements [3.3].

Several issues have been recognised elsewhere as potential drawbacks which may affect the sustainability of AnMBR technology treating urban wastewater (UWW). One key issue is the competition between Methanogenic *Archaea* (MA) and Sulphate Reducing Bacteria (SRB) for the available substrate [3.4] when there is significant sulphate content in the influent, reducing therefore the available COD for methanisation [3.5]. For urban wastewater, which can easily present low COD/SO_4–S ratio, this competition can critically affect the amount and quality of the biogas produced. Specifically, 2 kg of COD are consumed by SRB in order to reduce 1 kg of influent SO_4-S (see, for instance, [3.5]). According to the theoretical methane yield under standard temperature and pressure conditions (350 $L_{CH4}\cdot kg^{-1}$COD), SRB reduces the production of approx. 700 L of methane per kg of influent SO_4-S (considering reduction of all sulphate to sulphide). Therefore, higher biogas productions would be achieved when there is little sulphate content in the influent (typical sulphate concentration in UWW fluctuates around 7-17 mg SO_4-S$\cdot L^{-1}$ [3.6]). On the other hand, due to the low-growth rate of anaerobic microorganism, high sludge retention times (SRTs) are required when operating at low temperatures in order to achieve suitable organic matter removal rates, especially for low-strength wastewaters like urban ones (typical COD levels below 1 g$\cdot L^{-1}$ [3.6]). However, as regards filtration process, operating AnMBRs at high SRT may imply operating at high mixed liquor total solid (MLTS) levels. This is considered to be one of the main constraints on membrane operating because it can result in a high membrane fouling propensity and therefore high energy demand for membrane scouring by gas sparging [3.7].

The objective of this study was to evaluate the operating cost of an AnMBR system treating sulphate-rich urban wastewater (UWW) at ambient temperature (ranging from 17 to 33ºC). To this aim, power requirements, energy recovery from methane (biogas methane and/or methane dissolved in the effluent), and sludge handling and recycling to land were evaluated at different operating conditions. In order to obtain reliable results that can be extrapolated to full-scale plants, this study was carried out in an AnMBR using industrial-scale hollow-fibre membrane units. This system was operated using effluent from the pre-treatment of the Carraixet WWTP (Valencia, Spain).

3.2 Materials and methods

3.2.1 AnMBR plant description

A semi-industrial AnMBR plant was operated using the effluent of a full-scale WWTP pre-treatment. The average AnMBR influent characteristics are shown in Table 3.1. This influent UWW was characterised by a low COD (around 650 mg·L^{-1}) and high sulphate concentration (around 105 mg SO_4-S·L^{-1}).

Table 3.1 Average characteristics of AnMBR influent.

Parameter	Mean ± SD
Treatment flow rate (m^3·day^{-1})	3.2 ± 0.7
TSS (mg·L^{-1})	313 ± 45
VSS (mg·L^{-1})	257 ± 46
COD (mg·L^{-1})	650 ± 147
SO_4-S (mg·L^{-1})	105 ± 13
NH_4-N (mg·L^{-1})	35 ± 3
PO_4-P (mg·L^{-1})	4 ± 1

The AnMBR plant consists of an anaerobic reactor with a total volume of 1.3 m^3 connected to two membrane tanks (MT1 and MT2) each one with a total volume of 0.8 m^3. Each membrane tank includes one ultrafiltration hollow-fibre membrane commercial system (PURON®, Koch Membrane Systems, 0.05 µm pore size, 30 m^2 total filtering area). The filtration process was studied from experimental data obtained from MT1 (operated recycling continuously the obtained permeate to the system), whilst the biological process was studied using experimental data obtained from MT2 (operated for the biological process without recycling the obtained permeate). Hence, different 20 ºC-standardised transmembrane fluxes (J_{20}) were tested in MT1, without affecting the hydraulic retention time (HRT) of the plant.

In addition to conventional membrane operating stages (filtration, relaxation and back-flushing), two additional stages were considered in the membrane operating mode: degasification and ventilation. Further details on this AnMBR can be found in Giménez *et al.* [3.5] and Robles *et al.* [3.8].

3.2.2 AnMBR operating conditions

The AnMBR plant was operated for around 920 days within a wide range of operating conditions for both filtration and biological process.

- *Filtration process*

Five operating scenarios related to filtration process (FP1-FP5) were considered to evaluate the energy consumption of the AnMBR plant (see Table 3.2). As Table 3.2 shows, the main operating conditions in these five scenarios were as follows: transmembrane pressure (TMP) during filtration: from 0.09 to 0.35 bar; J_{20} from 9 to 20 LMH; MLTS entering the membrane tank: from 12.5 to 32.5 $g \cdot L^{-1}$; sludge recycling flow in membrane tank and anaerobic reactor (SRF_{MT} and SRF_{AnR} respectively): 2.7 and 1 $m^3 \cdot h^{-1}$ respectively; specific gas demand per square metre of membrane area (SGD_m): controlled at 0.17 and 0.23 $m^3 \cdot h^{-1} \cdot m^{-2}$; and biogas recycling flow to the anaerobic reactor (BRF_{AnR}): 1.5 $m^3 \cdot h^{-1}$.

Table 3.2 Main operating conditions in scenarios FP1-FP5. **TMP**: transmembrane pressure; **J_{20}**: 20 ºC-standardised transmembrane flux; **MLTS**: mixed liquor total solids; **SRF_{MT}** and **SRF_{MT}:** sludge recycling flow to membrane tank and anaerobic reactor, respectively; **SGD_m**: specific gas demand per square metre of membrane area; and **BRF_{AnR}**: biogas recycling flow to anaerobic reactor.

Scenario	Period (days)	TMP (bar)	J_{20} (LMH)	MLTS ($g \cdot L^{-1}$)	SRF_{MT} ($m^3 \cdot h^{-1}$)	SRF_{AnR} ($m^3 \cdot h^{-1}$)	SGD_m ($m^3 \cdot m^{-2} \cdot h^{-1}$)	BRF_{AnR} ($m^3 \cdot h^{-1}$)
FP1	137-170	0.35	10.0	32.5	2.7	1	0.23	1.5
FP2	361-404	0.13	13.3	12.5	2.7	1	0.23	1.5
FP3	556-600	0.26	9.0	22.5	2.7	1	0.23	1.5
FP4	807-850	0.09	15.0	14	2.7	1	0.17	1.5
FP5	853-896	0.20	20.0	13	2.7	1	0.23	1.5

- *Biological process*

Variations in SRT and seasonal temperature were studied to account for the dynamics in methane and sludge productions over time. During the 920-day experimental period the plant was operated at ambient temperature ranging from 17 to 33 ºC and SRT varied from 30 to 70 days. Three different experimental scenarios related to biological process ($BP_{33°C,\ SRT\ 70days}$, $BP_{22°C,\ SRT\ 38days}$ and $BP_{17°C,\ SRT\ 30days}$) were considered to evaluate the energy consumption of the AnMBR plant (see Table 3.3): (1) a summer period of two months of operation resulting in high methane and low sludge productions ($BP_{33°C,\ SRT\ 70days}$) due to operating at high temperature (33 °C in average) and high SRT (70 days); (2) one year of operation resulting in moderate methane and sludge productions ($BP_{22°C,\ SRT\ 38days}$) due to operating at variable temperature (22 °C in average) and moderate SRT (38 days); and (3) a winter period of two months of operation resulting in low methane and moderate sludge productions ($BP_{17°C,\ SRT\ 30days}$) due to operating at relatively low temperature (17.1 °C in average) and moderate SRT (30 days). These three scenarios represent boundary ($BP_{33°C,\ SRT\ 70days}$: best conditions; and $BP_{17°C,\ SRT\ 30days}$: worst conditions) and average ($BP_{22°C,\ SRT\ 38days}$) of the operating conditions evaluated in the plant.

Table 3.3 Operating temperature (T) and sludge retention time (SRT), total methane production (V_{CH4}), biogas methane ($V_{CH4,BIOGAS}$), and methane dissolved in the effluent ($V_{CH4,EFFLUENT}$) per m^3 of treated water, and sludge production, for cases $BP_{33°C,\ SRT\ 70days}$, $BP_{22°C,\ SRT\ 38days}$ and $BP_{17°C,\ SRT\ 30days}$.

	T (ºC)	**SRT (days)**	**V_{CH4} (BIOGAS+EFFLUENT) (L·m^{-3})**	**$V_{CH4,BIOGAS}$ (L·m^{-3})**	**$V_{CH4,EFFLUENT}$ (L·m^{-3})**	**Sludge production (kg TSS·kg^{-1} COD removed)**
$BP_{33°C,\ SRT\ 70days}$	33	70	41.1	26.5	14.6	0.16
$BP_{22°C,\ SRT\ 38days}$	22	38	16.8	8.4	8.4	0.43
$BP_{17°C\ ,\ SRT\ 30days}$	17	30	8.5	1.4	7.1	0.55

In addition, several simulation scenarios were calculated in order to assess the AnMBR performance within the whole range of temperature (17-33 ºC) and SRT (30-70 days) evaluated in this study. Simulation results were obtained using the WWTP simulating software DESASS [3.9]. This simulation software features the mathematical model BNRM2 [3.10], which was previously validated using experimental data obtained in the AnMBR plant. Figure 3.1 shows the resulting effluent COD without including dissolved methane concentration (see Figure 3.1a); total methane production (see Figure 3.1b); and sludge production (Figure 3.1c) for the different temperature and SRT conditions simulated.

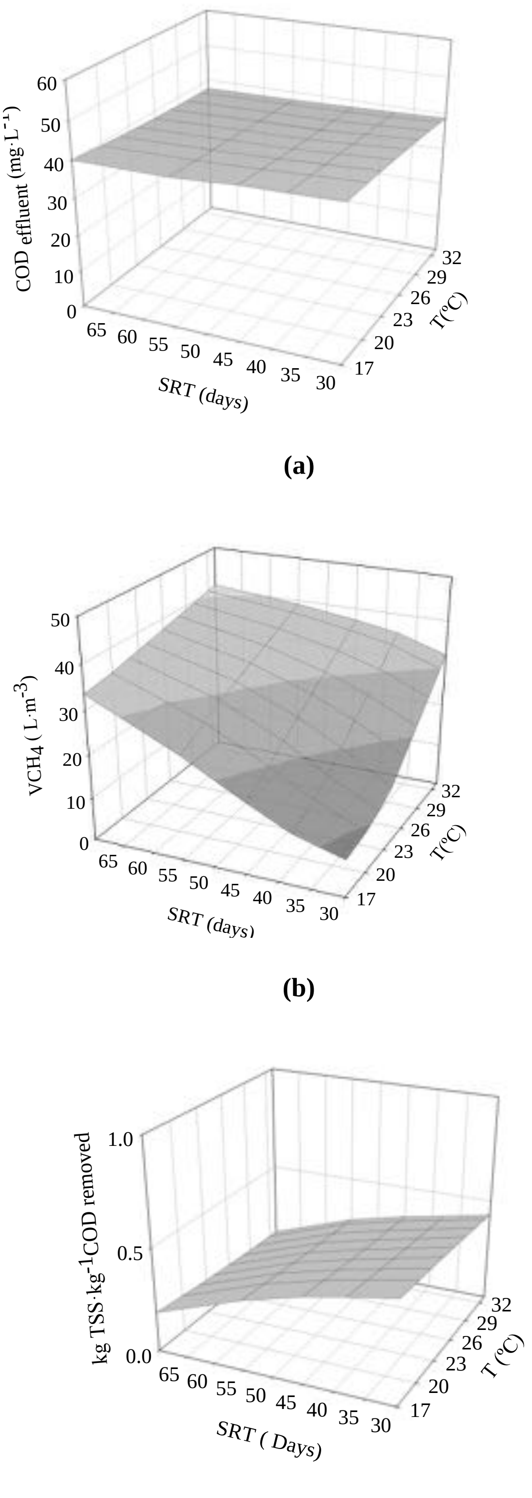

Figure 3.1 AnMBR performance at different temperature and SRT conditions: **(a)** effluent COD (without including dissolved methane concentration); **(b)** total methane production (V_{CH4}) (biogas methane and methane dissolved in the effluent); and **(c)** sludge production measured in kg TSS·kg^{-1} COD removed.

- *Influent sulphate concentration*

The effect of the influent sulphate on the AnMBR operating cost was also evaluated. As mentioned before, the UWW fed to the AnMBR plant was characterised by relatively low COD and high sulphate concentrations (see Table 3.1). Therefore, an important fraction of the influent COD was consumed by SRB. To be precise, the sulphate content in the influent was approx. 105 mg $S\text{-}SO_4\cdot L^{-1}$, from which approx. 98% was reduced to hydrogen sulphide (around 103 mg $S\text{-}SO_4\cdot L^{-1}$). Therefore, about 206 $mg\cdot L^{-1}$ of influent COD were consumed by SRB.

The results obtained in this study were compared to the theoretical results obtained in an AnMBR system treating low-sulphate UWW (10 mg $S\text{-}SO_4\cdot L^{-1}$). To this aim, the methane production when treating low-sulphate UWW was calculated on the basis of the theoretical methane yield under standard temperature and pressure conditions: 350 $L_{CH4}\cdot kg^{-1}COD$. Table 3.4 shows the theoretical methane production (including both biogas methane and methane dissolved in the effluent) obtained for cases $BP_{33°C,\ SRT\ 70days}$, $BP_{22°C,\ SRT\ 38days}$ and $BP_{17°C,\ SRT\ 30days}$ when treating low-sulphate UWW (10 mg $S\text{-}SO_4\cdot L^{-1}$). The distribution between gas and liquid phase of the produced methane was established on the basis of the experimental distribution obtained in the AnMBR plant.

Table 3.4 Theoretical methane production (V_{CH4}), biogas methane ($V_{CH4,BIOGAS}$), and methane dissolved in the effluent ($V_{CH4,EFFLUENT}$) per m^3 of treated water for cases $BP_{33°C,\ SRT\ 70days}$, $BP_{22°C,\ SRT\ 38}$ and $BP_{17°C,\ SRT\ 30days}$ when treating low-sulphate UWW.

	$V_{CH4,}$ (BIOGAS+EFFLUENT) ($L\cdot m^{-3}$)	$V_{CH4,BIOGAS}$ ($L\cdot m^{-3}$)	$V_{CH4,EFFLUENT}$ ($L\cdot m^{-3}$)
$BP_{33°C,\ SRT\ 70days}$	105.8	68.1	37.7
$BP_{22°C,\ SRT\ 38days}$	81.5	40.8	40.7
$BP_{17°C,\ SRT\ 30days}$	73.2	11.7	61.5

3.2.3 Analytical monitoring

The following parameters were analysed in mixed liquor and influent stream according to Standard Methods [3.11]: total solids (TS); total suspended solids (TSS); volatile suspended solids (VSS); sulphate (SO_4-S); nutrients (ammonium (NH_4-N) and orthophosphate (PO_4-P)); and chemical oxygen demand (COD). The methane fraction of the biogas was measured using a gas chromatograph equipped with a Flame Ionization Detector (GC-FID, Thermo Scientific) in accordance with Giménez *et al.* [3.5].

The dissolved methane fraction of the effluent was determined in accordance with Giménez ***et al.*** [3.12]. AMPTS® (Automatic Methane Potential Test System, Bioprocess Control) was employed for evaluating the biochemical methane potential (BMP) of the wasted sludge. Due to the low microbial activity of this sludge, BMP tests were inoculated using biomass coming from the anaerobic digester of the Carraixet WWTP. VSS and TSS levels in the wasted sludge were measured at the beginning and at the end of the BMP test, allowing the percentage of biodegradable volatile suspended solids (%BVSS) to be calculated. In this study, the sludge stabilisation criterion was set to 35% of BVSS.

3.2.4 Energy balance description

The energy balance of the AnMBR system consisted of: power requirements (W), and energy recovery from both biogas methane (E_{biogas}) and methane dissolved in the effluent ($E_{dissolved\ methane}$). The heat energy term (Q) was assumed negligible since the process was evaluated at ambient temperature conditions.

Therefore, the AnMBR energy consumption was evaluated in this study assuming the following terms: (1) energy consumption when non-capture of methane is considered; (2) net energy consumption including energy recovery from biogas methane; and (3) net energy consumption including energy recovery from both biogas methane and methane dissolved in the effluent.

The equipment considered in the W term consisted of the following: one anaerobic reactor feeding pump; one membrane tank sludge feeding pump; one anaerobic reactor sludge mixing pump; one permeate pump; one anaerobic reactor biogas recycling blower; one membrane tank biogas recycling blower; one rotofilter; and one dewatering system.

The energy requirements for each of the scenarios evaluated in this study were calculated using the simulation software DESASS, which includes a general tool that enables calculating the energy consumption of the different units comprising a WWTP.

- *Power requirements (W)*

As proposed by Judd and Judd [3.13], the energy consumption related to pumps and blowers (adiabatic compression), was calculated by applying the corresponding theoretical equations (Eq. 3.1, Eq. 3.2 and Eq. 3.3, respectively).

$$P_B\left(\frac{J}{S}\right) = \frac{(\mathrm{M}\cdot\mathrm{R}\cdot\mathrm{T_{gas}})}{(\alpha-1)\cdot\eta_{blower}}\left[\left(\frac{p_2}{p_1}\right)^{\frac{\alpha-1}{\alpha}}-1\right] \quad \textbf{(Eq. 3.1)}$$

where P_B is the blower power requirement (adiabatic compression), M ($mol\cdot s^{-1}$) is the molar flow rate of biogas, R ($J\cdot mol^{-1}\cdot K^{-1}$) is the gas constant for biogas, P_1 (atm) is the absolute inlet pressure, P_2 (atm) is the absolute outlet pressure, T_{gas} (K) is the biogas temperature, α is the adiabatic index and η_{blower} is the blower efficiency.

P_1 and M were taken from the data obtained in the AnMBR plant; P_2 and T_{gas} were calculated by the simulation software; and a value of 0.8 was considered for η_{blower} as a theoretical typical value.

$$P_g\left(\frac{J}{S}\right) = q_{imp}\cdot\rho_{liquor}\cdot g\cdot\frac{\left\{\left[\left(\frac{(\mathrm{L}+\mathrm{Leq})\cdot\mathrm{f}\cdot\mathrm{V}^2}{D\cdot 2\cdot g}\right)\mathrm{asp.}+\left(\frac{(\mathrm{L}+\mathrm{Leq})\cdot\mathrm{f}\cdot\mathrm{V}^2}{D\cdot 2\cdot g}\right)\mathrm{imp.}\right]+\left[Z_1-Z_2\right]\right\}}{\eta_{pump}} \quad \textbf{(Eq. 3.2)}$$

where P_g is the power requirement by the general pump, considering both pump aspiration and pump impulsion section, calculated from the impulsion volumetric flow rate ($q_{imp.}$ in $m^3\cdot s^{-1}$), liquor density (ρ_{liquor} in $kg\cdot m^{-3}$), acceleration of gravity (g in $m\cdot s^{-1}$), pipe length (L in m), pipe equivalent length of the punctual pressure drops (L_{eq} in m), liquor velocity (V in $m\cdot s^{-1}$), friction factor (f, dimensionless), diameter (d in m), difference in height (Z_1-Z_2, in m) and pump efficiency (η_{pump}).

q_{imp} and ρ_{liquor} were taken from the data obtained in the AnMBR plant; L, L_{eq}, D and Z_1-Z_2 were taken from the dimensions of the AnMBR plant; V and f were calculated by the modelling software; and a value of 0.8 was considered for η_{pump} as a theoretical typical value.

$$P_{stage(filtration,\ degasification\ or\ back-flushing)}\left(\frac{J}{S}\right) = \frac{\mathrm{q_{stage}}\cdot\mathrm{TMP_{stage}}}{\eta_{pump}} \quad \textbf{(Eq. 3.3)}$$

where P_{stage} is the permeate pump power requirement during filtration, degasification or back-flushing calculated from transmembrane pressure (TMP_{stage} in Pa), pump volumetric flow rate (q_{stage} in $m^3\cdot s^{-1}$) and pump efficiency (μ_{pump}).

TMP_{stage} and q_{stage} were taken from the data obtained in the AnMBR plant

To calculate the net power required by the permeate pump ($P_{permeate}$), the sum of the power consumed in the following four membrane operating stages was considered: filtration ($P_{filtration}$), back-flushing ($P_{back\text{-}flushing}$), degasification ($P_{degasification}$) and ventilation ($P_{ventilation}$). Eq. 3.4 was used to calculate the power in filtration, back-flushing and degasification. Eq. 3.3 was used to calculate the power in ventilation since the fluid does not pass through the membrane.

The energy consumption related to the rotofilter was obtained from a catalogue for full-scale implementation [3.14].

Concerning sludge handling, centrifuges with an average power consumption of 45 $kWh \cdot t^{-1}$ TSS [3.15] were selected in our study as sludge dewatering system.

- *Energy recovery from methane*

Since microturbines can run on biogas, they were selected as combined heat and power (CHP) technology [3.16]. Microturbine-based CHP technology has an overall efficiency of around 65.5%, assuming power energy efficiency of about 27% (see Eq. 3.4).

$$W_{biogas}(kW) = \frac{V_{biogas} \cdot \left(\%CH_4 \cdot CV_{CH4}\right) \cdot \%_{power\,effciency\,CHP}}{1000 \cdot 24 \cdot 3600} \quad \textbf{(Eq. 3.4)}$$

where W_{biogas} is the power generated by the Microturbine-based CHP system using biogas, V_{biogas} ($L \cdot d^{-1}$) is the biogas volume, $\%CH_4$ is the methane percentage and CV_{CH4} ($KJ \cdot m^{-3}$) is the methane calorific power.

It must be said that methane dissolved in the effluent was considered to be captured for obtaining power energy by using the Microturbine-based CHP system. Theoretical capture efficiency for the dissolved methane of 100% was considered in order to assess the maximum energy potential.

3.2.5 Operating cost assessment

The operating cost analysis was limited in this study to net energy demand, and sludge handling and recycling to land.

The net energy demand in scenarios FP1-FP5 was evaluated for cases $BP_{33°C,\ SRT\ 70days}$, $BP_{22°C,\ SRT\ 38days}$ and $BP_{17°C,\ SRT\ 30days}$ assuming, as previously mentioned, the following terms: (1) non-capture of methane;

(2) energy recovery from biogas methane; and (3) energy recovery from both biogas methane and methane dissolved in the effluent. The energy term considered in this study was €0.138 per kWh (according to the current electricity rates and prices in Spain [3.17]).

Concerning sludge handling and recycling to land, centrifuges require the use of polyelectrolyte for proper sludge conditioning. The dose of polyelectrolyte considered in our study was 6 $kg \cdot t^{-1}$ TSS [3.18], and the assumed polyelectrolyte cost was €2.52 per kg Polyelectrolyte [19]. The produced sludge was considered to be used as a fertiliser in agricultural land. The assumed cost for sludge recycling to land was €4.81 per t TSS [3.19].

3.3 Results and discussion

3.3.1 Overall process performance

Figure 3.2 shows the 20 ºC-standardised membrane permeability (K_{20}) and the MLTS level in the anaerobic sludge fed to the membrane tanks during 920 days of operation. Both K_{20} and MLTS are referred to its daily average value. This experimental period is divided into two stages, represented in Table 3.2 by a horizontal dashed line. Energy consumption was firstly evaluated in a period of about 790 days, which was mostly operated at sub-critical filtration conditions (scenarios FP1 to FP3). Overall, during this stage K_{20} decreased due to increasing membrane fouling over time (see days 300 to 790 in Figure 3.2). Around day 790 the membranes were chemically cleaned. After this chemical cleaning, the energy consumption was evaluated in a period of about 140 days, which was operated at critical filtration conditions (scenarios FP4 and FP5). During this second stage higher J_{20} were applied (see days 790 to 920 in Figure 3.2), making the AnMBR performance comparable to full scale aerobic MBRs [3.13].

Regarding the biological process, methane production increased significantly when operating at both high temperature and high SRT ($BP_{33°C,\ SRT\ 70days}$). To be precise, the average experimental methane production was 41.1, 16.8 and 8.5 $L_{CH4} \cdot m^{-3}$ for case $BP_{33°C,\ SRT\ 70days}$, $BP_{22°C,\ SRT\ 38days}$ and. $BP_{17°C,\ SRT\ 30days}$ (see Table 3.3), respectively. It can be considered that an increase in the ambient temperature and/or SRT leads to offset the low growth rate of MA [3.20]. In this respect, simulation results in Figure 3.1 show adequate effluent COD concentrations and increasing methane productions and decreasing sludge productions as temperature and/or SRT increases, within the range of operating conditions evaluated in this study.

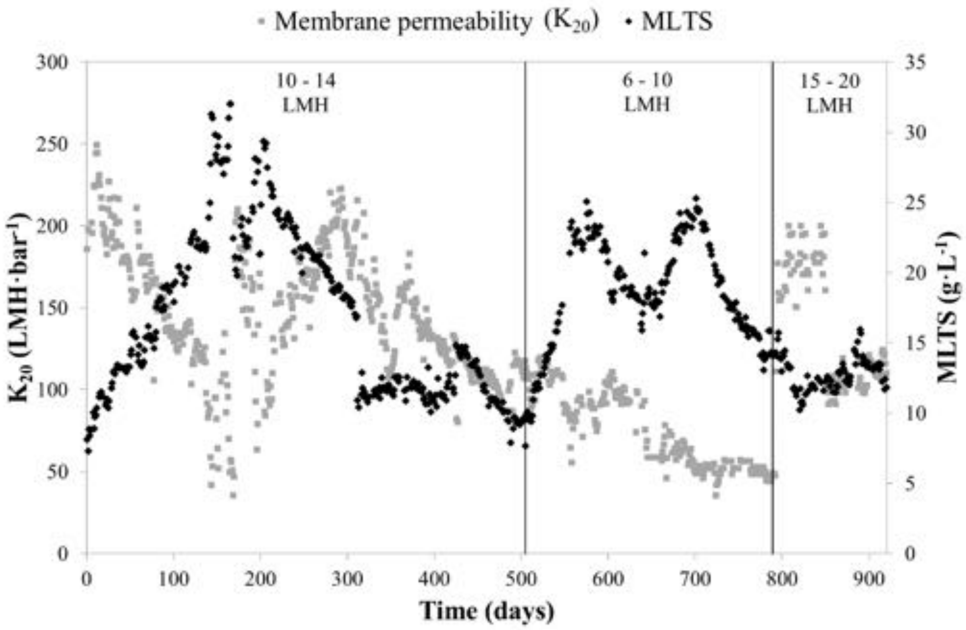

Figure 3.2 Evolution of K_{20} and MLTS throughout 920 days of operation.

Concerning sludge production, low/moderate amounts of sludge were generated. As Table 3.3 shows, the sludge production resulted in 0.16, 0.43 and 0.55 kgTSS·kg^{-1} $COD_{REMOVED}$ in average for cases $BP_{33°C,\ SRT\ 70days}$, $BP_{22°C,\ SRT\ 38days}$ and. $BP_{17°C,\ SRT\ 30days}$, respectively. The minimum sludge production corresponded to case $BP_{33°C,\ SRT\ 70days}$, due to operating at high temperature (33 ºC) and high SRT (70 days). On the other hand, the experimentally determined %BVSS resulted in values below 35% within the whole range of evaluated operating conditions, which indicated adequate sludge stabilities of the wasted sludge. For instance, %BVSS resulted in the highest value (31%) when operating under the most unfavourable conditions evaluated in this study (i.e. $BP_{17°C,\ SRT\ 30days}$). It is important to highlight that one key sustainable benefit of AnMBR technology is that the produced sludge is stabilised and no further digestion is required for its disposal on farmland. In addition, sludge production in anaerobic processes is expected to be lower than in aerobic processes.

3.3.2 Energy consumption and operating cost of the AnMBR system

- *Power requirements*

Table 3.5 shows the power requirements of the AnMBR plant for each of the five scenarios shown in Table 3.2 (FP1-FP5). This table also illustrates the weighted average distribution for the energy consumption of each particular equipment, i.e. pumps, blowers and rotofilter. The dotted line between scenario FP3 and FP4 differentiates the scenarios evaluated before and after chemically cleaning the membranes. Comparing the different scenarios assessed, it is worth to say that scenarios studied prior to chemically cleaning the membranes present higher energy consumptions (0.44, 0.32 and 0.49 kWh·m^{-3} for FP1, FP2 and FP3, respectively) than those studied afterwards (0.20 and 0.19 kWh·m^{-3} for FP4 and FP5, respectively). This is mainly due to the higher J_{20} applied in the second operating stage whilst operating at similar SGD_m. Specifically, the specific gas demands per permeate volume (SGD_P) resulted in the range from 21 to 32 in scenarios FP1-FP3, decreasing to approx. 14 in scenarios FP4 and FP5.

Table 3.5 Power requirements in scenarios FP1-FP5.

SCENARIO	TOTAL ENERGY CONSUMPTION (kWh·m^{-3})	PERMEATE PUMP (%)	MEMBRANE TANK BIOGAS RECYCLING BLOWER (%)	MEMBRANE TANK SLUDGE FEEDING PUMP (%)	STIRRING POWER REACTOR (%)	ANAEROBIC REACTOR FEEDING PUMP (%)	ROTOFILTER (%)
FP1	0.44	2.34	73.15	14.54	8.20	0.52	1.25
FP2	0.32	1.26	73.18	14.69	8.43	0.72	1.73
FP3	0.49	1.61	73.94	14.58	8.27	0.47	1.13
FP4	0.20	1.38	61.73	21.02	11.89	1.17	2.81
FP5	0.19	3.06	67.46	16.19	9.18	1.21	2.90

Figure 3.3 shows the weighted average distribution for the power requirements in the first (scenarios FP1 to FP3 in Table 3.5) and second operating period (scenarios FP4 and FP5 in Table 3.5). This figure shows that the most important item contributing the power input was the membrane tank biogas recycling blower, representing about two-thirds (60-75%) of the total AnMBR power requirements. The next in importance was the membrane tank sludge feeding pump, which represented about 15-20% of the total AnMBR power requirements. Therefore, the main terms contributing the total AnMBR power requirements were related to filtration (representing about 85-90%). This highlights the need of optimising filtration in any operating range to improve the feasibility of AnMBR technology to treat UWW.

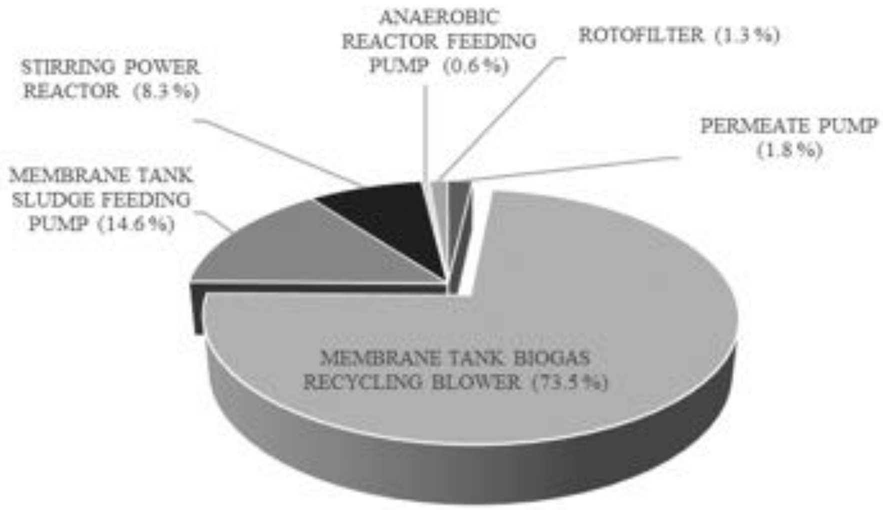

(a)

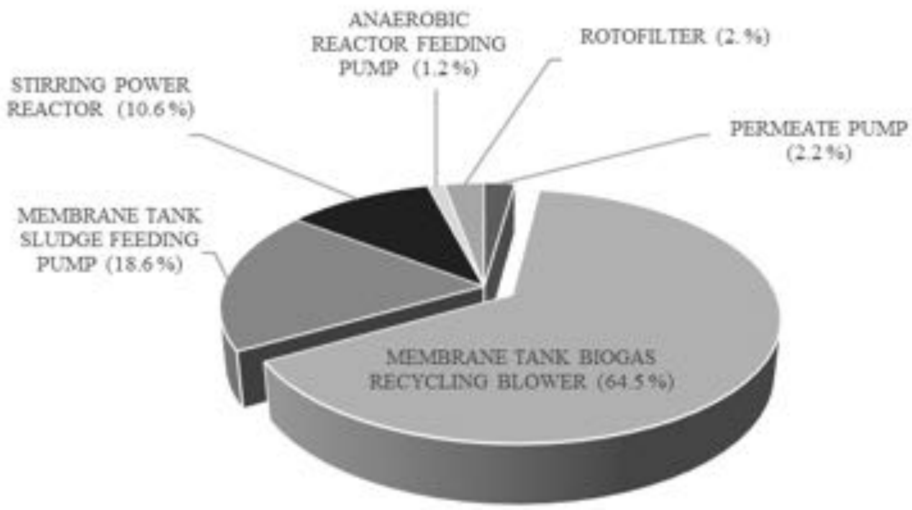

(b)

Figure 3.3 Weighted average distribution for the AnMBR power requirements in scenarios: **(a)** FP1 to FP3; and **(b)** FP4 and FP5.

To keep long operating periods without applying membrane chemical cleaning (i.e. minimising irreversible fouling problems: first 790 days in Figure 3.2), low J_{20} and/or high SGD_m are required. On the other hand, increasing the chemical cleaning frequency allows operating at high J_{20} and/or low SGD_m (i.e. low SGD_P), which reduces considerably the net energy demand (days 790 to 920 in Figure 3.2). To be precise, scenario FP5 was operated with the lowest SGD_P (14.4), resulting in the lowest power input

(0.19 kWh·m^{-3}). Hence, it is of vital importance to reduce the energy consumption by minimising SGD_P, which indirectly increases the membrane chemical cleaning frequency. Nevertheless, increasing the frequency of membrane chemical cleaning means high chemical reagent consumption and may affect the membrane lifetime, resulting therefore in an increase in membrane replacement and maintenance costs. Therefore, further research is required to evaluate the most suitable AnMBR operating strategy from an economical and environmental point of view including not only energy consumption but also investment and maintenance costs.

- *Net energy consumption*

Figure 3.4 shows the net energy consumption of the AnMBR for each of the five scenarios shown in Table 3.2 (FP1-FP5). This net energy consumption includes both power requirements and energy recovery from methane. As mentioned earlier, each scenario (FP1-FP5) was evaluated for three different methane productions ($BP_{33°C,\ SRT\ 70days}$, $BP_{22°C,\ SRT\ 38days}$ and $BP_{17°C,\ SRT\ 30days}$) and two different levels of energy recovery (biogas methane, and biogas methane and methane dissolved in the effluent).

Figure 3.4 shows considerable reductions in the AnMBR energy demand (in comparison with results shown in Table 3.5) whenever the generated methane is used as energy resource. For example, the energy consumption in scenario FP5 was 0.19 kWh·m^{-3} when methane was not captured (see Table 3.5); whilst the net energy demand in scenario FP5 decreased to 0.17 kWh·m^{-3} for case $BP_{17°C,\ SRT\ 30days}$ when capturing both the biogas methane and the methane dissolved in the effluent. In addition, operating at high ambient temperature and/or high SRT further enhances the energy balance of the system. For instance, the energy consumption in scenario FP5 could be reduced up to 0.07 and 0.14 kWh·m^{-3} when recovering energy from both biogas methane and methane dissolved in the effluent for cases $BP_{33°C,\ SRT\ 70days}$ and $BP_{22°C,\ SRT\ 38days}$, respectively (see Figure 3.4b).

Therefore, operating at high ambient temperature and/or high SRT allows achieving significant energy savings whenever the methane generated is captured and used as energy resource.

- *Operating cost*

Figure 3.5 shows the operating cost of the AnMBR system including energy recovery from methane (biogas methane and methane dissolved in the effluent) and sludge handling and recycling to land. As Figure 3.5 illustrates, the most favourable situation as regards operating cost corresponded to case $BP_{33°C,\ SRT\ 70days}$. By way of example, the operating cost in scenario FP5 when capturing both the biogas methane and the methane dissolved in the effluent was €0.011, €0.027 and €0.032 per m^3 of treated water for cases $BP_{33°C,\ SRT\ 70days}$, $BP_{22°C,\ SRT\ 38days}$ and $BP_{17°C,\ SRT\ 30days}$, respectively. In this respect, savings of up to 64% from winter to summer seasons could be achieved. This highlights the feasibility of AnMBR technology to treat UWW in warm climate regions, as well as the necessity of optimising SRT for a given ambient temperature to maximise methane production and minimise sludge production.

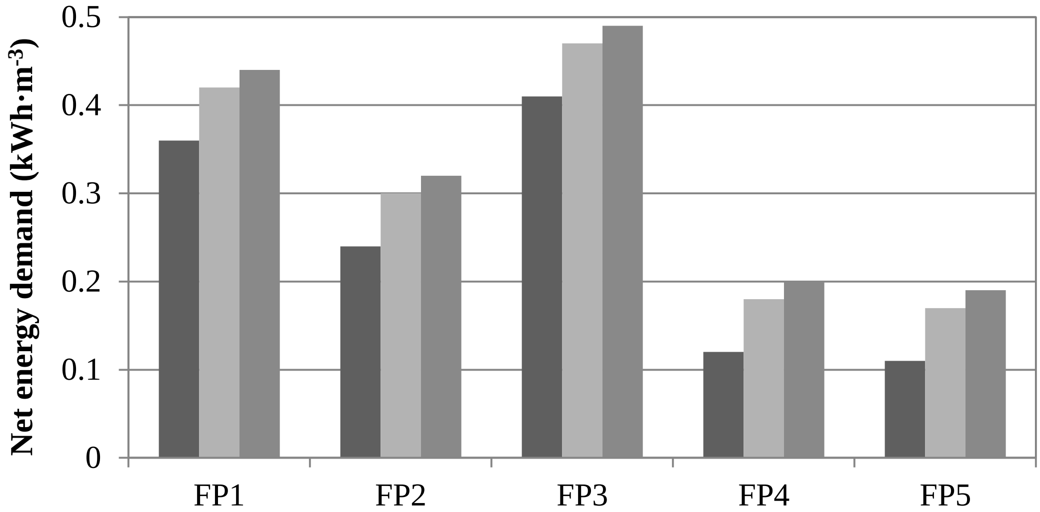

(a)

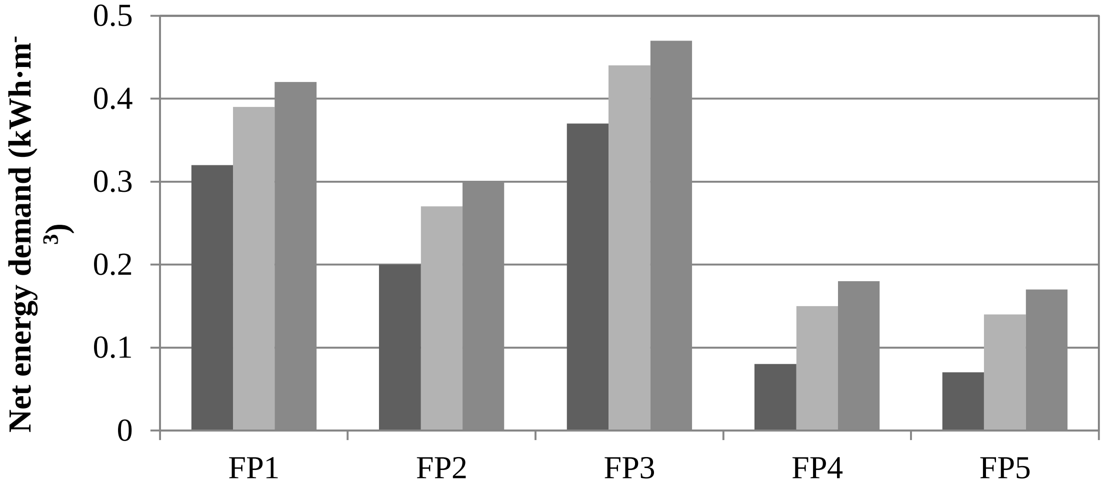

(b)

Figure 3.4 Net energy consumption in scenarios FP1-FP5 for cases $BP_{33°C,\ SRT\ 70days}$ (■), $BP_{22°C,\ SRT\ 38}$ (■) and $BP_{17°C,\ SRT\ 30days}$ (■) including energy recovery from: **(a)** biogas methane; and **(b)** biogas methane and methane dissolved in the effluent.

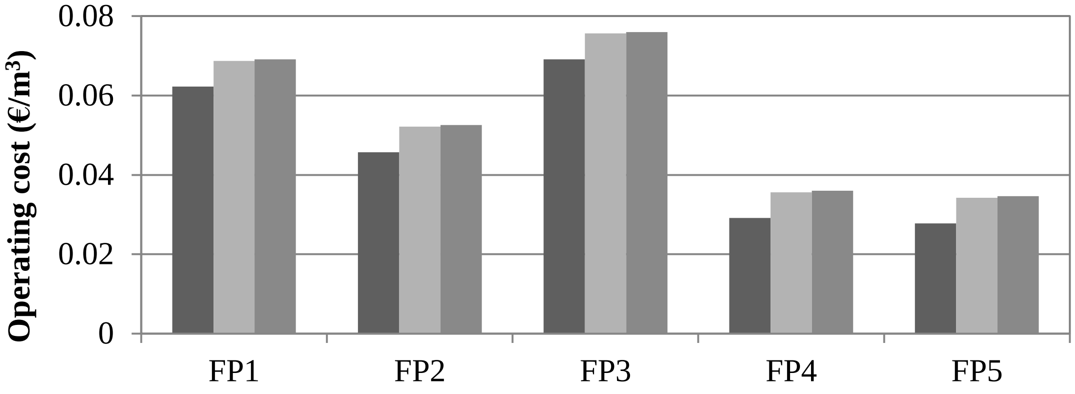

(a)

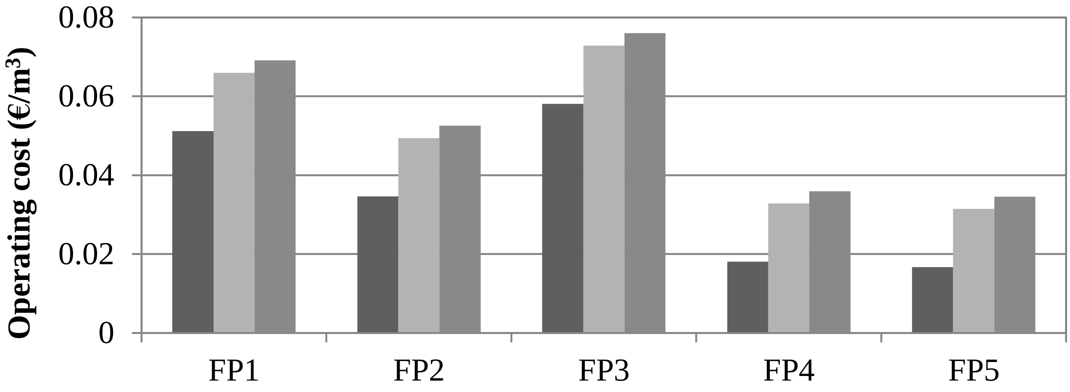

(b)

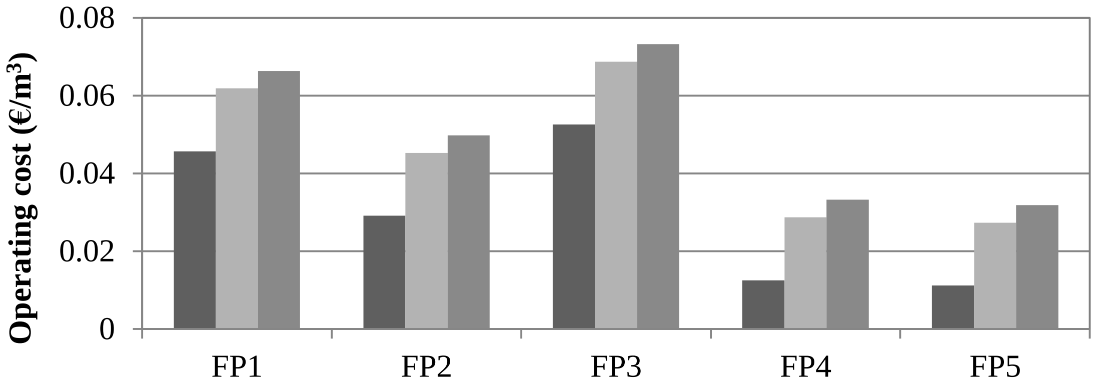

(c)

Figure 3.5 Operating cost (net energy consumption and sludge handling and recycling to land) in scenarios FP1-FP5 for cases $BP_{33°C,\ SRT\ 70days}$ (■), $BP_{22°C,\ SRT\ 38days}$ (■) and $BP_{17°C,\ SRT\ 30days}$ (■): **(a)** non-capture of methane; **(b)** energy recovery from biogas methane; and **(c)** energy recovery biogas methane and methane dissolved in the effluent.

On the other hand, it is worth pointing out the reduction in the operating cost if energy is recovered from methane. To be precise, scenario FP5 for case $BP_{33°C,\ SRT\ 70days}$ resulted in an operating cost of €0.028, €0.017 and €0.011 per m^3 of treated water when considering non-energy recovery from methane, energy recovery from biogas methane, and energy recovery from biogas methane and methane dissolved in the effluent, respectively (see Figure 3.5).

Therefore, the energy recovery from methane enables reducing considerably the operating cost of AnMBRs treating sulphate-rich UWW at ambient temperature. This highlights the need of developing feasible technologies for capturing the methane dissolved in the effluent stream not only to reduce its environmental impact (e.g. due to methane release to the atmosphere from the effluent), but also to enhance the economic feasibility of AnMBR technology.

As previously commented, several simulation scenarios were calculated in order to assess the AnMBR performance within the whole range of temperature and SRT evaluated in this study. Figure 3.6 shows the simulation results regarding the theoretical influence of temperature and SRT on the AnMBR operating cost (when treating sulphate-rich UWW), including energy recovery from methane (biogas methane and methane dissolved in the effluent) and sludge handling and recycling to land. Specifically, this study shows the results obtained for three SGD_P levels (22.3, 33.4 and 14.4) corresponding to scenarios FP2, FP3 and FP4, respectively. As shown in Figure 3.6, from a biological process perspective, the operating cost is reduced when temperature and/or SRT increase; whilst, from a filtration process perspective, the operating cost is reduced when SGDp decreases.

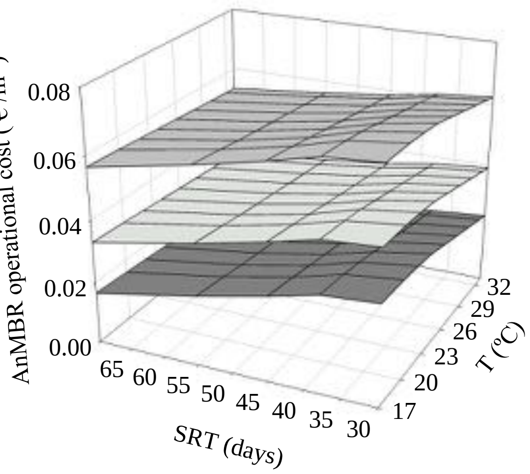

Figure 3.6 AnMBR operational cost (power requirements, energy recovery from total methane production, and sludge handling and recycling to land) at different temperature and SRT conditions for three SGD_P levels: (■) SGDp 33.4; (■) SGDp 22.3; and (■) SGDp 14.3.

3.3.3 Effect of influent sulphate content on AnMBR operating cost

As mentioned before, Table 3.4 shows the total volume of methane produced (including both biogas methane and methane dissolved in the effluent) for the cases referred as $BP_{33°C,\ SRT\ 70days}$, $BP_{22°C,\ SRT\ 38days}$ and $BP_{17°C,\ SRT\ 30days}$ when treating low-sulphate UWW (10 mg $S\text{-}SO_4 \cdot L^{-1}$). Similar to treating high-sulphate UWW, methane production increases significantly when operating at high ambient temperature and/or high SRT ($BP_{33°C,\ SRT\ 70days}$). When treating low-sulphate UWW, since a little amount of COD is consumed by SRB, the amount of influent COD transformed into methane increases significantly compared to treating high-sulphate UWW (see Table 3.4 and Table 3.3).

Figure 3.7 illustrates the operating cost of the AnMBR system when treating low-sulphate UWW. As Figure 3.7 shows, a significant decrease in the AnMBR operating cost could be achieved when treating low-sulphate UWW in comparison with treating high-sulphate UWW. For instance, for scenario FP5 and case $BP_{33°C,\ SRT\ 70days}$, the operating cost could be reduced from €0.017 per m^3 (see Figure 3.5c) to €0.001 per m^3 (see Figure 3.7c) when recovering energy from biogas methane. This highlights the possibility of improving the feasibility of AnMBR technology when treating low/non sulphate-loaded wastewaters.

Mention must also be made of the potential of AnMBR to be net energy producer (surplus electricity that can be exploited in other parts of the WWTP) when treating low-sulphate UWW. Specifically, Figure 3.7c shows that when methane is captured from both biogas and effluent, scenario FP5 presents very low operating cost (€0.006 per m^3) for case $BP_{17°C,\ SRT,\ 30days}$; whilst this cost decreases up to €0.002 per m^3 for case $BP_{22°C,\ SRT\ 38days}$. Moreover, null operating cost (or even income if the surplus energy is exploited and/or sold to the market) could be achieved for case $BP_{33°C,\ SRT\ 70days}$: theoretical maximum benefit of up to €0.014 per m^3.

Therefore, in mild/warm climates (i.e. tropical or Mediterranean), AnMBR technology is likely to be a net energy producer when treating low/non sulphate-loaded wastewaters: a theoretical maximum energy production of up to 0.11 $kWh \cdot m^{-3}$ could be obtained by capturing the methane from both biogas and effluent.

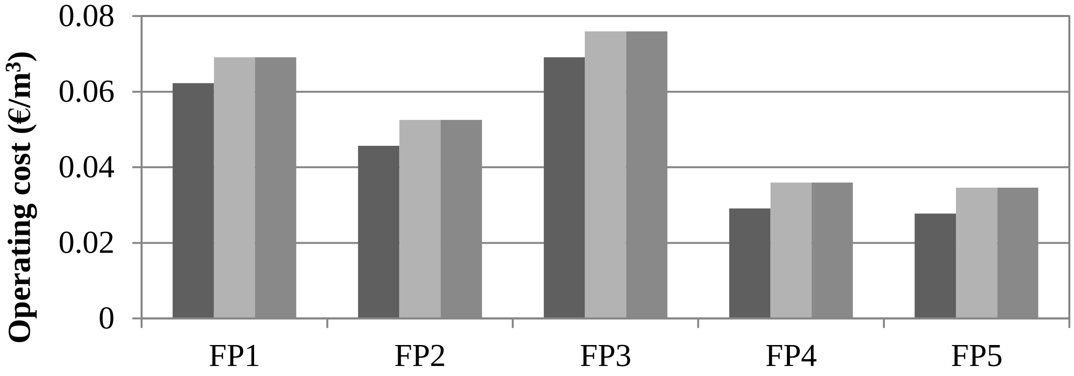

(a)

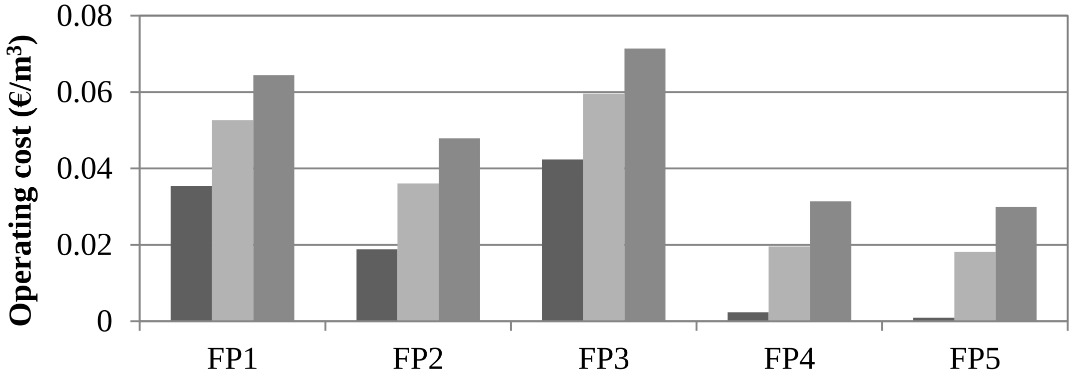

(b)

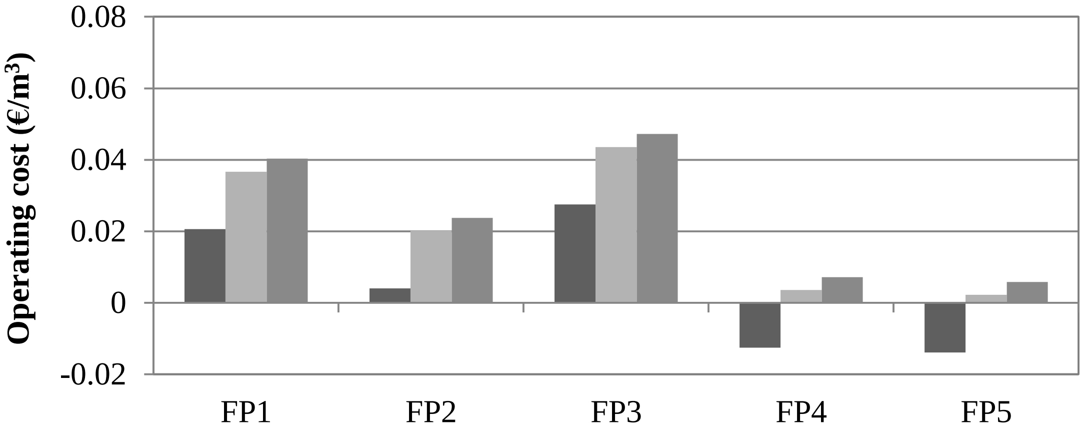

(c)

Figure 3.7 Operating cost (net energy consumption and sludge handling and recycling to land) in scenarios FP1-FP5 for cases $BP_{33°C,\ SRT\ 70days}$ (■), $BP_{22°C,\ SRT\ 38days}$ (■) and $BP_{17°C,\ SRT\ 30days}$ (■) when treating low-sulphate UWW: **(a)** non-capture of methane; **(b)** energy recovery from biogas methane; and **(c)** energy recovery biogas methane and methane dissolved in the effluent.

3.3.4 Comparison with other existing technologies

According to recent literature [3.13], the full-scale aerobic MBR from Peoria (USA) has a membrane and total aeration energy demand of around 0.34 and 0.55 $kWh \cdot m^{-3}$, which is low compared to the consumption of other full-scale municipal aerobic MBRs (e.g. Running Springs MBR WWTP, USA, consuming around 1.3-3 $kWh \cdot m^{-3}$). On the other hand, the conventional activated sludge system in Schilde (Belgium) consumed 0.19 $kWh \cdot m^{-3}$ [3.21]. In our study, the theoretical minimum energy requirements treating sulphate-rich UWW resulted in 0.07 $kWh \cdot m^{-3}$. Therefore, from an energy perspective, AnMBR operating at ambient temperature is a promising sustainable system compared to other existing urban wastewater treatment technologies. Nevertheless, it is important to consider that the energy demand from the AnMBR system evaluated in our study does not take into account the energy needed for nutrient removal, which it is considered in the wastewater treatment plants that has been mentioned as references.

According to Xing *et al*. [3.22], sludge production in activated sludge processes is generally in the range of 0.3-0.5 kg $TSS \cdot kg^{-1}$ $COD_{REMOVED}$. As expected, low/moderate amounts of sludge were obtained in our study (0.16, 0.43 and 0.55 kg $TSS \cdot kg^{-1}$ $COD_{REMOVED}$ for cases $BP_{33°C,\ SRT\ 70days}$, $BP_{22°C,\ SRT\ 38days}$ and. $BP_{17°C,\ SRT\ 30days}$, respectively). Moreover, the produced sludge was considered stabilised, which allows, as mentioned before, its direct disposal on farmland without requiring further digestion.

3.4 Conclusions

The results obtained reinforce the importance of optimising SGD_P and SRT (for given ambient temperature conditions) to minimise the energy requirements of AnMBRs treating sulphate-rich UWW (minimum value: 0.07 $kWh \cdot m^{-3}$). Operating at high ambient temperature and/or high SRT allows achieving significant energy savings whenever the methane generated is used as energy resource. Moreover, low/moderate sludge productions were obtained (minimum value: 0.16 kg $TSS \cdot kg^{-1}$ $COD_{REMOVED}$), which further enhanced the AnMBR operating cost (minimum value: €0.01 per m^3). On the other hand, the sulphate content in the UWW significantly affected the final production of methane and thereby affected the overall energy consumption. Indeed, AnMBR technology is likely to be a net energy producer when treating low/non sulphate-loaded wastewaters in warm/hot climates: theoretical maximum energy productions of up to 0.11 $kWh \cdot m^{-3}$ could be achieved

3.5 Acknowledgements

This research work was possible thanks to projects CTM2011-28595-C02-01/02 (funded by the Spanish Ministry of Economy and Competitiveness jointly with the European Regional Development Fund) and aqualia INNPRONTA IISIS IPT-20111023 (partially funded by the Centre for Industrial Technological Development (CDTI) and supported by the Spanish Ministry of Economy and Competitiveness).

3.6 References

3.1 X.M. Guo, E. Trably, E. Latrille, H. Carrère, J.P. Steyer, Hydrogen production from agricultural waste by dark fermentation: A review, Int. J. Hydrog. Energy 35 (2010) 10660–10673.

3.2 A. Gallego, A. Hospido, M.T. Moreira, G. Feijoo, Environmental performance of wastewater treatment plants for small populations, Resour. Conser. Recy. 52 (2008) 931–940.

3.3 L. Raskin, Anaerobic Membrane Bioreactors for Sustainable Wastewater Treatment, WERF Report U4R08, June 2012.

3.4 L.W. Hulshoff Pol, Treatment of sulphate-rich wastewaters: microbial and process technological aspects TMR Summer School Programme, The Biological Sulfur Cycle: Environmental Science and Technology, April, Wageningen, The Netherlands, 1998.

3.5 J.B. Giménez, A. Robles, L. Carretero, F. Durán, M.V. Ruano, M.N. Gattib, J. Ribes, J. Ferrer, A. Seco, Experimental study of the anaerobic urban wastewater treatment in a submerged hollow-fiber membrane bioreactor at semi-industrial scale, Bioresour. Technol. 102 (2011) 8799–8806.

3.6 Miliarium Aureum, S.L, Portal de referencia para la Ingeniería Civil, Construcción y el Medio Ambiente, Available on: http://www.miliarium.com/prontuario/Tablas/Aguas/CaracterizacionAguasResidualesUrbanas.asp, (Accessed February 6, 2014).

3.7 A. Robles, M.V. Ruano, J. Ribes, J. Ferrer, Sub-critical long-term operation of industrial scale hollow-fibre membranes in a submerged anaerobic MBR (HF-AnMBR) system, Sep. Purif. Technol. 100 (2012) 88–96.

3.8 A. Robles, M.V. Ruano, J. Ribes, J. Ferrer, Factors that affect the permeability of commercial hollow-fibre membranes in a submerged anaerobic MBR (HF-AnMBR) system, Water Res. 47 (2013) 1277–1288.

3.9 J. Ferrer, A. Seco, J. Serralta, J. Ribes, J. Manga, E. Asensi, J.J. Morenilla, F. Llavador, DESASS: A software tool for designing, simulating and optimising WWTPs, Environ. Modell. Softw. 23 (2008) 19–26.

3.10 R. Barat, J. Serralta, M.V. Ruano, E. Jiménez, J. Ribes, A. Seco, J. Ferrer, Biological Nutrient Removal Model Nº 2 (BNRM2): A general model for Wastewater Treatment Plants, Water Sci. Technol. 67 (2013) 1481–1489.

3.11 *Standard methods for the Examination of Water and Wastewater*, 21th edn, American Public Health Association/American Water Works Association/Water Environmental Federation, Washington DC, USA, 2005.

3.12 J.B. Giménez, N. Martí, J. Ferrer, A. Seco, Methane recovery efficiency in a submerged anaerobic membrane bioreactor (AnMBR) treating sulphate-rich urban wastewater: Evaluation of methane losses with the effluent, Bioresour. Technol. 118 (2012) 67–72.

3.13 S. Judd, C. Judd, Principles and Applications of Membrane Bioreactors in Water and Wastewater Treatment. Second Edition, Elsevier, London, UK, 2011, chapter 3 and 5.

3.14 AGUA TÉCNICA, Equipos mecánicos para tratamiento de aguas, Tamiz rotativo para sólidos finos, Available on: http://www.aguatecnica.es/index.php?option=com_content&view=article&id=50&Itemid=59, (Accessed September 7, 2012).

3.15 X. Elias-Castell, Vías de tratamiento y valorización de fangos de depuradora. Ediciones Díaz de santos, Madrid, España, 2012.

3.16 EPA, Environmental Protection Agency, Combined Heat and Power Partnership, Agency of the United States federal government, 2012.

3.17 Spanish electricity tariff, Iberdrola S.A, 2013.

3.18 J.A. Sainz-Lastre, Tecnologías para la sosteniblidad, Procesos y operaciones unitarias en depuración de aguas residuales, Colección EOI, 2005.

3.19 Miliarium Aureum, S.L, Portal de referencia para la Ingeniería Civil, Construcción y el Medio Ambiente, Available on: http://www.miliarium.com/Proyectos/Depuradoras/introduccion/edar.asp, (Accessed May 5, 2013).

3.20 Lettinga. G, Rebac. S, Zeeman. G, Challenge of psychrophilic anaerobic wastewater treatment. Trends Trends Biotechnol. 19 (2001) 363–370.

3.21 A. Fenu, J. Roels, T. Wambecq, K. De Gussem, C. Thoeye, G. De Gueldre, B. Vand De Steene, Energy audit of a full scale MBR system, Desalination 262 (2010) 121–128.

3.22 C.-H. Xing, W.-Z. Wu, Y. Quian, E. Tardieu, Excess sludge production in membrane bioreactors: a theoretical investigation, J. Environ. Eng. ASCE, 129 (2003) 291–297

CHAPTER 4:

Design methodology for submerged anaerobic membrane bioreactors (AnMBR): A case study

Abstract

The main objective of this study is to propose guidelines for designing submerged anaerobic MBR (AnMBR) technology for municipal wastewater treatment. The design methodology was devised on the basis of simulation and experimental results from an AnMBR plant featuring industrial-scale hollow-fibre membranes. The proposed methodology aims to minimise both capital expenditure and operating expenses, and the key parameters considered were: hydraulic retention time, solids retention time, mixed liquor suspended solids concentration in the membrane tank, 20 °C-standardised critical flux, specific gas demand per square metre of membrane area, and flow of sludge being recycled from the membrane tank to the anaerobic reactor. An AnMBR WWTP operating at 15 and 30 °C with both sulphate-rich (5.7 mg COD·mg^{-1} SO_4-S) and low-sulphate (57 mg COD·mg^{-1} SO_4-S) municipal wastewater was designed. The minimum cost of the designed plant was €0.097 and €0.070 per m^3 when treating sulphate-rich and low-sulphate wastewater, respectively.

Keywords

CAPEX/OPEX; design methodology; industrial-scale hollow-fibre membranes; submerged anaerobic MBR (AnMBR); municipal wastewater treatment

Highlights

A design methodology for AnMBR technology is proposed in this study.
Different design and operating parameters were evaluated to minimise CAPEX and OPEX.
Optimum design and operation were determined at different operating conditions.
The AnMBR total cost when treating sulphate-rich municipal wastewater was €0.097 per m^3.
Cost savings of up to 25% can be achieved when treating low-sulphate wastewater.

J. Ferrer, R. Pretel, F. Durán, J.B. Giménez, A. Robles, M.V. Ruano, J. Serralta, J. Ribes, A.Seco
Design methodology for submerged anaerobic membrane bioreactors (AnMBR): A case study
Sep. Purif. Technol. 141 (2015) 378–386

4.1 Introduction

Anaerobic wastewater treatment has several advantages in comparison with conventional aerobic treatment: i) lower sludge production because of the low yield of anaerobic microorganisms; ii) lower energy consumption because no aeration is required; and iii) potential resource recovery because energy (from biogas production) and nutrients (NH_4^+ and PO_4^{3-}) can be obtained from the anaerobic degradation process. As a result, anaerobic processes are viewed as an attractive choice for sustainable low-strength wastewater treatment (e.g. municipal wastewater). However, anaerobic processes have certain drawbacks that currently prevent them from being used in the full-scale treatment of low-strength wastewater.

As regards the anaerobic treatment of municipal wastewater, the low COD (chemical oxygen demand) of municipal wastewater (typically less than 1 $g \cdot L^{-1}$) means that little methane is produced. Therefore, an external energy source would be needed to heat the reactor to mesophilic conditions [4.1]. At low temperatures, the growth rates of anaerobic microorganisms are greatly reduced and long sludge retention times (SRT) are necessary – not only to meet appropriate effluent and sludge standards and produce considerable amounts of biogas, but also to prevent biomass washout [4.2]. Therefore, the success of anaerobic treatment of municipal wastewater at low temperatures depends on the ability to detach SRT from hydraulic retention time (HRT). In this respect, submerged anaerobic membrane bioreactors (AnMBRs) are considered a feasible alternative for municipal wastewater treatment at low temperatures.

Jeison [4.3] reported reductions of up to 90% in the sludge produced when AnMBR technology was used, therefore this technology is a promising alternative for the anaerobic treatment of low-strength wastewater. In addition, depending on the operating conditions, the produced sludge could be enough stabilised to be disposed of directly on farmland with no further digestion step (no pathogens and low biological methane production).

On the other hand, when municipal wastewater containing sulphate is anaerobically treated, the sulphate is reduced to sulphide. The production of this end product can cause technical problems such as: i) hydrogen sulphide is toxic to anaerobic microorganisms; ii) the amount of biogas produced is reduced because some of the influent COD (approx. 2 g COD per g SO_4-S) is consumed by sulphate-reducing microorganisms (SRB); iii) the quality of the produced biogas is reduced because some of the hydrogen sulphide produced will end up in the biogas; iv) hydrogen sulphide can cause corrosion in pipes, engines and boilers, entailing higher maintenance and replacement costs; and v) downstream oxygen demand may be required for oxidising hydrogen sulphide. For municipal wastewater, which can easily present low COD/SO_4-S ratios, the competition between Methanogenic Archaea (MA) and SRB can critically affect the amount and quality of the biogas produced. According to the theoretical methane yield under standard temperature and pressure conditions (350 L CH_4 per kg COD), SRB reduces the production of approx. 700 L of methane per kg of influent SO_4–S (considering reduction of all sulphate to sulphide). Therefore, higher biogas productions would be achieved at low sulphate influent concentrations [4.4].

As regards filtration, the high SRTs applied in AnMBR technology usually mean high levels of mixed liquor suspended solids (MLSS) which contribute to membrane fouling [4.5]. In order to minimise any kind of membrane fouling and thereby increase membrane lifespan, the main operating challenge for AnMBRs is to optimise membrane operation and configuration [4.6; 4.7; 4.8]. It is therefore necessary to optimise filtration whilst minimising not only capital expenditure but also operating and maintenance costs. Hence the AnMBR design strategy must be carefully selected since depending on the design strategy, different design criteria can be adopted.

The main points of fouling control strategies as regards membrane operation are: optimising the frequency and duration of the physical cleaning stages (back-flush and relaxation) [4.9,4.10]; optimising different operating variables such as gas sparging intensity or permeate/influent flow rate ratios; and operating membranes under the sub-critical filtration conditions bounded by critical flux (J_C) [4.11, 4.12]. Thus, one such design strategy entails operating membranes in sub-critical filtration conditions. Operating membranes sub-critically increases membrane lifespan, which reduces maintenance costs, but it usually increases investment and/or operating expenses (i.e. it increases the membrane area needs and/or the intensity of the gas sparging used for membrane scouring). MLSS and gas sparging intensity (usually measured as specific gas demand per membrane area, SGD_m) have been widely identified as the factors that affect J_C most. As for MLSS, an optimum combination of reactor volume and filtration area must be selected in order to keep MLSS at sub-critical levels for a given SGD_m. In addition, membrane scouring by air/biogas is a key process that allows minimising energy consumption of MBR plants because it is the most energy-consuming process in full-scale MBRs (see, for instance, [4.12]). Therefore, one of the main challenges when designing an AnMBR plant is to achieve acceptable membrane performances at minimum levels of SGD_m whilst minimising membrane fouling.

Another design criterion entails operating membranes in supra-critical filtration conditions. This strategy means lower initial investment because it requires lower operating volumes (i.e. operating at higher MLSS levels) and/or smaller membrane surfaces than operating membranes at sub-critical filtration conditions. However, maintenance and operating expenses are probably higher. For instance, for a given SGD_m, an increase in MLSS usually means greater membrane fouling, which in turn increases membrane maintenance costs because the membranes are chemically cleaned more often. In addition, increasing the frequency of membrane chemical cleaning affects the membrane lifespan, which also increases membrane replacement costs.

Although AnMBR technology has not been yet applied to full-scale municipal wastewater treatment, recent literature [4.13; 4.14; 4.15; 4.16; 4.17] has reported increasing interest by the scientific community in the use of AnMBRs for municipal wastewater treatment. However, a design methodology that holistically considers the key operating factors that affect both biology and filtration is still necessary in order to lay the foundations for the optimum design of full-scale AnMBRs for municipal wastewater treatment. The aim of this paper is to provide guidelines for designing AnMBR technology under different scenarios. To this aim, a design methodology was developed based on the knowledge and operation experience gained from an AnMBR plant featuring industrial-scale hollow-fibre membranes that was fed with sulphate-rich wastewater from the pre-treatment of a municipal WWTP located in Valencia (Spain). The proposed methodology aims to minimise total annual costs, which are defined as the sum of capital and operating expenses (CAPEX/OPEX). OPEX take into account energy requirements, methane production and capture, sludge handling and disposal, and membrane maintenance and replacement. In this respect, the key operating parameters considered when designing the biological process were hydraulic retention time (*HRT*) and solids retention time (*SRT*); and, when designing the filtration process, the levels of mixed liquor suspended solids in the membrane tank ($MLSS_{MT}$), the 20 ºC-standardised critical fluxes (J_{20}), SGD_m and the recycling sludge flow rate from the membrane tank to the anaerobic reactor (Q_{rec}).

The proposed methodology was used to design an AnMBR WWTP handling municipal wastewater with high and low levels of sulphate (5.7 and 57 mg COD·mg^{-1} SO_4-S, respectively) at 15 and 30 ºC.

4.2 Materials and methods

As mentioned earlier, the proposed design methodology is based on the knowledge and the results obtained from the operation of an AnMBR plant fitted with industrial-scale membranes that was operated using real sulphate-rich municipal wastewater. The WWTP simulating software DESASS [4.18], which enables a wide range of wastewater treatment schemes (including AnMBR systems) to be evaluated, was used to simulate the AnMBR WWTP

4.2.1 AnMBR plant description

This study was conducted in the AnMBR demonstration plant already described in Chapter 3. It consists of an anaerobic reactor with a total volume of 1.3 m^3 connected to two membrane tanks, each with a total volume of 0.8 m^3. Each membrane tank features one ultrafiltration hollow-fibre membrane commercial system (PURON®, Koch Membrane Systems, 0.05 µm pore size, and outside-in filtration). Each module consists of 9 hollow-fibre bundles of 1.8-m length that give a total of 30 m^2 membrane surface. In order to scour the membranes, thus minimising cake layer formation, a fraction of the produced biogas is continuously recycled to the membrane tanks through the bottom of each fibre bundle.

As mentioned above, this plant was fed with sulphate-rich municipal wastewater from the pre-treatment of the Carraixet WWTP (Valencia, Spain), which involves screening, degritting and grease removal. Further details of this AnMBR can be found in Giménez *et al.* [4.19] and Robles *et al.* [4.9].

4.2.2 AnMBR plant operation

The AnMBR plant was operated for more than 4 years under different operating conditions [4.4; 4.9]. Regarding the biological process, the plant was operated at four different SRT (20, 30, 40 and 70 days), with controlled HRT ranging from 5 to 30 hours, and organic load rates (OLR) ranging from 0.5 to 2 kg $COD \cdot m^{-3} \cdot d^{-1}$. The impact of temperature on process performance was evaluated in the 14 – 33 ºC range. During the operating period, the pH in the mixed liquor remained stable around 6.8 ± 0.2. As regards filtration, the membranes were operated at J_{20} from 6 to 20 LMH and SGD_m from 0.1 to 0.5 $m^3 \cdot m^{-2} \cdot h^{-1}$. The MLSS ranged from 5 to 30 $g \cdot L^{-1}$.

The influent wastewater was characterised using 24-hour composite samples. The following parameters were analysed daily: Total Suspended Solids (TSS), Volatile Suspended Solids (VSS), Volatile Fatty Acids (VFA), carbonate alkalinity (Alk), sulphate (SO_4-S), ammonium (NH_4-N), and orthophosphate (PO_4-P). The following parameters were determined once a week: total and soluble COD (T-COD and S-COD, respectively); total and soluble biological oxygen demand (T-BOD_{20} and S-BOD_{20}, respectively); and total nitrogen (TN) and total phosphorous (TP). Solids, COD, sulphate, and nutrients were determined according to Standard Methods [4.20]. Alk and VFA were determined by titration using the method proposed by WRC [4.21].

4.2.3 AnMBR WWTP simulation

Figure 4.1 shows a flow diagram of the AnMBR WWTP designed to remove organic matter, which is based on the AnMBR plant mentioned earlier. The proposed AnMBR WWTP also includes a sludge dewatering system for conditioning the resulting sludge; a degassing membrane for capturing the dissolved methane in the effluent, and a combined heat and power (CHP) system enabling energy to be recovered from methane. This plant was simulated using a new version of DESASS [4.18] which features a modified version of the mathematical model BNRM2 [4.22] including the competition between both acetogenic and methanogenic microorganisms and sulphate-reducing microorganisms [4.23]. This mathematical model was validated beforehand using experimental data obtained from the AnMBR plant [4.23].

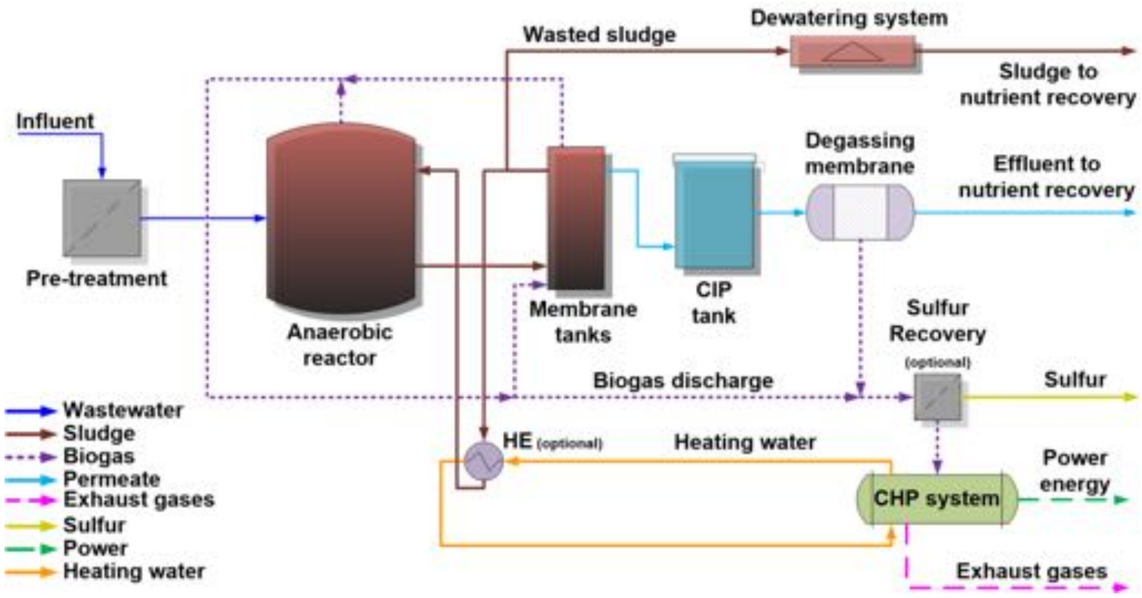

Figure 4.1 Process flow diagram for the proposed AnMBR WWTP (CIP: clean-in-place; HE: heat exchanger; CHP: combined heat and power).

The proposed AnMBR was designed to handle an influent flow of 50,000 $m^3 \cdot d^{-1}$ with the characteristics shown in Table A.4.1. Two different simulation scenarios were evaluated: the treatment of (1) sulphate-rich municipal wastewater (5.7 mg $COD \cdot mg^{-1}$ SO_4-S) and (2) low-sulphate municipal wastewater (57 mg $COD \cdot mg^{-1}$ SO_4-S).

Table A.4.1 Characteristics of the wastewater entering the anaerobic reactor used for designing the proposed AnMBR WWTP (**sulphate-rich municipal wastewater;* ***low-sulphate municipal wastewater*).

Parameter	Unit	Value
TSS	mg TSS·L^{-1}	315
VSS	mg VSS·L^{-1}	254
T-COD	mg COD·L^{-1}	568
S-COD	mg COD·L^{-1}	83
T-BOD_{20}	mg COD·L^{-1}	363
S-BOD_{20}	mg COD·L^{-1}	64
VFA	mg COD·L^{-1}	8
SO_4-S	mg S·L^{-1}	100*/10**
TN	mg N·L^{-1}	55
NH_4-N	mg N·L^{-1}	33
TP	mg P·L^{-1}	10.3
PO_4-P	mg P·L^{-1}	4.1
Alk	mg $CaCO_3$·L^{-1}	337
pH		7.7

4.3 Design methodology

In the proposed methodology, HRT, SRT and $MLSS_{MT}$ are the key operating parameters when designing the biological process in AnMBR technology, and J_{20}, SGD_m and $MLSS_{MT}$ are the key operating parameters when designing the filtration process in AnMBR technology.

The design methodology proposed in this study (summarised in Figure A.4.1) aims to minimise total annual costs (CAPEX plus OPEX), and consists of two main stages. The first stage involves optimising two parameters related to the anaerobic reactor, i.e. anaerobic reactor volume (V) and sludge recycling flow rate from the membrane tank to the anaerobic reactor (i.e. Q_{rec}). At a given operating temperature and influent flow and load, the AnMBR system is simulated under different SRT and $MLSS_{MT}$ (for Q_{rec} = influent flow). The SRT values used in the simulations must be above the minimum SRT needed to meet effluent standards and sludge stabilisation criteria. These simulation results are used to determine the optimum combination of anaerobic reactor volume and sludge recycling flow rate (see 4.3.1) for each SRT and $MLSS_{MT}$. The optimum combination ($V(opt)$, $Q_{rec}(opt)$) is the one that gives the lowest anaerobic reactor cost, including the following cost items: construction of the anaerobic reactor

including pumps and pipes, and the energy required for reactor stirring and sludge pumping. The cost of the biological process is then calculated for each SRT and $MLSS_{MT}$, also taking into account the costs of sludge handling and disposal, and the savings made by recovering energy from methane capture.
The second stage involves optimising J_{20} at the different $MLSS_{MT}$ levels evaluated in the simulations of stage 1. Before applying this methodology, the 20 ºC-standardised critical flux (J_{C20}) must be experimentally determined at different $MLSS_{MT}$ and SGD_m. The SGD_m considered in this study was selected on the basis of previous experimental results (data not shown), and J_{C20} was calculated for the different $MLSS_{MT}$. The following variables are then calculated for different values of J_{20} above and below J_{C20}: membrane tank volume, membrane filtration area (A_m), flow rate of biogas recycled into membrane tank (Q_G), transmembrane pressure (*TMP*), membrane permeability (*K*) and the amount of chemical reagents required for chemical membrane cleaning recommended by the membrane manufacturer. These values are then used to calculate the filtration cost, taking into account the following cost items: membrane area, membrane tank, biogas sparging, blowers and pipes, permeate pumping, chemical reagent, and membrane replacement. Then, for each level of $MLSS_{MT}$ the optimum operating J_{20} ($J_{20}(opt)$) is selected, which is the one that gives the lowest filtration cost.

Finally, the optimum design values (*SRT*, *HRT*, Q_{rec}, $\mathrm{MLSS_{MT}}$, J_{20} and A_m), i.e. those giving the lowest total cost, in worst-case seasonal conditions (i.e. winter) are selected, and then the optimum operating strategy for the best-case scenario (i.e. summer) is established

4.3.1 Biological process design

Table 4.1a shows how the selected design criteria (SRT, $\mathrm{Q_{rec}}$, $\mathrm{MLSS_{MT}}$) affects the above-mentioned factors that contribute to the cost of the biological process. As Table 4.1a shows, higher SRTs increase construction and stirring costs but also increase biogas production, resulting in more energy being recovered from methane capture. Increases in $\mathrm{Q_{rec}}$ reduce the reactor volume for a given $\mathrm{MLSS_{MT}}$, but increase the sludge pumping cost. Therefore, the optimum AnMBR design must include the optimum combination of SRT and $\mathrm{Q_{rec}}$. Finally, the higher the $\mathrm{MLSS_{MT}}$, the lower the reactor volume and stirring costs. However, an increase in $\mathrm{MLSS_{MT}}$ leads to higher filtration costs. Since the costs of the biological and filtration processes depend on MLSS levels, the design and operation of both the anaerobic reactor and the membrane tank must be simultaneously optimised for different $\mathrm{MLSS_{MT}}$. The range of 5 to 25 $g \cdot L^{-1}$ used in this paper was adopted on the basis of experimental data from the AnMBR plant.

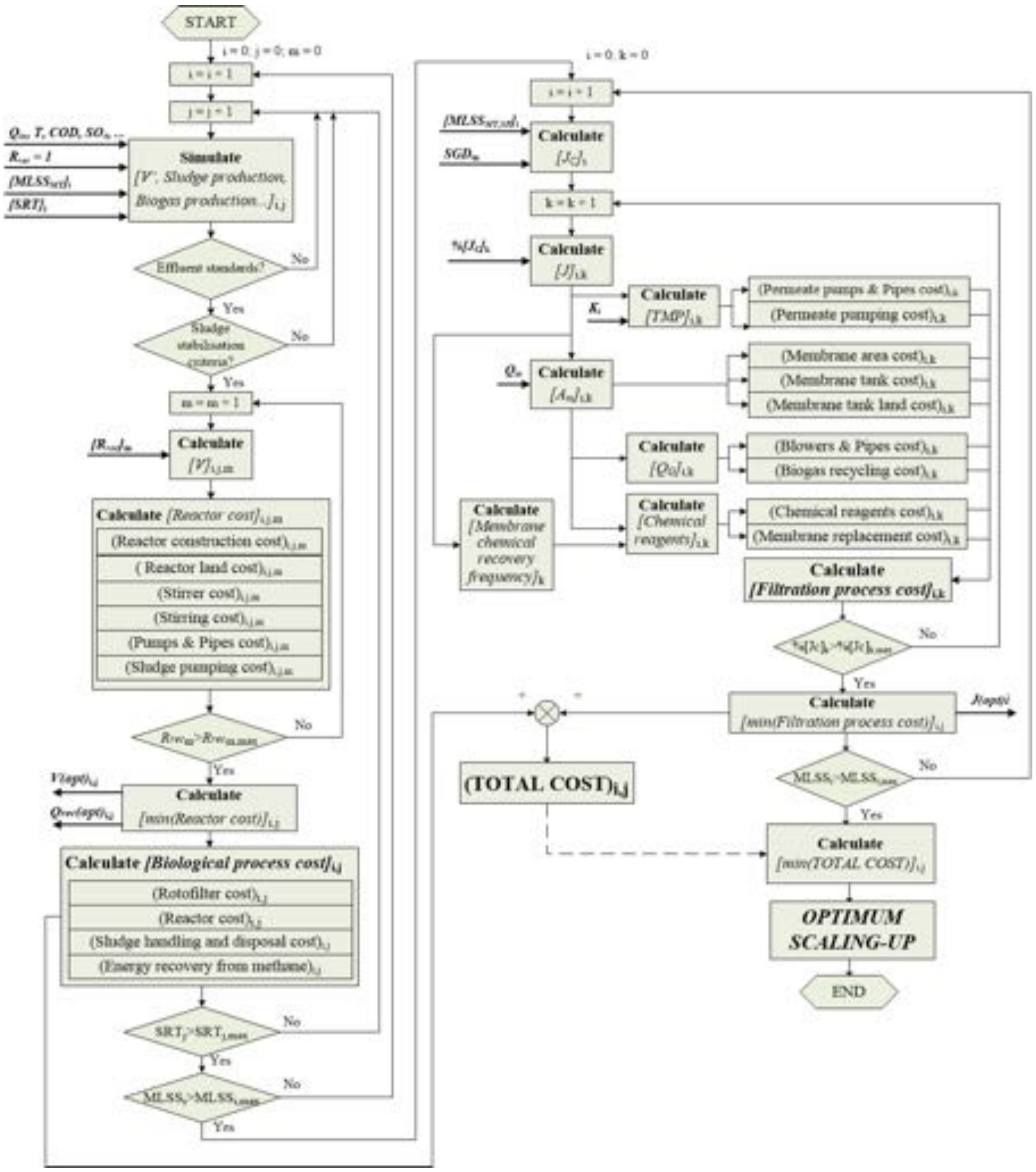

Figure A.4.1 Proposed design methodology for AnMBR technology.

Table 4.1 Impact of design parameters on cost of **(a)** biological process and **(b)** filtration.

	Cost of				
	Construction	Stirring sludge	Sludge recycling	Sludge handling	Energy recovery
SRT ↑	↑	↑		↓	↑
Q_{rec} ↑	↓	↓	↑		
$MLSS_{MT}$ ↑	↓	↓			

(a)

	Cost of			
	Membrane area + membrane tank	Biogas recycling	Permeate pumping	Chemical reagent
$MLSS_{MT}$ ↑		↑	↑	↑
J_{20} ↑	↓	↓	↑	↑
SGD_m ↑		↑		↓

(b)

The performance of the anaerobic reactor at each $MLSS_{MT}$ must be simulated at different SRT and Q_{rec}. SRT values should be above the minimum SRT stipulated in effluent standards and sludge stabilisation criteria.

At a given SRT and $MLSS_{MT}$, the higher the sludge recycling flow rate, the lower the reactor volume. Our study found the following relationship between the anaerobic reactor volume and the sludge recycling flow rate (see Eq. 4.1):

$$\frac{V}{V'} = a + \frac{b}{R_{rec}} - \frac{c}{{R_{rec}}^2} + \frac{d}{{R_{rec}}^3} \qquad \textbf{(Eq. 4.1)}$$

where V is the reactor volume, R_{rec} is the sludge recycling ratio defined as Q_{rec} per influent flow, V' is the reference reactor volume obtained for R_{rec} = 1, and a, b, c and d are fine-tuning parameters (in this study, 0.5039, 0.5003, $4.2453 \cdot 10^{-3}$ and $3.2861 \cdot 10^{-5}$, respectively, obtained from the simulation results shown in Figure 4.2).

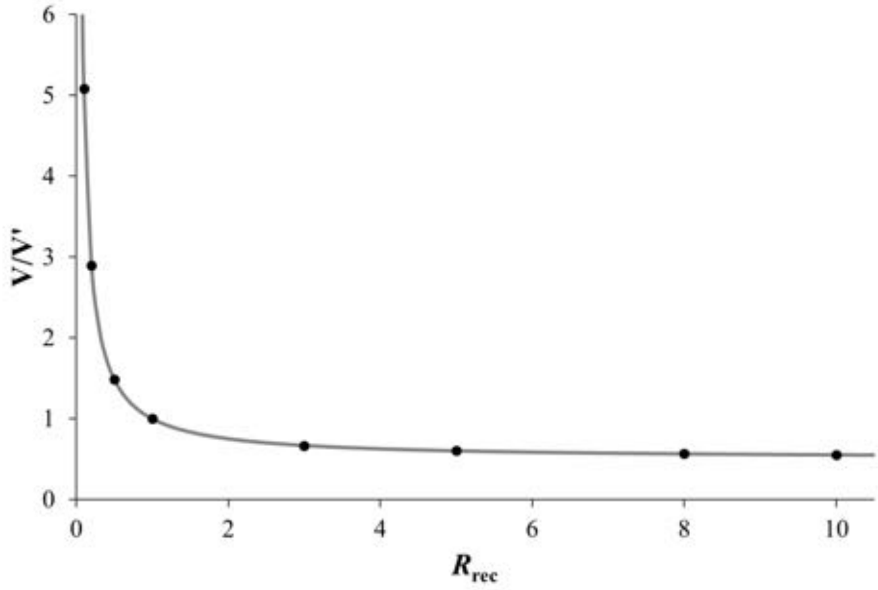

Figure 4.2 Correlation between the sludge recycling ratio (R_{rec} = sludge recycling flow from the membrane tank to the anaerobic reactor per influent flow) and the ratio between the reactor volume (V) and the reference reactor volume obtained for R_{rec} = 1 (V').

The correlation shown in Eq. 4.1 significantly reduces the number of simulations required to obtain optimum design values. In this respect, the performance of the biological process at each selected $MLSS_{MT}$ is simulated at different SRTs for Q_{rec} = influent flow (R_{rec} = 1), which gives the defined reference reactor volume V'. Different R_{rec} are then selected for each $MLSS_{MT}$ and SRT, and the respective anaerobic reactor volumes (V) are calculated using Eq. 4.1 (with the V' previously determined and each of the R_{rec} selected). The optimum combination of R_{rec} and V is the one that gives the lowest anaerobic reactor cost taking into account the following cost items: anaerobic reactor construction including pumps and pipes, anaerobic reactor stirring (including equipment and energy requirements) and sludge pumping.

The different simulations carried out during the biological process design give the following information that is used to calculate the capital and operating expenses of the biological process: anaerobic reactor volume, sludge recycling flow rate, biogas production, and flow rate and characteristics of the wasted sludge.

4.3.2 Filtration design

As mentioned earlier, the cost of the following items was taken into account when calculating filtration costs: membrane area, membrane tank including blowers and pipes, biogas sparging, permeate pumping (including equipment and energy requirements), chemical reagent and membrane replacement. The main operating parameters that affect filtration costs are J_{20}, $MLSS_{MT}$ and SGD_m.

Table 4.1b shows the effect of these operating parameters on the above-mentioned costs. As Table 4.1b shows, the lower the $MLSS_{MT}$, the lower the filtration cost. However, as stated before, the higher the $MLSS_{MT}$, the lower the cost of the biological process. Therefore, the sum of the biological and filtration costs must be minimised by optimising $MLSS_{MT}$. To do so, the filtration cost was calculated for each $MLSS_{MT}$ at different J_{20} values above and below the experimentally-determined critical flux (J_{20} varying from 80 to 120% of the respective J_{C20}).

Filtration costs were calculated in each scenario using the following parameters: membrane tank volume, membrane filtration area (A_m, Eq 4.2), membrane permeability (K, Eq 4.3), transmembrane pressure (TMP, Eq. 4.4) and the biogas recycling flow rate (Q_{gas}, Eq. 4.5).

$$\left[A_m\right]_{i,k} = \frac{Q_{in}}{\left[J_{20}\right]_{i,k}} \qquad \textbf{(Eq 4.2)}$$

where $[A_m]_{i,k}$ is the membrane filtration area for each $MLSS_{MT}$ (denoted by i) and $\%J_{20,C}$ (denoted by k), Q_{in} is the influent flow rate, and $[J_{20}]_{i,k}$ is the 20 ºC-standardised transmembrane flux for each i and k.

$$\left[K\right]_i = -a \cdot \left[MLSS_{MT}\right]_i + b \qquad \textbf{(Eq 4.3)}$$

where $[K]_i$ is the membrane permeability in LMH·bar^{-1} for each level of mixed liquor suspended solids in the membrane tank (denoted by $[MLSS_{MT}]_i$), and a and b are fine-tuning parameters obtained from previous studies [4.24].

$$\left[TMP\right]_{i,k} = \frac{\left[J_{20}\right]_{i,k}}{\left[K\right]_i} \qquad \textbf{(Eq. 4.4)}$$

where $[TMP]_{i,k}$ is the transmembrane pressure for each $MLSS_{MT}$ (denoted by i) and $\%J_{20,C}$ (denoted by k), $[J_{20}]_{i,k}$ is the 20 ºC-standardised transmembrane flux of each i and k, and $[K]_i$ is the membrane permeability of each i.

$$\lfloor Q_G \rfloor_{i,k} = SGD_m \cdot \lfloor A_m \rfloor_{i,k} \qquad \textbf{(Eq. 4.5)}$$

where $[Q_G]_{i,k}$ is the biogas recycling flow rate for each $MLSS_{MT}$ (denoted by i) and each $\%J_{20,C}$ (denoted by k), SGD_m is the specific gas demand per membrane area, and $[A_m]_{i,k}$ is the membrane filtration area for each i and k.

The results obtained from Eq 4.2, Eq 4.3, Eq. 4.4, and Eq. 4.5 were used to calculate the capital and operating expenses of filtration process.

4.3.3 Total annual cost

The total annual cost (*TAC*) of the biological and filtration processes was calculated by adding the annual investment cost (*IC*) to the annual operating and maintenance costs (*O&MC*), as shown in Eq. 4.6 [4.25]:

$$TAC = \frac{\mathrm{r}(1+\mathrm{r})^{\mathrm{t}}}{(1+r)^{t}-1} \cdot IC + O \,\&\, MC \qquad \textbf{(Eq. 4.6)}$$

where *TAC* is the total annual cost, *IC* is the investment cost, *O&MC* are the annual operating and maintenance costs, *r* is the annual discount rate, and *t* is the depreciation period in years.

The *IC* of the proposed AnMBR WWTP includes construction work (anaerobic reactor and membrane tank) and equipment (membranes, blowers, pumps and pipes). The *O&MC* of the proposed AnMBR WWTP includes energy requirements, energy recovery from methane capture, chemical reagents used to clean membranes, and sludge handling and disposal. Maintenance expenditure refers to the pumps and blowers, and membrane replacement.

4.4 Case study

The proposed methodology was used to design an AnMBR WWTP handling sulphate-rich wastewater at 15 and 30 ºC. Firstly, the optimum design parameters were determined for this AnMBR WWTP under the worst-case operating conditions (15 ºC), and then the optimum operating strategy was calculated for the best-case operating conditions (30 ºC).

Table A.4.2 shows the unit costs used to calculate the capital and operating expenses (CAPEX/OPEX) of the proposed AnMBR WWTP. The main considerations taken into account when calculating CAPEX and OPEX are summarized as follows:

- *Capital/investment cost (IC):*
  - Depreciation: A depreciation period of 20 years was used to calculate the total annual cost (*TAC*), with an annual discount rate (*r*) of 5%.
  - Membrane tank: The membrane tank volume was estimated according to a commercial membrane unit (PURON®, Koch Membrane Systems, PUR-PSH1500, 0.05 µm pore size, 1500 m^2 total filtering area).
  - Biogas, sludge and permeate pipeline: The velocity of the fluids in the pipes was set to 1 $m \cdot s^{-1}$ to calculate the pipe diameter.

- *Operating cost (OC):*
  - Power requirements*:* The simulation software DESASS was used to calculate the power requirements of the sludge and permeate pumps (associated with the filtration and back-flushing phases), biogas blowers, anaerobic reactor stirrers and sludge dewatering system as shown in Pretel *et al.* [4.26].
  - Energy recovery from methane (biogas methane and dissolved methane in the effluent): The selected technology for capturing the dissolved methane in the effluent was degassing membranes (see Table A.4.2). The chosen CHP technology for energy recovery from methane consisted of microturbines. The power and heat efficiency of this technology is approximately 27.0 and 33.5%, respectively [4.27].
  - Chemical reagents used to clean membranes*:* According to Judd and Judd [4.6] and previous experiments (see, for instance, [4.28]), 9.5 months can be set as the interval for membrane cleaning with chemicals when operating under critical filtration conditions. Therefore, in this study, the membrane chemical cleaning frequency ranged from 2 months (operating at J_{20} = 120% of J_{C20}) to 18 months (operating at J_{20} = 80% of J_{C20}). Sodium hypochlorite and citric acid are the two reagents required for cleaning the membranes chemically. In compliance with the membrane cleaning protocol proposed by the membrane manufacturer, 2000 ppm was adopted as the dose of both sodium hypochlorite and citric acid and the contact with each chemical was set to 5 hours.
  - Membrane physical cleaning: The downtime for membrane physical cleaning through back-flushing was set to 2.4% of the membrane operating time. This downtime was established based on the experimental results obtained by a model-based supervisory controller implemented in the AnMBR plant which optimised, among others, back-flushing frequency [4.10].

- Membrane replacement cost: As regards membrane lifespan, the cost of replacing the membrane was contemplated in order to evaluate the entire lifecycle cost of the system. The maximum total contact with chlorine permissible before membrane replacement according to the supplier is 500,000 ppm-hours cumulative. Therefore, the membrane lifetime (determining the membrane replacement cost) was calculated accounting for: 1) the maximum total contact with chlorine permissible and 2) the interval for membrane chemical cleaning.
- Sludge treatment cost: Centrifuges were selected for sludge dewatering. To ensure adequate sludge conditioning, polyelectrolyte is required and the dose considered in our study was 6 $kg \cdot t^{-1}$ TSS [4.29]. The sludge produced was used as fertiliser on farmland.
- Equipment replacement and maintenance*:* The lifetime of blowers and pumps was as per manufacturers' recommendations (see Table A.4.2). Membrane lifetime was estimated according to the total chlorine contact specified by the manufacturer (see Table A.4.2).

4.4.1 Simulation results

Figure 4.3 a shows the simulation results of the effect of SRT on the biodegradable volatile suspended solids (BVSS) fraction of the sludge and on methane production, at 15 and 30ºC. This figure shows that the BVSS fraction falls and methane production rises when either the temperature or SRT increases. As Figure 4.3 a illustrates, an SRT of more than 10 days would be necessary in order to comply with the sludge stabilisation criteria (%BVSS<35%) at 30 ºC, whereas the minimum SRT required at 15 ºC would increase up to 35 days.

However, at 15 ºC no methane production is envisaged on the basis of the model with SRTs of less than 35 days. In sulphate-rich wastewaters, methanogenic and sulphate-reducing organisms compete for the available substrates. In this respect, the available substrates will be consumed first by sulphate-reducing organisms because their growth rate is higher than methanogenic organisms.

Figure 4.3 b shows the simulation results of the effect of SRTs on effluent COD and BOD (excluding methane COD) at 15 and 30ºC. The upper and lower horizontal lines mark the COD and BOD discharge limits, respectively, as specified by European discharge quality standards. As can be seen in Figure 4.3 b, the COD and BOD of the effluent are both forecast to be well below said standards in the ranges of SRT and temperature used in our simulations. These results indicate that the membrane retention capacity will enable effluent of a good quality, i.e. containing acceptable levels of organic matter, to be obtained across a wide range of SRTs and temperatures.

Table A.4.2 Unit costs used to evaluate capital and operating expenses (CAPEX/OPEX) in the proposed AnMBR WWTP scheme.

Unit costs of capital and operating expenses		**Reference**
Steel pipe (DN: 0.4 m)/(DN: 1.4 m), €·m^{-1}	115/520	[4.31]
Concrete wall/slab, €·m^{-1}	350/130	[4.31]
Ultrafiltration hollow-fibre membrane (500,000 ppm·h cumulative), € per m^2	35	PURON®, Koch Membrane Systems
Energy, € per kWh	0.138	[4.32]
Sodium hypochlorite, (NaOCl Cl active 5% PRS-CODEX), €·L^{-1}	11	Didaciencia S.A.
Acid citric (Acid citric 1-hidrate PRS-CODEX), €·t^{-1}	23600	Didaciencia S.A.
Polyelectrolyte, €·kg^{-1}	2.35	[4.33]
Residual sludge for farming, €·t^{-1}	4.81	[4.34]
Blower (ELEKTROR RD 84, Q_B= 5400 m^3·h^{-1}; Lifetime: 50000 hours), €	5900	Elektror S.A.
Sludge recycling pump (ARS200-34CI/35CR, Q_P= 500 m^3·h^{-1}; Lifetime: 65000 hours), €	25000	[4.35]
Submersible stirrer (AGS 400-3SHG/6.1; Lifetime: 100000 hours; 3.4 kW; anaerobic reactor=5W·m^{-3};anoxic reactor=15 W·m^{-3}), €	11699	[4.35]
Rotofilter (PAM 630/2000; pitch diameter=0.5 mm; Q=320 m^3·h^{-1}; Lifetime: 87600 hours, 11.45 kW), €	7796	Procesos Auto-Mecanizados S.L
Microturbine-based CHP system (size: 30 kW), capital cost, €/kW and O&M cost, €/kWh (applying an exchange rate of: 0.729 €/$)	1968/0.015	[4.27]
Degassing membrane, (flow rate=30 m^3·h^{-1}; pressure drop= 60 kPa), Capital cost, €	7300	DIC Corporation
Land cost , €·m^{-2}	0.97	[4.36]

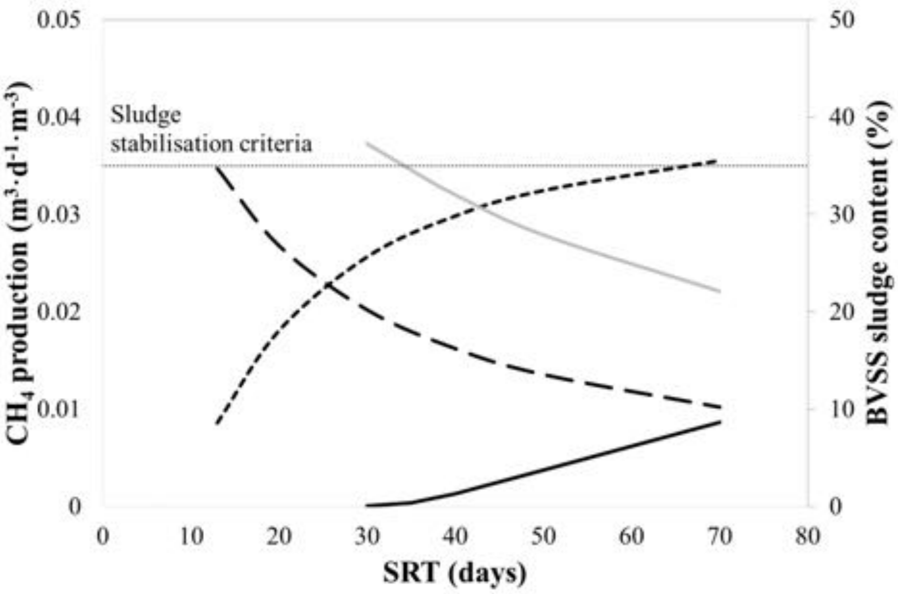

(a)

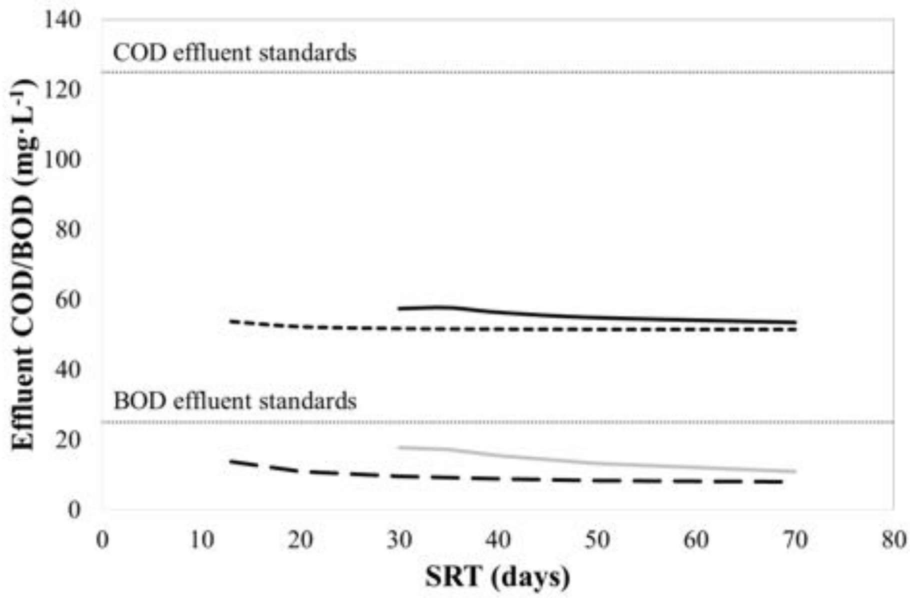

(b)

Figure 4.3 Simulation results. Influence of SRT on: (a) methane present in biogas stream at 15 ºC (▬▬) and 30 ºC (‒ ‒ ‒ ‒), and percentage of BVSS in the mixed liquor at 15 ºC (▬▬) and 30 ºC (▬ ▬); and (b) effluent COD (not including methane dissolved in effluent) at 15 ºC (▬▬) and 30 ºC (‒ ‒ ‒ ‒), and effluent BOD (not including methane dissolved in effluent) at 15 ºC (▬▬) and 30 ºC (▬ ▬).

4.4.2 Optimum design in winter conditions

Figure 4.4a shows the total annual filtration cost (CAPEX and OPEX) per cubic meter of treated water with a gas sparging intensity of 0.1 $m^3 \cdot h^{-1} \cdot m^{-2}$, $MLSS_{MT}$ ranging from 5 to 25 $g \cdot L^{-1}$ and J_{20} below and above the critical flux (J_{20} varying from 80 to 120% of J_{C20}). On the basis of the results of our experiments, we set SGD_m to 0.1 $m^3 \cdot h^{-1} \cdot m^{-2}$ in this study because this value gave adequate long-term membrane performance within the range of operating conditions evaluated, whilst resulting in minimum operating costs.

Figure 4.4a illustrates a similar tendency in the filtration costs at each $MLSS_{MT}$ evaluated, with minimum costs occurring when the operating transmembrane flux was around the critical flux (J_{20} = approx. 100 - 110% J_{C20}). Operating at critical fluxes above this value (approx. 115 – 120% J_{C20}) significantly increases filtration costs. In this respect, although operating at a high J_{20} reduces both the energy needed to scour the membrane with biogas and the membrane area investment cost, operating at high J_{20} commonly means high membrane chemical cleaning frequencies. This causes a high consumption of chemical reagents and a lower membrane lifetime, and hence higher membrane maintenance costs.

Figure 4.4b illustrates the main items that are included in total filtration costs, i.e. membrane area (approx. 55% of total filtration costs); membrane scouring by biogas (approx. 28% of total filtration costs); chemical reagents for membrane cleaning (approx. 14% of total filtration costs); and others which include the cost of: membrane tank (including the land required), blowers, permeate pumps, pipeline system and permeate pumping (approx. 3 % of total filtration costs). As Figure 4.4b shows, filtration costs decrease as $MLSS_{MT}$ decreases. However, as mentioned earlier, the cost of the biological process increases as $MLSS_{MT}$ decreases.

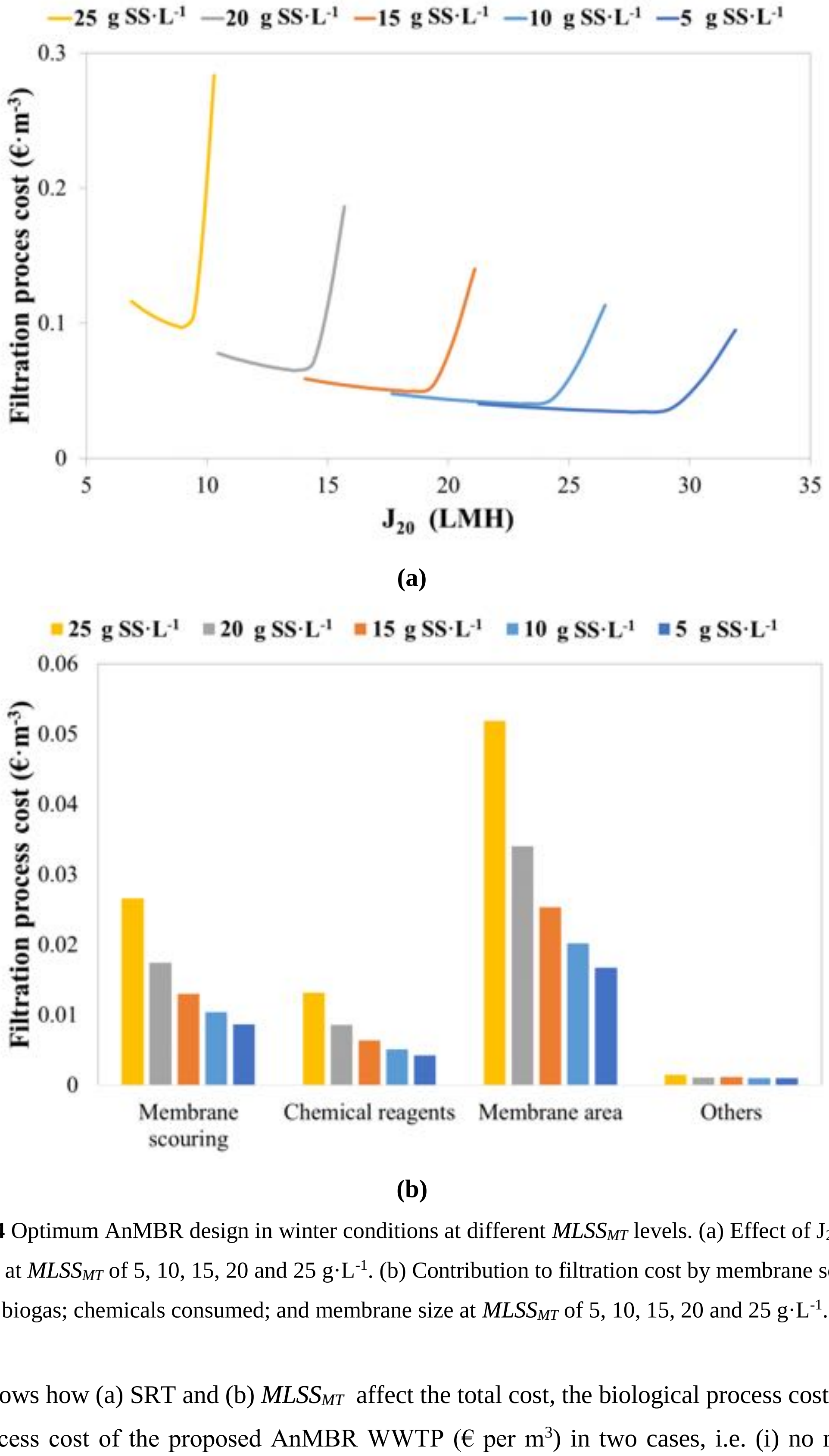

Figure 4.4 Optimum AnMBR design in winter conditions at different $MLSS_{MT}$ levels. (a) Effect of J_{20} on filtration cost at $MLSS_{MT}$ of 5, 10, 15, 20 and 25 g·L^{-1}. (b) Contribution to filtration cost by membrane scouring using biogas; chemicals consumed; and membrane size at $MLSS_{MT}$ of 5, 10, 15, 20 and 25 g·L^{-1}.

Figure 4.5 shows how (a) SRT and (b) $MLSS_{MT}$ affect the total cost, the biological process cost and the filtration process cost of the proposed AnMBR WWTP (€ per m^3) in two cases, i.e. (i) no methane capture, and (ii) energy recovered from methane (biogas methane and methane dissolved in the effluent).

As Figure 4.5a shows, biological process costs are lowest when the SRT that enables the sludge stabilisation criterion to be met is also lowest (see Figure 4.3 a), a criterion defined in this study as when the BVSS sludge content is 35%. It is important to note that an increase in SRT requires a higher reactor volume in order to maintain a given level of $MLSS_{MT}$. This increase in the reactor volume affects not only investment costs but also the operating costs of the biological process (i.e. stirring costs). As a result, the higher methane production observed when SRT was increased (see Figure 4.3 a) did not offset the higher total cost caused by increasing the reactor volume. Hence, the optimum operating SRT in winter was 35 days – which tallies with the minimum SRT mentioned earlier that enables sludge stabilisation criteria to be met.

It is worth to point out that when treating sulphate-rich municipal wastewater at 15 ºC, until reaching an SRT of around 45 days the total cost of the system when capturing methane was higher than the cost when methane was not captured (see Figure 4.5a). These results are caused by the low methane productions achieved when operating at SRTs below 45 days, which did not offset the cost of the technology considered for recovering energy from methane (degassing membranes and CHP). Nevertheless, recovering the dissolved methane from the effluent is necessary for making feasible the implementation of AnMBR technology at full-scale, so as to minimise the greenhouse potential impact resulting from discharging significant concentrations of methane (a powerful greenhouse gas) with the effluent.

As Figure 4.5b illustrates, filtration costs rise as $MLSS_{MT}$ increases. This result is due to the increase in both investment costs (mainly related to the required membrane area) and operating and maintenance costs (mainly related to membrane scouring by biogas and chemical cleaning). Therefore, as mentioned earlier, minimising filtration costs means decreasing $MLSS_{MT}$. Nevertheless, as Figure 4.5b shows, decreasing $MLSS_{MT}$ causes the cost of the biological process to climb, i.e. decreasing $MLSS_{MT}$ (at a given J_{20} and R_{rec}) means reducing the MLSS concentration entering the membrane tank, which therefore requires larger reactor volumes.

Figure 4.5b shows the optimum $MLSS_{MT}$ level giving the lowest AnMBR WWTP costs taking into account (i) no methane capture and (ii) energy recovered from methane (biogas methane and methane dissolved in the effluent). As this figure shows, also illustrated in Figure 4.5a, negligible energy is recovered from methane when sulphate-rich municipal wastewater is treated at low temperatures and SRTs below 45 days (mainly due to low hydrolysis rates), which did not offset the cost of the technology considered for recovering energy from methane (degassing membranes and CHP). Nonetheless, the optimum operating $MLSS_{MT}$ was 16 g·L^{-1} in both instances, i.e. J_{20} = 18 LMH, R_{rec} = 3.2, and HRT = 17 hours.

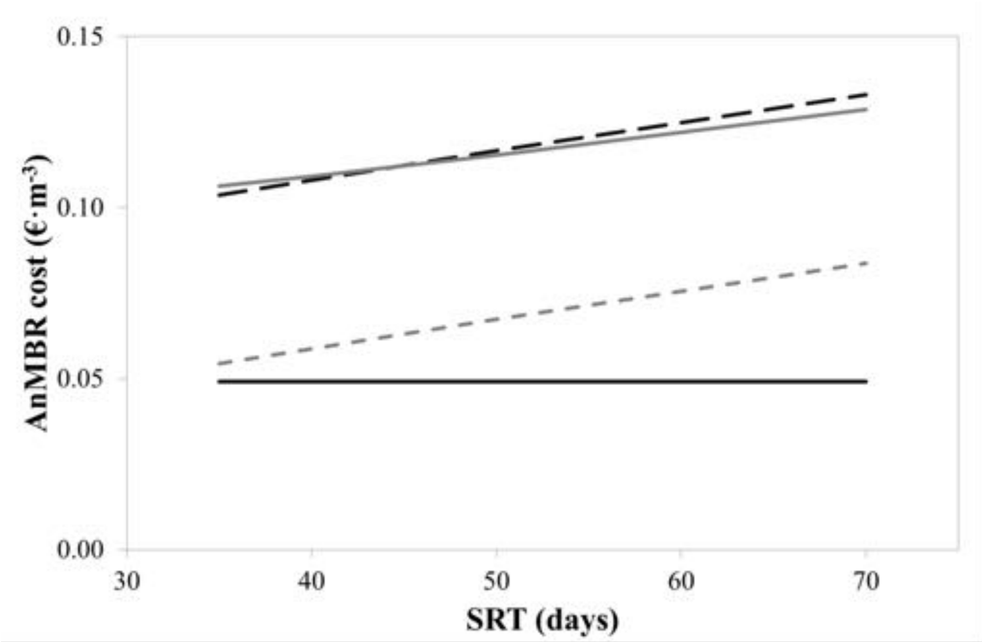

(a)

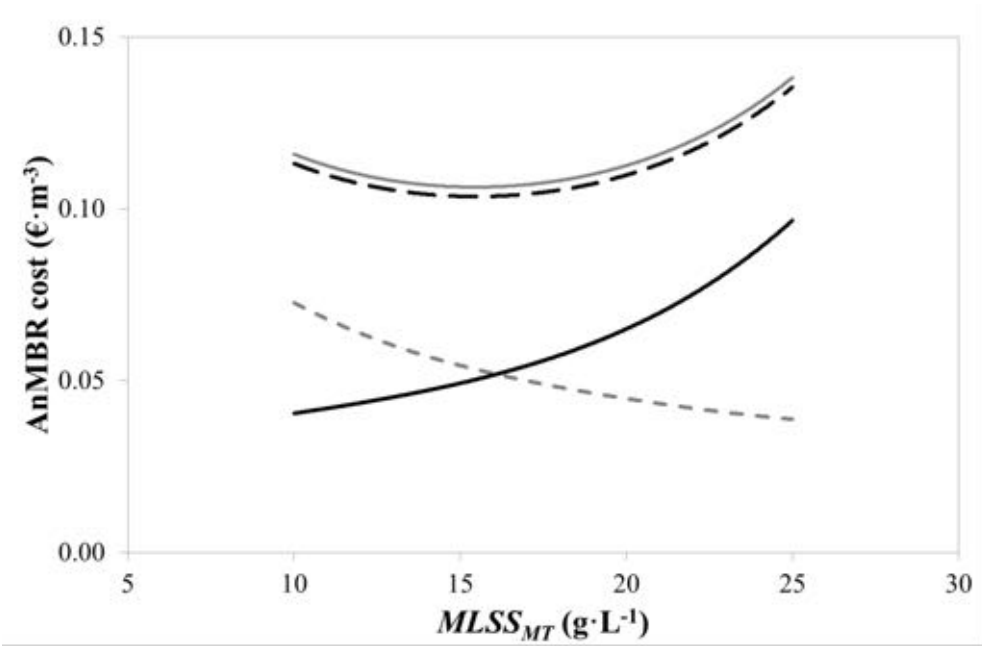

(b)

Figure 4.5 Optimum AnMBR design in winter conditions (T = 15 ºC). Effect on AnMBR cost of: **(a)** SRT; and **(b)** $MLSS_{MT}$. Cost of biological process (- - - -); cost of filtration (▬▬); total cost without energy recovery (▬ ▬); and total cost including energy recovery from methane (▬▬).

Table 4.2a summarises the optimum design values when treating sulphate-rich municipal wastewater in winter conditions.

Table 4.2 Optimum design values using the operating variables evaluated in this case study when treating **(a)** sulphate-rich municipal wastewater and **(b)** low-sulphate municipal wastewater. * J_{20} values based on the experimentally-determined critical flux in the AnMBR plant [4.24].

	Winter (T = 15 ºC)	Summer (T = 30 ºC)
SRT (days)	35	27
HRT (hours)	17	17
R_{rec}	3.2	1.8
J_{20} (LMH) *	18	21
$MLSS_{MT}$ (g·L^{-1})	16	12
TMP (bar)	0.1	0.1
SGD_m (m^3·m^{-2}·h^{-1})	0.1	0.1

(a)

	Winter (T = 15 ºC)	Summer (T = 30ºC)
SRT (days)	41	23
HRT (hours)	17	17
R_{rec}	3.2	1.2
J_{20} (LMH) *	18	21
$MLSS_{MT}$ (g·L^{-1})	15	12
TMP (bar)	0.1	0.1
SGD_m (m^3·m^{-2}·h^{-1})	0.1	0.1

(b)

Table A.4.3 illustrates the main performance values experimentally obtained in the AnMBR plant in winter conditions versus the corresponding simulation results at the optimum design values. As this table shows, the experimental results are in accordance with the simulation results.

Table A.4.3 Average performance values experimentally obtained in the AnMBR plant versus the corresponding simulation results (data in brackets) obtained for the optimum design values in winter and summer conditions.

	Winter	Summer
Methane production ($m^3·d^{-1}·m^{-3}$)	0.001 (0.006)	0.025 (0.022)
Effluent COD (mg $COD·L^{-1}$)	58.1 (57.8)	51.9 (55.7)
Membrane tank COD (g $COD·L^{-1}$)	7.6 (8.1)	8.7 (8.3)

The resulting minimum AnMBR total costs were €0.104 and €0.106 per m^3 of treated water taking into account (i) no methane capture and (ii) energy recovered from methane (biogas methane and methane dissolved in the effluent), respectively. The net energy consumption in winter conditions was 0.23 and 0.20 kWh per m^3, respectively.

4.4.3 Optimum operating strategy in summer conditions

Once the AnMBR WWTP had been designed for winter conditions (worst-case scenario), it was possible to determine the optimum operating strategy for summer conditions (best-case scenario). Figure 4.6 shows the effect of (a) SRT and (b) R_{rec} on the operating and maintenance costs in summer conditions taking into account (i) no methane capture and (ii) energy recovered from methane. As Figure 4.6a illustrates, the operating and maintenance costs are considerably lower when the methane is captured for energy recovery. Indeed, the average methane production when treating sulphate-rich municipal wastewater in summer conditions (operating at 30 ºC) was enough to offset the cost of the technology considered for recovering energy from methane (degassing membranes and CHP). In addition, increasing the SRT in summer conditions increases the amount of methane produced considerably (see Figure 4.3 a), resulting in lower operating costs. However, increasing the SRT for a given R_{rec} also increases the $MLSS_{MT}$, resulting in higher filtration operating and maintenance costs. Therefore, in summer conditions, the SRTs must be optimised in order to minimise operating and maintenance costs in AnMBR technology. In this study, the optimum SRT in summer conditions resulted in 27 days when methane was captured from both biogas and permeate.

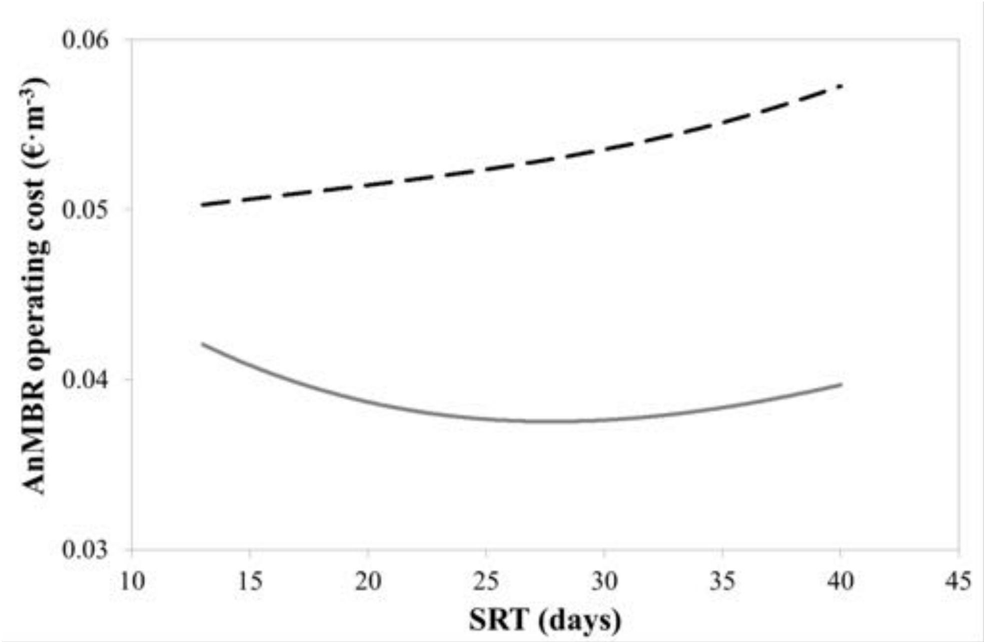

(a)

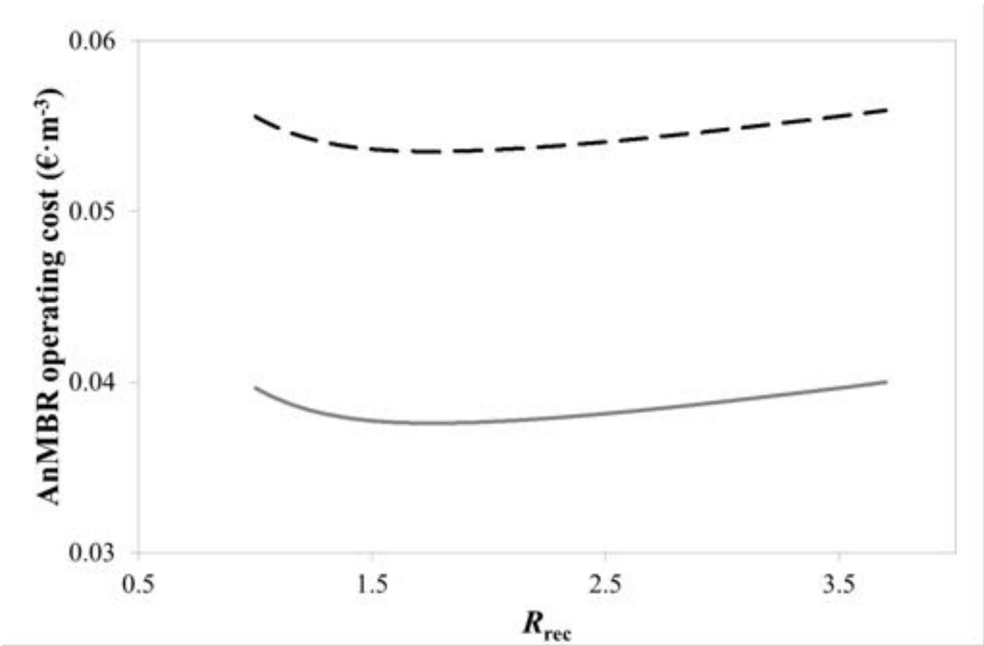

(b)

Figure 4.6 Optimum AnMBR operating strategy in summer conditions (T = 30 ºC). Effect on AnMBR cost of: **(a)** SRT; and **(b)** sludge recycling ratio (R_{rec} = sludge recycling flow from the membrane tank to the anaerobic reactor / influent flow). Operating cost without energy recovery (— —); and operating cost including energy recovery from methane (——).

However, since the volume of the anaerobic reactor depends on the winter design and the SRT is optimised in order to maximise methane production, it is only possible to optimise the $MLSS_{MT}$ in summer conditions by modifying R_{rec}. As Figure 4.6b illustrates, operating and maintenance costs can be minimised by optimising R_{rec}, which indirectly optimises $MLSS_{MT}$. Specifically, a decrease in R_{rec} causes $MLSS_{MT}$ to increase, leading to higher operating and maintenance costs related mainly to membrane scouring by biogas, chemical cleaning and membrane replacement. On the other hand, an increase in R_{rec} causes $MLSS_{MT}$ to fall but increases the cost of pumping sludge. Finally, the optimum summer R_{rec} was 1.8 which resulted in an $MLSS_{MT}$ of approx. 12 $g \cdot L^{-1}$, i.e. an optimum operating J_{20} of 21 LMH.

Table 4.2a shows the optimal values for the operating parameters evaluated in this study when treating sulphate-rich municipal wastewater in summer conditions. Table A.4.3 also illustrates the main performance values experimentally obtained in the AnMBR plant in summer conditions versus the corresponding simulation results at the optimum design values. Also for this scenario, the experimental results are in accordance with the simulation results.

The resulting optimum operating and maintenance costs were €0.099 and €0.089 per m^3 of treated water when (i) no energy was recovered from methane and (ii) energy was recovered from methane. The net energy consumption in summer conditions was 0.21 and 0.08 kWh per m^3, respectively.

4.4.4 Effect of sulphate levels in influent on AnMBR total cost

Following the methodology proposed in this paper, Table 4.2b summarises the optimum design and operating values when treating low-sulphate municipal wastewater in winter and summer conditions, respectively.

Table 4.3 gives the total annual cost of the proposed AnMBR WWTP and its energy requirements when treating sulphate-rich and low-sulphate municipal wastewater. Table 4.3 shows that the total cost of an AnMBR WWTP is significantly lower when treating low-sulphate rather than sulphate-rich municipal wastewater (cost savings of up to 28% were estimated in this study). This demonstrates that, thanks to its very low costs, AnMBR technology is more feasible for treating low/non sulphate-loaded wastewaters.

Table 4.3 Optimum cost and energy requirements of the proposed AnMBR WWTP when treating sulphate-rich and low-sulphate municipal wastewater.

	Total AnMBR cost (€ per m^3)		AnMBR energy requirements (kWh per m^3)	
	Sulphate-rich municipal wastewater	Low-sulphate municipal wastewater	Sulphate-rich municipal wastewater	Low-sulphate municipal wastewater
No methane capture	0.101	0.097	0.22	0.21
Energy recovered from methane (biogas methane and methane dissolved in the effluent)	0.097	0.070	0.14	-0.07

It must also be said that AnMBR technology has the potential to be a net energy producer when treating low-sulphate municipal wastewater. Table 4.3 shows that when methane is captured from both biogas and effluent, it is possible to obtain surplus energy that can be utilised and/or sold, giving a maximum theoretical energy production of 0.07 kWh per m^3.

In comparison with other existing technologies for municipal wastewater treatment, for instance, Judd and Judd [4.6] reported that the full-scale aerobic MBR from Peoria (USA) has a membrane and total aeration energy demand of around 0.34 and 0.55 kWh per m^3. This energy demand is low compared to the consumption of other full-scale municipal aerobic MBRs. With regard to conventional activated sludge systems, Schilde (Belgium) WWTP consumed 0.19 kWh per m^3 [4.30]. Therefore, from an energy perspective, AnMBR is a promising sustainable system compared to other existing municipal wastewater treatment technologies. However, it is important to consider that the energy demand from the AnMBR system evaluated in this study does not take into account the energy needed for nutrient removal, which is considered in the wastewater treatment plants that has been mentioned as references.

4.5 Conclusions

The proposed methodology was used to design an AnMBR WWTP treating sulphate-rich and low-sulphate municipal wastewater at 15 and 30 ºC. The total annual cost of the proposed AnMBR WWTP when treating sulphate-rich municipal wastewater was €0.101 and €0.097 per m^3 of treated water when (i) no energy was recovered from methane and (ii) energy was recovered from methane (biogas methane and methane dissolved in the effluent), respectively. The total cost when treating low-sulphate municipal wastewater resulted in €0.097 and €0.070 per m^3 of treated water for the two aforementioned scenarios, respectively. These results demonstrate that AnMBR is a feasible technology for treating low/non sulphate-loaded wastewater.

4.6 Acknowledgements

This research work was possible thanks to projects CTM2011-28595-C02-01/02 (funded by the Spanish Ministry of Economy and Competitiveness jointly with the European Regional Development Fund and Generalitat Valenciana GVA-ACOMP2013/203) and FCC Aqualia INNPRONTA IISIS IPT-20111023 (partially funded by the CDTI (Centre for Industrial Technological Development) and supported by the Spanish Ministry of Economy and Competitiveness).

4.7 References

4.1 B. Lew, S. Tarre, M. Beliavski, C. Dosoretz, M. Green, Anaerobic membrane bioreactor (AnMBR) for domestic wastewater treatment, Desalination 243 (2009) 251-257.

4.2 G. Lettinga, S. Rebac, G. Zeeman, Challenge of psychrophilic anaerobic wastewater treatment, Trends Biotechnol. 19 (2001) 363-370.

4.3 D. Jeison, Anaerobic membrane bioreactor for wastewater treatment: Feasibility and potential applications, PhD thesis, Wageningen University, Wageningen, The Netherlands, 2007.

4.4 R. Pretel, A. Robles M.V. Ruano, A. Seco, J. Ferrer, The operating cost of an anaerobic membrane bioreactor (AnMBR) treating sulphate-rich urban wastewater, Sep. Purif. Technol. 126 (2014) 30 – 38.

4.5 S. Judd, The status of membrane bioreactor technology, Trends Biotechnol. 26 (2008) 109 – 116.

4.6 S.J. Judd, C. Judd, Principles and Applications of Membrane Bioreactors, in: Water and Wastewater Treatment, Second Edition. Elsevier, London, UK, 2011.

4.7 A. Drews, Membrane fouling in membrane bioreactors – Characterization, contradictions, causes and cures, J Membrane Sci. 253 (2010) 1 – 28.

4.8 S.I. Patsios, A.J. Karabelas, An investigation of the long-term filtration performance of a membrane bioreactor (MBR): The role of specific organic fractions, J. Membrane Sci. 253(2011) 102 – 115.

4.9 A. Robles, M.V. Ruano, J. Ribes, J. Ferrer, Factors that affect the permeability of commercial hollow-fibre membranes in a submerged anaerobic MBR (HF-AnMBR) system, Water Res. 47 (2013a) 1277-1288.

4.10 A. Robles, M.V Ruano, J. Ribes, A. Seco, J. Ferrer, Model-based automatic tuning of a filtration control system for submerged anaerobic membrane bioreactors (AnMBR), J. Membrane Sci. 465 (2014) 14 – 26.

4.11 R.W. Field, D. Wu, J.A. Howell, B.B. Gupta, Critical flux concept for microfiltration fouling, J. Membrane Sci. 100 (1995) 259 – 272.

4.12 B. Verrecht, T. Maere, I. Nopens, C. Brepols, S. Judd, The cost of a large-scale hollow fibre MBR, Water Res. 44 (2010) 5274 – 5283.

4.13 H. Ozgun, R.K. Dereli, M.E. Ersahin, C. Kinaci, H. Spanjers, J.B. van Lier, A review of anaerobic membrane bioreactors for municipal wastewater treatment: Integration options, limitations and expectations, Sep. Purif. Technol. 118 (2013) 89-104.

4.14 L.M. Raskin, Anaerobic Membrane Bioreactors for Sustainable Wastewater Treatment. WERF Report U4R08, 2012.

4.15 A.L. Smith, L.B. Stadler, N.G. Love, S.J. Skerlos, L. Raskin, Perspectives on anaerobic membrane bioreactor treatment of domestic wastewater: A critical review, Bioresour. Technol. 122 (2012) 149-159.

4.16 D.C. Stuckey, Recent developments in anaerobic membrane reactors, Bioresour. Technol. 122 (2012) 137–148.

4.17 H. Lin, W. Peng, M. Zhang, J. Chen, H. Huachang, Y. Zhang, A review on anaerobic membrane bioreactors: Applications, membrane fouling and future perspectives, Desalination 314 (2013) 169–188.

4.18 J. Ferrer, A. Seco, J. Serralta, J. Ribes, J. Manga, E. Asensi, J.J. Morenilla , F. Llavador, DESASS: A software tool for design, simulating and optimising WWTPs, Environ. Modell. Softw. 23 (2008) 19-26.

4.19 J.B. Giménez, A. Robles, L. Carretero, F. Durán, M.V. Ruano, M.N. Gatti, J. Ribes, J. Ferrer, A. Seco, Experimental study of the anaerobic urban wastewater treatment in a submerged hollow-fibre membrane bioreactor at pilot scale. Bioresour. Technol. 102 (2011) 8799 – 8806.

4.20 APHA. Standard Methods for the Examination of Water and Wastewater, 21st edition. American Public Health Association/American Water Works Association/Water Environmental Federation, Washington DC, USA, 2005.

4.21 WRC, Simple titration procedures to determine H2CO3* alkalinity and short-chain fatty acids in aqueous solutions containing known concentrations of ammonium, phosphate and sulphide weak acid/bases, Report No. TT 57/92, Water Research Commission, University of Cape Town, Pretoria, Republic of South Africa, 1992.

4.22 R. Barat, J. Serralta, M.V. Ruano, E. Jiménez, J. Ribes, A. Seco, J. Ferrer, Biological nutrient removal model Nº 2 (BNRM2): a general model for wastewater treatment plants, Water Sci. Technol. 67 (2013) 1481-1489.

4.23 F. Durán, Mathematical modelling of the anaerobic urban wastewater treatment including sulphate-reducing bacteria. Application to an anaerobic membrane bioreactor (Modelación matemática del tratamiento anaerobio de aguas residuales urbanas incluyendo las bacterias sulfatorreductoras, Aplicación a un biorreactor anaerobio de membranas), Ph.D. thesis, Dept. of Hydraulic Engineering and Environment, Universitat Politècnica de València, Spain, 2013.

4.24 A. Robles, M.V. Ruano, J. Ribes, J. Ferrer, Performance of industrial scale hollow-fibre membranes in a submerged anaerobic MBR (HF-AnMBR) system at mesophilic and psychrophilic conditions, Sep. Purif. Technol. 104 (2013) 290–296.

4.25 M. Molinos-Senante, F. Hernández-Sancho, R. Sala-Garrido, M .Garrido-Baserba, Economic feasibility study for wastewater treatment: a cost-benefit analysis. Sci. Total Environ. 408 (2011), 953-957.

4.26 R. Pretel, A. Robles M.V. Ruano, A. Seco, J. Ferrer, Environmental impact of submerged anaerobic MBR (AnMBR) technology used to treat urban wastewater at different temperatures, Bioresour. Technol. 149 (2013) 532 – 540.

4.27 EPA, Environmental Protection Agency, Combined Heat and Power Partnership, Agency of the United States Federal Government, 2012.

4.28 A. Robles, M.V Ruano, J. Ribes, J. Ferrer, Sub-critical long-term operation of industrial scale hollow-fibre membranes in a submerged anaerobic MBR (HF-AnMBR) system, Sep Purif Technol. 100 (2012) 88–96.

4.29 X. Elias-Castell, Routes of treatment and recovery of sewage sludge (Vías de tratamiento y valorización de fangos de depuradora), Ediciones Díaz de Santos, Madrid, Spain, 2012.

4.30 Fenu, J. Roels, T.Wambecq, K. De Gussem, C. Thoeye, G. De Gueldre, B. Vand De Steene, Energy audit of a full scaleMBR system, Desalination, 262 (2010) 121–128.

4.31 Bank BEDEC - ITeC database, In Construmatica, Available on http://www.construmatica.com/bedec. (Accessed February 1, 2013).

4.32 Iberdrola S.A., Spanish electricity tariff (Tarifa eléctrica España). In Iberdrola. Available on https://www.iberdrola.es/clientes/empresas/info/mercado-energetico, (Accessed March 5, 2013).

4.33 J.A. Sainz-Lastre, Technologies for sustainability, Processes and unit operations in wastewater treatment (Tecnologías para la sostenibilidad, Procesos y operaciones unitarias en depuración de aguas residuales), Colección EOI Medio Ambiente, Madrid, Spain, 2005.

4.34 Miliarium Aureum, S.L, Approximate cost of WWTP (Coste estimativo EDAR), In Miliarium.com - Ingeniería Civil y Medio Ambiente, Available on http://www.miliarium.com/Proyectos/Depuradoras/introduccion/edar.asp, (Accessed April 20, 2013).

4.35 Bombas Ideal S.A., Distribution Catalogue (Catálogo Distribución), In Bombas Ideal, Available on http://www.bombas-ideal.com/pdf/CAT%20C9%20ES%20%5BD-100512%5D.pdf, (Accessed March 5, 2013).

4.36 MAGRAMA. Official website of the Ministry of Agriculture, Food and Environment. Spanish government, Madrid. Survey land prices 2012. Available on http://www.magrama.gob.es/es/estadistica/temas/estadisticas, agrarias/Encuesta_Precios_Tierra_2012_tcm7-298705.pdf (Accessed May 5, 2014).

CHAPTER 5:

Filtration process cost in submerged anaerobic membrane bioreactors (AnMBRs) for urban wastewater treatment

Abstract

The objective of this study was to evaluate the effect of the main factors affecting the cost of the filtration process in submerged anaerobic membrane bioreactors (AnMBRs) for urban wastewater (UWW) treatment. To this aim, capital and operating expenses (CAPEX/OPEX) related to filtration were evaluated at different levels of specific gas demand per square metre of membrane area (SGDm), mixed liquor suspended solids (MLSS) concentration and 20ºC-standardised transmembrane flux (J_{20}). Experimental data for CAPEX/OPEX calculations was obtained in an AnMBR system featuring industrial-scale hollow-fibre (HF) membranes that treated UWW. Results showed that operating at J_{20} slightly higher than the critical flux results in minimum CAPEX/OPEX. The minimum filtration process cost ranged from €0.03 to €0.12 per m³, mainly depending on SGD_m (from 0.05 to 0.3 m³·h⁻¹·m⁻²) and MLSS (from 5 to 25 g·L⁻¹). The optimal SGD_m resulted in approx. 0.1 m³·h⁻¹·m⁻².

Keywords

Submerged anaerobic MBR (AnMBR); CAPEX/OPEX; industrial-scale hollow-fibre membranes; urban wastewater (UWW)

Highlights

CAPEX/OPEX were evaluated for the filtration process in AnMBR systems.
SGD_m, MLSS and J_{20} were selected as the factors affecting the filtration cost most.
An optimum J_{20} slightly higher than the critical flux was determined.
Operating at low MLSS levels reduces the filtration process cost.
The results revealed an optimum filtration cost ranging from €0.03 to €0.12 per m³.

R. Pretel, A. Robles, M.V. Ruano, A.Seco, J. Ferrer
Filtration process cost in submerged anaerobic membrane bioreactors (AnMBRs) for urban wastewater treatment
Separ. Sci. Technol. (2015)

5.1 Introduction

Recent studies (see, for instance, [5.1; 5.2; 5.3]) have reported the need to address future research efforts on submerged anaerobic membrane bioreactors (AnMBRs) for urban wastewater (UWW) treatment towards sustainable full-scale implementation and operation. Specifically, it is required to establish adequate filtration strategies from an economical point of view, accounting not only for power requirements but also for investment, maintenance, and replacement costs. Gas sparging intensity for membrane scouring (commonly measured as specific gas demand per square metre of membrane area: SGD_m), mixed liquor suspended solids (*MLSS*) concentration and 20 ºC-standardised transmembrane flux (J_{20}) are key operating parameters that must be optimised in order to minimise capital and operating expenses (*CAPEX*/*OPEX*) in AnMBR systems [5.4; 5.5; 5.6].

The objective of this study was to evaluate the effect of the main factors affecting the filtration process cost in AnMBR technology for UWW treatment. To this aim, *CAPEX*/*OPEX* related to filtration were evaluated at different levels of SGD_m, J_{20} and *MLSS*. In order to obtain adequate results that can be extrapolated to full-scale plants, experimental data used in this study were obtained in an AnMBR system featuring industrial-scale hollow-fibre (HF) membrane units that was fed with the effluent from the pre-treatment of the Carraixet WWTP (Valencia, Spain).

5.2 Materials and methods

In order to assess the effect of the main factors affecting the design and operation of the filtration process in AnMBR technology for UWW, *CAPEX*/*OPEX* were evaluated at different levels of SGD_m (from 0.05 to 0.30 $m^3 \cdot m^{-2} \cdot h^{-1}$), J_{20} (varying from 80 to 120% of the experimentally determined 20 ºC-standardised critical flux: J_{C20}) and *MLSS* (from 5 to 25 $g \cdot L^{-1}$).

5.2.1 AnMBR plant description

Experimental data required for calculating *CAPEX*/*OPEX* were obtained using data obtained from the previously introduced AnMBR system (see Chapter 3). It mainly consists of an anaerobic reactor with a total volume of 1.3 m^3 connected to two membrane tanks each one with a total volume of 0.8 m^3. Each membrane tank includes one ultrafiltration hollow-fibre membrane commercial system (PURON®, Koch Membrane Systems, 0.05 µm pore size, 30 m^2 total filtering area). Further details on this AnMBR can be found in Giménez *et al.* [5.7] and Robles *et al.* [5.8].

5.2.2 CAPEX/OPEX calculation

Figure 5.1 shows the methodology used in this study for calculating *CAPEX*/*OPEX* in AnMBRs treating UWW. This methodology was extracted from the design methodology proposed in Ferrer *et al.* [5.3]. The terms considered for *CAPEX* calculation were: acquisition of ultrafiltration hollow-fibre membranes, equipment acquisition (blowers, pumps and pipes) and reinforced concrete structures. The terms considered for *OPEX* calculation were: membrane scouring by gas sparging, permeate pumping, chemical reagent consumption for membrane recovery, membrane replacement at the end of membrane lifetime, and equipment reposition (blowers, pumps and pipes). The total annualised equivalent cost (*TAEC*) was calculated by adding the annualised *CAPEX* to the annual *OPEX*. Further details on *CAPEX*/*OPEX* calculations and the unit cost values used in this study can be found in Ferrer *et al.* [5.3].

5.3 Results and discussion

5.3.1 Effect of MLSS on filtration process cost

Figure 5.2 illustrates the effect of *MLSS* on *TAEC* when operating at different levels of SGD_m (from 0.05 to 0.30 $m^3 \cdot m^{-2} \cdot h^{-1}$) and J_{20} ranging below and above the critical filtration region (from 80 to 120 % of J_{C20}). Specifically, this figure shows the resulting *TAEC* when operating at *MLSS* of 5 (Figure 5.2a), 15 (Figure 5.2b) and 25 $g \cdot L^{-1}$ (Figure 5.2c).

As Figure 5.2 shows, increasing *MLSS* from 5 to 25 $g \cdot L^{-1}$ considerably increases *TAEC* (up to 91%) for a given SGD_m level, mainly due to increasing *CAPEX*. This *CAPEX* increase is related to the reduction in J_{C20} as *MLSS* increases (for a given SGD_m), which results in a subsequent increase in the required membrane area. On the other hand, increasing *MLSS* from 5 to 25 $g \cdot L^{-1}$ considerably increases *TAEC* (up to 82%) for a given J_{20} due to increasing *OPEX*. This *OPEX* increase is related to the necessity of increasing SGD_m as *MLSS* increases in order to maintain sustainable membrane fouling propensities, which results in a consequent increase in the cost of membrane scouring by gas sparging.

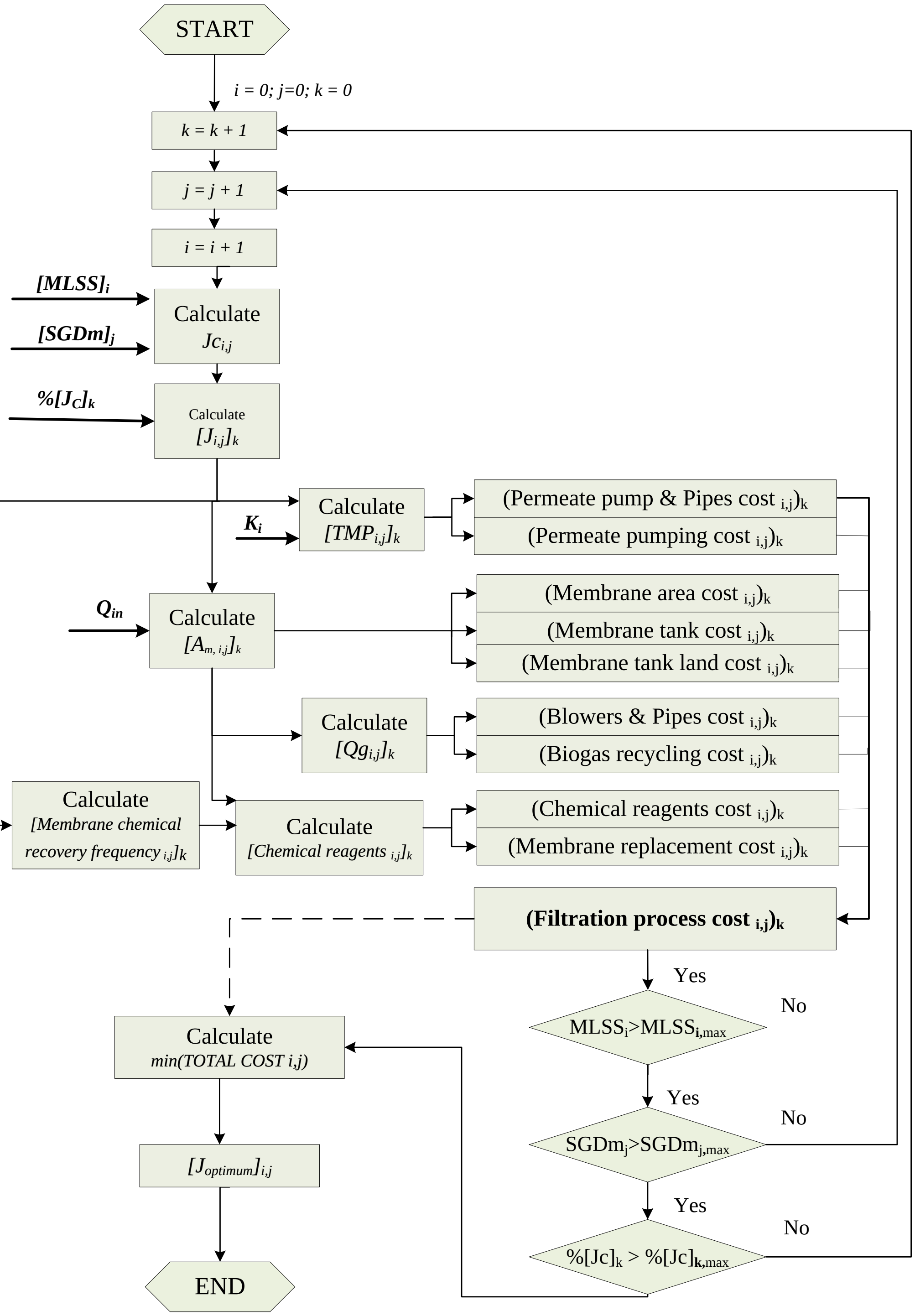

Figure 5.1 Proposed methodology for *CAPEX*/*OPEX* calculations related to filtration in AnMBR technology treating UWW (extracted from Ferrer *et al.*, [5.3]).

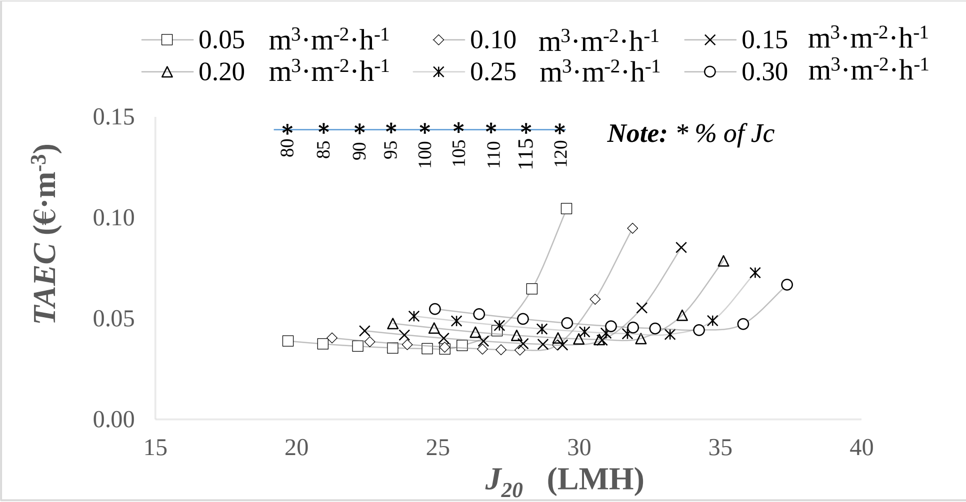

(a)

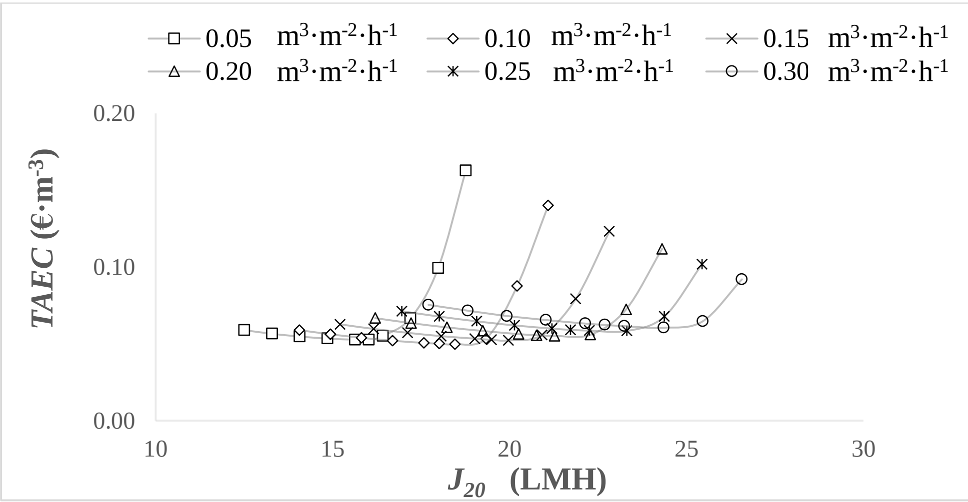

(b)

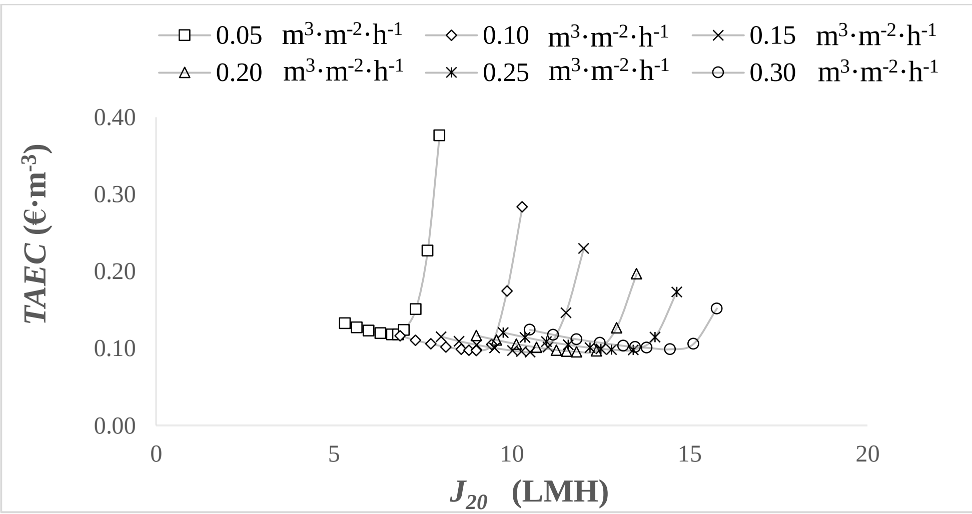

(c)

Figure 5.2 Effect of J_{20} and SGD_m on *TAEC* at different levels of *MLSS:* **(a)** 5 g·L^{-1} **(b)** 15 g·L^{-1} and **(c)** 25 g·L^{-1}.

High operating *MLSS* concentrations could be reached when operating at high sludge retention times (*SRTs*), which may be required when running AnMBR technology at low temperatures (i.e. psychrophilic temperature conditions) in order to achieve proper organic matter removal rates. As can be seen in Figure 5.2, high *MLSS* concentrations would result in an increase in *TAEC* mainly caused by an increase in the gas sparging intensity for membrane scouring and/or the required membrane area. Nevertheless, this drawback can be avoided by increasing the volume of the anaerobic reactor thus reducing the operating *MLSS* level for a given *SRT*. Hence, it is required to optimise not only the filtration process cost but also the biological process cost (i.e. reactor volume) in order to optimise the design and operation of AnMBR technology for UWW treatment (see [5.3]).

5.3.2 Effect of J_{20} on filtration process cost

Figure 5.2 also illustrates the effect of the operating J_{20} on *TAEC* at different levels of SGD_m (from 0.05 to 0.30 $m^3 \cdot m^{-2} \cdot h^{-1}$) and *MLSS* (5, 15 and 25 $g \cdot L^{-1}$). As Figure 5.2 shows, there is an optimal operating J_{20} that results in minimum *TAEC* for any combination of SGD_m and *MLSS*. Specifically, for SGD_m from 0.05 to 0.30 $m^3 \cdot m^{-2} \cdot h^{-1}$, the optimal operating J_{20} determined in this study ranged around 5-15, 15-25, and 25-35 LMH when operating at 25, 15 and 5 $g \cdot L^{-1}$ of *MLSS*, respectively. This optimal operating J_{20} corresponds to a J_{20} slightly higher than the experimentally determined J_{C20} (around 100-110% of the J_{C20}).

By way of example, Table 5.1 illustrates the effect of selecting a J_{20} value below and above the critical filtration region (80, 100 and 120% of the J_{C20}) on *TAEC*. Results in Table 5.1 were determined at 15 $g \cdot L^{-1}$ of *MLSS* and SGD_m of 0.10 $m^3 \cdot m^{-2} \cdot h^{-1}$. As this table shows, operating at J_{20} above J_{C20} reduces both investment (i.e. decreases the required membrane filtration area) and membrane scouring costs (i.e. increases the net permeate flow per membrane area whilst maintaining SGD_m). However, operating at J_{20} above J_{C20} increases chemical cleaning frequency, increasing therefore chemical reagent consumption whilst decreasing membrane lifetime (i.e. increases membrane replacement cost). A considerable increase in *TAEC* is observed when operating at J_{20} above the upper boundary of the critical filtration region (approx. for J_{20} values above 110 % of the J_{C20}). Therefore, since membrane replacement is a key factor affecting the total cost of the filtration process, considerable attention should be paid to the optimisation of membrane lifetime by operating under a sustainable regime. Indeed, the optimal operating J_{20} determined in this study corresponded to the maximum J_{20} for which membrane replacement was not required.

Table 5.1 Effect of J_{20} on the filtration process cost at SGD_m of 0.10 $m^3 \cdot m^{-2} \cdot h^{-1}$ and *MLSS* of 15 $g \cdot L^{-1}$.

		CAPEX		***OPEX***								***TAEC***
J_{20}		Membrane area and membrane tank		Membrane scouring		Chemical reagent consumption		Total operating cost		Membrane replacement		
LMH	% of J_{C20}	€·m^{-3}	%	€·m^{-3}	%	€·m^{-3}	%	€·m^{-3}	%	€·m^{-3}	%	€·m^{-3}
14	80	0.033	61.0	0.018	32.1	0.004	6.8	0.021	38.9	0.000	0.0	0.055
18	100	0.027	57.5	0.014	30.6	0.005	11.7	0.020	42.3	0.000	0.0	0.047
22	120	0.022	17.3	0.011	8.4	0.036	26.2	0.047	34.6	0.067	49.0	0.136

5.3.3 Effect of SGD_m on filtration process cost

Figure 5.2 also illustrates the effect of SGD_m on *TAEC* when operating at different levels of *MLSS* (5, 15 and 25 $g \cdot L^{-1}$) and J_{20} ranging below and above the critical filtration region (from 80 to 120 % of J_{C20}). As shown in Figure 5.2, for J_{20} around 80-95%, at every *MLSS*, the minimum *TAEC* corresponded to a low SGD_m level, around 0.05-0.10 $m^3 \cdot m^{-2} \cdot h^{-1}$. However, considering a J_{20} around 115-120% of J_{C20}, the optimal SGD_m value was around 0.30 $m^3 \cdot m^{-2} \cdot h^{-1}$. As commented before, the optimal J_{20} is reached when operating at J_{20} of approx. 100-110% of J_{C20}. Figure 5.3 illustrates the effect of SGD_m on *TAEC* when operating at different *MLSS* (from 5 to 25 $g \cdot L^{-1}$) for the optimal J_{20} ($J_{20\ optimal}$) determined from the results shown in Figure 5.2. The results shown in Figure 5.3 reveal that, in this study, the optimal SGD_m value which results in minimum *TAEC* was around 0.10 $m^3 \cdot m^{-2} \cdot h^{-1}$ for every *MLSS* level.

Hence, the results shown in this study revealed that decreasing SGD_m below 0.10 $m^3 \cdot m^{-2} \cdot h^{-1}$ increases *TAEC* due to increasing membrane fouling propensity (i.e. low shear intensities were applied on the membrane surface), which increases membrane chemical cleaning requirements and reduces membrane lifetime. On the other hand, increasing SGD_m above 0.10 $m^3 \cdot m^{-2} \cdot h^{-1}$ allows reducing the costs related to membrane maintenance (i.e. it allows reducing membrane fouling propensity) and/or investment (i.e. it allows increasing $J_{20\ optimal}$). Nonetheless, the higher cost related to membrane scouring by gas sparging offsets these possible savings thus resulting in an increase in *TAEC.*

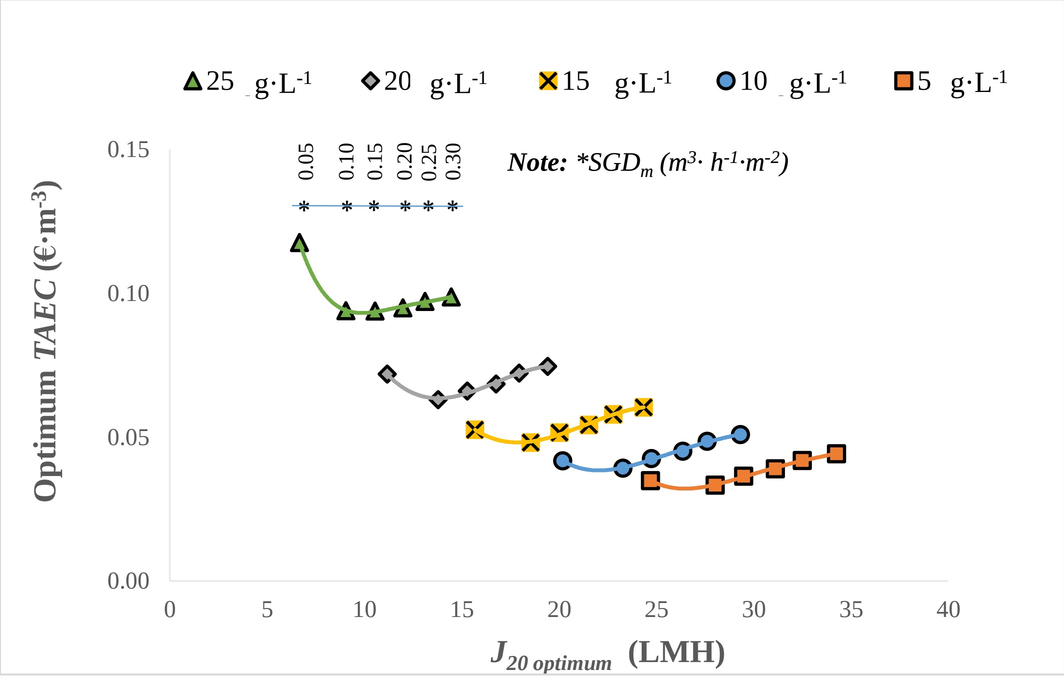

Figure 5.3 Effect of $J_{20\ optimal}$, SGD_m and *MLSS* on the optimum *TAEC*.

5.3.4 Optimum design and operation of filtration in AnMBR technology for UWW treatment

As commented above, Figure 5.3 shows the optimal J_{20} and *TAEC* calculated in this study for SGD_m from 0.05 to 0.30 $m^3{\cdot}m^{-2}{\cdot}h^{-1}$ and *MLSS* from 5 to 25 $g{\cdot}L^{-1}$. As previously commented, $J_{20\ optimal}$ corresponded to a J_{20} value slightly higher than J_{C20}, whilst the optimal SGD_m resulted in values around 0.10 $m^3{\cdot}m^{-2}{\cdot}h^{-1}$ (see Figure 5.3). On the other hand, Figure 5.3 shows how *TAEC* decreases as *MLSS* decreases. For instance, the optimum *TAEC* decreases from €0.10 to €0.03 per m^3 of treated water when decreasing *MLSS* from 25 to 5 $g{\cdot}L^{-1}$, respectively, at SGD_m of 0.10 $m^3{\cdot}m^{-2}{\cdot}h^{-1}$. Thus, it seems to be obvious that the optimum design and operation of the filtration process in AnMBR technology for UWW treatment is achieved when operating membranes at the lowest allowable *MLSS* concentration. However, as previously commented, decreasing *MLSS* means increasing the volume of the anaerobic reactor for a given *SRT*. According to Ferrer *et al*. [5.3], it is required to optimise not only the filtration process but also the biological process (i.e. reactor volume) in order to optimise the cost of AnMBR technology for UWW treatment. Nonetheless, the results shown in this study highlight the necessity of optimising design and operation of filtration in order to improve the feasibility of AnMBR technology to treat UWW since selecting adequate combinations of J_{20}, SGD_m and *MLSS* considerably reduces *TAEC*.

5.3.5 Effect of membrane and energy costs on filtration process cost

A future decrease in the membrane acquisition cost (or selecting more economical membrane types or suppliers) may reduce the effect of this term on the design and operation of AnMBR technology. However, nowadays membrane acquisition cost represents a great weight in the total filtration cost of AnMBR technology, thus it is necessary to maximise membrane lifetime whilst minimising the required membrane area.

On the other hand, the future trends in energy cost are a determining factor for *TAEC* in AnMBR technology. A 'worst case' of a 10% annual increase in energy cost, corresponding to a doubling of energy prices roughly every 10 years, increases the total cost of the filtration process around 16 and 54% when operating at SGD_m of 0.05 and 0.30 $m^3 \cdot m^{-2} \cdot h^{-1}$, respectively, along the 20 years of the depreciation of the plant.

Hence, it is important to emphasise that the results shown in this study are strongly dependent on energy and membrane costs. Therefore, one key point for maximising the long-term economic feasibility of the filtration process in AnMBR technology is decreasing power requirements, whilst maximising membrane lifetime thus limiting membrane replacement cost.

5.4 Conclusions

The effect of the main factors (J_{20}, *MLSS*, and SGD_m) affecting the cost of the filtration process in AnMBR technology treating UWW has been assessed. The results shown in this study revealed that operating at J_{20} slightly higher than the critical flux (around 100-110% of the J_{C20}) results in minimum *TAEC*. Moreover, the results revealed that the lowest the operating *MLSS* the lowest *TAEC* related to filtration. The optimal SGD_m resulted in approx. 0.1 $m^3 \cdot m^{-2} \cdot h^{-1}$ for *MLSS* ranging from 5 to 25 $g \cdot L^{-1}$ when operating at the corresponding optimal J_{20} (around 100-110% of the J_{C20}). The optimum *TAEC* estimated in this study ranged from €0.03 to €0.12 per m^3 of treated water.

5.5 Acknowledgements

This research work was possible thanks to projects CTM2011-28595-C02-01/02 (funded by the Spanish Ministry of Economy and Competitiveness jointly with the European Regional Development Fund) and FCC Aqualia INNPRONTA IISIS IPT-20111023 (partially funded by the Centre for Industrial

Technological Development (CDTI), and supported by the Spanish Ministry of Economy and Competitiveness).

5.6 References

5.1 H. Lin, J. Chen, F. Wang, L. Ding, H. Hong, Feasibility evaluation of submerged anaerobic membrane bioreactor for municipal secondary wastewater treatment. Desalination 280 (2011) 120–126.

5.2 A.L. Smith, S.J. Skerlos, L. Raskin, Psychrophilic anaerobic membrane bioreactor treatment of domestic wastewater. Water Res. 15 (2012) 47 (4) 1655–65.

5.3 J. Ferrer, R. Pretel, F. Durán, J.B Giménez, A. Robles, M.V. Ruano, J. Serralta, J. Ribes, A. Seco, Design methodology for anaerobic membrane bioreactors (AnMBR): A case study, Sep. Purif. Technol. 141 (2015), 378-386.

5.4 A. Robles, M.V. Ruano, F. García-Usach, J. Ferrer, Sub-critical filtration conditions of commercial hollow-fibre membranes in a submerged anaerobic MBR (HF-SAnMBR) system: The effect of gas sparging intensity. Bioresour. Technol. 114 (2012) 247–254.

5.5 I. Martin Garcia, M. Mokosch, A. Soares, M. Pidou, B. Jefferson, Impact on reactor configuration on the performance of anaerobic MBRs: Treatment of settled sewage in temperate climates. Water Res. 47 (2013) 4853–4860.

5.6 H. Lin, W. Peng, M. Zhang, J. Chen, H. Huachang, Y. Zhang, A review on anaerobic membrane bioreactors: Applications, membrane fouling and future perspectives, Desalination 314 (2013) 169–188.

5.7 J.B. Giménez, A. Robles, L. Carretero, F. Durán, M.V. Ruano, M.N. Gatti, J. Ribes, J. Ferrer, A. Seco, Experimental study of the anaerobic urban wastewater treatment in a submerged hollow-fibre membrane bioreactor at pilot scale. Bioresour. Technol. 102 (2011) 8799–8806.

5.8 A. Robles, M.V. Ruano, J. Ribes, J. Ferrer, Factors that affect the permeability of commercial hollow-fibre membranes in a submerged anaerobic MBR (HF-SAnMBR) system, Water Res. 47 (2013) 1277–12.

CHAPTER 6:

Designing an AnMBR-based WWTP for energy recovery from urban wastewater: the role of primary settling and anaerobic digestion

Abstract

The main objective of this paper is to assess different treatment schemes for designing a submerged anaerobic membrane bioreactor (AnMBR) based WWTP. The economic impact of including a primary settling (PS) stage and further anaerobic digestion (AD) of the wasted sludge has been evaluated. The following operating scenarios were considered: sulphate-rich and low-sulphate urban wastewater (UWW) treatment at 15 and 30 °C. To this aim, the optimum combination of design/operating parameters that resulted in minimum total cost (CAPEX plus OPEX) for the different schemes and scenarios was determined. The AnMBR design was based on both simulation and experimental results from an AnMBR plant featuring industrial-scale hollow-fibre membranes fed with UWW from the pre-treatment of a municipal WWTP located in Valencia (Spain). AnMBR without PS and AD was identified as the most economic option for an AnMBR-based WWTP treating low-sulphate UWW (minimum cost of €0.05 per m^3 and a maximum surplus energy of 0.1 kWh per m^3), whilst AnMBR with PS and AD was the optimum option when treating sulphate-rich UWW (minimum cost of €0.05 per m^3 and a maximum surplus energy of 0.09 kWh per m^3).

Keywords

CAPEX/OPEX; full-scale design; industrial-scale hollow-fibre membranes; submerged anaerobic MBR (AnMBR); urban wastewater treatment

Highlights

Primary settling (PS) and anaerobic digestion (AD) in AnMBR-based WWTP was assessed.
High- and low-sulphate UWW at 15 and 30 °C were considered for the different schemes.
AnMBR without PS and without AD was the most economic option for low-sulphate UWW.
AnMBR with PS and AD was the most economic option when treating sulphate-rich UWW.

R. Pretel, F. Durán, A. Robles, M.V. Ruano, J. Ribes, J. Serralta, J. Ferrer
Designing an AnMBR-based WWTP for energy recovery from urban wastewater: the role of primary settling and anaerobic digestion
Sep.Purif.Technol.(2015)

6.1 Introduction

In recent years, urban wastewater (UWW) is being looked at more as a resource than as a waste, a renewable source potential of energy, water and nutrients [6.1]. In this respect, anaerobic membrane bioreactors (AnMBR) technology has been reported as an emerging technology for sustainable low-strength wastewater treatment (e.g. UWW) rather than traditional aerobic wastewater treatment (see, for instance, [6.2; 6.3; 6.4]).

On the one hand, as an anaerobic process this technology presents: i) low sludge production because of the low yield of anaerobic microorganisms; ii) low energy consumption because no aeration is required; and iii) potential resource recovery because energy (from biogas production) and nutrients (NH_4^+ and PO_4^{3-}) can be obtained from the anaerobic degradation process. Indeed, complete anaerobic treatment of UWW has the potential to achieve net energy production while meeting stringent effluent standards [5.1]. Moreover, AnMBR technology may produce more net energy and had lower life cycle environmental emissions than conventional UWW treatment processes [6.5].

On the other hand, the treatment capacity of membrane bioreactors (MBR) has increased significantly, enabling them to be used even in large municipal wastewater treatment plants (WWTPs). However, WWTPs fitted with MBRs use aerobic processes which require considerable aeration in order to remove organic matter, apart from the required air to scour the membrane surface.

As regards the biological treatment of UWW, the low influent COD (typically less than 1 $g \cdot L^{-1}$) results in low methane productions. Therefore, an external energy source is usually needed to heat the reactor to mesophilic conditions [6.6]. According to Martín *et al.* [6.7], if the influent wastewater temperature is around 15 ºC, then COD levels must be higher than 4 – 5 $g \cdot L^{-1}$ in order to generate enough biogas to heat the reactor to 35 °C. Hence, the only economically feasible option for the anaerobic treatment of UWW is to operate at ambient temperature conditions. AnMBR technology allows treating UWW at ambient temperature because hydraulic retention time (HRT) and sludge retention time (SRT) are decoupled due to the filtration process. AnMBR can be operated at high SRT without requiring high anaerobic reactor volumes.

The main biological operating parameters in AnMBR systems are SRT, organic loading rate (OLR) and temperature which finally determine, among others, the use of the wastewater's energy potential. Among the different schemes that can be found in literature, AnMBR based-technology could be proposed as itself or with primary settling and further anaerobic digestion of the wasted sludge [6.1]. When ambient temperature is not so high, including a previous settling step and anaerobic digestion in the AnMBR based-scheme could reduce the reactor volume required to achieve the same methane production. Due to the high COD in primary and wasted sludge, anaerobic digestion can be operated at 35ºC using the biogas produced. Therefore, the SRT required in the anaerobic digestion will be lower than in the AnMBR system.

As regards the filtration process, one key challenge for sustainable full-scale AnMBR operation consists in achieving proper membrane performances under minimum operating cost whilst minimising membrane fouling, particularly irrecoverable/permanent fouling that cannot be removed by chemical cleaning. The extent of irrecoverable/permanent fouling is what ultimately determines the membrane lifespan (see, for instance, [6.4; 6.8]). It is therefore necessary to optimise filtration whilst minimising not only capital expenditure (CAPEX) but also operating and maintenance expenditure (OPEX). Gas sparging intensity, usually measured as the specific gas demand per permeate volume (SGD_P) or as the specific gas demand per membrane area (SGD_m), is considered a key operating parameter to maximise energy savings in AnMBRs (see, for instance, [6.9; 6.10]).

In this study we have evaluated the total cost of the following treatment schemes: AnMBR, AnMBR + anaerobic digester (AD), primary settler (PS) + AnMBR + AD for different operating scenarios: sulphate-rich and low-sulphate UWW treatment at 15 and 30 ºC. To select the most appropriate treatment scheme for each scenario, the optimum combination of design/operating parameter values that resulted in minimum cost was determined for each AnMBR WWTP scheme. The AnMBR design was based on both simulation and experimental results from an AnMBR plant featuring industrial-scale hollow-fibre membranes that was fed with UWW from the pre-treatment of a municipal WWTP located in Valencia (Spain).

6.2 Materials and methods

As mentioned earlier, this study establishes the optimum design for AnMBR WWTPs for UWW treatment with and without primary settling and further anaerobic digestion of the wasted sludge. To this aim, the design methodology proposed by Ferrer *et al.* [6.11] was used. This methodology is based on both simulation and experimental results. Experimental data were obtained from an AnMBR plant fitted with industrial-scale membranes that was fed with UWW. Simulation results were obtained using the WWTP simulating software DESASS [6.12] which enables a wide range of wastewater treatment schemes (including AnMBR systems) to be evaluated.

6.2.1 AnMBR plant description and operation

The previously described AnMBR demonstration plant entailing industrial-scale HF membranes (see Chapter 3) was used to conduct this study. As mentioned above, this plant was fed with UWW coming from the pre-treatment of the Carraixet WWTP (Valencia, Spain), which involves screening, degritting and grease removal. Further details of this AnMBR can be found in Giménez *et al.* [6.13].

This AnMBR plant was run for more than 5 years under different operating conditions (see, for instance, [6.14; 6.15]). Regarding the biological process, the plant was operated at sludge retention times ranging from 20 to 70 days, with controlled HRT ranging from 5 to 30 hours, and OLR ranging from 0.5 to 2 kg COD·m^3·d^{-1}. The impact of temperature on process performance was evaluated in the range of 14 – 33 ºC. As regards filtration, the membranes were operated at 20 ºC-standardised transmembrane fluxes (J_{20}) ranging from 6 to 20 LMH and SGD_m from 0.05 to 0.5 m^3·m^{-2}·h^{-1}. The mixed liquor suspended solids (MLSS) concentration ranged from around 5 to 30 g·L^{-1}.

6.2.2 AnMBR WWTP simulation

Figure 6.1 illustrates a flow diagram of the different treatment schemes to be assessed. As Figure 6.1 shows, all the schemes include the following common units: 1) a pre-treatment unit; 2) a clean-in-place tank; 3) a degassing membrane for capturing the dissolved methane in the effluent; 4) a combined heat and power (CHP) system enabling energy to be recovered from methane; and 5) a dewatering system for conditioning the resulting sludge.

The three different treatment schemes considered in this study for designing an AnMBR WWTP are (see Figure 6.1): a) AnMBR; b) AnMBR + AD fed with the sludge coming from the AnMBR; c) PS + AnMBR + AD fed with the sludge coming from both PS and AnMBR. However, the last treatment scheme was modified when low-sulphate UWW was treated. As it will be shown in the results section the SRT in the AnMBR required to fulfil the effluent criteria was high enough to meet sludge stabilisation criteria. Pumping the wasted sludge to the anaerobic digester leads to a significant increase in its volume but an almost negligible increase in the methane production. Therefore, it was decided to feed the anaerobic digester only with primary sludge. In addition, the variation of total cost due to including a sludge thickener in treatment schemes with AD has also been estimated.

As previously commented, the proposed AnMBR WWTP was simulated using a new version of DESASS [6.12]. This simulating software features a modified version of the mathematical model

BNRM2 [16] including the competition between both acidogenic and methanogenic microorganisms and sulphate-reducing microorganisms [6.17]. In other words, sulphate reduction to sulphide and stripping of hydrogen sulphide from the liquid phase were considered in the extended version of BNRM2. The mathematical model (BNRM2) built into DESASS was validated beforehand using experimental data obtained from the AnMBR plant [6.17].

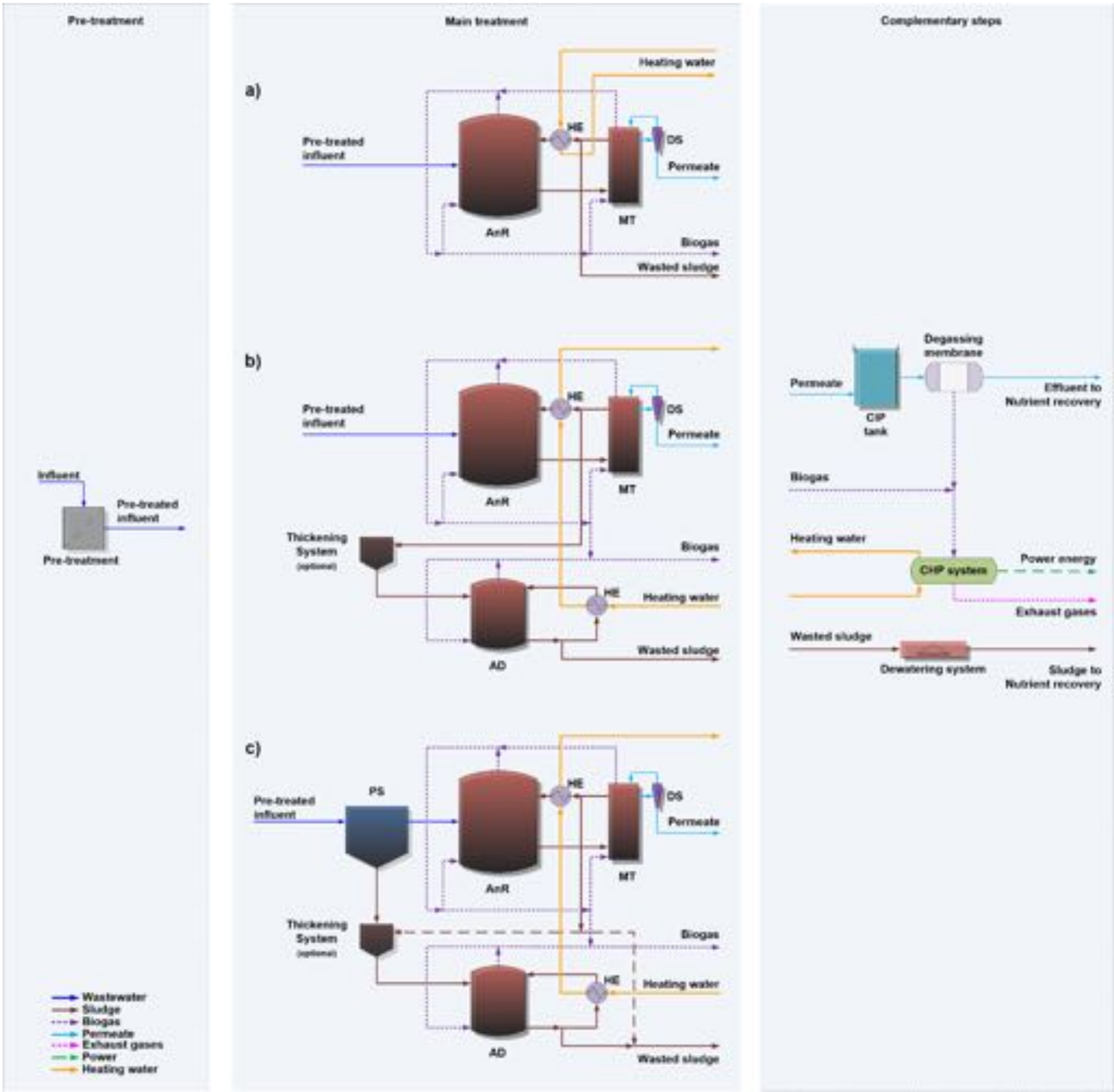

Figure 6.1 Flow chart of the different schemes considered for designing an AnMBR-based WWTP: **a)** AnMBR; **b)** AnMBR+AD; **c)** PS+AnMBR+AD. **PS**: Primary settler; **AnR**: Anaerobic Reactor; **MT**: Membrane Tank; **DV**: Degasification Vessel; **AD**: Anaerobic Digester; **HE**: Heat Exchanger; **CIP**: clean-in-place; and **CHP**: Combined Heat and Power.

The influent wastewater pattern proposed in the Benchmark Simulation Model n.1 [6.18] was used in this study. Therefore, the proposed AnMBR WWTP was designed to handle an influent flow of 18,446 $m^3 \cdot d^{-1}$. The full characterisation of the UWW used in this study is shown in Table 6.1. The following four simulation scenarios were evaluated: the treatment at i) 15 and ii) 30 ºC of sulphate-rich UWW (3.8 mg COD·mg^{-1} SO_4-S, corresponding to an influent sulphate concentration of 100 mg SO_4-S); and the treatment at iii) 15 and iv) 30 ºC of low-sulphate UWW (38.1 mg COD·mg^{-1} SO_4-S, corresponding to an influent sulphate concentration of 10 mg SO_4-S).

Table 6.1 Characteristics of the wastewater entering the anaerobic reactor used for designing the proposed AnMBR WWTP ([*]*sulphate-rich municipal wastewater;* [**]*low-sulphate municipal wastewater*).

Parameter	Unit	Value
TSS	mg TSS·L^{-1}	200
VSS	mg VSS·L^{-1}	160
T-COD	mg COD·L^{-1}	381
S-COD	mg COD·L^{-1}	99.5
T-BOD_{20}	mg COD·L^{-1}	300
S-BOD_{20}	mg COD·L^{-1}	69.5
VFA	mg COD·L^{-1}	10
SO_4-S	mg S·L^{-1}	100[*]/10[**]
TN	mg N·L^{-1}	50
NH_4-N	mg N·L^{-1}	31.5
TP	mg P·L^{-1}	6.9
PO_4-P	mg P·L^{-1}	5
Alk	mg $CaCO_3$·L^{-1}	350
pH		7

6.2.3 Design methodology

The following terms were considered for OPEX calculation: rotofilter operation, membrane scouring by biogas sparging, mixing, sludge pumping, permeate pumping, chemical reagent consumption for membrane cleaning, replacing membranes at the end of membrane lifespan, equipment replacement, sludge settling, sludge thickening, sludge handling and disposal (including dewatering system and polyelectrolyte consumption), AD heating input energy, energy recovery from AD biogas, energy recovery from AnMBR biogas, and energy recovery from methane dissolved in the AnMBR effluent.

On the other hand, the following terms were considered for CAPEX calculation: rotofilter, pumping equipment, piping system, stirrers, ultrafiltration hollow-fibre membranes, reinforced concrete structures, circular suction scraper bridges (primary settler and sludge thickener), sludge dewatering system (centrifuges) and land needed. The total cost of the technology needed for energy recovery (degassing membrane for capturing the methane dissolved in the effluent and microturbine-based CHP for energy recovery) was also considered.

6.2.3.1 AnMBR design

The methodology proposed by Ferrer *et al.* [6.11] was applied in this study for designing the AnMBR-based WWTP. According to this methodology, HRT, SRT and the level of suspended solids in the mixed liquor in the membrane tank ($MLSS_{MT}$) are the key operating parameters when designing the biological process in AnMBR technology and J_{20}, SGD_m and $MLSS_{MT}$ are the key operating parameters when designing the filtration process.

This design methodology aims to minimise total cost, and consists of two main stages. The first stage involves optimising two parameters related to the anaerobic reactor, i.e. anaerobic reactor volume (V) and the sludge recycling flow rate from the membrane tank to the anaerobic reactor (Q_{rec}). At a given operating temperature and influent flow and load, the AnMBR performance is simulated at different SRT and $MLSS_{MT}$ (for Q_{rec} = influent flow). The SRT values used in the simulations must be above the minimum SRT needed to meet effluent standards (COD < 125 mg·L^{-1} and BOD < 25 mg·L^{-1}) and sludge stabilisation criteria (percentage of biodegradable volatile suspended solids (%BVSS < 35%)). For the treatment schemes in which AnMBR technology is combined with AD or PS and AD the sludge stabilisation criteria was applied to the sludge wasted from the AD unit.

These simulation results are used to determine the optimum combination of anaerobic reactor volume and sludge recycling flow rate for each SRT and $MLSS_{MT}$. The optimum combination ($V(opt)$, Q_{rec} (opt)) is the one that minimises the total cost for the biological process. Therefore, the minimum cost of the biological process is calculated for each SRT-$MLSS_{MT}$ combination. This calculation also takes into account the costs of sludge handling and disposal, and the savings made by recovering energy from methane capture.

The second stage involves optimising the operating parameters SGD_m and J_{20} for the different $MLSS_{MT}$ levels evaluated in the simulations carried out to calculate the cost of the filtration process (see [6.19]). Before applying this methodology, the 20 ºC-standardised critical flux (J_{C20}) must be experimentally determined at different $MLSS_{MT}$ and SGD_m. Once J_{C20} has been experimentally obtained, the following variables are calculated for different J_{20} values above and below J_{C20}: membrane tank volume, membrane filtration area (A_m), biogas flow rate recycled into membrane tank (Q_G), transmembrane pressure (TMP), membrane permeability (K) and the amount of chemical reagents required for chemical membrane cleaning according to the membrane manufacturer recommendations. These values are used to calculate the filtration cost, taking into account the following cost items: membrane area, membrane tank, biogas sparging, blowers and pipes, permeate pumping, chemical reagents and membrane replacement. Then, for each level of $MLSS_{MT}$ the optimum values of J_{20} and SGD_m are selected, i.e. the ones leading to the lowest filtration cost.

Further details of this AnMBR design methodology can be found in Ferrer *et al.* [6.11].

6.2.3.2 Primary settler design

As Figure 6.1 shows, one AnMBR-based WWTP treatment scheme including primary settling is considered in this study (see Figure 6.1c). HRT is the key operating parameter when designing the primary settling step. The required number of PSs was determined based on a maximum unit diameter of 30 meters. As a result, one unit was required for designing the primary settling step, resulting in a HRT value of around 3 hours.

6.2.3.3 Anaerobic digester design

As Figure 6.1 illustrates, two treatment schemes including an anaerobic digestion step for the sludge wasted from the AnMBR are considered in this study. As previously commented, the AD unit was initially fed with the sludge coming from both PS and AnMBR. However, the sludge wasted from the AnMBR when treating low-sulphate UWW was stabilised and it was not worth to pump it into the anaerobic digester.

The AD unit was simulated at different SRT (from 5 to 30 days) under mesophilic temperature conditions (35 ºC). All the values selected for SRT were above the minimum SRT needed to meet the sludge stabilisation criteria (%BVSS < 35%). The cost of the AD unit was then calculated for each SRT taking into account the following cost items: construction of the digester including pumps and pipes, energy required for stirring and sludge pumping, savings made by recovering energy from methane capture, and the heat energy requirement to maintain the operating temperature.

6.2.3.4 Total annualised cost

The total annualised cost of the different scenarios was calculated by adding the annualised capital expenditure to the annual operating and maintenance expenditure, as shown in Eq. 6.1 [6.20]:

$$TAC = \frac{r(1+r)^{t}}{(1+r)^{t}-1} \cdot CAPEX + OPEX \qquad \textbf{(Eq. 6.1)}$$

where *r* is the annual discount rate, and *t* is the depreciation period in years.

CAPEX includes construction work (primary settler, anaerobic reactor, membrane tank, anaerobic digester, sludge thickener, and the corresponding required land) and equipment (pumps, blowers, pipes, membranes, stirrers, rotofilter, sludge dewatering system, microturbine-based CHP system, degassing membrane for recovering the methane dissolved in the effluent and circular suction scraper bridge (for primary settler and sludge thickener)). OPEX includes energy requirements (heat and power), energy recovery from methane capture (biogas methane and methane dissolved in the effluent), chemical reagents used to clean membranes, and sludge handling and disposal. Maintenance expenditure refers to pumps, blowers, stirrers, rotofilter and membrane replacement.

Further details on CAPEX/OPEX calculations in AnMBR, as well as the unit cost values used in this study, can be found in Ferrer *et al.* [6.11] and Pretel *et al.* [6.19]. In addition, the following considerations have been also taken into account when calculating CAPEX and OPEX in this work:

- For the sludge dewatering system, flow treatment of 55 $m^3 \cdot h^{-1}$, power consumption of 45 $kWh \cdot t^{-1}$ TSS and 265 k€ of CAPEX have been considered.
- For the circular suction scraper bridge for primary settler and sludge thickener, power consumption of 0.75 kW and 245 k€ of CAPEX have been considered.
- According to MAGRAMA [6.21], the following final disposal of the wasted sludge was considered in this study the: 80% to farmland (cost of 4.81 $€ \cdot t^{-1}$), 10% to incineration (cost of 250 $€ \cdot t^{-1}$) and 10% to landfilling (cost of 30.05 $€ \cdot t^{-1}$).

6.3 Results and discussion

6.3.1 Optimum design values

Table 6.2 summarises the optimum design values for the AnMBR and AD units included in the different schemes proposed for designing an AnMBR-based WWTP treating low-sulphate and sulphate-rich UWW at 15 and 30 ºC.

Table 6.2 Optimum design values for the **(a)** AnMBR and **(b)** AD units included in the three schemes considered for designing an AnMBR-based WWTP when treating low-sulphate and sulphate-rich UWW.

	AnMBR configuration				AnMBR+AD configuration				PS+AnMBR+AD configuration			
	low-sulphate UWW		sulphate-rich UWW		low-sulphate UWW		sulphate-rich UWW		low-sulphate UWW		sulphate-rich UWW	
T (ºC)	15	30	15	30	15	30	15	30	15	30	15	30
SRT (days)	35	12	60	22	35	12	8	2	33	10	6	2
HRT (hours)	14	7	23	10	14	8	9	4	10	4	6	3
Q_{rec}/*influent flow*	1.4	1.0	1.8	1.2	1.4	1.0	1.0	0.5	1.1	0.7	0.6	0.5
J_{20} (LMH)	19	19	16	19	19	24	24	26	24	26	24	29
$MLSS_{MT}$ ($g \cdot L^{-1}$)	15	10	18	15	15	10	10	8	10	8	10	5
SGD_m ($m^3 \cdot m^{-2} \cdot h^{-1}$)	0.1	0.1	0.1	0.1	0.1	0.1	0.1	0.1	0.1	0.1	0.1	0.1

(a)

	AnMBR+AD				PS+AnMBR+AD			
	low-sulphate UWW		sulphate-rich UWW		low-sulphate UWW		sulphate-rich UWW	
T (ºC)	15	30	15	30	15	30	15	30
SRT (days)	10	10	15	15	15	15	20	20
$MLSS_{AD}$ ($g \cdot L^{-1}$)	34	34	27	26	14	12	23	23

(b)

As Table 6.2a shows, the optimal SRT for the AnMBR unit when it is not combined with primary settling and further anaerobic digestion of the wasted sludge was lower when treating low-sulphate rather than sulphate-rich UWW. Specifically, the optimal SRT when operating at 15 ºC resulted in 35 and 60 days when treating low-sulphate and sulphate-rich UWW, respectively, whilst when operating at 30 ºC it resulted in 12 and 22 days, respectively. When sulphate-rich UWW is treated, the BOD is mainly biodegraded by sulphate-reducing bacteria (SRB). SRB have a biomass yield much higher than methanogenic archaea (MA) (see [6.17]). Therefore, the simulation results for this case study showed that the biomass production is much higher when treating sulphate-rich UWW and, consequently, a higher SRT is required for meeting the sludge stabilisation criteria (%BVSS < 35%). In addition, when treating sulphate-rich UWW no methane production was envisaged on the basis of the model since as abovementioned BOD is mainly biodegraded by SRB instead of by MA.

It is worth to point out that the optimum SRTs for sulphate-rich UWW corresponded with the minimum SRT required for meeting the sludge stabilisation criteria. However, the optimum SRTs for low-sulphate UWW corresponded with the minimum SRT required for meeting the European discharge quality standards for BOD.

In contrast with the results obtained in the AnMBR configuration, the optimal SRT for the AnMBR unit when it is combined with AD or PS and AD was lower when treating sulphate-rich UWW than when treating low-sulphate UWW (see Table 6.2a). In this case, shorter SRTs are required in the AnMBR unit since further degradation of the organic matter is conducted in the AD. Therefore, there is no minimum SRT limitation in the AnMBR unit as regards sludge stabilisation. Thus, the optimal SRT for the AnMBR corresponded with the minimum SRT required for meeting the European discharge quality standards for BOD. Hence, the optimal SRT for the AnMBR unit when treating low-sulphate UWW, which was already limited by the European discharge quality standards, could not be reduced when an additional anaerobic digestion step was included in the treatment scheme.

Regarding the design of the AD unit in the AnMBR+AD and PS+AnMBR+AD configurations, Table 6.2b shows that the optimal SRT for this element was higher when treating sulphate-rich rather than low-sulphate UWW. This is the consequence of the higher degree of sludge stabilisation reached in the AnMBR sludge when treating low-sulphate UWW

As regards the effect of temperature, Table 6.2a shows that, as expected, increasing the operating temperature from 15 to 30 ºC results in a decrease of the optimum SRT. Hence, lower SRTs are required for meeting both sludge stabilisation criteria (%BVSS < 35%) and effluent quality standards for BOD (25 mg $BOD \cdot L^{-1}$) when operating in warm climate areas.

With regard to including primary settling in the AnMBR-based configuration, as Table 6.2 illustrates, for the four scenarios considering PS allows reducing slightly the optimal SRT in the AnMBR unit, but increases the resulting SRT in the AD unit.

Concerning the rest of parameters included in Table 6.2, the corresponding optimal values are determined by minimising the resulting total cost for the different units included in the considered treatment schemes, as it has been described in Section 2.3. Variations on these parameters were mainly related to variations in SRT and MLSS (affected by the fate of the influent particulate organic matter). It is important to highlight that operating at low MLSS levels in the anaerobic reactor allows commonly reducing the optimal design values for the following parameters (see Table 6.2): Q_{rec}, which allows reducing sludge pumping cost; and $MLSS_{MT}$, which allows increasing J_{20} thus reducing membrane scouring cost for a given SGD_m due to the consequent membrane area reduction. In this respect the lowest design values for $Q_{rec,}$ HRT and $MLSS_{MT}$ correspond to the PS+AnMBR+AD scheme.

6.3.2 Minimum energy demand when treating low-sulphate UWW

Figure 6.2 illustrates the energy requirements of the three schemes considered for designing an AnMBR-based WWTP treating low-sulphate UWW at 15 and 30 ºC. Specifically, this figure shows the minimum energy requirements resulting from the corresponding optimum design values illustrated in Table 6.2.

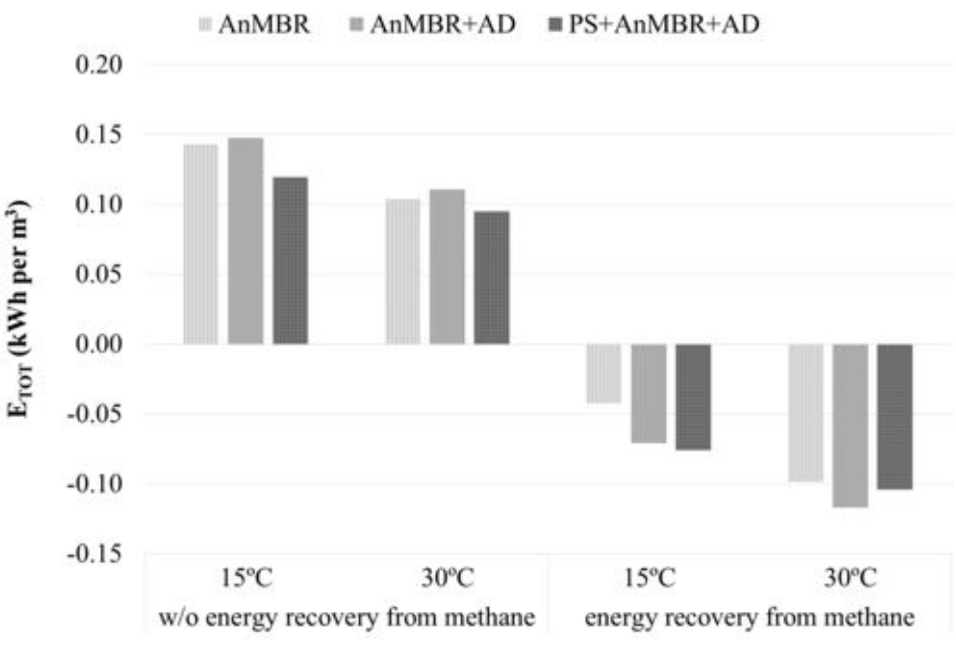

Figure 6.2 Energy requirements of the three schemes considered for designing an AnMBR-based WWTP when treating low-sulphate UWW.

As Figure 6.2 shows, the energy requirements of the WWTP slightly increase when including an additional anaerobic digestion step in the case of no methane capture. This is because of the addition of new mechanical equipment to the treatment scheme (e.g. stirrers for anaerobic digester). Nevertheless, these energy requirements are reduced when including a PS unit due to reducing the particulate organic matter entering the AnMBR unit, which allows decreasing MLSS in the anaerobic reactor. As a result, Q_{rec} and HRT are reduced in the AnMBR unit in order to optimise $MLSS_{TM}$ (see Table 6.2). Moreover, lower optimal $MLSS_{TM}$ levels were reached in the PS+AnMBR+AD configuration, which allowed increasing the operating J_{20} for a given SGD_m due to meeting higher critical fluxes [6.22]. Thus, it is important to highlight that increasing $MLSS_{MT}$ raises filtration costs mainly due to decreasing the optimal operating J_{20} (i.e. increasing membrane filtration area) for a given SGD_m, but decreases anaerobic reactor costs (mainly construction, stirring and sludge pumping costs). Hence, it is necessary to optimise the total AnMBR unit cost by optimising $MLSS_{MT}$ in order to meet optimum construction, stirring, sludge pumping and filtration costs [6.11].

Concerning the effect of operating temperature on power consumption, Figure 6.2 illustrates a reduction in the energy requirements of the different treatment schemes as the temperature increases. This reduction is attributed to an increase in the hydrolysis rate as temperature increases. Hence, lower optimal $MLSS_{TM}$ levels were reached at 30 ºC, which allowed, as previously commented, not only increasing J_{20} but also decreasing Q_{rec} and HRT in the AnMBR unit.

As regards energy recovery from methane, Figure 6.2 shows that all the considered treatment schemes have significant potential to be net energy producers when treating low-sulphate UWW. Indeed, this figure shows that in case of capturing the methane it was possible to obtain surplus energy that could be exploited and/or sold, giving a maximum theoretical energy production of 0.08 and 0.12 kWh per m^3 when treating low-sulphate UWW at 15 and 30 ºC, respectively.

Figure 6.2 shows that PS+AnMBR+AD resulted in the lowest energy demand (energy surplus of 0.08 kWh per m^3) when treating low-sulphate UWW at 15 ºC. Nevertheless, this behaviour was not reproduced when treating low-sulphate UWW at 30 ºC. When operating at 15 ºC, the energy recovery potential of the plant was enhanced by increasing the amount of organic matter that was biodegraded in the AD unit at mesophilic temperature conditions. On the other hand, when operating at 30 ºC most of the influent organic matter was already biodegraded in the AnMBR at mesophilic temperature conditions, thus the addition of primary settling (i.e. PS+AnMBR+AD) did not significantly enhanced the energy recovery potential of the WWTP. Nevertheless, adding an additional anaerobic digestion step, AnMBR+AD, allowed improving somewhat the energy recovery potential of the WWTP (maximum theoretical energy production of 0.12 kWh per m^3) since the residual organic matter was biodegraded at 35 ºC in the AD unit (against the temperature of 30 ºC of the AnMBR unit). In addition, the optimal SRT for the AD unit when treating low-sulphate UWW at 30 ºC was lower in AnMBR+AD than in PS+AnMBR+AD (see Table 6.2), which resulted in lower power requirements also due to a reduction in the stirring power consumption.

Nevertheless, the total cost of the different treatment schemes must be evaluated to determine the more feasible option when treating low-sulphate UWW at 15 and 30 ºC.

6.3.3 Minimum total cost when treating low-sulphate UWW

Figure 6.3 illustrates the total cost of the three schemes considered for designing an AnMBR-based WWTP treating low-sulphate UWW at 15 and 30 ºC. Specifically, this figure shows the minimum total cost resulting from the corresponding optimised values illustrated in Table 6.2.

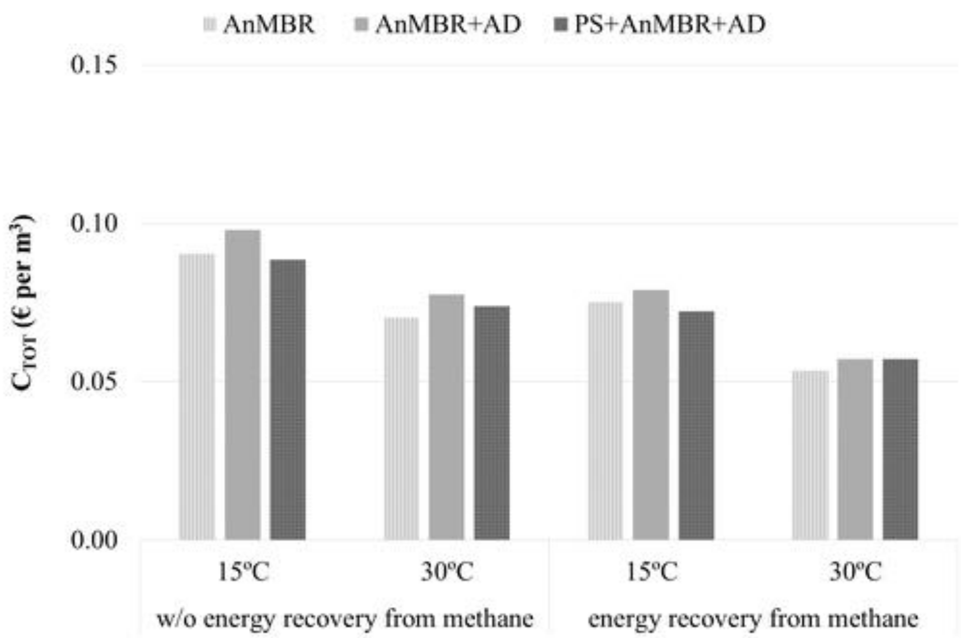

Figure 6.3 Total cost of the three schemes considered for designing an AnMBR-based WWTP when treating low-sulphate UWW.

As Figure 6.3 shows, no significant differences were detected in the total cost of the proposed treatment schemes for each of the evaluated scenarios. As regards the additional anaerobic digestion step, Figure 6.3 shows that adding an AD unit to the WWTP without including a primary settling step resulted in a slight increase of the total cost when treating low-sulphate UWW at 15 and 30 ºC. On the other hand, the total cost analysis revealed that the AnMBR scheme presented similar costs to PS+AnMBR+AD scheme mainly because of non-significant COD was consumed by SRB. Thus, most of the influent COD can be converted into methane in the AnMBR unit. Hence, AnMBR without primary settling and without further anaerobic digestion of the wasted sludge can be identified as the most feasible option for designing an AnMBR-based WWTP due to the following: 1) simplicity of the treatment scheme; and 2) reduced total cost.

6.3.4 Minimum energy demand when treating sulphate-rich UWW

Figure 6.4 illustrates the energy requirements of the different schemes proposed for designing an AnMBR-based WWTP treating sulphate-rich UWW at 15 and 30 ºC. Specifically, this figure shows the minimum energy requirements resulting from the corresponding optimised values gathered in Table 6.2.

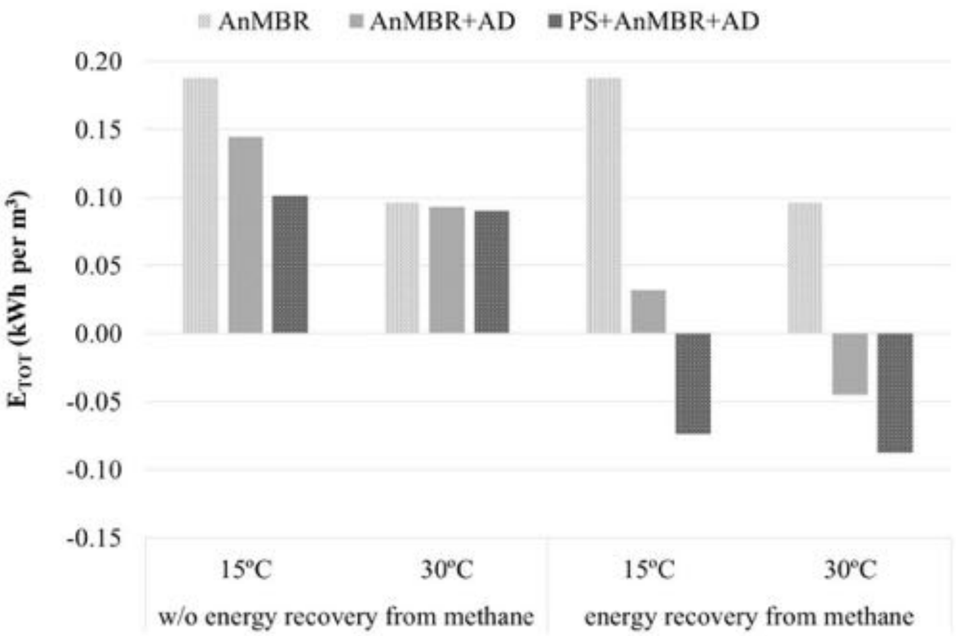

Figure 6.4 Energy requirements of the three schemes considered for designing an AnMBR-based WWTP when treating sulphate-rich UWW.

As Figure 6.4 illustrates, the power requirements (in the case of not considering energy recovery from methane) of the AnMBR WWTP operating at 15 ºC can be reduced including an AD unit (AnMBR+AD scheme) and can be reduced even more including also the PS unit (PS+AnMBR+AD scheme). As previously commented, the optimal SRT for the AnMBR unit is decreased when AnMBR is combined with AD or PS and AD (see Table 6.2a). In these configurations (AnMBR+AD and PS+AnMBR+AD), shorter SRTs for the AnMBR were required since further degradation of the organic matter was conducted in the AD (there was no minimum SRT limitation in the AnMBR as regards sludge stabilisation). Hence, lower MLSS were reached in the AnMBR depending on HRT, which resulted, as commented before, in a reduction in the optimal design values for the following parameters (see Table 6.2): Q_{rec}, which allowed reducing sludge pumping cost; and $MLSS_{MT}$, which allowed increasing J_{20} thus reducing membrane scouring cost for a given SGD_m due to the consequent membrane area reduction. Similar results but in a lesser extent were obtained in the case of treating sulphate-rich UWW at 30 ºC.

Concerning energy recovery from methane, Figure 6.4 shows that it is possible to considerably reduce energy requirements in an AnMBR WWTP treating sulphate-rich UWW by including primary settling and further anaerobic digestion of the wasted sludge. Indeed, this figure shows that energy surplus could be achieved not only in the PS+AnMBR+AD configuration operating at 15 and 30 ºC, but also in the AnMBR+AD configuration operating at 30 ºC. However, it is important to highlight that the AnMBR unit is not used as a source of biogas when treating this sulphate-rich UWW. In these scenarios, the AnMBR unit aimed at meeting the effluent standards for COD/BOD since most of the influent COD was consumed by SRB. Therefore, the whole methane production came from the AD unit where the organic matter was biodegraded at 35 ºC by MA. Hence, the higher the amount of organic matter that is introduced to the AD unit the higher the energy recovery potential of the WWTP. In this respect, the PS+AnMBR+AD configuration resulted in the lowest power requirements due to the introduction of a fraction of the influent particulate organic matter directly to the AD system after settling in the PS unit, reducing therefore the amount of COD available in the AnMBR unit for sulphate reduction by SRB.

Nevertheless, the total cost of the different treatment schemes must be evaluated to determine the more economic option when treating sulphate-rich UWW at 15 and 30 ºC.

6.3.5 Minimum total cost when treating sulphate-rich UWW

Figure 6.5 illustrates the total cost of the three schemes considered for designing an AnMBR-based WWTP treating sulphate-rich UWW at 15 and 30 ºC. In particular, this figure shows the minimum total cost resulting from the corresponding optimised values illustrated in Table 6.2.

As Figure 6.5 shows, the cost of the AnMBR-based WWTP treating sulphate-rich UWW was significantly reduced by adding primary settling and anaerobic digestion of the wasted sludge. As commented before, this is the result of taking advantage of the influent COD for biomethanisation in the AD against being introduced into the AnMBR, where a considerable fraction of the organic matter is consumed by SRB. Hence, the total cost analysis revealed that PS+AnMBR+AD is, for this case study, the best option for treating sulphate-rich UWW since less COD is consumed by SRB, thus increasing the energy recovery potential of AnMBR technology.

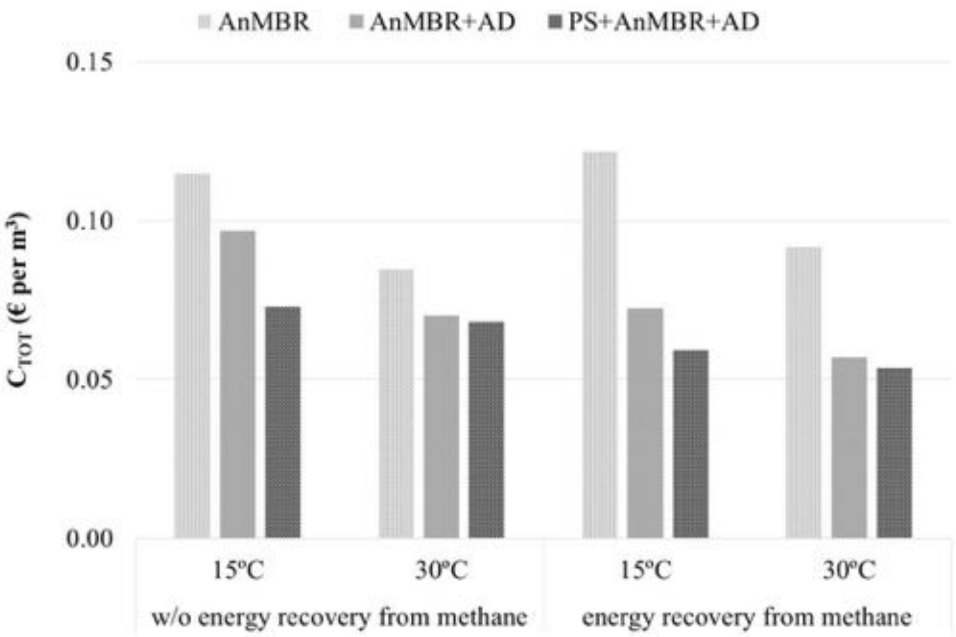

Figure 6.5 Total cost of the three schemes considered for designing an AnMBR-based WWTP when treating sulphate-rich UWW.

6.3.6 Optimum treatment scheme for designing an AnMBR-based WWTP

Table 6.3 summarises the total cost and the power requirements of the different AnMBR-based WWTP schemes evaluated at 15 and 30 ºC for treating sulphate-rich and low-sulphate UWW

As aforementioned, Table 6.3 shows that there are no significant differences in the total cost of the different schemes for treating low-sulphate UWW. Hence, as commented before, AnMBR without primary settling and without further anaerobic digestion of the wasted sludge is proposed in this study as the more feasible option for designing an AnMBR-based WWTP for low-sulphate UWW treatment due to the following: 1) simplicity of the treatment scheme; and 2) reduced total cost.

On the other hand, Table 6.3 shows that it is possible to meet considerable cost savings in an AnMBR-based WWTP treating sulphate-rich UWW by including primary settling and anaerobic digestion of the wasted sludge. Specifically, cost savings of up to 40 and 50% can be achieved by including an additional anaerobic digestion step and primary settling and additional anaerobic digestion step, respectively.

Table 6.3 also shows that the total cost of an AnMBR WWTP is significantly lower when treating low-sulphate rather than sulphate-rich UWW (cost savings of up to 45% were estimated in this study). This demonstrates that, thanks to its very low costs, AnMBR technology is a feasible option for treating low/non sulphate-loaded wastewaters.

Table 6.3 Optimum cost and energy requirements (considering energy recovery from methane) of the three schemes considered for designing an AnMBR-based WWTP at 15 ºC and 30ºC when treating **(a)** low-sulphate and **(b)** sulphate-rich UWW.

(a)

	Total cost (€ per m^3)		Energy requirements (kWh per m^3)	
	15ºC	30ºC	15ºC	30ºC
AnMBR configuration	0.08	0.05	-0.04	-0.10
AnMBR+AD configuration	0.08	0.06	-0.06	-0.12
PS+AnMBR+AD configuration	0.07	0.06	-0.08	-0.10

(b)

	Total cost (€ per m^3)		Energy requirements (kWh per m^3)	
	15ºC	30ºC	15ºC	30ºC
AnMBR configuration	0.12	0.09	0.19	0.09
AnMBR+AD configuration	0.07	0.06	0.03	-0.04
PS+AnMBR+AD configuration	0.06	0.05	-0.07	-0.09

It must also be highlighted that AnMBR has the potential to be a net energy producer when treating low-sulphate UWW. Table 6.3 shows that when methane is captured, it is possible to obtain surplus energy that can be exploited and/or sold, giving a maximum theoretical energy production of 0.12 kWh per m^3. Moreover, it is worth to point out that AnMBR combined with primary settling and anaerobic digestion of the wasted sludge has also the potential to be a net energy producer when treating sulphate-rich UWW. In this case, it would be possible to achieve a maximum theoretical energy production of up to 0.09 kWh per m^3.

6.4 Conclusions

AnMBR without primary settling and without further anaerobic digestion of the wasted sludge was the most economic option (minimum cost of €0.05 per m^3) for designing an AnMBR WWTP treating low-sulphate UWW at mild temperatures (above 15 ºC). Indeed, when methane is captured, it is possible to obtain surplus energy of 0.1 kWh per m^3. The combination PS+AnMBR+AD was the most economic option when treating sulphate-rich UWW (minimum cost of €0.05 per m^3). The total cost of the AnMBR WWTP was significantly lower when treating low-sulphate rather than sulphate-rich UWW (cost savings of up to 45% can be met).

6.5 Acknowledgements

This research work was possible thanks to projects CTM2011-28595-C02-01/02 (funded by the Spanish Ministry of Economy and Competitiveness jointly with the European Regional Development Fund and Generalitat Valenciana GVA-ACOMP2013/203) and FCC Aqualia INNPRONTA IISIS IPT-20111023 (partially funded by the Centre for Industrial Technological Development (CDTI), and supported by the Spanish Ministry of Economy and Competitiveness).

6.6 References

6.1 P.L. McCarty, J. Bae, J. Kim, Domestic wastewater treatment as a net energy producer–can this be achieved? Environ. Sci. Technol. 45 (2011) 7100–7106.

6.2 Ozgun, R.K. Dereli, M.E. Ersahin, C. Kinaci, H. Spanjers, J.B. van Lier, A review of anaerobic membrane bioreactors for municipal wastewater treatment: Integration options, limitations and expectations, Sep. Purif. Technol. 118 (2013) 89-104.

6.3 A.L. Smith, L.B. Stadler, N.G. Love, S.J. Skerlos, L. Raskin, Perspectives on anaerobic membrane bioreactor treatment of domestic wastewater: A critical review, Bioresour. Technol. 122 (2012) 149-159.

6.4 H. Lin, W. Peng, M. Zhang, J. Chen, H. Huachang, Y. Zhang, A review on anaerobic membrane bioreactors: Applications, membrane fouling and future perspectives, Desalination 314 (2013) 169–188.

6.5 A. L, Smith, L.B. Stadler, L. Cao, N.G, Love, L. Raskin, S.J. Skerlos, 2014. Navigating Wastewater Energy Recovery 1 Strategies: A Life Cycle Comparison of Anaerobic Membrane Bioreactor and Conventional Treatment Systems with Anaerobic Digestion, Environ Sci. Technol. 48 (2014), 5972-5981.

6.6 B. Lew, S. Tarre, M. Beliavski, C. Dosoretz, M. Green, Anaerobic membrane bioreactor (AnMBR) for domestic wastewater treatment, Desalination 243 (2009) 251-257.

6.7 I. Martin, M. Pidou, A. Soares, S. Judd, B. Jefferson, Modelling the energy demands of aerobic and anaerobic membrane bioreactors for wastewater treatment, Environ. Technol. 32 (2011), 921–932.

6.8 Z. Wang, J. Ma, C.Y. Tang, K. Kimura, Q. Wang, X. Han, Membrane cleaning in membrane bioreactors: A review. J. Membrane Sci. 468 (2014), 276-307.

6.9 A. Robles, M.V Ruano, J. Ribes J. Ferrer, Advanced control system for optimal filtration in submerged anaerobic, J. Membrane Sci. 430 (2013), 330-341.

6.10 A. Robles, M.V Ruano, J. Ribes, A. Seco, J. Ferrer, Model-based automatic tuning of a filtration control system for submerged anaerobic membrane bioreactors (AnMBR), J. Membrane Sci. 465 (2014) 14 – 26.

6.11 J. Ferrer, R. Pretel, F. Durán, J.B Giménez, A. Robles, M.V. Ruano, J. Serralta, J. Ribes, A. Seco, Design methodology for anaerobic membrane bioreactors (AnMBR): A case study, Sep. Purif. Technol. 141 (2015), 378-386.

6.12 J. Ferrer, A. Seco, J. Serralta, J. Ribes, J. Manga, E. Asensi, J.J. Morenilla , F. Llavador, DESASS: A software tool for design, simulating and optimising WWTPs, Environ. Modell. Softw. 23 (2008) 19-26.

6.13 J.B. Giménez, A. Robles, L. Carretero, F. Durán, M.V. Ruano, M.N. Gatti, J. Ribes, J. Ferrer, A. Seco, Experimental study of the anaerobic urban wastewater treatment in a submerged hollow-fibre membrane bioreactor at pilot scale, Bioresour. Technol. 102 (2011) 8799 – 8806.

6.14 A. Robles, M.V. Ruano, J. Ribes, J. Ferrer, Factors that affect the permeability of commercial hollow-fibre membranes in a submerged anaerobic MBR (HF-AnMBR) system, Water Res. 47 (2013) 1277-1288.

6.15 R. Pretel, A. Robles M.V. Ruano, A. Seco, J. Ferrer, The operating cost of an anaerobic membrane bioreactor (AnMBR) treating sulphate-rich urban wastewater, Sep. Purif. Technol. 126 (2014) 30 – 38.

6.16 R. Barat, J. Serralta, M.V. Ruano, E. Jiménez, J. Ribes, A. Seco, J. Ferrer, Biological nutrient removal model Nº 2 (BNRM2): a general model for wastewater treatment plants, Water Sci. Technol. 67 (2013) 1481-1489.

6.17 F. Durán, Mathematical modelling of the anaerobic urban wastewater treatment including sulphate-reducing bacteria. Application to an anaerobic membrane bioreactor (Modelación matemática del tratamiento anaerobio de aguas residuales urbanas incluyendo las bacterias sulfatorreductoras, Aplicación a un biorreactor anaerobio de membranas), Ph.D. thesis, Dept. of Hydraulic Engineering and Environment, Universitat Politècnica de València, Spain, 2013.

6.18 J. Alex, L. Benedetti, J. Copp, J., K.V. Gernaey, U. Jeppsson, I. Nopens, M-N Pons., L. Rieger, C. Rosen, J.P Steyer, P. Vanrolleghem, S. Winkler, Benchmark Simulation Model no. 1 (BSM1). Dept. of Industrial Electrical Engineering and Automation Lund University, 2008.

6.19 R. Pretel, A. Robles M.V. Ruano, A. Seco, J. Ferrer, Filtration process cost in anaerobic membrane bioreactors (AnMBRs) for urban wastewater treatment, Sent to Sep. Sci. Technol.

6.20 M. Molinos-Senante, F. Hernández-Sancho, R. Sala-Garrido, M .Garrido-Baserba, Economic feasibility study for wastewater treatment: a cost-benefit analysis, Sci. Total Environ. 408 (2011), 953-957.

6.21 MAGRAMA. Official website of the Ministry of Agriculture, Food and Environment. Spanish government, Madrid. Available on http://www.magrama.gob.es/es/calidad-y-evaluacion-ambiental/temas/prevencion-y-gestion-residuos/flujos/lodos-depuradora/ (Accessed May 21, 2015).

6.22 A. Robles, M.V. Ruano, J. Ribes, J. Ferrer, Performance of industrial scale hollow-fibre membranes in a submerged anaerobic MBR (HF-SAnMBR) system at mesophilic and psychrophilic conditions, Sep. Purif. Technol. 104 (2013) 290–296.

CHAPTER 7:

Environmental impact of submerged anaerobic MBR (AnMBR) technology used to treat urban wastewater at different temperatures

Abstract

The objective of this study was to assess the environmental impact of a submerged anaerobic MBR (AnMBR) system in the treatment of urban wastewater at different temperatures: ambient temperature (20 and 33 °C), and a controlled temperature (33 °C). To this end, an overall energy balance (OEB) and life cycle assessment (LCA), both based on real process data, were carried out. Four factors were considered in this study: (1) energy consumption during wastewater treatment; (2) energy recovered from biogas capture; (3) potential recovery of nutrients from the final effluent; and (4) sludge disposal. The OEB and LCA showed AnMBR to be a promising technology for treating urban wastewater at ambient temperature (OEB = 0.19 kWh m^{-3}). LCA results reinforce the importance of maximising the recovery of nutrients (environmental impact in eutrophication can be reduced up to 45%) and dissolved methane (positive environmental impact can be obtained) from AnMBR effluent.

Keywords

Energy balance; global warming potential; life cycle assessment; submerged anaerobic MBR (AnMBR); environmental impact.

Highlights

A sustainability study of a AnMBR system was conducted at different temperatures.
Energy consumption, nutrient recovery and sludge disposal were studied.
Operating at ambient temperature resulted in low energy demands: about 0.19 kWh m^{-3}.
Capture of methane dissolved in the effluent means considerable energy savings.
The life cycle assessment revealed the importance of capturing methane and nutrients.

R. Pretel, A. Robles, M.V. Ruano, A.Seco, J. Ferrer
Environmental impact of submerged anaerobic MBR (AnMBR) technology used to treat urban wastewater at different temperatures
Bioresour. Technol. 149 (2013), 532-540

7.1 Introduction

Urban wastewater treatment (WWT) is an energy-intensive activity whose operating energy requirements vary considerably from one WWTP to another depending on the type of influent, treatment technology and required effluent quality. Hence, electricity consumption is a key element in the overall environmental performance of a WWTP [7.1; 7.2]. Specifically, some studies indicate that bioreactor aeration could account for up to 60% of total WWTP energy consumption [7.3; 7.4]. In addition, from a sustainability viewpoint, aerobic urban WWT does not exploit the potential energy contained in the organic matter and the fertiliser value of nutrients.

It is, therefore, particularly important to implement new energy-saving technologies that reduce the overall WWTP carbon footprint and improve environmental sustainability. In recent years there has been increased interest in the feasibility of using submerged anaerobic MBRs (AnMBRs) to treat urban wastewater. In this respect, AnMBRs can provide the desired step towards sustainable wastewater treatment [7.5, 7.6; 7.7]. This alternative WWT is more sustainable because it transforms wastewater into a renewable source of energy and nutrients, whilst providing a recyclable water resource. Biogas capture is a key operating opportunity of AnMBR technology which further improves energy balance [7.8] and thereby reduces operating costs.

Other aspects of sustainable urban WWT that must be taken into account are the quality and nutrient recovery potential of the effluent, the quantity and quality of the sludge generated, all of which are of vital importance when conducting an environmental assessment of a WWTP [7.1].

Tools are needed to analyse the likely overall environmental burdens of any wastewater management system. Life cycle assessment (LCA) is a tool for measuring environmental impact that has been widely used in recent decades in the realm of WWT, and is useful for evaluating different WWT technologies [7.1; 7.17.9; 7.2; 7.10].

The aim of this study was to assess the environmental impact of AnMBR technology in the treatment of urban wastewater at different temperatures: ambient temperature (20 and 33 ºC), and a controlled temperature (33 ºC) requiring energy input. To this aim, an overall energy balance (OEB) and an LCA, both based on real process data, were carried out. Four factors were considered in this study: (1) energy consumption during urban wastewater treatment; (2) energy recovered from biogas capture; (3) final effluent discharged, considering its nutrient recovery potential; and (4) sludge disposal. In order to obtain reliable results directly comparable to the results from existing full-scale plants, this study was carried out using data from an AnMBR system featuring industrial-scale, hollow-fibre (HF) membrane units that was operated using effluent from the pre-treatment of the Carraixet WWTP (Valencia, Spain).

7.2 Materials and methods

7.2.1 Scenarios

The environmental impact of an AnMBR system to treat urban wastewater (i.e. reducing its organic load to comply with COD effluent standards), by applying OEB and LCA was evaluated. In this respect, since temperature is one of the key operating variables that determine the biological process performance in AnMBR technology, the following three scenarios at three different operating temperatures were evaluated:

- Scenario 1a: AnMBR operating at ambient temperature of 20 ºC (warm climate)
- Scenario 1b: AnMBR operating at ambient temperature of 33 ºC (hot/tropical climate)
- Scenario 2: AnMBR operating at 33 ºC when the ambient temperature is 20 ºC (controlled temperature requiring energy input).

In addition, within these three scenarios, working at ambient temperatures and controlled temperatures when an energy input is required was also assessed to evaluate the environmental impact of AnMBRs treating urban wastewater.

The three scenarios were studied using the new version of the WWTP simulation software DESASS [7.11] which features the mathematical model BNRM2 [7.12] and a general tool enabling the OEB of the different units in a WWTP to be calculated.

In accordance with recent literature [7.13; 7.2] in order to ensure comparable results, it is necessary to define the functional unit used (e.g. person equivalent, volume of treated wastewater, eutrophication associated with the effluent in terms of kg PO_4^{3-} eq. removed, etc). The functional unit (FU) adopted in this study was the volume of treated wastewater (m^3). This approach may have the advantage of being based on physical data.

Four factors were considered when determining the environmental performance of the AnMBR system being evaluated: (1) the energy consumption of the urban wastewater treatment; (2) energy from biogas capture; (3) the final discharge of effluent (including supernatant from sludge dewatering) taking its nutrient recovery potential into account; and (4) sludge disposal.

The SimaPro 7.3.3 programme was used to quantify the environmental impact of the AnMBR system being evaluated in the above-mentioned scenarios. SimaPro is widely used in LCA studies and covers a large number of databases (Ecoinvent v.2.2, BUWAL 250, ETH-ESU 96, IDEMAT 2001...) and methodologies (Eco-Indicator 99, CML 2 baseline 2000, EPS 2000, IPCC Global warming potential (GWP) 100a…).

7.2.2 System boundaries

The following system boundaries were considered in this study:

- Wastewater treatment operations and the treated water discharge were considered to be the stages that significantly contribute to the total environmental impact [7.13].
- The operating phase was considered to have far more of an impact than the investment phase [7.14; 7.13] so the construction phase (including membrane investment cost) was not included in the LCA. Nevertheless, although recent advances in MBR technology have reduced significantly its capital cost, the impact related to this phase should be also considered to assess whether it is important or not.
- Pre-treatment processes (e.g. screening, degritting, and grease removal) were not included in this study because they were assumed to feature in all WWTPs.
- Final effluent was evaluated taking into account its possible re-use for irrigation purposes.
- Sludge transport was not contemplated in the calculations presented in the manuscript.
- The demolition phase was ignored in this study as it was identified to be relatively insignificant in others studies [7.15].
- CO_2 emissions due to sludge dewatering and biogas capture were not taken into account because CO_2 is classified as biogenic according to IPCC guidelines.
- GWP was defined as GWP100 (i.e. GWP with a 100 year horizon). Electricity consumption was considered to be the main contributor to greenhouse gases [7.1].
- The thermal impact of the final effluent upon natural water courses (when operating at a controlled temperature) was not contemplated in this study.

7.2.3 Description of AnMBR plant

This study was carried out using data obtained from an AnMBR system featuring industrial-scale HF membrane units, which was fed with the effluent from a full-scale pre-treatment WWTP (screening, degritter, and grease removal). Table 7.1a shows the average characteristics of the urban wastewater influent at the AnMBR plant.

The same AnMBR plant described in Chapter 3 was used to conduct this study. In order to control the temperature when necessary, the anaerobic reactor is jacketed and connected to a water heating/cooling system.The filtration process was studied using experimental data obtained from MT1 (operated whilst continuously recycling the permeate back into the system), whilst the biological process was studied using experimental data obtained from MT2 (operated without recycling the permeate). Hence, different transmembrane fluxes (J) were tested in MT1, without affecting the hydraulic retention time (HRT) of the process.

In addition to conventional membrane operating stages (filtration, relaxation and back-flushing), two additional stages were considered: degasification and ventilation. Degasification consists of a period of high-flow filtration intended to improve filtration efficiency by removing the accumulated biogas from the top of the dead-end fibres. To capture the bubbles of biogas in the permeate leaving the membrane tank, two degasification vessels (DV) were installed, one between the respective MT and vacuum pump. The funnel-shaped section of conduit makes the biogas accumulate at the top of the DV. During ventilation, permeate is pumped into the membrane tank through the DV instead of through the membrane in order to recover the biogas accumulated in the DV.

Further details of this AnMBR system can be found in Giménez *et al.* [7.5] and Robles *et al.* [7.6].

Table 7.1 (a) Average characteristics of AnMBR influent. **(b)** Average characteristics of AnMBR effluent in scenarios 1a, 1b and 2**. (c)** Effluent characteristics after irrigation of AnMBR effluent on farmland. *Nomenclature:* ***OT****: Operating Temperature; and* ***AT****: Ambient Temperature.*

COD, Kg·m^{-3}	0.518
BOD, Kg·m^{-3}	0.384
VFA, Kg·m^{-3}	0.009
N_T, Kg·m^{-3}	0.049
NH_4, Kg·m^{-3}	0.041
P_T, Kg·m^{-3}	0.008
PO_4, Kg·m^{-3}	0.009
SO_4, Kg·m^{-3}	0.285
SST, Kg·m^{-3}	0.267
SSNV, Kg·m^{-3}	0.056
Alkalinity, Kg·m^{-3}	0.351

(a)

Effluent discharge	**Scenario 1a (OT=AT= 20ºC)**	**Scenario 1b (OT=AT=33ºC)**	**Scenario 2 (OT 33ºC, AT 20ºC)**
COD, Kg·m^{-3}	0.1718	0.1656	0.1647
NH_4, Kg·m^{-3}	0.0564	0.0573	0.0573
PO_4, Kg·m^{-3}	0.0186	0.0191	0.0192
SO_4, Kg·m^{-3}	0.0002	0.0001	0.0001
CH4, Kg·m^{-3}	0.0173	0.0190	0.0181
H_2S, Kg·m^{-3}	0.1003	0.1001	0.0999

(b)

Effluent discharge	**Scenario 1a (OT=AT= 20ºC)**	**Scenario 1b (OT=AT=33ºC)**	**Scenario 2 (OT 33ºC, AT 20ºC)**
NH_4, Kg·m^{-3}	0.0282	0.0286	0.0286
PO_4, Kg·m^{-3}	0.0056	0.0057	0.0057

(c)

7.2.4 AnMBR plant operation

The plant was operated with an SRT of 70 days at two different operating temperatures: 20 and 33 ºC. The treatment flow (set by MT2) was 2.12 m^3 d^{-1}. The filtration process (studied in MT1) was conducted at sub-critical filtration conditions: the 20 ºC-normalised transmembrane flux (J_{20}) was set to 14.5 LMH; the membranes were operated at 13.5 g L^{-1} of MLTS, and the specific gas demand per square meter of membrane area (SGD_m) was 0.1 $Nm^3 \cdot m^{-2} \cdot h^{-1}$. The resulting transmembrane pressure (TMP) was approximately 10, -10 and 20 kPa in filtration, back-flushing and degasification respectively. The sludge recycling flow in the anaerobic reactor and membrane tank was 0.4 and 2.1 $m^3 \cdot h^{-1}$, respectively.

7.2.5 Analytical monitoring

The same parameters described in chapter 3 and 4 were analysed according to Standard Methods [7.16] in mixed liquor and effluent stream: total solids (TS); sulphate (SO_4-S); sulphide (HS-S); nutrients (ammonium (NH_4-N) and orthophosphate (PO_4-P)); and total chemical oxygen demand (COD_T). The methane fraction of the biogas was measured using a gas chromatograph equipped with a Flame Ionization Detector (GC-FID, Thermo Scientific) in accordance with Giménez *et al.* [7.5].

7.2.6 Overall energy balance description

In this study, the AnMBR plant was considered to be a continuous, steady-state reactor. The resulting OEB in this system is expressed by Eq. 7.1 thus:

$$OEB = W + Q - E_{biogas} \qquad \textbf{(Eq. 7.1)}$$

where OEB is net energy consumption, consisting of mechanical energy demand (*W*), heat energy (*Q*), and the energy from biogas capture (E_{biogas}).

7.2.6.1 Mechanical Energy Demands (W)

The equipment of the AnMBR plant considered when calculating *W* consists of the following: one anaerobic reactor feeding pump; one membrane tank sludge feeding pump; one anaerobic reactor sludge mixing pump; one permeate pump; one anaerobic reactor biogas recycling blower; one membrane tank biogas recycling blower; one rotofilter; and one sludge dewatering system.

As proposed by Judd and Judd [7.17], the energy consumption of the blowers (adiabatic compression), the general pumps (feeding and recycling) and the permeate pump was calculated by applying Eq.7.2, Eq. 7.3 and Eq.7.4, respectively.

$$P_B(\frac{J}{S}) = \frac{(M \cdot R \cdot T_{gas})}{(\alpha - 1) \cdot \eta_{blower}} \left[\left(\frac{p_2}{p_1} \right)^{\frac{\alpha - 1}{\alpha}} - 1 \right] \qquad \textbf{(Eq.7.2)}$$

where P_B is the power requirement (adiabatic compression), M ($mol \cdot s^{-1}$) is the molar flow rate of biogas, R ($J \cdot mol^{-1} \cdot K^{-1}$) is the gas constant for biogas, P_1 (atm) is the absolute inlet pressure, P_2 (atm) is the absolute outlet pressure, T_{gas} (K) is the biogas temperature, α is the adiabatic index and η_{blower} is the blower efficiency.

$$P_g(\frac{J}{S}) = q_{imp} \cdot \rho_{liquor} \cdot g \cdot \frac{\left\{ \left[\left(\frac{(L + Leq) \cdot f \cdot V^2}{D \cdot 2 \cdot g} \right) asp. + \left(\frac{(L + Leq) \cdot f \cdot V^2}{D \cdot 2 \cdot g} \right) imp. \right] + [Z_1 - Z_2] \right\}}{\eta_{pump}} \qquad \textbf{(Eq. 7.3)}$$

where P_g is the power requirement by the general pump, considering both pump aspiration and pump impulsion section, calculated from the impulsion volumetric flow rate ($q_{imp.}$ in $m^3 \cdot s^{-1}$), liquor density (ρ_{liquor} in $kg \cdot m^{-3}$), acceleration of gravity (g in $m \cdot s^{-1}$), pipe length (L in m), equivalent pipe length of accidental pressure drops (L_{eq} in m), the velocity (V in $m \cdot s^{-1}$), friction factor (f, dimensionless), diameter (d in m), difference in height (Z_1-Z_2, in m) and pump efficiency (η_{pump}).

$$P_{stage(filtration, \deg asification\ or\ back-flushing)}(\frac{J}{S}) = \frac{q_{stage} \cdot TMP_{stage}}{\eta_{pump}} \qquad \textbf{(Eq.7.4)}$$

where P_{stage} is the power requirement during filtration, degasification or back-flushing calculated from transmembrane pressure (TMP_{stage} in Pa), pump volumetric flow rate (q_{stage} in $m^3 \cdot s^{-1}$) and pump efficiency (μ_{pump}).

To calculate the net power required by the permeate pump ($P_{permeate}$), the sum of the power consumed in the following four membrane operating stages was considered: filtration ($P_{filtration}$), back-flushing ($P_{back\text{-}flushing}$), degasification ($P_{degasification}$) and ventilation ($P_{ventilation}$). Eq.7.4 was used to calculate the power in filtration, back-flushing and degasification. Eq. 7.3 was used to calculate the power in ventilation since the fluid does not pass through the membrane.

The energy consumption of the rotofilter was obtained from a catalogue of full-scale equipment [7.18]. When designing the sludge dewatering, a centrifuge with an average power consumption of 45 $kWh \cdot t^{-1}$ TSS was chosen.

7.2.6.2 Heat Energy Demands (Q)

In scenarios 1a and 1b, Q was not considered because the plant was operated at ambient temperatures of 20 and 33 ºC, respectively. In scenario 2 (operating at 33 ºC when the ambient temperature is 20 ºC), the intake temperature was increased by heating the system.

Q was assumed to be the sum of the following: the energy required to heat the inflow if necessary ($Q_{REQUIRED}$, Eq. 7.5); the heat dissipated through the walls of the reactor ($Q_{DISSIPATED}$, Eq. 7.6); the heat generated or released in the gas decompression process ($Q_{DECOMPRESSION}$, Eq. 7.7 and Eq. 7.8); and the heat generated or consumed by the biological reactions taking place in the wastewater treatment process ($Q_{ENTHALPY}$, Eq. 7.9).

$$Q_{REQUIRED}\left(\frac{Kcal}{h}\right) = C_P \cdot q \cdot \rho \cdot \left(T_{fixed} - T_{inflow}\right) \qquad \textbf{(Eq. 7.5)}$$

where C_P is the specific heat (1 $Kcal \cdot Kg^{-1} \cdot K^{-1}$ for water), q ($m^3 \cdot h^{-1}$) is the inlet flow rate, ρ ($kg \cdot m^{-3}$) is the density of the sludge and T_{fixed}-T_{inflow} (K) is the difference in temperature between the intake temperature and the temperature desired in the reactor.

$$Q_{DISSPATED}\left(\frac{Kcal}{h}\right) = \Sigma U \cdot S \cdot \Delta T \qquad \textbf{(Eq. 7.6)}$$

where U ($Kcal \cdot h^{-1} \cdot m^{-2} \cdot K^{-1}$) is the overall heat transfer coefficient calculated by Eq. 7, S (m^2) is the surface of the reactor and ΔT *(K)* is the difference in temperature between the inside and the outside of the reactor.

$$U_{non-buried}\left(\frac{Kcal}{h \cdot m^2 \cdot K}\right) = \frac{1}{\Sigma \frac{\delta_{reactor}}{K_{reactor}} + \frac{1}{h_{air}}}; \quad U_{buried}\left(\frac{Kcal}{h \cdot m^2 \cdot K}\right) = \frac{1}{\Sigma \frac{\delta_{reactor}}{K_{reactor}} + \frac{\delta_{soil}}{K_{soil}}} \qquad \textbf{(Eq. 7.7)}$$

where $U_{non\text{-}baried}$ and U_{buried} are the heat transfer coefficient in the surface and buried sections of the reactor respectively, $\delta_{reactor}$ (m) is the reactor thickness, δ_{soil} (m) is the thickness of the soil in contact with the reactor wall, $k_{reactor}$ (Kcal·h^{-1}·m^{-1}·K^{-1}) is the conductivity of the reactor material, h_{air} (Kcal·h^{-1}·m^{-2}·K^{-1}) is the convective heat transfer coefficient of the air, and k_{soil} (Kcal·h^{-1}·m^{-1}·K^{-1}) is the soil conductivity.

$$Q_{DECOMPRESSION}\ (\frac{Kcal}{h}) = \frac{R \cdot T_4}{\alpha - 1}\left[\left(\frac{P_1}{P_2}\right)^{\frac{\alpha-1}{\alpha}} - 1\right] \cdot \frac{M}{\Sigma(MW \cdot \%)_i \cdot 4.187} \qquad \textbf{(Eq. 7.8)}$$

where P_1 (atm) is the absolute head space pressure, P_2 (atm) is the absolute output blower pressure, T_4 (K) is the final temperature of the biogas, $\sum(MW{\times}\%)_i$ is the sum of the molecular weight of each gaseous component in g·mol^{-1}, M is the mass flow rate of biogas in Kg·h^{-1}, and α is the adiabatic index.

$$Q_{ENTHALPY} = \Delta H^{\circ}_{T}\ (\frac{Kcal}{mol}) = \left(\eta \Delta H^{\circ}_{F}\right)_{PRODUCTS} - \left(\eta \Delta H^{\circ}_{F}\right)_{REACTANTS} + \int_{298.15}^{T} \Sigma\, \eta \cdot C_P \qquad \textbf{(Eq. 7.9)}$$

where ΔH^{o}_{T} is the enthalpy of the reaction at a given temperature (T); $(\eta\ \Delta H^{o}_{F})_{PRODUCTS}$ is the enthalpy of the products; $(\eta\ \Delta H^{o}_{F})_{REACTANTS}$ is the enthalpy of the reactants; η is the stoichiometric number; and C_P (Kcal·mol^{-1}·K^{-1}) is the specific heat of each component of the reaction.

7.2.6.3 Energy from biogas capture

The CHP technology in this study uses microturbines because they can run on biogas. Although the electrical efficiency of microturbines is usually lower than other CHP systems, they operate adequately because of their simple design [7.19]. Microturbine-based CHP technology has an overall efficiency of around 60.5%. Power and heat efficiency may be about 27.0 and 33.5%, respectively. Eq. 7.10 and Eq. 7.11 show the energy from biogas capture in terms of heat (Q_{biogas}) and power (W_{biogas}), respectively.

$$Q_{biogas}(\frac{Kcal}{h}) = \frac{Vbiogas \cdot (\%CH_4 \cdot CV_{CH4} + \%H_2 \cdot CV_{H2}) \cdot \%_{heat\ effciency\ CHP}}{1000 \cdot 24 \cdot 4.187} \qquad \textbf{(Eq. 7.10)}$$

$$W_{biogas}(kW) = \frac{Vbiogas \cdot (\%CH_4 \cdot CV_{CH4} + \%H_2 \cdot CV_{H2}) \cdot \%_{power\ effciency\ CHP}}{1000 \cdot 24 \cdot 3600} \qquad \textbf{(Eq. 7.11)}$$

where V_{biogas} (l·d^{-1}) is the biogas volume; $\%CH_4$ is the methane percentage; CV_{CH4} (KJ·m^{-3}) is the methane calorific power; $\%H_2$ is the hydrogen percentage; and CV_{H2} (KJ·m^{-3}) is the hydrogen calorific power.

7.2.7 Life cycle inventory and life cycle impact assessment

Life cycle inventory (LCI) methods are described in ISO 14041. The inventory analysis is a list of the volumes of the inflows that a system extracts from the natural environment and the outflows released into it. The energy consumed/generated and final matter discharged by the AnMBR system were simulated using DESASS. The potential impact of these parameters was then assessed by applying SimaPro and its built-in Ecoinvent database. Simapro was chosen because it provides the most up-to-date and reliable LCI data worldwide [7.20].

Life cycle impact assessment (LCIA) methods are described in ISO 14042. The methodology chosen to assess and evaluate the environmental impact of the system under study is the Centre of Environmental Science (CML) 2 baseline 2000. The impact categories considered in this study are as follows: eutrophication, GWP, acidification, abiotic depletion, ozone layer depletion (ODP), human toxicity, marine aquatic ecotoxicity, fresh water aquatic ecotoxicity, photochemical oxidation and land ecotoxicity.

Environmental loads are calculated by multiplying the amount of emission or consumption by a characterisation factor. Normalised results are calculated by taking into account the characterisation factor of total emissions and the depletion of resources caused by a benchmark system over a given period (in this instance, Europe 1995, the most recent figures available from SimaPro). The normalised value can then be used to calculate the environmental impact of the system under study.

7.2.7.1 Electricity consumption data

The data on the resources used to generate the electricity used to run the AnMBR system were updated in this study according to data obtained from the Spanish electricity network [7.21].

7.2.7.2 Wastewater effluent data

In this study, the impact of the effluent discharged into natural water courses was assessed after part of its nutrients was used for irrigating farmland (as fertiliser). Since fertiliser can be partially avoided, ammonium sulphate and diammonium phosphate were assumed to be generic N and P sources, which could substitute 50 and 70% respectively of the N and P provided by the effluent [7.22].

7.2.7.3 Sludge disposal data

The stability of the sludge in the three scenarios was evaluated using % VSS (volatile suspended solids) and BVSS (biodegradable volatile suspended solids). The BVSS was calculated theoretically by the WWTP simulation software DESASS which features the mathematical model BNRM2 (Barat *et al.,* 2013). The heavy metal content of the sludge in Spain proposed by Kidd *et al.* [7.23] was adopted in this study.

As the sludge could be used as fertiliser on farmland, the synthetic fertiliser can be partially avoided, using the same percentages of N and P as the wastewater effluent (mentioned in section 7.2.7.2) according to Bengtsson *et al.* [7.22]. In addition, nitrogen was emitted: 25.81% in the form of NH_3-N and 1.18% in the form of N_2O-N [7.24]. On the other hand, heavy precipitation and erosion caused some phosphorus in the sludge spread on land to enter both surface and groundwater by filtering through the soil. The transfer coefficient of phosphorus from sludge into groundwater is 0.57% and into surface water is 2.005% [7.24].

7.3 Results and discussion

7.3.1 OEB results

The OEB results of the three operating scenarios of the AnMBR system evaluated, including energy consumption (mechanical and heat energy) and energy production (heat and power from biogas) (Table 7.2a). The possible energy obtained by capturing methane dissolved in the effluent was also evaluated (see Table 7.2b), although it is not included in the OEB results.

7.3.1.1 Energy consumption and energy from biogas capture

The mechanical energy was similar in all scenarios (around 0.22 kWh·m^{-3}) (see Table 7.2a). Nevertheless, considering the energy from biogas capture, the net energy requirements were 0.20 kWh·m^{-3} (scenario 1a), 0.18 kWh·m^{-3} (scenario 1b) and 36.71 kWh·m^{-3} (scenario 2), since the high temperature (33 ºC in scenarios 1b and 2) increased the final biogas production. However, a considerable amount of heat energy was needed in the second scenario to maintain a temperature of 33 ºC (131649 kJ·m^{-3}, see Table 7.2). Therefore, increasing the operating temperature from 20 ºC (ambient temperature) to 33 ºC when using AnMBR technology to treat urban wastewater may be assumed to be unsustainable because of the considerable heat energy needed. On the other hand, the low energy requirements recorded when operating at ambient temperature (scenario 1a and 1b) make AnMBR a promising sustainable technology from an energy viewpoint. Moreover, when operating at hot/tropical ambient temperatures (e.g. 33 ºC) more biogas was captured than at warm ambient temperatures (e.g. 20 ºC), which slightly reduced overall energy consumption (from 0.20 to 0.18 kWh·m^{-3} in this scenario) when capturing biogas.

Table 7.2 (a) OEB of scenarios 1a, 1b and 2 divided into mechanical and heat energy consumption; power energy heat energy fuelled by biogas; and net power and heat energy. **(b)** Energy from capture of methane dissolved in effluent considering an extraction efficiency of 100%. *Nomenclature: **OT**: Operating Temperature; and **AT**: Ambient Temperature. *N/A: not applicable*

	Scenario 1a (OT=AT= 20ºC)	**Scenario 1b (OT=AT=33ºC)**	**Scenario 2 (OT 33ºC, AT 20ºC)**
Energy consumption			
Mechanical energy consumption , kWh·m^{-3}	0.219	0.218	0.218
Anaerobic reactor sludge mixing pump	0.0005	0.0004	0.0004
Anaerobic reactor wastewater feeding pump	0.0022	0.0022	0.0022
Membrane tank sludge feeding pump	0.0857	0.0853	0.0853
Permeate Pump	0.0052	0.0052	0.0052
Anaerobic reactor biogas recycling blower	0.0113	0.0113	0.0113
Membrane tank biogas recycling blower	0.1017	0.1019	0.1017
Rotofilter	0.0055	0.0055	0.0055
Sludge dewatering	0.0067	0.0064	0.0064
Heat energy consumption, KJ· m^{-3}	0.0000	0.0000	131649
Heat required for heating inflow (Qrequired)	*N/A**	*N/A**	54408
Heat dissipated through reactor (Qdissipated)	*N/A**	*N/A**	75428
Heat in the gas decompression (Qdecompression)	*N/A**	*N/A**	-271
Heat enthalpy of the biological reactions (Qenthalpy)	*N/A**	*N/A**	2085
Energy from biogas capture			
Power energy production , kWh·m^{-3}	0.021	0.042	0.044
Heat energy production , KJ· m^{-3}	65.897	132.031	136.417
Net power energy, kWh·m^{-3}	0.198	0.176	0.174
Net heat energy, KJ· m^{-3}	-65.897	-132.031	131512
OEB, kWh·m^{-3}	0.20	0.18	36.71

(a)

Scenarios			**Power energy generated**	**Heat energy generated**	**Total energy recovered**
	mg$_{CH4}$·l^{-1}	l$_{CH4}$·dia^{-1}	kWh·m^{-3}	KJ·m^{-3}	kWh·m^{-3}
Scenario 1a (OT=AT= 20ºC)	70.53	56.13	0.075	235.78	0.075
Scenario 1b (OT=AT=33ºC)	77.89	61.99	0.083	260.38	0.083
Scenario 2 (OT 33ºC, AT 20ºC)	76.13	60.589	0.081	254.50	0.152

(b)

7.3.1.2 Impact of physical separation process

As shown in Table 7.2a, the most important item contributing to the mechanical energy consumption in the three scenarios was the membrane tank biogas recycling blower, which accounts for some 45% of total mechanical energy requirements (some 0.10 kWh·m^{-3} in absolute terms). According to Lin *et al.* [7.25] the energy consumed by gas scouring accounted for the largest percentage of operating costs, followed by the membrane tank sludge feed pump, which accounted for 43% (approx. 0.09 kWh·m^{-3} in absolute terms). The resulting weighted average distribution of mechanical energy consumption highlights the need to optimise filtration in all operating ranges to improve the feasibility of AnMBR technology being used to treat urban wastewater. In this regard, operating at low SGD_P (specific gas demand per m^3 of treated water) reduces net energy consumption considerably.

7.3.1.3 Impact of energy from capture of methane dissolved in effluent

As shown in Table 7.2b, the theoretical amounts of energy from the capture of methane dissolved in effluent were 0.075, 0.083 and 0.152 kWh·m^{-3} in scenarios 1a, 1b and 2, respectively, assuming a methane capture efficiency of 100%.

It is important to emphasise that the energy from the methane dissolved in effluent is not contemplated in this study. If it was, it might reduce the energy consumed in scenarios 1a and 1b considerably (up to 57 and 47%, respectively). This highlights the need to develop technologies for the capture of methane dissolved in effluent not only in order to reduce the environmental impact (i.e. the release of dissolved methane into atmosphere) but also to enhance the OEB of AnMBR technology.

7.3.1.4 Impact of sulphate content in influent

Because of the significant sulphate content in the influent in this particular study, an important fraction of COD is consumed by sulphate-reducing bacteria (SRB). To be precise, sulphate content in the influent was approx. 97 mg SO_4-S L^{-1}, almost all of which was reduced to sulphide (approx. 98%). In this respect, 190 mg COD L^{-1} were theoretically consumed by SRB (calculated using the stoichiometric ratio of kg of COD degraded per kg of sulphate reduced to sulphide).

Therefore, considerably far more power and heat could have been generated if low/non sulphate-loaded wastewaters had been used. If the sulphate content in the influent is considered to be zero, the amount of influent COD transformed into methane increases significantly (up to 37% of the influent COD).

Therefore, the resulting methane generated will increase up to 141 $L_{CH4}·day^{-1}$ (calculated on the basis of the theoretical methane yield under standard temperature and pressure conditions: 350 L_{CH4} $kg^{-1}COD$). Consequently, in absolute terms, the energy from methane capture (present in biogas and dissolved in the effluent assuming a capture efficiency of 100%) would increase to 0.19 $kWh·m^{-3}$ (power energy) and 592.17 $KJ·m^{-3}$ (heat energy), respectively.

7.3.1.5 Comparison with other technologies

According to Judd and Judd [7.17], the full-scale aerobic MBR in Nordkanal (Germany) had a specific energy demand of 0.9 $kWh·m^{-3}$, which is low compared to the consumption (approx. 3.9 $kWh·m^{-3}$) at other full-scale municipal aerobic MBRs (e.g. Immingham Docks MBR WWTP, United Kingdom). On the other hand, conventional activated sludge (CAS) in Schilde (Belgium) consumed 0.19 $kWh·m^{-3}$ [7.26]. For this study, the energy consumption in scenarios 1a and 1b (operating at ambient temperatures of 20 and 33 ºC, respectively) is much lower (0.20 and 0.18 $kWh·m^{-3}$, respectively) than at Nordkanal MBR and similar to Schilde CAS. On the other hand, scenario 2 (operating at 33 ºC when the ambient temperature was 20 ºC) far exceeds the above-mentioned values. Hence, it can be concluded that from an energy perspective, AnMBR operating at ambient temperatures is a promising sustainable wastewater technology in comparison with other existing urban WWT technologies. Nevertheless, it is important to note that AnMBR energy demand does not include the energy needed to remove nutrients unlike at Nordkanal MBR, Immingham Docks MBR and Schilde CAS.

7.3.2 LCA results

As mentioned earlier, the SimaPro programme (using Ecoinvent data) was used to assess the potential impact of the AnMBR system evaluated in this study (energy consumption and production, and matter discharged).

Table 7.3 shows the LCA results of each impact category (eutrophication, abiotic depletion, etc) in the three scenarios evaluated (1a, 1b and 2). This table is divided into five columns corresponding to the impact of: (1) the four factors of the inventory analysis considered in this study (total impact); (2) energy consumption; (3) energy from biogas capture; (4) sludge disposal; and (5) effluent discharge. The fourth column is divided into two columns to show the impact of the sludge, depending on the percentage considered: (1) for use as fertiliser on farmland (85%); and (2) sent to landfill (15%).

Table 7.3 LCA of AnMBR operating at: **(a)** ambient temperature of 20 ºC (scenario 1a); **(b)** ambient temperature of 33 ºC (scenario 1b); and **(c)** at 33 ºC when the ambient temperature is 20 ºC (scenario 2). *Method: CML 2 baseline 2000 V2.05/ / West Europe, 1995 / Normalisation / Excluding infrastructure processes/ Excluding long-term emissions. Negative values correspond to a positive environmental impact.*

Impact category	Total ($\cdot 10^{-14}$)	Energy consumption ($\cdot 10^{-14}$)	Energy from biogas capture ($\cdot 10^{-14}$)	Sludge disposal: Farmland ($\cdot 10^{-14}$)	Sludge disposal: Landfill ($\cdot 10^{-14}$)	Effluent discharge ($\cdot 10^{-14}$)
Eutrophication	158.8726	0.1958	-0.0188	3.3025	1.9280	153.4651
Marine aquatic ecotoxicity	11.6750	2.1077	-0.2031	9.8158	0.0247	-0.0700
Acidification	7.7487	1.0630	-0.1024	6.7452	0.0568	-0.0140
Terrestrial ecotoxicity	7.4031	0.1481	-0.0143	6.8798	0.0051	0.3843
Fresh water aquatic ecotox.	70.7456	0.0436	-0.0042	5.2833	0.0013	65.4215
Abiotic depletion	3.2047	3.4399	-0.3314	-0.0047	0.1425	-0.0415
Global warming (GWP100)	2.5455	1.3511	-0.1302	-0.0017	1.3403	-0.0141
Human toxicity	69.7208	0.1389	-0.0134	1.5487	0.0013	68.0453
Photochemical oxidation	0.3407	0.1426	-0.0137	-0.0003	0.2141	-0.0019
Ozone layer depletion (ODP)	0.0061	0.0068	-0.0007	0.0000	0.0001	-0.0001

(a)

Impact category	Total ($\cdot 10^{-14}$)	Energy consumption ($\cdot 10^{-14}$)	Energy from biogas capture ($\cdot 10^{-14}$)	Sludge disposal: Farmland ($\cdot 10^{-14}$)	Sludge disposal: Landfill deposition ($\cdot 10^{-14}$)	Effluent discharge ($\cdot 10^{-14}$)
Eutrophication	159.1307	0.1949	-0.0376	2.8386	1.8213	154.3135
Marine aquatic ecotoxicity	10.9076	2.0981	-0.4051	9.2609	0.0233	-0.0695
Acidification	6.6890	1.0582	-0.2042	5.7957	0.0537	-0.0143
Terrestrial ecotoxicity	7.0542	0.1474	-0.0285	6.5077	0.0049	0.4227
Fresh water aquatic ecotox.	76.8873	0.0434	-0.0084	5.0006	0.0013	71.8504
Abiotic depletion	2.8501	3.4241	-0.6612	-0.0041	0.1346	-0.0433
Global warming (GWP100)	2.3352	1.3449	-0.2597	-0.0015	1.2661	-0.0146
Human toxicity	76.3144	0.1383	-0.0267	1.4693	0.0012	74.7322
Photochemical oxidation	0.3145	0.1419	-0.0274	-0.0003	0.2023	-0.0020
Ozone layer depletion (ODP)	0.0055	0.0068	-0.0013	0.0000	0.0001	-0.0001

(b)

Impact category	Total ($\cdot 10^{-14}$)	Energy consumption ($\cdot 10^{-14}$)	Energy from biogas capture ($\cdot 10^{-14}$)	Sludge disposal: Farmland ($\cdot 10^{-14}$)	Sludge disposal: Landfill deposition ($\cdot 10^{-14}$)	Effluent discharge ($\cdot 10^{-14}$)
Eutrophication	191.6357	32.8911	-0.0727	2.8414	1.8213	154.1547
Marine aquatic ecotoxicity	362.4733	354.0457	-0.7843	9.2609	0.0233	-0.0723
Acidification	184.0135	178.5680	-0.3954	5.8015	0.0537	-0.0143
Terrestrial ecotoxicity	31.7411	24.8815	-0.0551	6.5077	0.0049	0.4021
Fresh water aquatic ecotox.	80.7569	7.3244	-0.0162	5.0006	0.0013	68.4468
Abiotic depletion	576.6242	577.8171	-1.2801	-0.0041	0.1346	-0.0433
Global warming (GWP100)	227.7044	226.9572	-0.5028	-0.0015	1.2661	-0.0146
Human toxicity	95.9476	23.3368	-0.0517	1.4693	0.0012	71.1920
Photochemical oxidation	24.0949	23.9479	-0.0530	-0.0003	0.2023	-0.0020
Ozone layer depletion (ODP)	1.1397	1.1422	-0.0025	0.0000	0.0001	-0.0001

(c)

By way of example, Figure 7.1 shows the LCA of the inventory analysis of each impact category of the final effluents discharged after irrigation, taking into account whether the methane dissolved in the effluent is captured (Figure 7.1b) or not (Figure 7.1a).

The impact of the factors contemplated in the inventory analysis are addressed below (on the basis of the results shown in Table 7.3 and Figure 7.1):

7.3.2.1 Impact of the final effluent discharge

Table 7.1b shows the average AnMBR effluent characteristics (COD_T, NH_4, PO_4, SO_4, CH_4 and H_2S). The nutrient content of the effluent shows how temperature affects the rate of hydrolysis: the nutrient content was slightly higher at 33ºC (scenarios 1b and 2). In accordance with Bengtsson *et al.* [7.22], Table 7.1c shows the amount of nutrients that is not used by plants (i.e. the nutrients in effluents discharged into natural water courses).

The impact of reusing AnMBR effluent for irrigation is positive because it avoids the direct discharge of nutrients into natural water courses and reduces the use of synthetic fertiliser containing nitrogen (N) and phosphorous (P) [7.27]. Table 7.3 shows that the effluent discharged after part of its nutrients is used for irrigating farmland, contributes to environmental impact by eutrophication, with environmental loads with normalised values of $153.5 \cdot 10^{-14}$ in scenario 1a, and $154.3 \cdot 10^{-14}$ in scenarios 1b and 2. A significant increase in the environmental impact of eutrophication occurs if the effluent is directly discharged into natural water courses, resulting in environmental loads with normalised values of $336.3 \cdot 10^{-14}$ and $341.8 \cdot 10^{-14}$, respectively. The other impact categories are not affected by the final destination of effluent nutrients (irrigation or discharge).

It is important to highlight that the nutrient discharge has an equal environmental impact in the two scenarios conducted at 33 ºC (scenarios 1b and 2). Scenario 1a (conducted at 20 ºC) has a slightly lower environmental impact than scenarios 2 and 1b, mainly due to the hydrolysis rate. In this respect, the nutrient discharge concentrations (shown in Table 7.1b and Table 7.1c) reveal that temperature seems to have little influence on the hydrolysis rate: similar effluent results were obtained in both scenarios. This is due to operating at 70 days of SRT. This SRT is enough to hydrolyse the main part of the particulate biodegradable organics (XC_B): 95% of the XC_B is hydrolysed at 20ºC and 98% of the XC_B is hydrolysed at 33ºC. Therefore, as shown in Table 7.1b, similar concentrations of NH_4 (0.0564, 0.0573 and 0.0573 kg m^{-3}) and PO_4 (0.0186, 0.0191 and 0.0192 kg m^{-3}) were observed in all scenarios (1a, 1b and 2, respectively).

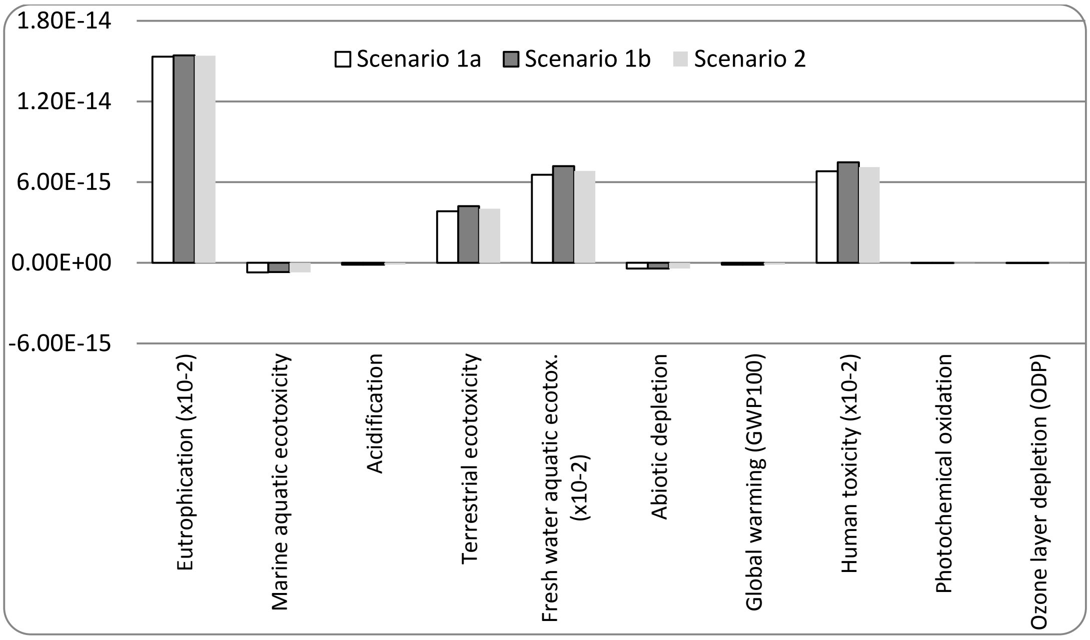

(a)

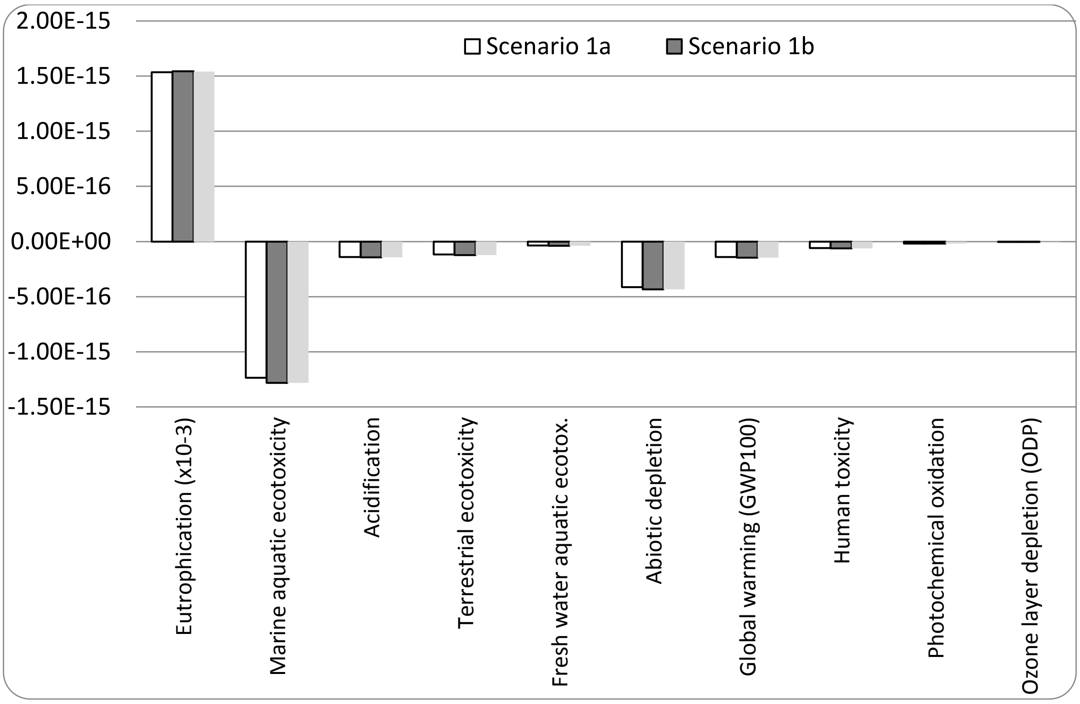

(b)

Figure 7.1 LCA of treated effluent discharge (in normalised values per m^3) considering: **(a)** non-capture of methane dissolved in effluent; and **(b)** capture of methane dissolved in effluent. Scenario 1a: operating at ambient temperature of 20 ºC; scenario 1b: operating at ambient temperature of 33 ºC); and scenario 2: operating at 33 ºC when the ambient temperature is 20 ºC. *Method: CML 2 baseline 2000 V2.05 / West Europe, 1995 / Normalisation / Excluding infrastructure processes / Excluding long-term emissions.*

Final effluent nutrient discharge after irrigating farmland has a slightly positive environmental impact (negative values) in all the evaluated impact categories (except eutrophication) due to partially replacing part of the required fertiliser (see Figure 7.1b). However, when the methane dissolved in the effluent is not captured, some of the impact categories are negatively affected (see Figure 7.1a or Table 7.3).

As shown in Figure 7.1a, different impact categories are affected by discharging the methane dissolved in the effluent, such as human toxicity (resulting in environmental loads with normalised values of $68.0 \cdot 10^{-14}$, $74.7 \cdot 10^{-14}$, $71.2 \cdot 10^{-14}$, in scenarios 1a, 1b and 2, respectively), fresh water aquatic ecotoxicity (resulting in environmental loads with normalised values of $65.4 \cdot 10^{-14}$, $71.9 \cdot 10^{-14}$, $68.4 \cdot 10^{-14}$, in scenarios 1a, 1b and 2, respectively) and to a lesser extent, terrestrial ecotoxicity and marine aquatic ecotoxicity.

7.3.2.2 Impact of energy consumption

Electricity consumption affects all the impact categories assessed. As shown in Table 7.3, the main environmental impacts caused by electricity consumption are abiotic depletion (resulting in environmental loads with normalised values of $3.4 \cdot 10^{-14}$ in scenarios 1a and 1b, and $577.8 \cdot 10^{-14}$ in scenario 2), marine aquatic ecotoxicity (resulting in normalised environmental loads with normalised values of $2.1 \cdot 10^{-14}$ in scenarios 1a and 1b, and $354.0 \cdot 10^{-14}$ in scenario 2) followed to a lesser extent by GWP (resulting in environmental loads with normalised values of $1.4 \cdot 10^{-14}$, $1.3 \cdot 10^{-14}$ and $227.0 \cdot 10^{-14}$, in scenarios 1a, 1b and 2, respectively) and acidification (resulting in environmental loads with normalised values of $1.1 \cdot 10^{-14}$ in scenarios 1a and 1b, and $178.6 \cdot 10^{-14}$ in scenario 2). Note that the environmental impact of electricity consumption on all the impact categories evaluated in this study is considerably higher in scenario 2 than in scenarios 1a and 1b due to the considerable amount of heat energy needed in scenario 2 to maintain an operating temperature of 33 ºC (131649 $kJ \cdot m^{-3}$, see Table 7.3). It must be said that ideally, this study should have contemplated the impact of discharging effluent to the natural water courses at 13 ºC above the ambient temperature. In this respect, this higher temperature would increase the adverse environmental impact even more in scenario 2.

7.3.2.3 Impact of energy from biogas capture

Energy from biogas capture has a positive impact (shown in Table 7.3 as negative figures) on all the impact categories evaluated because it is considered to be an energy saving. As Table 7.3 shows, the main environmental benefits of energy from biogas capture are abiotic depletion (resulting in environmental loads with normalised values of $-0.3 \cdot 10^{-14}$, $-0.7 \cdot 10^{-14}$ and $-1.2 \cdot 10^{-14}$, in scenarios 1a, 1b and 2, respectively), marine aquatic ecotoxicity (resulting in environmental loads with normalised values of $-0.2\cdot10^{-14}$, $-0.4\cdot10^{-14}$ and $-0.8\cdot10^{-14}$, in scenarios 1a, 1b and 2, respectively) and GWP (resulting in environmental loads with normalised values of $-0.1\cdot10^{-14}$, $-0.3\cdot10^{-14}$ and $-0.5\cdot10^{-14}$, in scenarios 1a, 1b and 2, respectively). In this case, the environmental benefits when operating at 33 ºC (scenarios 2 and 1b) are greater than when operating at 20 ºC (scenario 1a) due to higher methane production. Although in scenario 2 the heat energy generated by captured biogas can be used for heating purposes, it is a very small amount in comparison with the total energy required to achieve the operating temperature.

7.3.2.4 Overall inventory results

It must be said that heating the process from 20 to 33 ºC (see Table 7.3) increases the environmental impact caused by electricity consumption considerably (because it affects abiotic depletion, marine aquatic ecotoxicity, GWP and acidification categories). Electricity consumption is therefore the major contributor to overall environmental impact, and the most significant impact categories, in descending order, are: abiotic depletion, marine aquatic ecotoxicity, global warming and acidification. The environmental loads related to electricity consumption in scenario 1b are slightly lower than in scenario 1a because, as mentioned before, of the greater volume of biogas produced at higher temperatures. According to the IPCC method, greenhouse gas emissions are considerably higher in scenario 2 (10.98 kg CO_2 equivalents) than in scenarios 1a and 1b (0.13 and 0.12 kg CO_2 equivalents, respectively). Therefore, in order for AnMBR technology to be feasible, it is important to operate at ambient temperature which, furthermore, avoids the heating impact caused by discharging effluent which is hotter than the temperature of natural water courses.

When operating at ambient temperature (scenario 1), the effluent treated (either reused for irrigation or discharged directly onto the natural water courses) is the main contributor to overall environmental impact through eutrophication. In addition, if the methane dissolved in the effluent is not captured, human toxicity and fresh water aquatic ecotoxicity are also significant (see Figure 7.1). This highlights the importance of maximising the recovery of nutrients (which mainly affects eutrophication) and dissolved methane (which mainly affects human toxicity and fresh water aquatic ecotoxicity, see Figure 7.1) from AnMBR effluent.

Disposing of sludge upon farmland slightly affects marine aquatic ecotoxicity, terrestrial ecotoxicity, acidification and fresh water aquatic ecotoxicity (see Table 7.3). Disposing of sludge in landfills has barely any environmental impact on the system, in comparison with other factors.

Effluent discharge through eutrophication is the factor that affects the LCA results most. Nevertheless, the resulting overall environmental impact when operating at different ambient temperature (scenario 1a and 1b) is quite similar. These results reveal that the different operating temperatures seem to have little influence on the hydrolysis rate (due to operating at high SRT), and thus on effluent discharge. When an input energy is required, electricity consumption is the factor that affects the LCA results most, and significant differences in overall environmental impact among the compared scenarios (scenario 1 and 2) are obtained.

7.3.2.5 Impact of sludge disposal

Table 7.4 shows average sludge production and stability. Sludge production was 0.25, 0.23 and 0.23 kg TSS kg^{-1} $COD_{REMOVED}$ in scenarios 1a, 1b and 2, respectively. Moreover, the produced sludge was stabilised, %BVSS below 20. This table shows the impact of temperature on both sludge production and stability: slightly lower sludge production and slightly higher sludge stability were obtained at 33 ºC (scenarios 1b and 2) than at 20 ºC (scenario 1a).

Table 7.4 Average characteristics of AnMBR sludge production and stability in scenarios 1a, 1b and 2. *Nomenclature: **OT**: Operating Temperature; and **AT**: Ambient Temperature.*

Sludge	Scenario 1a (OT=AT= 20ºC)	Scenario 1b (OT=AT=33ºC)	Scenario 2 (OT 33ºC, AT 20ºC)
Kg TSS· kg^{-1} $COD_{REMOVED}$	0.25	0.23	0.23
VSS, %	56.3	53.8	53.8
BVSS, %	19.7	9.8	9.8

The main sustainable benefits of an AnMBR is that lower volumes of sludge are generated and no further digestion is expected to be necessary to enable the sludge to be disposed of on farmland. According to Xing *et al.* [7.28], sludge production in activated sludge processes is generally in the range of 0.3 - 0.5 kg TSS kg^{-1} $COD_{REMOVED}$. As expected, low amounts of sludge were obtained in all scenarios. In addition, the sludge was already stabilised and could therefore be used directly as fertiliser on farmland or sent to a landfill.

As shown in Table 7.3, the main environmental impacts of sludge disposal on farmland are marine aquatic ecotoxicity (resulting in environmental loads with normalised values of $9.8\cdot10^{-14}$ and $9.3\cdot10^{-14}$, in scenarios 1a, 1b and 2, respectively), terrestrial ecotoxicity (resulting in environmental loads with normalised values of $6.9\cdot10^{-14}$ and $6.5\cdot10^{-14}$, in scenarios 1a, 1b and 2, respectively), acidification (resulting in environmental loads with normalised values of $6.7\cdot10^{-14}$ and $5.8\cdot10^{-14}$ in scenarios 1a, 1b and 2, respectively) and fresh water aquatic ecotoxicity (resulting in environmental loads with normalised values of $5.3 \cdot 10^{-14}$ and $5.0 \cdot 10^{-14}$, in scenarios 1a, 1b and 2, respectively). As mentioned earlier, one promising alternative for the disposal of sludge is to spread it on land – with the advantage of reusing the nutrient content in the sludge as fertiliser. Although the environmental impact of disposing of sludge in landfills is slightly lower (only 15 % of all sludge generated is disposed of in landfills), the environmental impact of major factors such as abiotic depletion, global warming and photochemical oxidation can be positive if sludge is used as a fertiliser.

7.4 Conclusions

The environmental impact of an AnMBR system treating urban wastewater at different operating temperatures was evaluated. OEB results highlight the importance of operating at ambient temperature and optimising membrane filtration (average 0.19 $kWh \cdot m^{-3}$). Moreover, maximising the capture of methane from both in both biogas and effluent streams enables considerable energy savings in AnMBRs, which enhances the feasibility of this technology in comparison with others. Furthermore, LCA results revealed the importance of operating at ambient temperature, and maximising the recovery of nutrients (eutrophication can be reduced up to 50%) and dissolved methane (positive environmental impact can be achieved) from AnMBR effluent.

7.5 Acknowledgements

This research work has been supported by the Spanish Ministry of Science and Innovation (MICINN, Project CTM2011-28595-C02-01/02) jointly with the European Regional Development Fund (ERDF) which are gratefully acknowledged.

7.6 References

7.1 A. Gallego, A. Hospido, M.T. Moreira, G. Feijoo, Environmental performance of wastewater treatment plants for small populations. Resour. Conser. Recy. 52 (2008), 931-940.

7.2 G. Rodriguez-Garcia, M. Molinos-Senante, A. Hospido, F. Hernández-Sancho, M.T. Moreira, G. Feijoo, Environmental and economic profile of six typologies of wastewater treatment plants. Water Res. 45 (2011), 5997-6010.

7.3 G. Tchobanoglous, F.L. Burton, H.D. Stensel, Metcalf & Eddy, Inc. Wastewater Engineering. Treatment and Reuse. 4th ed. New York: McGraw-Hill, Fourth edition. pp. 1704 15-5, 2003.

7.4 F. Hernandez-Sancho, M. Molinos-Senante, R. Sala-Garrido, Energy efficiency in Spanish wastewater treatment plants: A non-radial DEA approach. Sci. Total Environ. 409 (2011), 2693-2699.

7.5 J.B. Giménez, A. Robles, L. Carretero, F. Durán, M.V. Ruano, M.N Gatti, J. Ribes, J. Ferrer, A. Seco, Experimental study of the anaerobic urban wastewater treatment in a submerged hollow-fibre membrane bioreactor at semi-industrial scale. Bioresour. Technol. 102 (2011), 8799–8806.

7.6 A. Robles, M.V. Ruano, F. García-Usach, J. Ferrer, Sub-critical filtration conditions of commercial hollow-fibre membranes in a submerged anaerobic MBR (HF-AnMBR) system: The effect of gas sparging intensity. Bioresour. Technol. 114 (2012), 247–254.

7.7 H. Lin, W. Peng, M. Zhang, J. Chen, H. Hong, Y. Zhang, A review on anaerobic membrane bioreactors: Applications, membrane fouling and future perspectives. College of Geography and Environmental Sciences, Zhejiang Normal University, Jinhua, 321004, PR China. Desalination 314 (2013), 169–188.

7.8 L. Raskin, Anaerobic Membrane Bioreactors for Sustainable Wastewater Treatment. WERF Report U4R08, June 2012.

7.9 J. Foley, D. de Hass, K. Hartley, P. Lant, Comprehensive life cycle inventories of alternative wastewater treatment systems. Water Res. 44 (2010), 1654-1666.

7.10 D. Godin. C. Bouchard, A. Vanrolleghem, Net environmental benefit. Introducing a new LCA approach on wastewater treatment systems. Wat. Sci. Technol. 65.9 (2012), 1624-1631.

7.11 J. Ferrer, A. Seco, J. Serralta, J. Ribes, J. Manga, E. Asensi, J.J. Morenilla, F. Llavador, DESASS: A software tool for designing, simulating and optimising WWTPs. Environ. Modell. Softw. 23 (2008), 19-26.

7.12 R. Barat, J. Serralta, M.V. Ruano, E. Jiménez, J. Ribes, A. Seco, J. Ferrer, Biological Nutrient Removal Model Nº 2 (BNRM2): A general model for Wastewater Treatment Plants. Water Sci. Technol. 67 (2013), 1481 – 1489.

7.13 S. Lassaux, R. Renzoni, A. Germain, Life Cycle Assessment of Water from the Pumping Station to the Wastewater Treatment Plant. Int. J. Life Cycle Ass. 12 (2007) 118 – 126.

7.14 S. Lundie, G.M. Peters, P.C. Beavis, Life Cycle Assessment for Sustainable Metropolitan Water Systems Planning. Environ. Sci. Technol. 38 (2004), 3465-3473.

7.15 R.H.C. Emmerson, G.K Morse, J.N. Lester, D.R. Edge, The Life-Cycle Analysis of Small- Scale Sewage-Treatment Processes. J. CIWEM (1995) 317-325.

7.16 Standard methods for the Examination of Water and Wastewater 21th edn, American Public Health Association/American Water Works Association/Water Environmental Federation, Washington DC, USA, 2005.

7.17 S.J. Judd, C. Judd, Principles and Applications of Membrane Bioreactors in Water and Wastewater Treatment. Second Edition, Elsevier, London, UK, 2011.

7.18 AGUA TÉCNICA. Equipos mecánicos para tratamiento de aguas. Tamiz rotativo para sólidos finos. Available on: http://www.aguatecnica.es/index.php?option=com_content&view=article&id=50&Itemid=59, (Accessed May 3, 2012).

7.19 EPA. Environmental Protection Agency. Combined Heat and Power Partnership. Agency of the United States federal government, 2012.

7.20 R. Frischknecht, G. Rebitzer,G, The ecoinvent database system: a comprehensive web-based LCA database. J. Clean. Prod. 13 (2005), 1337-1343.

7.21 REE. Spanish Electrical System. La Red Eléctrica de España, Alcobendas, Madrid, 2010.

7.22 M. Bengtsson, M. Lundin, S. Molander, Life cycle assessment of wastewater systems: case studies of conventional treatment, urine sorting and liquid composting in three Swedish municipalities. Report 1997:9. Chalmers University of Technology, Gothenburg, Sweden.

7.23 P.S. Kidd, M.J. Dominguez-Rodriguez, J. Diez, C. Monterroso, Bioavailability and plant accumulation of heavy metals and phosphorus in agricultural soils amended by long-term application of sewage sludge. Chemosphere, 66 (2007), 1458-1467.

7.24 G. Doka, Life cycle inventories of waste treatment services. Ecoinvent report no.13. Swiss centre for life cycle inventories, Dübendorf, 2009.

7.25 H. Lin, J. Chen, F. Wang, L. Ding, H.Hong Feasibility evaluation of submerged anaerobic membrane bioreactor for municipal secondary wastewater treatment. Desalination 280 (2011), 120–126.

7.26 A. Fenu, J. Roels, T. Wambecq, K. De Gussem, C. Thoeye, G. De Gueldre, B. Vand De Steene, Energy audit of a full scale MBR system. Desalination 262 (2010), 121-128.

7.27 M. Meneses, J.C. Pasqualino, F. Castells, Environmental assessment of urban wastewater reuse: Treatment alternatives and applications. Chemosphere 81 (2010), 266–272.

7.28 C.H. Xing, W.Z. Wu, Y. Quian, E. Tardieu, Excess sludge production in membrane bioreactors: a theoretical investigation. J. Environ. Eng. ASCE, 129 (2003), 291–297

CHAPTER 8:

Navigating Environmental, Economic, and Technological Trade-Offs in the Design and Operation of Submerged Anaerobic Membrane Bioreactors (AnMBRs)

Abstract

Anaerobic membrane bioreactors (AnMBRs) enable energy recovery from wastewater while simultaneously achieving high levels of treatment. The objective of this study was to elucidate how detailed design and operational decisions of submerged AnMBRs influence the technological, environmental, and economic sustainability of the system across its life cycle. Specific design and operational decisions evaluated included: solids retention time (SRT), mixed liquor suspended solids (MLSS) concentration, sludge recycling ratio (r), flux (J), and specific gas demand per membrane area (SGD). The possibility of methane recovery (both as biogas and as soluble methane in reactor effluent) and bioenergy production, nutrient recovery, and final destination of the sludge (land application, landfill, or incineration) were also evaluated. The implications of these design and operational decisions were characterized by leveraging a quantitative sustainable design (QSD) framework which integrated steady-state performance modeling across seasonal temperatures (using pilot-scale experimental data and the simulating software DESASS), life cycle cost (LCC) analysis, and life cycle assessment (LCA). Sensitivity and uncertainty analyses were used to characterize the relative importance of individual design decisions, and to navigate trade-offs across environmental, economic, and technological criteria. Based on this analysis, there are design and operational conditions under which submerged AnMBRs could be net energy positive and contribute to the pursuit of carbon negative wastewater treatment.

Keywords

Anaerobic MBR; biomethane; global warming potential; life cycle analysis; renewable energy; carbon neutral

Highlights

A quantitative sustainable design for submerged AnMBR is proposed in this study
Operational decisions were evaluated to assess environmental/economic sustainability
Flux, gas sparging and suspended solids results in trade-offs across sustainability
Suspended solids and flux had the greatest influence in environmental/economic terms
Energy positive treatment can be achieved at higher operating temperatures

R. Pretel, B.D. Shoener, J. Ferrer and J. S. Guest
Navigating Environmental, Economic, and Technological Trade-Offs in the Design and Operation of Submerged Anaerobic Membrane Bioreactors (AnMBRs)
Water Res. (2015)

8.1 Introduction

Wastewater treatment plants (WWTPs) predominantly utilize aerobic bioprocesses, which rely on the delivery of air (or oxygen) to achieve contaminant degradation to meet effluent standards. This approach has been highly effective at achieving organic carbon removal from municipal wastewaters, but has resulted in resource-intensive treatment that has broad environmental consequences. Wastewater management in the United States, for example, is estimated to represent roughly 3% of U.S. electricity demand [8.1]. With an estimated 0.3-0.6 kWh of electricity consumed per m^3 of wastewater treated [8.2], this energy demand equates to roughly 0.4-0.8 tonnes of CO_2 emitted per day by a WWTP treating 10 $ML \cdot d^{-1}$ (assuming the 2012 Spanish electricity mix). In addition to impeding progress toward carbon neutral (or negative) WWTPs, these high levels of electricity consumption inflate operating costs and incur a diverse set of life cycle environmental impacts stemming from electricity production processes.

In recent years, there has been increasing interest in the development of mainstream (i.e., main liquid stream) anaerobic treatment processes. In particular, submerged anaerobic membrane bioreactors (AnMBRs) have gained attention for their ability to produce methane-rich biogas during the treatment of urban wastewaters [8.3; 8.4; 8.5; 8.6]. AnMBRs circumvent several critical barriers to the environmental and economic sustainability of wastewater treatment by eliminating aeration, reducing sludge production, and generating methane (a usable form of energy) from organic contaminants in the wastewater [8.7]. However, given the early stage of development and uncertainties around AnMBR performance, it is unclear how detailed design and operational decisions influence the environmental and economic impacts of AnMBR [8.8].

Recent studies (e.g., [8.9]) have identified the need to focus future research efforts on achieving sustainable operation of AnMBRs treating urban wastewater. Although environmental and economic criteria have been used to evaluate submerged AnMBRs relative to alternative aerobic technologies [8.8], a critical barrier to advancing AnMBR development has been the lack of understanding of how detailed design decisions influence system sustainability; a barrier stemming from the lack of a calibrated and validated AnMBR process model to predict system performance under various design and operational scenarios. Ferrer *et al.* [8.10] implemented a computational software called DESASS for designing, simulating, and optimizing both aerobic and anaerobic technologies. The simulation software incorporates a plant-wide model, biological nutrient removal model No. 2 (BNRM2) [8.11], and has been calibrated and validated across a wide range of operating conditions in an industrial-scale AnMBR system [8.12]. By leveraging semi industrial-scale data and modeling, Ferrer *et al.* [8.13] and Pretel *et al.* [8.14] have established an economic basis for the minimum cost design of AnMBRs suitable for implementation in full-scale WWTPs by considering the key parameters affecting membrane performance. However, the environmental impacts of design and operational decisions, as well as the resulting trade-offs across environmental and economic dimensions of sustainability, have not been characterized.

The aim of this study was to elucidate and navigate sustainability trade-offs in the detailed design of submerged AnMBRs by evaluating the full range of feasible design alternatives using technological, environmental, and economic criteria. To this end, the implications of AnMBR design and operational decisions were characterized using a quantitative sustainable design framework (QSD; [8.15]) integrating a calibrated and validated process performance model with life cycle assessment (LCA) and life cycle costing (LCC) under uncertainty. By integrating pilot-scale performance data into this QSD framework, our goal was to characterize the relative importance of individual design and operational decisions of submerged AnMBR, while also shedding light on key elements of the system that warrant further research and development. Finally, QSD was used to optimize a submerged AnMBR system to demonstrate how this methodology can be leveraged to navigate sustainability trade-offs in the design and operation of treatment systems, including low energy and energy-producing wastewater technologies.

8.2 Methodology

8.2.1 Experimental AnMBR Plant

This study was carried out using five years of data from the same AnMBR plant described in Chapter 3, using also the same industrial scale hollow-fibre (HF) membrane units. Further details of this AnMBR system can be found in Giménez *et al.* [8.3] and Robles *et al.* [8.4].

8.2.2 Design and Operational Decision-Making

Recent work leveraging this pilot-scale system has identified that costs of the system are most sensitive to the following design and operational parameters [8.13; 8.14]: sludge retention time (*SRT*); mixed liquor suspended solids in the membrane tank (*MLSS*); sludge recycling ratio (*r*; the ratio of recycled sludge to forward flow); 20 ºC-standardized critical fluxes (*J*); and specific gas demand per membrane area (*SGD*). These parameters influence both the design (i.e., reactor/pump/membrane sizing and construction; Section 8.3.1) and operation (Section 8.3.2) of submerged AnMBR. Based on extensive experimental data from the AnMBR plant and DESASS modeling (Section 8.2.3), acceptable ranges of these critical parameters were identified to be the following: *SRT* from 13 to 70 days (minimum *SRT* values were set based on treatment efficacy, effluent standard, and sludge stabilization criteria); *r* from 0.5 to 8; *MLSS* entering the membrane tank from 5 to 25 g·L^{-1}; *SGD* from 0.05 to 0.3 m^3·m^{-2}·h^{-1}; and *J* from 80 to 120% of the respective critical flux (J_C). To enable more detailed discussion of decision-making, the evaluation of the AnMBR system is divided into its two sub-components: (i) the *biological process*, which includes the anaerobic reactor and its hydraulic connection with the membrane tank, and (ii) the *filtration process*, which includes the membranes and any related maintenance or fouling mitigation.

Beyond these continuous decision variables, three discrete choices/options were also considered in the design of the AnMBR system: the decision of whether to release or recover methane (both biogas and soluble methane in the effluent) for energy production (via a microturbine); whether or not treated effluent is used for fertigation (i.e., irrigation with nutrient-rich water) to offset fertilizer needs; and the final fate of wasted sludge (land application to achieve fertilizer offsets, incineration, or landfilling). The process flow diagram of the submerged AnMBR is shown in Figure S.8.1, and the full range of design and operational decisions can be found in Table S.8.1.

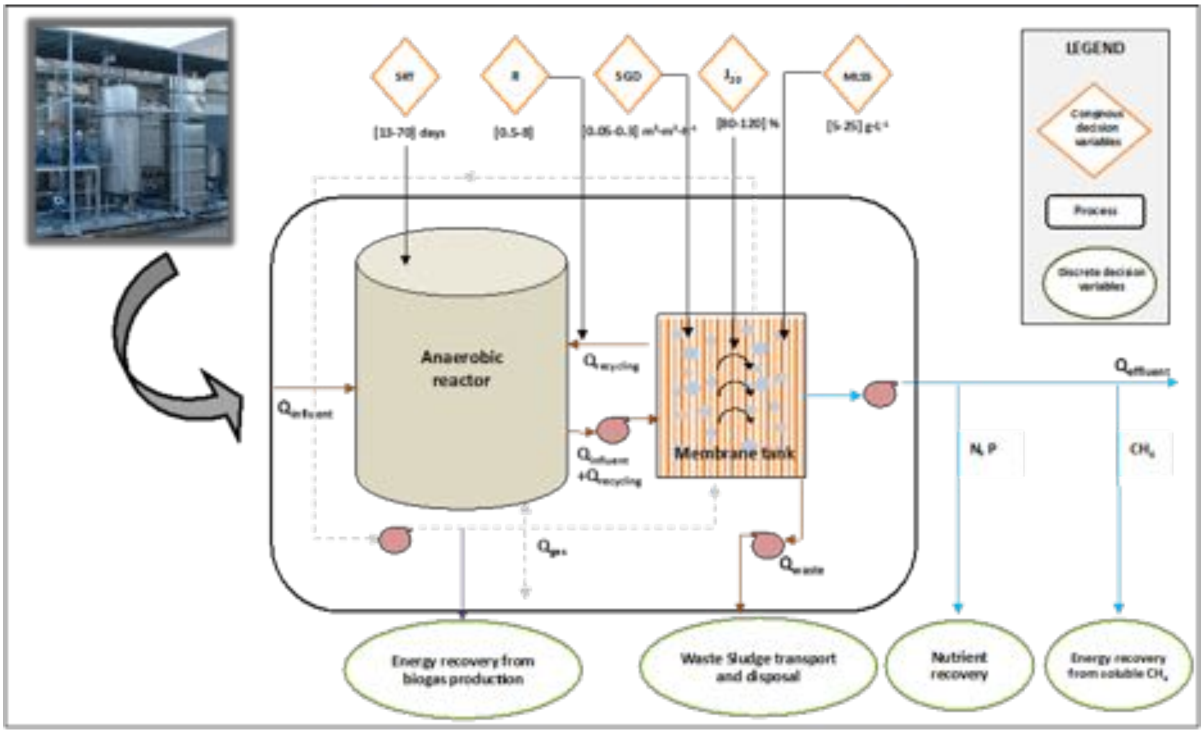

Figure S.8.1 Process diagram flow of the AnMBR design including the operation range of the key parameters in the filtration and biological process over the four seasons of the year, from 15 to 30 ºC. Minimum *SRT* values vary depending on temperature in order to meet effluent standards and sludge stabilization criteria.

Table S.8.1 Full range of design and operational decisions (*T, SRT, r, MLSS, SGD,* and *J*) for the submerged AnMBR system used to characterize environmental, economic, and technological trade-offs.

T, ºC	**15**	**20**	**25**	**30**
SRT, days	41,50,60,70	28,40,50,70	19,30,40,70	13,20,30,70
r	0.5, 1, 1.5, 2, 2.5, 3, 3.5, 4, 6, 8			
MLSS, $g \cdot L^{-1}$	5, 10, 15, 20, 25			
SGD, $m^3 \cdot m^{-2} \cdot h^{-1}$	0.05, 0.10, 0.15 ,0.20, 0.25, 0.30			
J , %J_C	80, 85, 90, 95, 100, 105, 110, 115, 120			

8.2.3 Performance Modeling

The simulated AnMBR system was designed to treat an influent flow of 50,000 $m^3 \cdot d^{-1}$, with a chemical oxygen demand (COD) of 600 $mg \cdot L^{-1}$ and low sulfate content (10 $mg \cdot L^{-1}$). The full characterization of the sewage entering the AnMBR plant can be found in Ferrer *et al.* [8.13]. The system was simulated using DESASS [8.10] with BNRM2 [8.11]. A total of 80 simulations were executed in DESASS and leveraged to characterize system performance across 43,200 scenarios using an Excel-based model that also incorporated an energy consumption tool, enabling the calculation of the overall energy balance (OEB) of the different units at the WWTP. The methodology for the OEB followed the approach of Pretel *et al.* [8.16], which includes procedures for mechanistically calculating mechanical energy demand and energy recovery from biogas.

8.2.4 LCA Implementation

Implementation of a LCA framework was conducted in accordance with ISO 14040 [8.17] and following industry best practices [8.18]. In order to define the goal and scope, the environmental impacts of the AnMBR system associated with water line operations (i.e., primary and secondary wastewater treatment as well as final discharge of the treated effluent) and sludge line treatment (i.e., stabilization to comply with discharge standards) were evaluated. A functional unit of one m^3 of treated wastewater was used for the comparison of the different design alternatives (i.e., the combinations of the SRT, MLSS, J, SGD, and r simulated under four temperatures resulting in a total of 43,200 scenarios; Table S.8.1). Figure 8.1 shows the system boundary used for the LCA and LCC, including the inventory data of the individual materials and processes in this study. As shown in Figure 8.1, the construction, operation, and demolition phases of the WWTP as well as transportation of the materials, reagents, and sludge were all included, but structural concrete and pipes were excluded from the demolition phase because their useful life was greater than that of the project itself. A maximum useful membrane life of 20 years was assumed, with operational fluxes higher than J_C resulting in decreased membrane life (for detailed discussion, see [8.13]). Briefly, membrane life was set from 8 years (when J = 120% of J_C) to 20 years (when J = 80% of J_C), according to the maximum total contact with chlorine permissible (500,000 ppm·h cumulative) and the interval for membrane chemical cleaning. Following the recommendations of Judd and Judd [8.2], 9.5 months was set as the interval for membrane cleaning with chemicals when operating under critical filtration conditions and with a *SGD* value of 0.1 $m^3 \cdot m^{-2} \cdot h^{-1}$. Cleaning frequency was adjusted based on the flux (80-120% of the J_C) and *SGD* by leveraging experimental data extracted in the semi-industrial AnMBR system (e.g., [8.4]; as described in [8.13]). Pre-treatment processes (e.g., screening, grit removal, and grease removal), rotofilter use, equalization tanks, and CIP were not included in this study because their design and operation (and thus, their costs and environmental impacts) were not influenced by the design and operational decisions of the AnMBR process itself. As a result, these supporting processes would not influence the comparative assessment of AnMBR design and operation, and were subsequently placed outside the system boundary. Final effluent was either discharged to natural surface waters or re-used for fertigation. Fugitive CH_4 emissions were accounted when methane was not captured and recovered for energy production. The CML characterization factor of 23 kg CO_2 eq. per kg of CH_4 was used for evaluating the climate implications of fugitive methane. Direct CO_2 releases (i.e., fugitive CO_2 emissions) during sludge dewatering and biogas capture were not quantified because the released CO_2 is classified as biogenic according to IPCC guidelines [8.19]. Direct emissions to air (e.g., CO, SO_2, NO_2, non-methane volatile organic compounds) resulting from methane combustion through a microturbine-based CHP system were excluded because of a lack of information.

The life cycle inventories (LCI) of individual materials and processes were compiled using the Ecoinvent Database v.3 accessed via SimaPro 8.01 (PRé Consultants; The Netherlands). The Centre of Environmental Science (CML) 2 baseline 2000 methodology was used to conduct the impact assessment. The impact categories considered in this study were as follows: eutrophication (kg PO_4 eq.), global warming potential with a 100-year time horizon (GWP_{100}; kg CO_2 eq.), abiotic depletion (AD, kg Sb eq.), and marine aquatic ecotoxicity (kg 1,4-DB eq.). No grouping, weighting, or aggregation of impact categories was used.

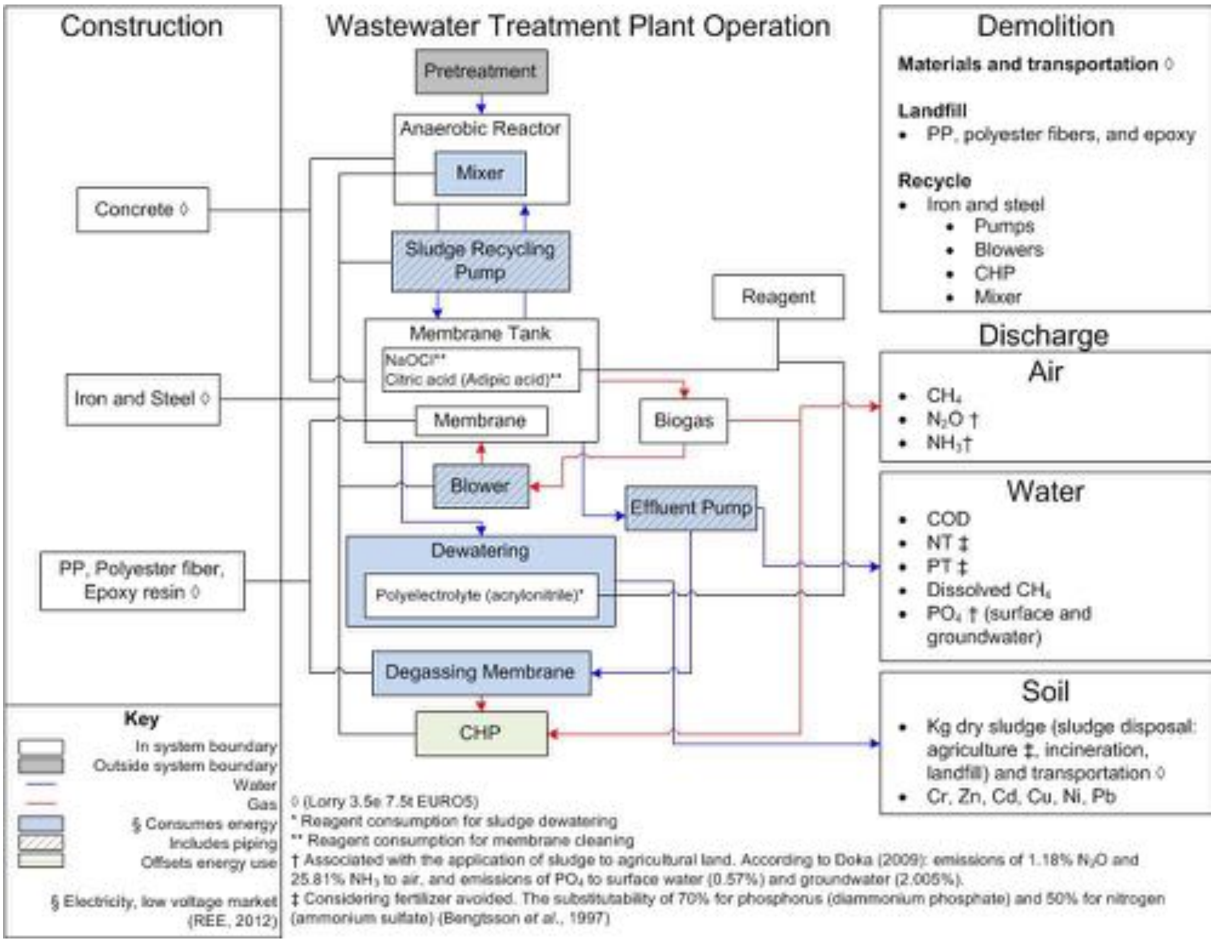

Figure 8.1 System boundary for the LCA and LCC of the submerged AnMBR.

8.2.5 LCC Implementation

In order to determine the LCC of the system, all costs were converted to uniform annual cost. Capital costs were annualized assuming a discount rate of 10% and a project lifetime of 20 years. Annual operating and maintenance (O&M) costs were estimated based on energy and reagent consumption, sludge handling and disposal, as well as the replacement of the equipment required. Unit costs and further details about the LCC methodology can be found in Table S.8.2 as well as Ferrer *et al.* [8.13] and Pretel *et al.* [8.14].

Table S.8.2 Unit costs used to evaluate capital and operating expenses (CAPEX/OPEX) in the proposed AnMBR WWTP scheme.

Unit costs of capital and operating expenses		**Reference**
Steel pipe (DN: 0.4 m)/(DN: 1.4 m), €·m^{-1}	115/520	[8.34]
Concrete wall/slab, € per m	350/130	[8.34]
Ultrafiltration hollow-fibre membrane, (maximum chloride contact of 500,000 ppm·h cumulative), € per m^2	35	PURON®, Koch Membrane Systems
Energy, € per kWh	0.138	[8.35]
Sodium hypochlorite, (NaOCl Cl active 5% PRS-CODEX), € per L	11	Didaciencia S.A.
Acid citric (Acid citric 1-hidrate PRS-CODEX), € per kg	23.6	Didaciencia S.A.
Polyelectrolyte, € per kg	2.35	[8.36]
Wasted sludge for farming, € per t	4.8	[8.37]
Wasted sludge for landfill, € per t	30.1	[8.37]
Wasted sludge for incineration, € per t	250.0	e-REdING, 2014
Blower (ELEKTROR RD 84, Q_B= 5400 m^3·h^{-1}; Lifetime: 50000 hours), €	5900	Elektror S.A.
Sludge recycling pump (BR 600-3GXX/12.3 , Q_P= 600-3000 m^3·h^{-1}; Lifetime: 65000 hours), €	29000	[8.38]
Rotary Lobe pump (INOXPA, Q_P 140 m^3·h^{-1})	25000	INOXPA, S.A
Submersible stirrer (AGS 400-3SHG/6.1; Lifetime: 100000 hours; 3.4 kW; anaerobic reactor=5W·m^{-3}; anoxic reactor=15W·m^{-3}), €	11699	[8.38]
Microturbine-based CHP system (size: 30kW), capital cost, $/ kW and O&M cost, $/ kWh	2700/0.02	[8.39]
Degassing membrane, (flow rate=30m^3·h^{-1}; pressure drop= 60Kpa), Capital cost, €	7300	DIC Corporation
Land cost , €·m^{-2}	0.97	[8.40]

8.2.6 Characterization of the Relative Importance of Design and Operational Decisions

In order to elucidate the relative importance of individual design and operational decisions on AnMBR system sustainability, a sensitivity analysis was conducted in two stages (Figure 8.2): Stage 1 evaluated the full decision space, and Stage 2 focused only on the designs that were likely to be chosen by decision-makers based on economic and environmental criteria (i.e., design and operational decisions resulting in costs below the 15th percentile; see Figure 8.2, left-center panel). The uncertainty around absolute values of cost and LCA results, as well as the relative sensitivity of results to key assumptions (including discount rate, membrane cost, electricity cost, concrete cost, energy for stirring, microturbine efficiency, transportation distance, and percent of produced methane dissolved in the effluent), were also evaluated, with details in the SD (Table S.8.3).

Table S.8.3 Parameters and their probability density functions used in uncertainty analysis.

Input parameters	Distribution	Values	
Electricity cost, €·kWh^{-1}	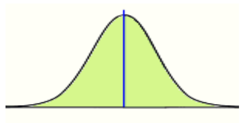	mean	0.138
		SD	0.0054
Discount rate, %		mean	10
		SD	0.7
Concrete cost, €·m^{-3}	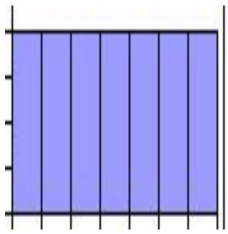	min	330
		max	350
Stirring consumption, W·m^{-3}		min	4
		max	6
Dissolved methane emitted to air, %		min	30
		max	70
Microturbine effciency, %		min	22.5
		max	27
Membrane cost, €·m^{-2}		min	25
		most likely	35
		max	45
Distance transport, km		min	10
		most likely	20
		max	30

To setup the sensitivity analysis, continuous (*MLSS*, *SRT*, *r*, *SGD*, and *J*) and discrete (fate of methane, fate of effluent, and fate of sludge) decisions were sampled from across the decision space, resulting in a total of 10,800 scenarios – where a *scenario* is a single, unique combination of design and operational decisions – at each of four temperatures (totaling 43,200 total simulations; see Table S.8.1 for the values sampled from each continuous decision). The costs and GWP_{100} stemming from capital, $O\&M_{15}$ (O&M at 15 ˚C), and $O\&M_{30}$ (O&M at 30 ˚C) were then quantified for each scenario. To quantify the effect that individual decisions had on environmental and economic criteria, the results were segregated across the decision space for each individual parameter. For Stage 1 of the sensitivity analysis, the median, 5th, 25th, 75th, and 95th percentiles were then calculated for a given parameter value or discrete decision, as was the global median (i.e., the median of all the results). The range between the maximum and minimum value for each percentile was then normalized to the global median in order to quantify how much the range and absolute value of output metrics change across the full decision space for each individual parameter (see the top panel of Figure 8.2 for a visual representation of this methodology).

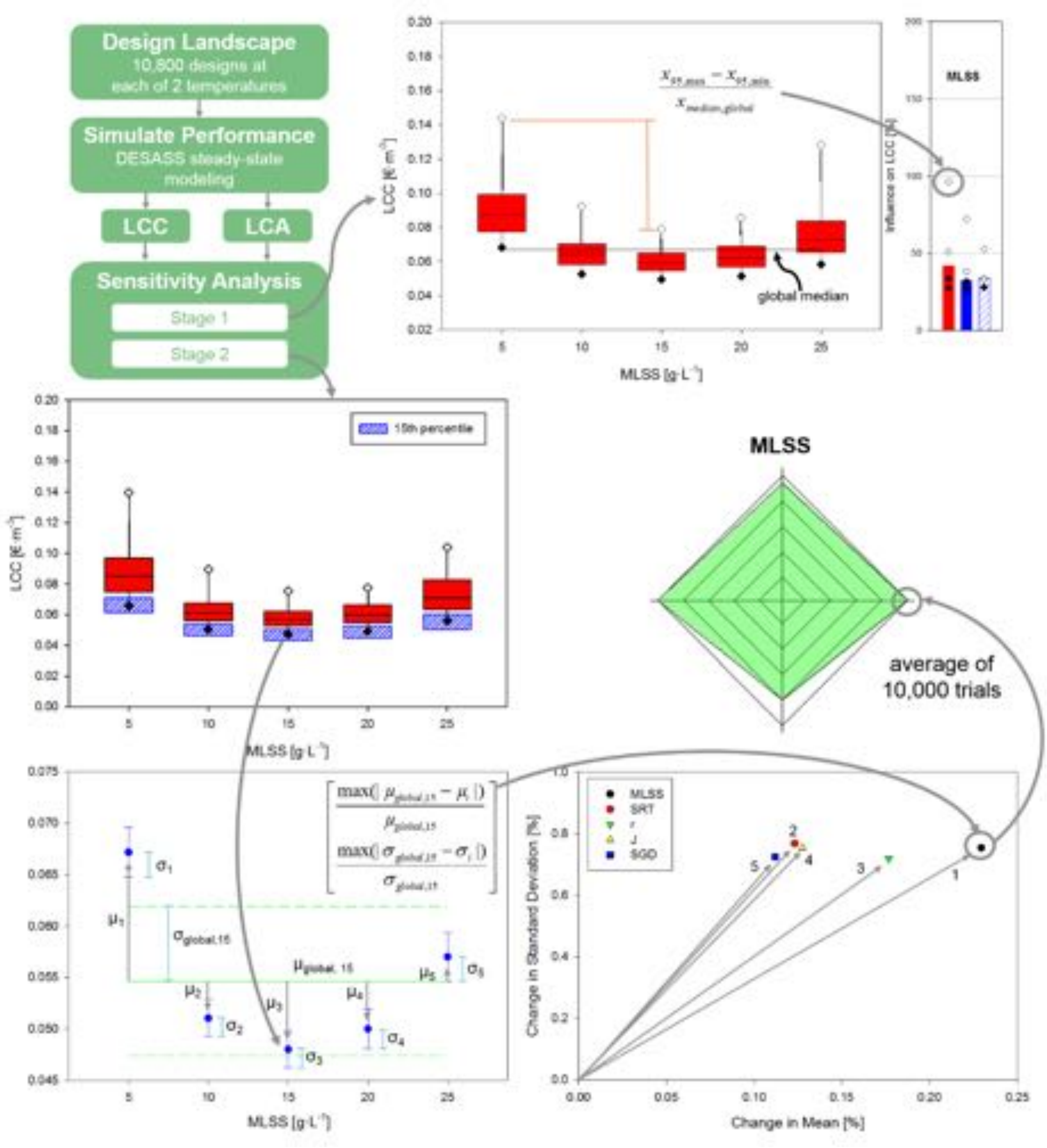

Figure 8.2 Sensitivity analysis methodology used to characterize the relative importance of individual design decisions on (Stage 1) the full range of possible designs or (Stage 2) the range of practical designs (where *practical* designs are those combinations of design and operational parameters that resulted in the lowest 15th percentile of cost or environmental impact, believed to be the most likely to be chosen by decision-makers for implementation). Results of this sensitivity analysis can be found in Figure 8.3 and Figure 8.4.

Recognizing that design and operational decisions resulting in costs below the 15th percentile are most likely to be chosen (so long as they meet treatment objectives) by WWTP designers and decision-makers, these scenarios were the focus of Stage 2 of the sensitivity analysis. Once this subset of scenarios was identified (consisting of the "practical" scenarios most likely to be chosen for implementation), the *practical* average and standard deviation of cost and GWP_{100} across all continuous decisions were determined. Next, the *local* average and standard deviation were calculated for each simulated value across the range of an individual design or operational decision (e.g., *MLSS* = 5, 10, 15, 20, and 25 $kg \cdot m^{-3}$). For a given decision, the greatest difference between a *local* and the *practical* average was then used to calculate the maximum percent shift from the practical average stemming from that decision (this calculation of the maximum percent shift was repeated for the *practical* standard deviation using *local* standard deviations; bottom-left graph in Figure 8.2). The relative importance of each continuous decision variable on a given metric (costs and GWP_{100} stemming from capital and average O&M) was determined by taking the sum of the percent change in average and percent change in standard deviation and ranking those sums in descending order (bottom-right graph in Figure 8.2), similar to the ranking process of Morris' one-at-a-time method [8.20]. As a final step in the Stage 2 sensitivity analysis, Monte Carlo simulation was conducted with 10,000 trials to examine the change in rank of the five continuous decision variables in order to characterize the robustness of these rankings.

8.3 Results and Discussion

Four main sections have been established in order to elucidate and navigate sustainability trade-offs stemming from detailed decision-making for submerged AnMBR: the relative importance of individual design and operational decisions (Section 8.3.1), navigating trade-offs across dimensions of sustainability (Section 8.3.2), optimization of the AnMBR process (Section 8.3.3), and uncovering how and why individual design/operational decisions impact AnMBR sustainability (Section 8.3.4). Taken altogether, these sections demonstrate how QSD can be used to optimize wastewater treatment technologies, including those targeting energy and broader resource recovery from wastewater. Results and discussion are centered on linking design decisions to costs and life cycle environmental impacts, with a focus on global warming potential with a 100 year time horizon (GWP_{100}) as a representative example of broader environmental impacts. It should be noted, however, that most environmental impact categories followed similar trends as those of GWP_{100}.

8.3.1 Relative Importance of Design and Operational Decisions to AnMBR Sustainability

Figure 8.3 shows the effect of the continuous (*MLSS*, *SRT*, *r*, *J*, and *SGD*) and discrete (methane fate, effluent fate, and sludge fate) decisions on costs and environmental impacts across capital, $O\&M_{15}$, and $O\&M_{30}$. Considering continuous variables, all five influenced costs to a similar degree, although *MLSS* and *J* were most responsible for the variance in the LCC results stemming from capital and O&M costs, respectively (Figure 8.3A). The variables *r*, *MLSS*, and *SGD* were the most significant contributors to the variance in LCA results, mostly due to O&M (Figure 8.3C). For almost all parameters, the largest variance in economic and environmental performance was observed at the 95th percentile and the lowest variance at the 5th percentile. Discrete variables had similar cost implications as the design and operational parameters (Figure 8.3A and Figure 8.3B), but disproportionately high GWP_{100} consequences (one to two orders of magnitude higher; see y-axis scales in Figure 8.3C and Figure 8.3D). This observation stemmed from the climate implications of fugitive methane (23 kg of CO_2 eq. per kg of fugitive CH_4), energy offsets (0.13 kg of CO_2 per kWh produced), and fertilizer offsets (2.68 kg of CO_2 equivalents per kg of N). In comparison to the baseline set of discrete decisions (recovery of biogas and soluble methane for electricity production, effluent reuse, and land application of biosolids), allowing fugitive methane emissions and managing sludge through incineration were the least preferable options in terms of cost (Figure 8.3B). Regarding LCA results, eliminating energy recovery from methane and final disposal of the sludge into landfill were the least preferable options (Figure 8.3D).

In order to provide insight into the role of individual design and operational decisions on the relative sustainability of practical designs (i.e., the final set of designs likely to be considered by decision-makers), Stage 2 of the sensitivity analysis focused on the scenarios below the 15th percentile for costs (as shown in Figure 8.2). The relative importance of the five continuous decision variables was evaluated across four categories: influence on costs and GWP_{100} stemming from capital and average O&M (i.e., average of O&M at 15 and 30˚C; Figure 8.4). The results of the Monte Carlo simulation (Figure 8.4 and Table S.8.4) show that *MLSS* consistently (71-100%) had the largest impact on capital costs and both LCA categories, and was ranked second for its impact on LCC O&M across all simulations. *SRT* only had a high impact on LCA Capital (ranked second), which is a result of its effect on tank volume, which in turn determines construction material requirements. *r* was most often ranked second for LCC Capital, which was due mainly to its effect on tank volume when building the plant. *SGD* consistently impacted LCA O&M (ranked second) because of electricity demand from blower operation. *J* was ranked first for LCC O&M (across all simulations) because of its effect on membrane operation and replacement cost. Thus, the factors driving environmental impacts were tankage and electricity for gas sparging, while costs were driven by tankage and membranes. In comparison to Figure 8.3 and the analysis of the full decision space, the results presented in Figure 8.4 provide much more meaningful insight for decision-makers by focusing on the scenarios most likely to be chosen. This analysis eliminates observations that are irrelevant (e.g., stemming from scenarios that would never be chosen), and also allows decision-makers to prioritize individual design and operational decisions as part of a participatory planning process incorporating locality-specific factors [8.21].

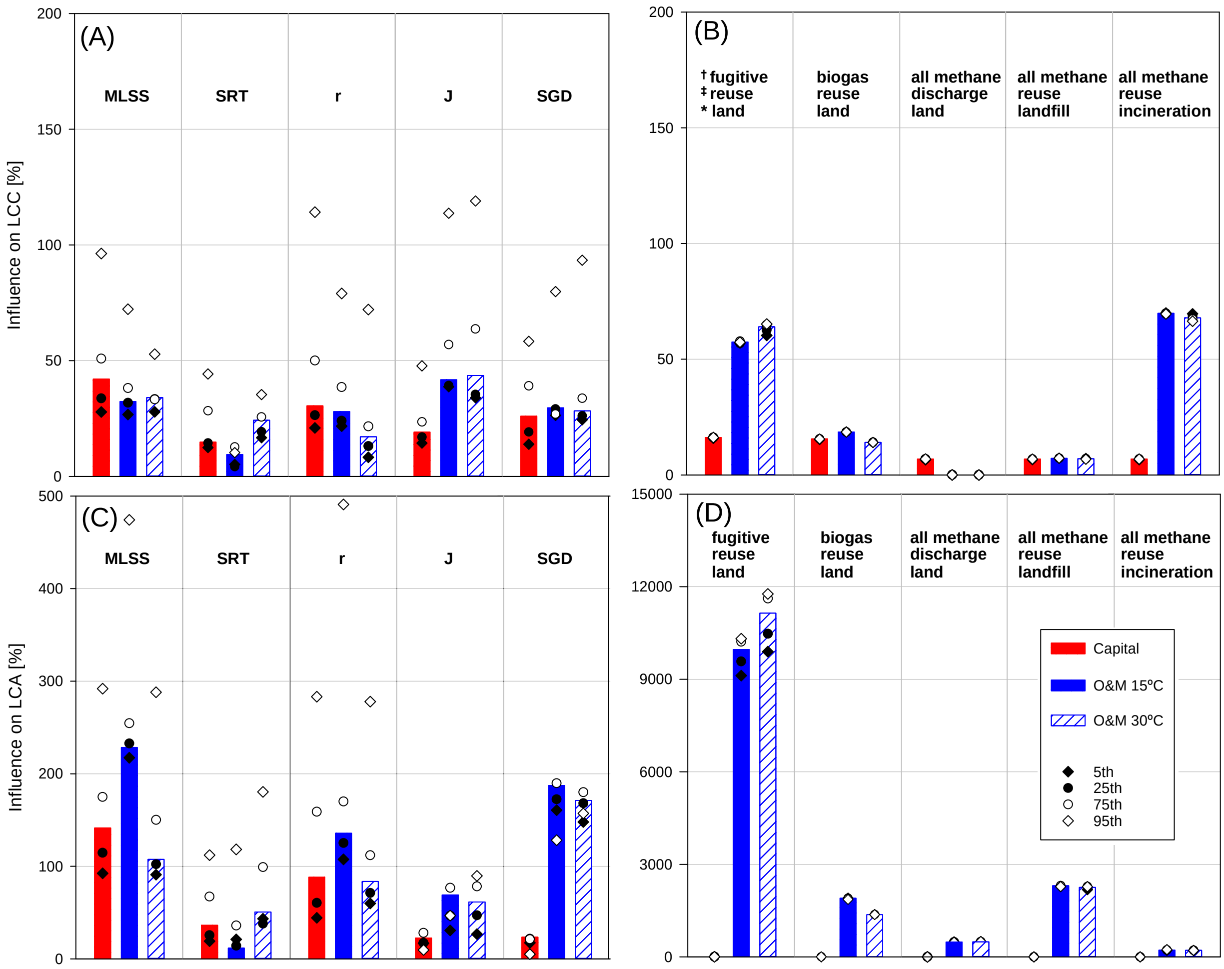

Figure 8.3 Effect of the continuous (*MLSS*, *SRT*, *r*, *J*, and *SGD*) and discrete (methane recovery, nutrient recovery, and sludge disposal) decisions on the outputs (LCC and LCA) stemming from capital, O&M$_{15}$, and O&M$_{30}$ and considering 5th, 25th, 75th, and 95th percentiles. As shown in the top right panel of Figure 8.2, the range between the maximum and minimum for each percentile was normalized by the global median. Discrete selections are listed as †methane fate (*fugitive* emission, *biogas* recovery for electricity production, total *methane* recovery – including biogas and soluble methane – for electricity production), ‡effluent fate (*reuse* for fertigation, direct *discharge*), and *residuals fate (*land* application, *landfill*, *incineration*). The baseline set of discrete decisions was fixed as total methane recovery, fertigation, and land application.

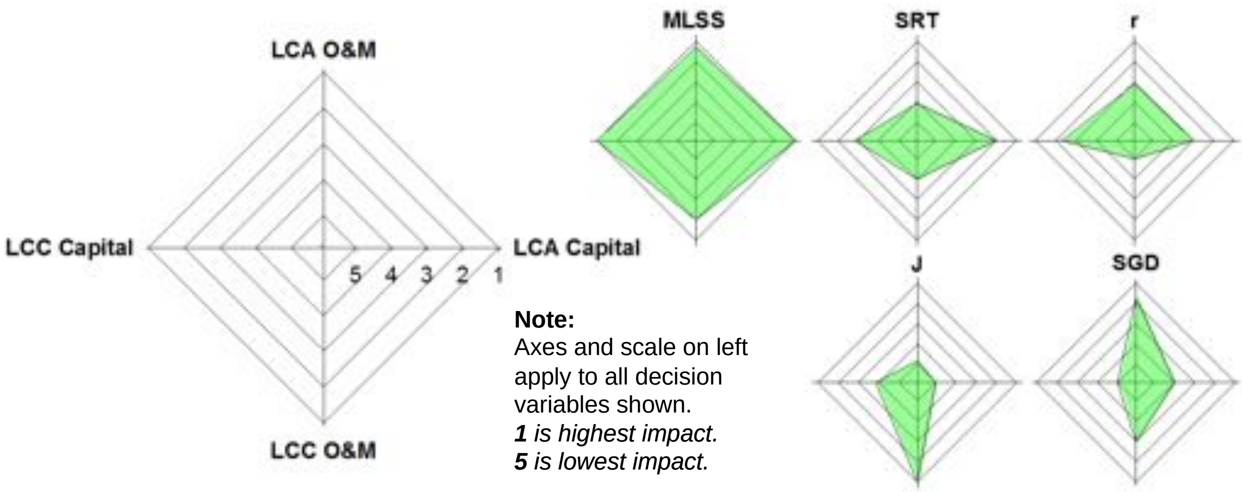

Figure 8.4 Radar plot showing the average relative importance of five continuous decisions (*MLSS, SRT, r, J, SGD*) on four outputs (LCC Capital and O&M, LCA Capital and O&M). The influence of each decision on LCC and LCA outputs was ranked from 1–5 – with one having the highest impact on each result – across 10,000 trials. The size of the green area represents the magnitude of the decision's impact. Average ranks and standard deviations (from the 10,000 trials) can be found in Table S.8.3.

Table S.8.4 Most probable ranks from 10,000 trials (Monte Carlo with Latin Hypercube Sampling) that were utilized to generate Figure 4. Values in parentheses are the probability that the variable was given this rank throughout the 10,000 trials (100% indicates that the variable had the same rank after every trial).

	MLSS	SRT	r	J	SGD
LCA Capital	1 (100%)	2 (100%)	3 (100%)	5 (100%)	4 (100%)
LCA O&M	1 (71%)	4 (72%)	3 (89%)	5 (83%)	2 (71%)
LCC Capital	1 (100%)	3 (84%)	2 (79%)	4 (91%)	5 (100%)
LCC O&M	2 (100%)	4 (100%)	5 (100%)	1 (100%)	3 (100%)

8.3.2 Navigating Trade-Offs Across Dimensions of Sustainability

In order to develop a final set of parameters, it becomes necessary to characterize the interactions among design and operational decisions. To this end, we evaluated relationships among decision variables to identify trade-offs and synergies, where *trade-offs* exist when adjusting a decision variable produces tension between sustainability metrics (i.e., to get better in one, you must get worse in the other), and *synergies* occur when changing a given decision variable moves sustainability metrics in the same direction (either both become more desirable, or both become less desirable).

When synergies exist between LCC and LCA results, it can be expected that designers would seek to simultaneously improve both costs and environmental impacts by adjusting the decision variable. If the LCC and LCA results follow opposing trends, trade-offs can be considered by comparing the ratio of additional costs (€) to the tonnes of CO_2 equivalents that are saved (i.e., not released to the environment). This approach to quantifying the tension between sustainability metrics enables the comparison of a given decision to an external benchmark – the carbon emissions trading system – which enables the purchase of carbon offsets (€·t CO_2^{-1}). In general, emissions trading seeks to reduce pollution by providing economic incentives for companies to limit their emissions [8.22]. The largest international framework for greenhouse gas emissions is the European Union Emission Trading Scheme, which currently spans power plants and industrial plants across 31 countries [8.23]. By using market prices for carbon offsets as a benchmark (e.g., in Spain the emissions trading system is currently around 6 €·tonne CO_2 saved^{-1} [8.24]), the rationality of having a WWTP incur additional costs to reduce carbon emissions can be evaluated.

Figure 8.5 shows the effect of *MLSS* (Figure 8.5A), *J* (Figure 8.5B), *SRT* (Figure 8.5C), and *SGD* (Figure 8.5D) in order to illustrate the potential for trade-offs and synergies between costs and environmental impacts. Although simulations were performed across the full range for all continuous decision variables, four illustrative examples (the min-max combinations of two other decision variables) are plotted in each figure. In Figure 8.5A, *MLSS* was varied from 5-25 g·L^{-1} for four possible design/operational scenarios at the min-max of *J* (80 and 120% of J_C) and *r* (0.5-8). For these example scenarios, costs and GWP_{100} were synergistic below *MLSS* values of 15 g·L^{-1}. In Figure 8.5B, flux was varied from 80-120% of J_C for four possible design/operational scenarios at the min-max *MLSS* (5 and 25 g·L^{-1}) and *SGD* (0.05 and 0.30 m^3·m^{-2}·h^{-1}). At a flux below 97% and above 112%, synergy occurs between the LCA and LCC results, which indicates that both impacts can be lessened by increasing or decreasing the flux in the direction of the synergy arrows shown in Figure 8.5B. However, between 97-112% of J_C, tension exists between economic and environmental impacts, thus requiring the navigation of trade-offs. In Figure 8.5C, *SRT* was varied from 13 to 70 days across combinations of *MLSS* (5 and 25 g·L^{-1}) and *r* (0.5-8) (when methane is not recovered), and was shown to be synergistic at all values examined, which indicates that LCC and GWP can be lessened by minimizing *SRT* across the entire decision space. In contrast, Figure 8.5D demonstrates that *SGD* often results in trade-offs across the full range of values considered (0.05 to 0.30 m^3·m^{-2}·h^{-1}), shown with combinations of *MLSS* (5 and 25 g·L^{-1}) and *J* (80 and 120% of J_C).

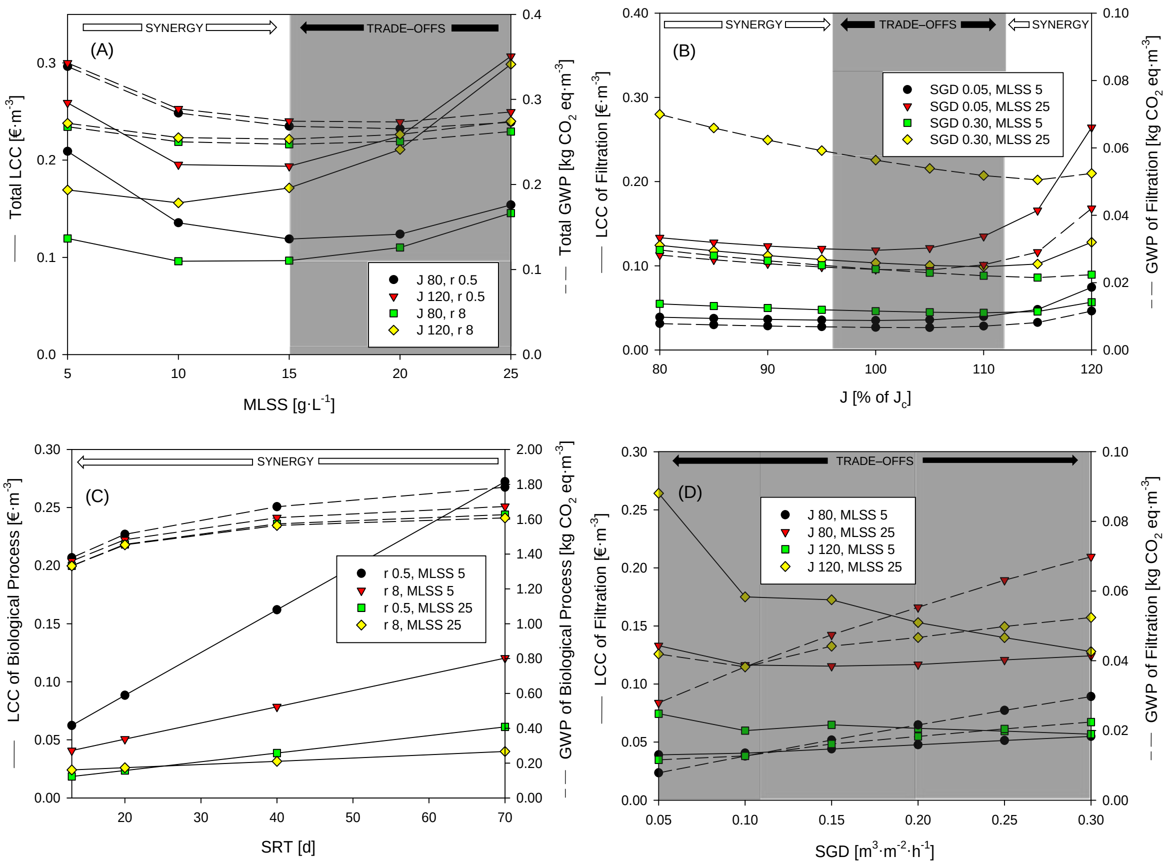

Figure 8.5 LCC (€·m^{-3}) and GWP (kg-CO_2 eq·m^{-3}) results of a subset of AnMBR scenarios showing trade-offs and synergies between economic and environmental criteria across the decision space for: (A) *MLSS* (g·L^{-1}); (B) *J* (% J_C); (C) *SRT* (days); and (D) *SGD* (m^3·m^{-2}·h^{-1}).

As one proposed approach to identify an optimal design, Figure 8.6 benchmarks the ratio of €·tonne-CO_2 saved^{-1} for the WWTP against the Spanish emissions trading system across the feasible range of *J* values (for this analysis, *SGD* = 0.30 m^3·m^{-2}·h^{-1} and *MLSS* = 25 g·L^{-1}). Across the bulk of the design space where trade-offs exist, the cost of mitigating carbon emissions at the WWTP was drastically higher than the market-based benchmark, with costs of up to 30,000 €·tonne-CO_2 saved^{-1} at the treatment plant. In this particular case, therefore, treatment plants seeking to lower their carbon footprint beyond leveraging synergies with cost may achieve a more meaningful environmental benefit at much less cost if they were to purchase credits on the trading market (if such an action is possible). In the future, however, this QSD framework may provide additional support for the creation of carbon crediting systems for the wastewater sector (proposed by Wang *et al*. [8.25] in the context of reducing nitrogenous greenhouse gas emissions); such a transition could enable utilities to take a more proactive posture and secure additional financial resources for the installation of low-energy and energy positive treatment technologies.

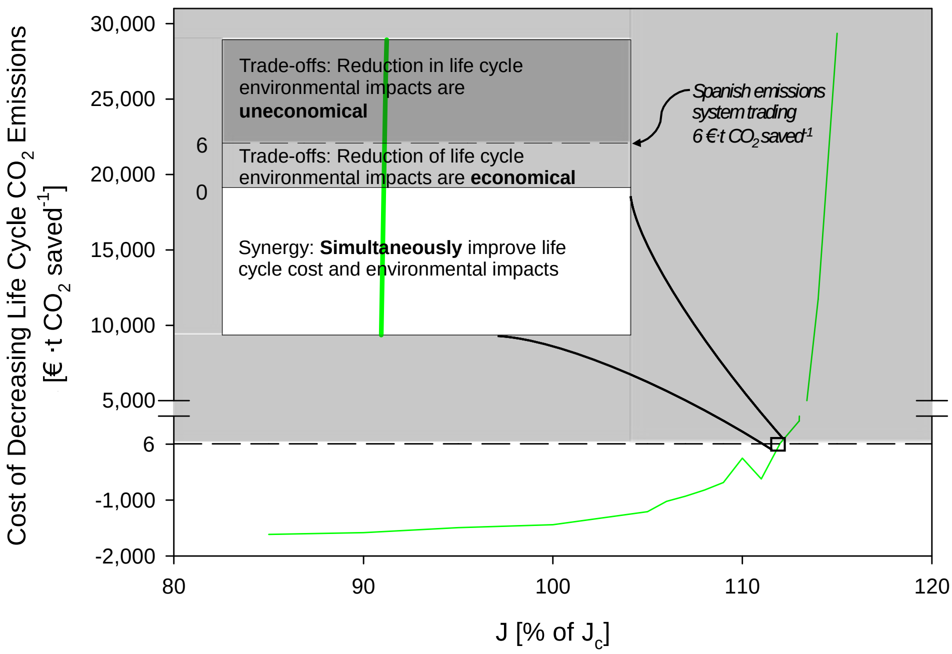

Figure 8.6 Evaluation of the ratio of €·tonne-CO_2 saved^{-1} in the selection *J* values (when *SGD* = 0.30 $m^3 \cdot m^{-2} \cdot h^{-1}$ and *MLSS* = 25 $g \cdot L^{-1}$) and comparison with the Spanish emissions trading system (6 €·t CO_2^{-1}) as a benchmark.

8.3.3 Optimization of Submerged AnMBR

We propose that the optimization of AnMBR design should minimize costs subject to effluent water quality constraints, and only consider further reducing greenhouse gas emissions when (i) there are no readily available, less expensive alternatives for greenhouse gases (GHG) reduction, and (ii) it is part of a transparent, inclusive planning and design process that addresses locality-specific factors in decision-making [8.15; 8.21]. For the submerged AnMBR system evaluated here, costs and GHG emissions were largely in synergy (reducing one reduced the other), and design conditions that resulted in trade-offs between costs and GWP_{100} had incurred costs for CO_2 mitigation that far exceeded the European Union Emission Trading Scheme (except for a very narrow band in which carbon could be offset at an expense to the utility of < 6 €·tonne-CO_2 saved^{-1}). Thus, the optimization of the submerged AnMBR system (detailed below) focused on cost minimization, with all potential designs subject to year-round treatment requirements with treatment efficacy confirmed through DESASS modeling under summer and winter conditions. It should be noted that this methodology leveraged pilot-scale experimental data for the design and simulation of a full-scale treatment process, and that additional scale-up challenges – although outside the scope of this study – may influence system sustainability.

8.3.3.1 Optimizing the Construction of the Submerged AnMBR System

Capital costs represented a meaningful fraction of life cycle costs across the full range of AnMBR design alternatives (with typical values of 45 ± 8%; average ± standard deviation), whereas life cycle environmental impacts were largely dominated by the O&M phase (e.g., 74 ± 14% for GWP_{100} when total methane is recovered, 99% if methane is released as fugitive emissions). Following the approach to optimization outlined immediately above (Section 8.3.3), the anaerobic reactor and membrane area were sized by selecting the configuration (based on 10,800 evaluated combinations of MLSS, SRT, r, J, and SGD) that resulted in the minimum LCC while enabling the plant to meet treatment requirements across all simulated temperatures (from 15 ºC to 30 ºC). In this respect, winter conditions (15 ºC) governed the sizing of the constructed system. *J* was set slightly above the critical flux (105% of J_C, based on the least favorable *SGD* and *MLSS* values), *r* was set to 3 and the anaerobic reactor volume was set in 35,190 m^3. By selecting the minimum cost values for these parameters as opposed to the minimum or maximum (17,800 m^3 or 373,440 m^3 for volume, 80% or 120% for *J*, and 0.5 or 8 for *r*, respectively), the overall LCC reduced by 35/70% (minimum/maximum) for volume, 17/47% for *J*, and 22/4% for *r*. When considering the LCA, there was no obvious benefit to selecting the optimum values for construction-phase elements because their impact on the life cycle environmental impacts was minimal.

8.3.3.2 Optimizing the Operating Submerged AnMBR

In the O&M phase, an operational volume (calculated from *r* and required to be below the constructed volume), an operational membrane area (calculated from the operating *J* for each *SGD* and *MLSS* value at a flux of 105% J_C, and required to be smaller than constructed area), and an operating *r* value (at or below the constructed *r* capacity) have been considered for the full range of feasible design alternatives in order to assess the overall LCC and LCA results for the AnMBR system. Further details on the interactions among the detailed design calculations with decision variables can be found in Ferrer *et al.* [8.13]. Based on economic and environmental criteria, the optimum operating parameters of the AnMBR design (*MLSS*, *r*, *SRT*, *SGD*, and *J*) were determined at different temperatures (see Table 8.1). Details of the mechanisms governing the selection of individual parameters is discussed in more detail in Section 8.3.4.

Table 8.1 Optimum operating parameters at different ambient temperatures of the AnMBR design and total cost.

Optimum Operational Parameters							Scenarios for Sludge Disposal			Scenarios for Methane Recovery	
T, ºC	MLSS, g·L^{-1}	SRT, days	r	SGD, m^3·m^{-2}·h^{-1}	J, % of J_C (in LMH)	Total cost†, €·m^{-3}	Land application‡, €·m^{-3}	Incineration‡, €·m^{-3}	Landfilling‡, €·m^{-3}	Biogas recovery*, €·m^{-3}	Total CH_4 recovery*, €·m^{-3}
15	15	41	3	0.10	105 (16)	0.130	0.001	0.049	0.006	- 0.021	- 0.005
20	15	28	2.5	0.10	105 (16)	0.125	0.001	0.049	0.006	- 0.022	- 0.004
25	10	19	2.5	0.10	105 (23)	0.094	0.001	0.049	0.006	- 0.024	- 0.004
30	10	13	2	0.10	105 (23)	0.079	0.001	0.050	0.006	- 0.026	- 0.002

† *Cost of the AnMBR system, excluding sludge disposal and methane recovery.*
‡ *Cost of sludge management and disposal assuming 100% of sludge is managed with a single method.*
* *Cost of 100% biogas or total methane (biogas and soluble methane) recovery (capital and operating cost of the technology are included). Negative values represent net profit.*

The uncertainty analysis was conducted on LCC and LCA results at 15 ºC (taking the scenario with the optimum operating parameters from Table 8.1), and an additional sensitivity analysis was performed to better understand the influence of individual assumptions. Based on the LCC considering fugitive methane emissions, the input parameters affecting the output were (in descending order): membrane cost, discount rate, energy for stirring and electricity cost. When methane was recovered, the microturbine efficiency became more important than the stirring energy and the electricity cost. Based on the LCA, when methane was not recovered, the only input parameter affecting the output was the percentage of dissolved methane emitted to air (where the balance of dissolved methane is assumed to be degraded to CO_2). When total methane recovery was considered, the efficiency of the microturbine became the most important (approximately 50%), followed by transportation distance (35%), and stirring energy (15%). The results showed that although there was uncertainty surrounding model outputs (Figure S.8.2), alternative values for these assumed parameters would not have changed the observed trends and narrative surrounding the sustainable design of submerged AnMBR.

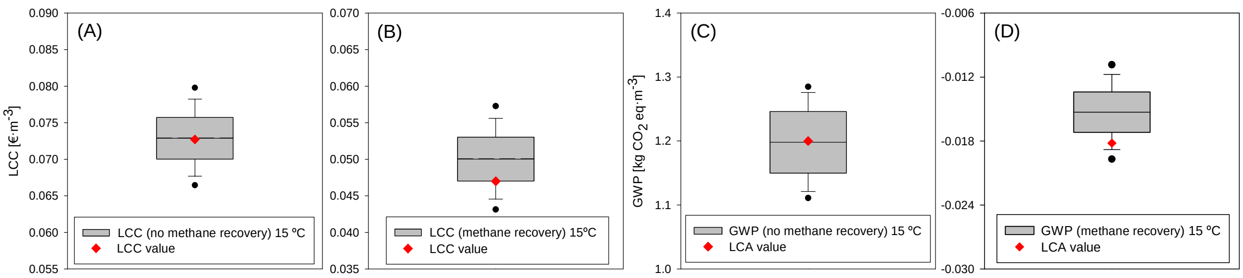

Figure S.8.2 Uncertainty analysis of the AnMBR design: LCC results (€·m^{-3}) with (A) fugitive methane emissions and (B) total methane recovery and use for electricity; and GWP results (kg CO_2·m^{-3}) with (C) fugitive methane emissions and (D) total methane recovery and use for electricity. The scenario with the minimum cost value at 15ºC was selected in order to assess uncertainty through LCC and LCA.

8.3.4 Connecting Design and Operational Decisions to Sustainability Metrics

8.3.4.1 The Impact of SGD and MLSS on Membrane Filtration

In order to better understand the mechanisms governing the impact of *SGD* and *MLSS* on LCA and LCC results, these values were varied across the decision space at a temperature of 15 ˚C. Other parameters corresponding to biological processes (i.e., *r* and *SRT*) were fixed at 3 and 41 days, respectively. Total methane recovery, nutrient recovery from effluent, and agricultural application of sludge were considered for the discrete decisions. Based on the LCC results, gas sparging was the most significant process at high *MLSS* and *SGD*, contributing nearly 62% of the total operating cost. However, reagent consumption had an increased impact when operating at high *MLSS* and low *SGD* values – representing up to 41% of the total operating cost – due to the increased membrane cleaning requirement.

When *MLSS* was held constant, *SGD* had a positive correlation with filtration costs, increasing the filtration operating cost by up to 0.063 $€\cdot m^{-3}$ (representing a 19% increase), but had no effect on biological costs. Similarly at a given *SGD* value, increasing *MLSS* increased filtration costs, but it also decreased costs associated with biological processes. Based on this, the optimum parameters for this study were the optimum value for *SGD* (0.10 $m^3\cdot m^{-2}\cdot h^{-1}$) and *MLSS* = 10-15 $g\cdot L^{-1}$ (Table 8.1). This value was chosen for *MLSS* because at larger values, the increase in filtration costs was not offset by a decrease in biological costs. Similarly, lower *MLSS* values increased biological costs much more than the filtration costs decreased (up to 85% of the total operating costs).

Methane recovery was not affected by changes in *MLSS* and *SGD*. Based on the LCA results, reagent consumption did not have a significant environmental impact (GWP_{100} = 0.003 kg $CO_2\cdot m^{-3}$ and marine ecotoxicity = 0.428 kg 1,4-DB$\cdot m^{-3}$). Gas sparging presented the greatest environmental impact based on GWP at high *MLSS* and *SGD*, increasing GWP to 0.051 kg $CO_2\cdot m^{-3}$ and marine ecotoxicity to 21.479 kg 1,4-DB$\cdot m^{-3}$. Biological processes had a beneficial impact on reducing GWP_{100} because of the decreased emissions from methane and by enabling nutrient recovery, achieving values as low as -0.039 kg $CO_2\cdot m^{-3}$ for GWP_{100} and -19.0 kg 1,4-DB$\cdot m^{-3}$ for marine ecotoxicity.

8.3.4.2 The Impact of r and MLSS on the Bioprocess

To better understand the underlying relationships among *r*, *MLSS*, and LCA and LCC outputs, these values were varied across the decision space while *SGD* and *J* were fixed at their optimum values (0.10 $m^3\cdot m^{-2}\cdot h^{-1}$ and 105% of J_C, respectively). Based on the LCC results, mixer operation was the most significant cost – comprising up to 80% of the total operating cost of 0.11 $€\cdot m^{-3}$ – and was highest at low *MLSS* and *r* values. The sludge recycling pump accounted for a small fraction of the operating cost (approximately 8%).

At a given *MLSS* value, decreasing *r* increased the cost of biological processes; at lower *MLSS* values, this increase was even more pronounced, raising the biological operating cost up to 0.091 $€\cdot m^{-3}$ (representing a 48% increase). Conversely, the filtration process costs was not affected by *r*. When *r* was fixed, *MLSS* had a similar trend in terms of biological process cost, but filtration costs also decreased. Therefore, the lowest total cost occurred at *r* = 2-3 and *MLSS* = 10-15 $g\cdot L^{-1}$ (Table 8.1).

Changes in *r* and *MLSS* had no effect on methane recovery. Based on the LCA results, the sludge recycling pump contributed very little to overall environmental impact (i.e., increases in GWP_{100} by 0.002 kg $CO_2\cdot m^{-3}$ and marine ecotoxicity by 1.14 kg 1,4-DB$\cdot m^{-3}$). Mixer operation had a much greater impact overall. At low *MLSS* and *r* values, GWP_{100} increased by 0.077 kg $CO_2\cdot m^{-3}$ and marine ecotoxicity increased by 40 kg 1,4-DB$\cdot m^{-3}$. When considering methane and nutrient recovery, however, GWP_{100} decreased to -0.039 kg $CO_2\cdot m^{-3}$ and marine ecotoxicity to -17.9 kg 1,4-DB$\cdot m^{-3}$.

8.3.4.3 The Impact of SRT and T on the Bioprocess

For the LCA, the effects of sludge disposal (agriculture), methane production, and effluent discharge were also evaluated by varying *SRT* across temperatures (*T*). At high *SRT* and *T*, biogas production and nutrient solubility were large. Sludge disposal, stirring, and sludge recycle pumping all contributed significantly to marine ecotoxicity (up to 13.1 kg 1,4-DB$\cdot m^{-3}$ for sludge disposal, which corresponded with the lowest value of SRT and up to 10.6 kg 1,4-DB$\cdot m^{-3}$ for the latter two, which corresponded with the highest value of SRT). When neither nutrients nor methane are recovered, emitted methane represented almost 100% of the GWP (increasing it up to 1.61 kg $CO_2\cdot m^{-3}$) and discharged nutrients increased eutrophication up to 0.042 kg $PO_4^{-3}\cdot m^{-3}$. However, if nutrients, biogas, and soluble methane are all recovered, this system achieved carbon offsets through resource recovery (up to -0.059 kg $CO_2\cdot m^{-3}$ for methane recovery and up to -0.067 kg $CO_2\cdot m^{-3}$ for nutrient recovery) as well as reductions in marine ecotoxicity (up to -18.6 kg 1,4-DB$\cdot m^{-3}$ for methane recovery and up to -37.3 kg 1,4-DB$\cdot m^{-3}$ for nutrient recovery). In terms of eutrophication, a reduction of around 50% can be achieved as a result of recovering nutrients in the effluent.

8.3.4.4 Energy, Nutrient, and Residuals Management

Regarding methane recovery, three options were considered: no recovery, only recovering biogas, or total methane recovery (recovery of both biogas and methane dissolved in the effluent). The LCC results show that cost savings of up to 16 and 36% (at 15 ˚C and 30 ˚C, respectively) are possible. By accounting for the energy offsets through on-site production, greenhouse gas savings up to 76-104% (at 15˚C and 30˚C, respectively) can be achieved. These calculations were made assuming methane in both biogas and effluent streams were recovered and utilized for energy generation. The total cost of the technologies needed for these processes (degassing membrane for dissolved methane and microturbine-based CHP for energy generation) were also considered. Based on this analysis, there may exist submerged AnMBR design/operational scenarios that have the potential to generate energy in excess of what is required to run the AnMBR system, making them net energy positive.

The framework in this study examined whether or not treated effluent is used for fertigation (i.e., irrigation with nutrient-rich water) to offset fertilizer needs. Note that calculations of fertilizer offsets from fertigation included assumptions of nitrogen and phosphorus bioavailability (50% and 70%, respectively), consistent with other studies [8.16; 8.26; 8.27; 8.28]. Based on the LCA data, nutrient recovery reduced eutrophication by approximately 50% and significantly reduced marine toxicity (around -37 kg 1,4-DB·m^{-3}), GWP (-0.07 kg CO_2·m^{-3}) and AD (-0.0005 kg Sb eq) due to the fertilizer avoided. For sludge disposal, three options were considered in this study: agricultural application, incineration, or landfilling. Based on the LCC results, there were savings of 50% or 90% using agricultural application over landfilling or incineration, respectively. Based on the LCA results, incineration could be a better option over agriculture in terms of GWP_{100} and eutrophication, because while agricultural application offsets fertilizer use, it still results in direct emissions to air (e.g., N_2O, NH_3), water (e.g., PO_4), and soil (heavy metals). Although the approach used to estimate emissions from land application and fertilizer offsets were consistent with other studies [8.16; 8.26; 8.27; 8.28], this approach does not account for direct fugitive emissions to air and water that stem from synthetic fertilizers. The negative consequences of land application in terms of GWP_{100} and eutrophication, therefore, would be reduced if direct emissions from synthetic fertilizers were included in the system boundary, since a portion of these emissions would be offset. Beyond GHG and nutrient emissions, agriculture also had the fewest negative impacts in AD and marine toxicity.

8.4 The Role of AnMBR in Carbon Neutral Wastewater Treatment

The main challenge of AnMBR technology is optimizing design and operation of the process in order to improve the sustainability of the technology to treat wastewaters. The AnMBR system may be suitable to treat most municipal wastewater streams, since it can achieve high quality effluent [8.9; 8.29] while also achieving meaningful steps toward sustainable wastewater treatment: lower inherent energy demand stemming from no aeration and energy recovery through methane production. Although conventional activated sludge treatment plants consume roughly 0.2-0.6 $kWh{\cdot}m^{-3}$ [8.2; 8.30; 8.31], a sub-set of design scenarios here achieved on-site energy production in excess of estimated on-site energy demands. However, consistent with findings from other energy assessments of AnMBRs [8.7; 8.8; 8.32], sparging remains a critical challenge as it accounts for the majority of AnMBR energy demand (with typical values of 52 ± 21%; average ± standard deviation), in this study). Fouling mitigation (during operation) and membrane capital costs – as well as anaerobic reactor construction and mixing – remain the dominant sources of costs, which are critical challenges to enable AnMBR to overtake activated sludge in practice [8.13; 8.33]. Additionally, maximizing the capture of methane is another key component of AnMBR technology for achieving energy savings and reducing the overall WWTP carbon footprint in a way that is financially viable. Particularly in this study, greenhouse gas savings up to 76-104% (at ambient temperature of 15 ˚C and 30 ˚C, respectively) were achieved by accounting for energy offsets through on-site production when methane (from both biogas and effluent streams) is captured and utilized for energy generation.

As we pursue improved designs of submerged AnMBR systems, the greatest opportunities for simultaneously improving economic and environmental performance will be through reduced energy consumption. Based on the QSD results presented here, it is also worth highlighting the importance of (i) reducing energy-intensive sparging, (ii) increasing flux to decrease required membrane area, and (iii) developing efficient dissolved methane recovery processes in order to maximize energy recovery and avoid direct greenhouse gas emissions. In any case, these pursuits to reduce life cycle environmental impacts should not jeopardize effluent quality – the primary responsibility of WWTPs. The high quality effluent provided by AnMBRs is one of the technology’s greatest strengths. The membranes help ensure robust treatment and can enable safe nutrient recovery through fertigation, the latter of which can have significant economic and environmental benefits through fertilizer and freshwater offsets.

8.5 Conclusions

A quantitative sustainable design process has been leveraged to develop a detailed design of submerged AnMBR by evaluating the full range of feasible design alternatives using technological, environmental, and economic criteria. Results showed that *J, SGD, MLSS,* and *r* required the navigation of sustainability trade-offs, but minimizing *SRT* simultaneously improved environmental/economic performance. Moreover, *MLSS* and *J* had the strongest influence over LCA results and capital costs, with *J* governing O&M costs. Based on this analysis, there are design and operational conditions under which submerged AnMBRs could be net energy positive at higher operating temperatures and contribute to the pursuit of carbon negative wastewater treatment. More broadly, this work demonstrates the use of QSD, which can be leveraged to quantify and navigate sustainability trade-offs in the optimization of wastewater treatment and resource recovery systems.

8.6 Acknowledgements

This research work was possible thanks to projects CTM2011-28595-C02-01/02 (funded by the Spanish Ministry of Economy and Competitiveness jointly with the European Regional Development Fund and Generalitat Valenciana GVA-ACOMP2013/203), by the European Regional Development Fund (ERDF), and by the King Abdullah University of Science and Technology (KAUST) Academic Partnership Program (UIeRA 2012-06291), which are gratefully acknowledged. The authors would like also to acknowledge the Jack Kent Cooke Foundation for partial funding for B.D. Shoener.

8.7 References

8.1 USEPA, Wastewater Management Fact Sheet: Energy Conservation, Office of Water, 2006.

8.2 J. Judd, C. Judd, Principles and Applications of Membrane Bioreactors in Water and Wastewater Treatment. Second Edition, Elsevier, London, UK, 2011.

8.3 J.B. Giménez, A. Robles, L. Carretero, F. Durán, M.V. Ruano, M.N. Gatti, J. Ribes, J. Ferrer, A. Seco, Experimental study of the anaerobic urban wastewater treatment in a submerged hollow-fibre membrane bioreactor at pilot scale. Bioresour.Technol. 102 (2011) 8799–8806.

8.4 A. Robles, M.V. Ruano, F. García-Usach, J. Ferrer, Sub-critical filtration conditions of commercial hollow-fibre membranes in a submerged anaerobic MBR (HF-SAnMBR) system: The effect of gas sparging intensity. Bioresour. Technol. 114 (2012) 247–254.

8.5 L. Raskin, Anaerobic Membrane Bioreactors for Sustainable Wastewater Treatment. WERF Report U4R08, June 2012.

8.6 A. L. Smith, S. J. Skerlos, L. Raskin, Psychrophilic anaerobic membrane bioreactor treatment of domestic wastewater. Water Res. 47 (2013), 1655-1665.

8.7 B.D. Shoener, I.M. Bradley, R.D. Cusick, J.S. Guest, J.S, Energy positive domestic wastewater treatment: the roles of anaerobic and phototrophic technologies. Environmental Science: Processes & Impacts 16 (2014), 1204-1222.

8.8 A. L. Smith, L. B Stadler, L. Cao, N.G. Love, L. Raskin, S. J Skerlos, Navigating Wastewater Energy Recovery 1 Strategies: A Life Cycle Comparison of Anaerobic Membrane Bioreactor and Conventional Treatment Systems with Anaerobic Digestion. Environ. Sci. Technol. 48 (2014), 5972-5981.

8.9 A.L. Smith, L.B. Stadler, N.G. Love, S.J. Skerlos, L. Raskin, Perspectives on anaerobic membrane bioreactor treatment of domestic wastewater: A critical review. Bioresour. Technology 122 (2012), 149-159.

8.10 J. Ferrer, A. Seco, J. Serralta, J. Ribes, J. Manga, E. Asensi, JJ. Morenilla, F. Llavador, DESASS: A software tool for designing, simulating and optimising WWTPs. Environ. Modell. Softw. 23 (2008), 19-26.

8.11 R. Barat, J. Serralta, M.V. Ruano, E. Jiménez, J. Ribes, A. Seco, J. Ferrer, Biological Nutrient Removal Model Nº 2 (BNRM2): A general model for Wastewater Treatment Plants. Water Sci.Technol. 67 (2013), 1481-1489.

8.12 F. Durán, Mathematical modelling of the anaerobic urban wastewater treatment including sulphate-reducing bacteria. Application to an anaerobic membrane bioreactor (Modelación matemática del tratamiento anaerobio de aguas residuales urbanas incluyendo las bacterias sulfatorreductoras. Aplicación a un biorreactor anaerobio de membranas). Ph.D. thesis. Dept. of Hydraulic Engineering and Environment. Universitat Politècnica de València, Spain, 2013.

8.13 J. Ferrer, R. Pretel, F. Durán, J.B. Giménez, A. Robles, M.V. Ruano, J. Serralta, J. Ribes, A. Seco, Design methodology for anaerobic membrane bioreactors (AnMBR): A case study. Sep. Purif. Technol. 141 (2015), 378-386.

8.14 R. Pretel, A. Robles, M.V. Ruano, A. Seco, J. Ferrer, Filtration process cost in anaerobic membrane bioreactors (AnMBRs) for urban wastewater treatment. Sent to Sep. Sci. Technol.

8.15 J.S. Guest, S.J. Skerlos, J.L. Barnard, M.B. Beck, G.T. Daigger, H. Hilger, S.J. Jackson, K. Karvazy, L. Kelly, L. Macpherson, J.R. Mihelcic, A. Pramanik, L. Raskin, M.C.M. Van Loosdrecht, D. Yeh, N.G. Love, A New Planning and Design Paradigm to Achieve Sustainable Resource Recovery from Wastewater. Environmental Science & Technology 43(2009), 6126–6130.

8.16 R. Pretel, A. Robles, M.V. Ruano, A. Seco, J. Ferrer, Environmental impact of submerged anaerobic MBR (AnMBR) technology used to treat urban wastewater at different temperatures. Bioresour. Technol. 149 (2013), 532 – 540.

8.17 ISOInternational Organization for Standardization (ISO) 14040: Environmental Management - Life Cycle Assessment--Principles and Framework (Geneva), 2006.

8.18 L. Corominas, J. Foley, J.S. Guest, A. Hospido, H.F. Larsen, S. Morera, A. Shaw, Life cycle assessment applied to wastewater treatment: State of the art. Water Res. 47 (2013), 5480-5495.

8.19 J. Hobson, CH_4 and N_2O emissions from wastewater handling. In: Good practice guidance and uncertainty management in National Greenhouse Gas Inventories. Geneve, Switzerland: Intergovernmental Panel on Climate Change (IPCC) Publications, 2000.

8.20 A. Saltelli, S. Tarantola, F. Campolongo, M. Ratto, M, Sensitivity Analysis in Practice: a Guide to Assessing Scientific Models. p 219, John Wiley & Sons Ltd, West Sussex, England, 2004.

8.21 J.S. Guest, S.J. Skerlos, G.T. Daigger, J.R.E. Corbett, N.G. Love, N. G, The use of qualitative system dynamics to identify sustainability characteristics of decentralized wastewater management alternatives. Water Science and Technology 61(2010), 1637.

8.22 R.N. Stavins, Chapter 9 Experience with market-based environmental policy instruments. In *Handbook of Environmental Economics*; Karl-Göran Mäler and Jeffrey R. Vincent, Ed.; Environmental Degradation and Institutional Responses; Elsevier, 2003; Vol. Volume 1, pp. 355–435.

8.23 EU. The EU Emissions Trading System (EU ETS), 2013.

8.24 REE, Spanish Electrical System. La Red Eléctrica de España, Alcobendas, Madrid, 2012.

8.25 J.S. Wang, S.P. Hamburg, D.E. Pryor, K. Chandran, G.T. Daigger. Emissions credits: Opportunity to promote integrated nitrogen management in the wastewater sector. Environmental Science & Technology, 45(2011), 6239–6246.

8.26 A. Gallego, A. Hospido, M.T. Moreira, G. Feijoo, Environmental performance of wastewater treatment plants for small populations. Resour, Conser. Recy. 52 (2008), 931-940.

8.27 G. Rodriguez-Garcia, M. Molinos-Senante, A. Hospido, F. Hernández-Sancho, M.T. Moreira, G. Feijoo, Environmental and economic profile of six typologies of wastewater treatment plants. Water Res. 45 (2011), 5997-6010.

8.28 M. Garrido-Baserba, A. Hospido, R. Reif, M. Molinos-Senante, J. Comas, M. Poch, Including the environmental criteria when selecting a wastewater treatment plant. Environ. Modell. Softw. (2013) 1-9.

8.29 H. Lin, W. Peng, M. Zhang, J. Chen, H. Huachang, Y. Zhang, A review on anaerobic membrane bioreactors: Applications, membrane fouling and future perspectives, Desalination 314 (2013) 169–188.

8.30 P.L. McCarty, J. Bae, J. Kim, Domestic wastewater treatment as a net energy producer–can this be achieved? Environ. Sci. Technol. 45 (2011) 7100–7106.

8.31 A. Fenu, J. Roels, T. Wambecq, K. De Gussem, C. Thoeye, G. De Gueldre, B. Vand De Steene, Energy audit of a full scale MBR system, Desalination 262 (2010) 121–128.

8.32 I. Martin Garcia, M. Mokosch, A. Soares, M. Pidou, B. Jefferson, Impact on reactor configuration on the performance of anaerobic MBRs: Treatment of settled sewage in temperate climates. Water Res. 47 (2013) 4853–4860.

8.33 H. Lin, J. Chen, F. Wang, L. Ding, H.Hong Feasibility evaluation of submerged anaerobic membrane bioreactor for municipal secondary wastewater treatment. Desalination 280 (2011), 120–126.

8.34 Bank BEDEC - ITeC database, 2013. In *Construmatica,* available on: http://www.construmatica.com/bedec. (Accessed February 1, 2013).

8.35 Iberdrola S.A, Spanish electricity tariff (Tarifa eléctrica España). In Iberdrola. Available on. https://www.iberdrola.es/clientes/empresas/info/mercado-energetico (Accessed February 1, 2013).

8.36 J.A. Sainz-Lastre, Technologies for sustainability. Processes and unit operations in wastewater treatment (Tecnologías para la sostenibilidad. Procesos y operaciones unitarias en depuración de aguas residuales). Colección EOI Medio Ambiente. Madrid, Spain, 2005.

8.37 Miliarium Aureum, S.L, Approximate cost of WWTP (Coste estimativo EDAR). *In Miliarium.com- Ingeniería Civil y Medio Ambiente.* Available on: http://www.miliarium.com/Proyectos/Depuradoras/introduccion/edar.asp. (Acceded April 20, 2013)

8.38 Bombas Ideal S.A, Distribution Catalogue (Catálogo Distribución). In Bombas Ideal. Available on: http://www.bombas-ideal.com/pdf/CAT%20C9%20ES%20%5BD-100512%5D.pdf. (Accessed April 20, 2013).

8.39 EPAEnvironmental Protection Agency. Combined Heat and Power Partnership, Agency of the United States federal government, 2012.

8.40 MAGRAMA, Official website of the Ministry of Agriculture, Food and Environment. Spanish government, Madrid. Survey land prices 2012. Available on: http://www.magrama.gob.es/es/estadistica/temas/estadisticas-agrarias/Encuesta_Precios_Tierra_2012_tcm7-298705.pdf. (Accessed May 5, 2014).

CHAPTER 9:

Economic and environmental sustainability of submerged anaerobic MBR-based (AnMBR-based) technology as compared to aerobic-based technologies for moderate-/high-loaded urban wastewater treatment

Abstract

The objective of this study was to assess the economic and environmental sustainability of submerged anaerobic membrane bioreactors (AnMBRs) in comparison with aerobic-based technologies for moderate-/high-loaded urban wastewater (UWW) treatment. To this aim, steady-state performance modelling, life cycle analysis (LCA) and life cycle costing (LCC) approaches have been integrated. Specifically, AnMBR (coupled to an aerobic-based post-treatment) was compared to aerobic membrane bioreactor (AeMBR), conventional activated sludge (CAS) and extended aeration activated sludge (EAAS). This study focussed on the removal of organic matter, nitrogen and phosphorus at ambient temperature of 20 °C when using the influent to a full-scale urban WWTP located in Valencia (Spain). The results showed that AnMBR coupled to an aerobic-based post-treatment (especially CAS-based) may be a promising sustainable technology for moderate-/high-loaded UWW treatment in comparison with the rest of evaluated systems. Significant reductions in energy consumption (minimum value of 0.04 kWh per m^3), LCC (minimum value of approx. €0.135 per m^3) and LCA (reductions in environmental impacts of up to 72, 66, 44 and 37% in abiotic depletion, GWP, acidification and marine aquatic ecotoxicity, respectively) could be achieved in AnMBR-based UWW treatment schemes.

Keywords

Global warming potential (GWP); life cycle analysis (LCA); life cycle costing (LCC); steady-state performance modelling; submerged anaerobic MBR (AnMBR).

Highlights

LCC and LCA of an AnMBR were compared to aerobic-based technologies for UWW at 20 °C.
AnMBR was coupled to an aerobic-based post-treatment for nutrient removal: CAS/AeMBR.
The minimum energy consumption in AnMBR resulted in 0.04 kWh per m^3.
Significant reductions in LCC (€0.135 per m^3) were achieved in AnMBR.
Significant environmental impact reductions (e.g. 66% in GWP) were achieved in AnMBR.

R. Pretel, A. Robles, M.V. Ruano, A.Seco, J. Ferrer
Economic and environmental sustainability of submerged anaerobic MBR (AnMBR) compared to aerobic-based technologies for moderate-/high-loaded urban wastewater treatment
J. Environ Manage (2015)

9.1 Introduction

Nowadays, meeting requirements in urban wastewater (UWW) treatment (e.g. restrictions in effluent standards, treatment costs and spatial constraints) might involve alternative technologies rather than traditional ones (i.e. conventional activated sludge (CAS) and extended aeration activated sludge (EAAS)) [9.1]. Recent technological advance in wastewater treatment includes membranes, in particular aerobic membrane bioreactors (AeMBR), which offers several advantages over traditional processes: high effluent quality, small footprint and reduced sludge production [9.2]. However, although the MBR market has recently risen, the competitiveness of this technology is threatened by the low operating cost of CAS systems [9.3]. On the other hand, current UWW treatment is mainly based on aerobic processes (i.e. CAS, EAAS and AeMBR), where significant energy input is required for aeration and energy recovery from organic matter is not maximised [9.4; 9.5].

Submerged anaerobic membrane bioreactor (AnMBR) technology for UWW treatment reduces sludge production, eliminates aeration and generates methane [9.6; 9.7; 9.8]. Hence, although AnMBR technology has not been applied to full-scale UWW treatment yet, recent literature (e.g. [9.9; 9.7; 9.10; 9.11; 9.5]) has reported increasing interest by the scientific community on its applicability.

Anaerobic processes are often operated at high temperatures in order to increase microorganism growth rate. Nevertheless, the feasibility of AnMBRs for treating UWW at lower temperatures (e.g. 15-20 °C) has been recently proven [9.6; 9.7; 9.12]. However, the lower the temperature the higher the amount of produced methane that is dissolved in the effluent [9.13]. In this respect, the possible emission of this dissolved methane to the atmosphere is one key issue in AnMBR technology. On the other hand, nutrient removal in AnMBR technology is minimal [9.14]. Thus, when downstream treatment or alternative water reuse application (agriculture irrigation) are not considered, the discharge of the nutrient-loaded AnMBR effluent may cause considerable environmental impacts. Hence, one key concern for sustainable UWW treatment using AnMBR technology is recovering the nutrients and methane from the effluent [9.5].

Mathematical models capable of predicting system performance under different design and operating scenarios might be useful tools for AnMBR development. Ferrer *et al.* [9.15] proposed a computational software called DESASS for modelling different aerobic and anaerobic wastewater treatment technologies. This software was later updated for including AnMBR. The updated-version of this software incorporates the plant-wide mathematical model BNRM2 [9.16].

On the other hand, Ferrer *et al.* [9.17] and Pretel *et al.* [9.18] established the basis of an economic framework (based on semi industrial-scale data and modelling) aimed at designing AnMBRs for full-scale UWW treatment by considering the key parameters affecting process performance. However, the selection of appropriate schemes for UWW treatment may consider not only economic items (i.e. investment, operation and maintenance) but also environmental concerns (e.g. eutrophication, global warming potential (GWP), marine ecotoxicity…). In this respect, life cycle analysis (LCA) and life cycle costing (LCC) approaches have become useful tools for assessing the sustainability of different UWW treatment schemes (see e.g. [9.19 ; 9.20; 9.21; 9.22; 9.23]). Indeed, in compliance with Corominas *et al.* [9.24], several studies have been published dealing with LCA applied to wastewater treatment. Nevertheless, LCC and LCA applied to AnMBR for UWW treatment must be further evaluated and compared to the results from other wastewater treatment systems. Pretel *et al.* [9.25], for instance, assessed the energy balance and LCA of an AnMBR system featuring industrial-scale membranes that treated UWW at different temperatures; whilst Pretel *et al.* [9.26] characterised the environmental impacts of design and operational decisions on AnMBR technology, as well as the resulting trade-offs across LCC and LCA frameworks.

The sustainability of AnMBR has been recently evaluated relative to alternative aerobic technologies [9.5]. However, no references have been found assessing the sustainability of AnMBR coupled to downstream processes for nutrient removal in comparison with conventional treatment schemes. In this respect, the objective of this study was to assess the economic and environmental sustainability of a possible AnMBR-based urban WWTP by integrating steady-state performance modelling (using the simulating software DESASS), LCA and LCC approaches. To this aim, AnMBR has been compared to AeMBR, CAS and EAAS applied to the removal of organic matter, nitrogen and phosphorus from moderate-/high-loaded UWW.

9.2 Methodology

The economic and environmental sustainability of an AnMBR-based WWTP (including an aerobic-based post-treatment for nutrient removal) was compared to three UWW treatment schemes based on CAS, EAAS and AeMBR. All these treatment schemes were designed for meeting the European discharge quality standards (sensitive areas and population of more than 100000 p-e) as regards solids (<35 $mg \cdot L^{-1}$ of TSS), organic matter (<125 and 25 $mg \cdot L^{-1}$ of COD and BOD, respectively) and nutrients (<10 and 1 $mg \cdot L^{-1}$ of N and P, respectively). In addition, a maximum value of 35% of biodegradable volatile suspended solids (BVSS) was stablished as sludge stabilisation criteria. The study accounted for effluent disinfection either by filtration (in MBR-based systems) or ultraviolet (UV) radiation.

The four wastewater treatment systems (CAS, EAAS, AeMBR and AnMBR) were designed and simulated using the updated version of the simulation software DESASS [9.15], which features the mathematical model BNRM2 [9.16]. This mathematical model was previously calibrated and validated for a wide range of operating conditions in an AnMBR system featuring industrial-scale membranes [9.27]. DESASS enables the energy balance of several wastewater treatment schemes (including AnMBR systems) to be evaluated [9.25].

For CAS, EAAS and AeMBR, two different simulation scenarios were evaluated depending on the technology employed to reduce the phosphorus content in the influent: (1) chemical removal of phosphorus, or (2) combined biological and chemical removal of phosphorus. It is worth to point out that, for this case study, biological removal of phosphorus by itself was not enough for meeting phosphorus effluent standards. Therefore, biological and chemical removal of phosphorus were combined in scenario 2. For the AnMBR-based treatment scheme, only chemical removal of phosphorus was evaluated since the acetic acid content in the AnMBR effluent was not enough for biological removal of phosphorus in the downstream aerobic-based treatment unit.

The results obtained from the above-mentioned scenarios were also compared to the results obtained when only nitrogen removal was applied.

9.2.1 WWTP design and operation

The evaluated wastewater treatment systems (i.e. CAS, EAAS, AeMBR and AnMBR) were simulated at ambient temperature of 20 ºC. The treatment flow rate was set to 50000 $m^3 \cdot d^{-1}$. The full characterisation of the influent UWW used in this study is shown in Table 9.1a. This characterisation corresponds with the effluent from the pre-treatment of the Carraixet WWTP (Valencia, Spain). This moderate-/high-loaded UWW was the one used for obtaining the experimental data related to the AnMBR unit evaluated in this study. Table 9.1b shows the values of the main operating parameters established in CAS, EAAS, AeMBR and AnMBR.

Table 9.1 (a) Characteristics of the UWW entering the WWTP; **(b)** main operational parameter values in CAS, EASS, AeMBR and AnMBR units; and **(c)** main operational parameter values in CAS- and AeMBR-based post-treatment units. Nomenclature: **SRT**: Sludge retention time; **MLSS**: mixed liquor suspended solids concentration in the reaction volume; **J_{20}**: 20 ºC-standardised transmembrane flux; **$S(A/G)D_m$**: specific air/gas demand per m^2 of membrane area; **AD**: anaerobic digestion; **N.A**: not-applicable; **UV**: ultraviolet . * [9.2]; ** [9.18].

Parameter	**Unit**	**Value**
T-COD	mg COD $\cdot L^{-1}$	945
T-BOD	mg $COD \cdot L^{-1}$	715
VFA	mg $VFA \cdot L^{-1}$	45
TN	mg $N \cdot L^{-1}$	47
NH_4-N	mg $N \cdot L^{-1}$	16
TP	mg $P \cdot L^{-1}$	13
PO_4-P	mg $P \cdot L^{-1}$	4
SO_4-S	mg $S \cdot L^{-1}$	10
TSS	mg $TSS \cdot L^{-1}$	429
VNSS	mg $VNSS \cdot L^{-1}$	100
Alkalinity	mg $CaCO_3 \cdot L^{-1}$	350

(a)

Technology	**SRT (days)**	**MLSS (g/L)**	**J_{20} (LMH)**	**$S(A/G)D_m$ ($m^3 \cdot m^{-2} \cdot h^{-1}$)**	**Sludge stabilisation**	**Tertiary treatment**
CAS	10	2.3			AD	UV
EAAS	20	3.5			N.A.	UV
AeMBR	10	6.5	14 *	0.3 *	AD	N.A.
AnMBR	40	11	20 **	0.1 **	N.A.	N.A.

(b)

Post-treatment Technology	**SRT (days)**	**MLSS (g/L)**	**J_{20} (LMH)**	**$S(A/G)D_m$ ($m^3 \cdot m^{-2} \cdot h^{-1}$)**	**Tertiary treatment**
CAS	10	2.3			UV
AeMBR	10	2.6	29 *	0.3 *	N.A.

(c)

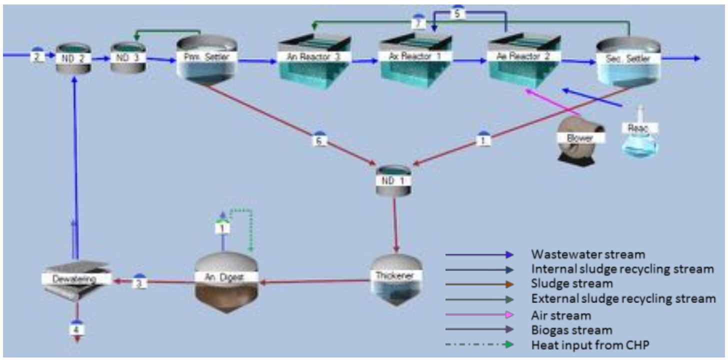

(a)

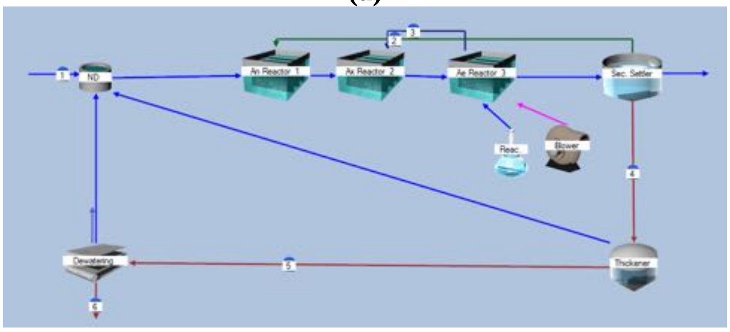

(b)

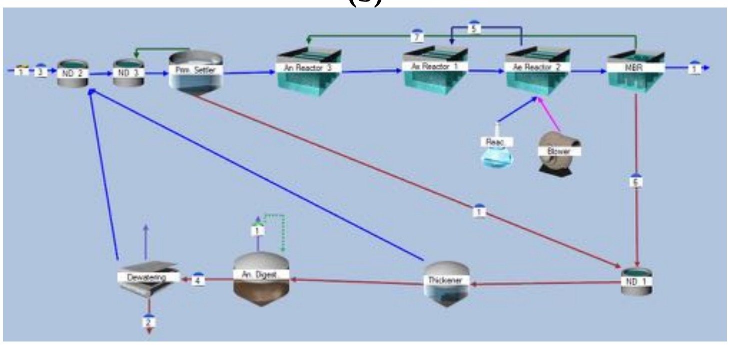

(c)

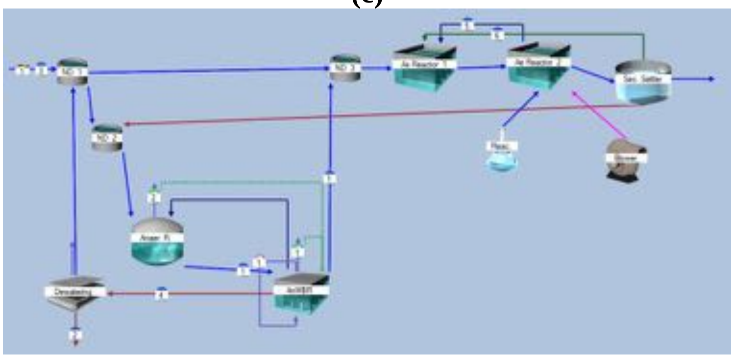

(d)

Figure 9.1 Process flow diagram of the proposed UWW treatment schemes designed in DESASS: **(a)** CAS, **(b)** EAAS, **(c)** AeMBR and **(d)** AnMBR + CAS. Nomenclature: **ND**: Chamber; **Prim. Settler:** Primary Settler; **Sec. Settler:** Secondary Settler; **An Reactor:** Anaerobic tank; **Ax Reactor:** Anoxic tank; **Ae Reactor:** Aerobic tank; **Reac.**: Reactant: (FeCl for P removal); **An. Digest.:** Anaerobic Digester; **MBR:** Membrane Bioreactor; **Anaer. R.**: Anaerobic Reactor; **AnMBR**: Anaerobic Membrane Bioreactor.

Figure 9.1 shows the process flow diagrams built in DESASS for the CAS, EAAS, AeMBR and AnMBR treatment schemes. The classical AO (anoxic – oxic) and A2O (anaerobic – anoxic – oxic) configurations were selected for designing the aerobic-based treatment units in scenarios 1 (chemical phosphorus removal) and 2 (biological and chemical phosphorus removal), respectively. The volume of anaerobic, anoxic and oxic tanks was defined as follows: 0, 40 and 60% of total reactor volume in scenario 1 and 40, 10 and 50% of total reactor volume in scenario 2, respectively. The ratio of nitrate being recycled into the influent flow was set to 4 times the influent flow.

As Figure 9.1 shows, CAS and AeMBR included an anaerobic digestion (AD) unit in order to meet the sludge stabilisation criteria.

In compliance with Judd and Judd [9.2], 2000 and 9000 ppm was adopted as the dose of sodium hypochlorite and citric acid, respectively, for membrane chemical cleaning in AeMBR units, whilst the chemical cleaning frequency was set to 12 months. On the other hand, tertiary treatment was not required in AeMBR since complete retention of the biomass was considered (i.e. membranes were considered tertiary treatment).

AnMBR technology

As Table 9.1b shows, the MLSS in the AnMBR membrane tank was established as 14 $g\cdot L^{-1}$. For this MLSS, the 20 ºC-standardised transmembrane flux (J_{20}) was set to 20 LMH, whilst the specific gas demand per square metre of membrane area (SGD_m) was set to 0.1 $m^3\cdot m^{-2}\cdot h^{-1}$. These J_{20} and SGD_m values were selected on the basis of previous experimental results obtained in an AnMBR system fitted with industrial-scale hollow-fibre membranes [9.28]. This MLSS-J_{20}-SGD_m combination corresponded to filtration conditions around the critical ones (J_{20} of around 105% of the experimentally-determined critical flux), since this operating mode resulted in minimum filtration costs in previous studies [9.18]. Nevertheless, a basic uncertainty analysis regarding SGD_m and J_{20} was carried out since AnMBR for full-scale UWW treatment is not a mature technology yet. Specifically, the effect of decreasing and increasing the operating SGD_m (0.05 and 0.30 $m^3\cdot m^{-2}\cdot h^{-1}$) and J_{20} (80 and 120% of the critical flux, corresponding with 15 and 22 LMH, respectively) was assessed and compared to the baseline evaluated in this study (SGD_m of 0.10 $m^3\cdot m^{-2}\cdot h^{-1}$ and J_{20} of 105% of the critical flux).

According to Judd and Judd [9.2] and previous experiments (see, for instance, [9.28]), 7.5 months was set in this study as the interval for membrane chemical cleaning when operating at J_{20} around 105% of critical flux. In compliance with the membrane manufacturer, 2000 ppm was adopted as the dose of both sodium hypochlorite and citric acid for cleaning the membranes chemically.

As Figure 9.1 shows, a post-treatment step based on AO (anoxic – oxic) configuration with addition of chemicals for phosphorus removal was included in the AnMBR-based treatment scheme in order to meet nutrient effluent standards. This step contemplated two possibilities: AeMBR-based post-treatment and CAS-based post-treatment. Table 9.1c illustrated the selected values for the main operating parameters in both configurations. The membrane cleaning protocol adopted for the AeMBR-based post-treatment was the same than the one proposed in AeMBR.

Two different scenarios were evaluated in the AnMBR-based treatment scheme depending on the fate of the methane dissolved in the effluent: (a) capture for energy production (using a degassing membrane for separation); and (b) use as organic matter source for denitrification in the corresponding post-treatment unit. A fraction of the influent wastewater was bypassed anyhow to the post-treatment unit in order to meet effluent quality standards (further organic matter was required for denitrification rather than the one contained in the AnMBR effluent). Specifically, around 27 and 16% of the wastewater entering the AnMBR-based WWTP was derived directly to the post-treatment unit when the dissolved methane was used for energy production and denitrification, respectively. Therefore, four different scenarios were considered in AnMBR depending on the fate of the methane dissolved in the effluent and the post-treatment considered: AnMBR+AeMBR and AnMBR+CAS when the dissolved methane was used for energy production, and AnMBR+AeMBR$_{CH4DN}$ and AnMBR+CAS$_{CH4DN}$ when the dissolved methane was used for denitrification.

Further digestion of the sludge was not required in AnMBR since this unit was already designed for meeting the sludge stabilisation criteria.

9.2.2 LCC implementation

The total annualised equivalent cost was calculated by adding the annual investment cost (considering a discount rate of 10% and a project lifetime of 20 years) to the annual operating and maintenance costs.

The investment cost included construction work using concrete (primary and secondary settler, anaerobic reactor, AO/A2O reactors, membrane tank, anaerobic digester, CIP (clean-in-place) tank, thickener, and equalisation tank); and equipment (pumping equipment (pumps and blowers), piping and valve system, aeration devices (diffusers) and their supports, air cleaning equipment, stirrers, rotofilter, dewatering system, ultrafiltration hollow-fibre membranes, circular suction scraper bridges for the primary and secondary settler and thickener, UV radiation system, combined heat and power (CHP), degassing membrane system and land needed). Construction work and equipment varied depending on the evaluated system (see Table 9.2).

Although a degassing membrane system was considered for completely recovering the methane dissolved in the effluent, it is important to note that degassing membrane is not a mature technology yet. In this respect, further development of efficient dissolved methane recovery technologies is needed in order to both maximise energy recovery and avoid direct greenhouse gas emissions.

The operating and maintenance costs consisted of: heat supply for maintaining a temperature of 35 ºC in the AD unit included in AeMBR and CAS; power energy requirements; energy recovery from methane capture (excluding EASS); chemical reagents used for membrane cleaning (in AnMBR and AeMBR); chemical reagents for diffusers cleaning; $FeCL_3$ dosage when applying chemical removal of phosphorus; and sludge handling and disposal, including dewatering system and polyelectrolyte consumption. Maintenance expenditure referred to replacement of pumps and blowers, stirrers, rotofilter, air diffusers for aeration system, and lamps for UV disinfection when necessary.

Table 9.3 shows the unit costs used to calculate the capital and operating expenses (CAPEX/OPEX) of the proposed treatment systems. Further details about the LCC methodology used in this study can be found in Ferrer *et al.* [9.17] and Pretel *et al.* [9.18].

9.2.3 LCA implementation

LCA methodology is subdivided into four stages [9.29]: (1) goals and scope of the study, where the definition of the activity, the purpose of the study, the functional unit, the system boundaries, and the employed methodology are established; (2) life cycle inventory (LCI), where the list of inputs (energy use and material sourcing) and outputs (emissions to atmosphere, water and soil) are determined; (3) life cycle impact assessment (LCIA), where the environmental impacts of the environmental resources and releases identified during the LCI are evaluated (comprising, among others, selection and definition of impact categories, classification, characterisation and normalisation); and (4) interpretation of results. The goal of this study was to evaluate the environmental impacts of different UWW treatment schemes associated to both water line operation (primary and secondary UWW treatment, and final discharge of the treated effluent) and sludge treatment (reduction of the organic matter content in the sludge to comply with the established stabilisation criteria). A functional unit based on the volume of treated wastewater (m^3) was used for the comparison of the different UWW treatment schemes.

Table 9.2 Factors affecting the investment cost of the proposed UWW treatment schemes (CAS, EAAS, AeMBR and AnMBR), including construction work and equipment

	CAS	EAAS	AeMBR	AnMBR+AeMBR	AnMBR+AeMBR$_{CH4DN}$	AnMBR+CAS	AnMBR+CAS$_{CH4DN}$
CONSTRUCTION							
Primary settler	V		V				
Secondary settler	V	V				V	V
Thickener	V	V	V				
Anaerobic reactor				V	V	V	V
Membrane tank			V	V	V	V	V
Anaerobic digester	V		V				
CIP (clean-in-place) tank			V	V	V	V	V
Equalisation tank			V	V	V	V	V
AO/A2O reactor	V	V	V	V	V	V	V
Land needed	V	V	V	V	V	V	V
EQUIPMENT							
Pumping equipment	V	V	V	V	V	V	V
Piping/valve system	V	V	V	V	V	V	V
Aeration devices (diffusers)	V	V	V	V	V	V	V
Air cleaning equipment	V	V	V	V	V	V	V
Stirrers	V	V	V	V	V	V	V
Rotofilter			V	V	V	V	V
Dewatering system	V	V	V	V	V	V	V
Ultrafiltration hollow-fibre membranes			V	V	V	V	V
Circular suction scraper bridges for primary settler	V		V				
Circular suction scraper bridges for secondary settler	V	V				V	V
Circular suction scraper bridges for thickener	V	V	V				
UV radiation system	V	V					
CHP system	V		V	V	V	V	V
Degassing membrane system				V		V	

Table 9.3 Unit costs used to evaluate capital and operating expenses (CAPEX/OPEX) in the proposed UWW treatment schemes.

Unit costs of capital and operating expenses		Reference
Steel pipe (depending on the Nominal Diameter (ND) and material: from ND 0.6m (cast iron) to ND 1.2m (concrete)), € per m	15/ 490	[9.32]
Concrete wall/slab, € per m	350/130	[9.32]
Ultrafiltration hollow-fibre membrane, (maximum chloride contact of 500,000 ppm·h cumulative), € per m^2	35	PURON®, Koch Membrane Systems
Energy, € per kWh	0.138	[9.33]
Sodium hypochlorite, (NaOCl Cl active 5% PRS-CODEX), € per L	11	Didaciencia S.A.
Citric acid (Citric acid 1-hidrate PRS-CODEX), € per kg	23.6	Didaciencia S.A.
Polyelectrolyte, € per kg	2.35	[9.34]
Iron (III) chloride, € per t	235	Quiminet S.L.
Wasted sludge for farming, € per t	4.8	[9.35]
Wasted sludge for landfill, € per t	30.1	[9.35]
Wasted sludge for incineration, € per t	250.0	e-REdING, 2014
Blower (ELEKTROR RD 84, Q_B= 5400 $m^3 \cdot h^{-1}$; Lifetime: 50000 hours), €	5900	Elektror S.A.
Sludge recycling pump (BR 600-3GXX/12.3 , Q_P= 600-3000 $m^3 \cdot h^{-1}$; Lifetime: 65000 hours), €	29000	[9.36]
Rotary Lobe pump (INOXPA, Q_P 140 $m^3 \cdot h^{-1}$)	25000	INOXPA, S.A
Submersible stirrer (AGS 400-3SHG/6.1; Lifetime: 100000 hours; 3.4 kW; anaerobic reactor=5$W \cdot m^{-3}$;anoxic reactor=15$W \cdot m^{-3}$), €	11699	[9.37]
Rotofilter (PAM 630/2000; pitch diameter=0.5mm; Q=320 $m^3 \cdot h^{-1}$; Lifetime: 87600 hours, 11.45 kW), €	7796	Procesos Auto-Mecanizados S.L
Circular suction scraper bridges (primary settler, 0.75 kW), €	246795	WWTP from Ibiza, Spain
Circular suction scraper bridges (secondary settler, 0.75 kW), €	60998	WWTP from Ibiza, Spain
Circular suction scraper bridges (thickener, 0.75 kW), €	12530	WWTP from Ibiza, Spain
Butterfly Valve (Bray 16”)	1102	[9.37]
Fine-bubble diffuser with removable 9” Membrane Disc Aeration Head (Flygt)	12	TFB-FLYGT, S.A
Dewatering system, centrifuge (55 $m^3 \cdot h^{-1}$;45 $kWh \cdot t^{-1}$ SS), €	265540	WWTP from Ibiza, Spain
UV radiation system, TrojanUV Solo Lamp 1000W, lifetime 15000 hours), €	435182	TrojanUVSigna
Microturbine-based CHP system (size: 30kW), capital cost, $/ kW and O&M cost, $/ kWh	2700/0.02	[9.38]
Degassing membrane, (flow rate=30$m^3 \cdot h^{-1}$;pressure drop= 60Kpa), Capital cost, €	7300	DIC Corporation
Land cost , $€ \cdot m^{-2}$	0.97	[9.39]

The LCA framework was implemented according to ISO 14040 (2006). The life cycle inventories (LCI) of individual materials and processes were compiled using the Ecoinvent Database v.3 accessed via SimaPro 8.03 (PRé Consultants; The Netherlands). The Centre of Environmental Science (CML) 2 baseline 2000 methodology was used to conduct the impact assessment. The impact categories considered in this study were: eutrophication (quantified as kg PO_4 eq.), global warming potential with a 100-year time horizon (GWP_{100}; quantified as kg CO_2 eq.), abiotic depletion (quantified as kg Sb eq.), marine aquatic ecotoxicity (quantified as kg 1,4-DB eq.), and acidification (quantified as kg SO_4 eq.).

System boundaries

The following system boundaries were considered in this study:

- Construction, operation and demolition phase (materials recycled or disposal to landfill), as well as the transport of materials, reagents and sludge (assuming a distance for transport of 10 km) were included within the system boundary. Nonetheless, structural concrete and pipes were excluded in the demolition phase because their useful life was greater than the lifetime of the project itself.
- A useful membrane lifetime of 20 years was assumed, according to the total chlorine contact specified by the manufacturer (see Table 9.3) and the established membrane chemical cleaning frequency.
- Pre-treatment processes (e.g. screening, degritting, and grease removal) were not included in this study because they were assumed to feature in all the evaluated systems.
- The fate of the wasted sludge was established as follows: 80% to fertilising purposes on farmland, 10% to incineration, and 10% to landfilling [9.30].
- CO_2 emissions resulting from sludge dewatering and biogas capture were not taken into account because CO_2 is classified as biogenic according to IPCC guidelines [9.31].
- Biogas and methane dissolved in the effluent stream were considered to be totally recovered and used for energy production. Thus, fugitive methane emissions into the atmosphere were not considered for evaluating climate implications. Therefore, the cost of both degassing membrane technology for dissolved methane recovering and microturbine-based CHP technology for energy generation were also considered.
- Emissions to air (e.g. CO, SO_2, NO_2, non-methane volatile organic compounds) resulting from biogas combustion (through microturbine-based CHP) were excluded due to a lack of information.

Table 9.4 shows the inventory data and the parameters used in the LCA study, including the Ecoinvent process and substances extracted from SimaPro 8.03. Six main factors were considered when determining the environmental performance of the evaluated treatment schemes: (1) energy consumption; (2) energy recovery from methane (biogas and dissolved methane capture); (3) consumption of chemical reagents ($FeCl_3$, polyelectrolyte, NaOCl and citric acid); (4) employment of construction materials (concrete, iron, chromium steel, polyester and epoxy resin, polypropylene, glass tube…); (5) final discharge of the effluent; and (6) sludge disposal taking into account its emissions.

9.3 Results and discussion

9.3.1 Energy balance results

Figure 9.2 illustrates the energy balance of CAS, EAAS, AeMBR and AnMBR (AnMBR+AeMBR, AnMBR+AeMBR$_{CH4DN}$, AnMBR+CAS, and AnMBR+CAS$_{CH4DN}$), including both power requirements and energy production.

As Figure 9.2 shows, power requirements for air pumping (organic matter removal and/or nitrification) accounted for the largest percentage of total power requirements (up to 49%) in all the proposed treatment schemes except in the ones incorporating an AeMBR unit. In these cases, membrane scouring by air sparging became the largest percentage of total power requirement (up to 46%). For the two scenarios including an AeMBR-based post-treatment unit (AnMBR+AeMBR and AnMBR+AeMBR$_{CH4DN}$), membrane scouring by air sparging and air pumping for nitrification presented both similar percentages (around 28 and 25%, respectively). EAAS and CAS presented considerable power requirements related to reactor stirring (around 44 and 29%, respectively). With regard to AnMBR schemes, all the proposed scenarios presented significant power requirements as regards membrane scouring by biogas sparging and anaerobic reactor stirring (both processes represented up to 19% of total power requirements).

In absolute terms, power requirements were high in AeMBR, with a value of 0.84 kWh·m^{-3} in scenario 1 (biological and chemical removal of phosphorus) and 0.81 kWh·m^{-3} in scenario 2 (chemical removal of phosphorus). It is important to highlight that this technology requires air for both membrane scouring and organic matter removal (air pumping). On the other hand, power requirements were low in AnMBR+CAS and AnMBR+CAS$_{CH4DN}$, with a value of 0.48 and 0.46 kWh·m^{-3}, respectively. These low values were the result of avoiding a secondary MBR-based process for nutrient removal (i.e. power for membrane scouring by air sparging was not required).

Table 9.4 Elements selected for the inventory of the proposed UWW treatment schemes. In brackets is included the Ecoinvent process extracted from SimaPro 8.03.

Construction Materials, kg·m^{-3}	Concrete *(Concrete, normal, at plant/CH S)* Iron & Chromium steel *(Cast iron, at plant/RER S & Chromium steel 18/8, at plant/RER S)* PP and polyester fibers and epoxy resine (*Polyester resin, unsaturated, at plant/RER S; Epoxy resin, liquid {GLO}| market for | Alloc Def, U; Polypropylene, granulate {GLO}| market for | Alloc Def, S)* UV Lamps *Glass tube, borosilicate {GLO}| market for | Alloc Def, S* Transport (*Lorry 3.5e7.5t EURO5*), t·km	
Energy consumption, Kwh·m^{-3} *(Electricity, low voltage {ES}| market for | Alloc Def, U*	Rotofilter Stirring of anaerobic digester & anaerobic reactor Stirring of AO/A2O reactors Air pumping Biogas pumping Permate pumping Rest of pumping system Circular suction scraper bridges (primary & secondary settler) Thickening and dewatering system UV radiation Heat requirement for anaerobic digester	
Energy avoided (energy recovery from methane), kWh·m^{-3} *(Electricity, low voltage {ES}| market for | Alloc Def, U*		
Reagent consumption, kg·m^{-3}	Polyelectrolyte *(Acrylonitrile from Sohio process, at plant/RER S)* NaOCl *(Sodium hypochlorite, 15% in H2O, at plant/RER S)* Citric acid *(Adipic acid, at plant/RER S)* $FeCL_3$ *(Iron (III) chloride, 40% in H2O, at plant/CH S)* Transport (*Lorry 3.5e7.5t EURO5*), t·km	
Discharge to water, kg·m^{-3}	Total nitrogen, Nt Total phosphorous, Pt Chemical oxygen demand, COD	
	Disposal to agriculture	Phosphate to river (PO^{3-}_4)
		Phosphate to groundwater (PO^{3-}_4)
	Biogenic methane, CH_4	
Discharge to air, kg·m^{-3}	Biogenic methane, CH_4	
	Disposal to agriculture	Ammonia to air (NH_3)
		Dinitrogen monoxide to air (N_20)
Discharge to soil, kg·m^{-3}	Disposal to agriculture *(Slurry spreading, by vacuum tanker/CH S)*	Solid waste
		N-based fertiliser *(Ammonium sulphate, as N, at regional storehouse/RER S)*
		P-based fertiliser *(Diammonium phosphate, as P2O5, at regional storehouse/RER S)*
		Cd to soil
		Co to soil
		Cr to soil
		Cu to soil
		Ni to soil
		Pb to soil
		Zn to soil
	Disposal to landfill (*Disposal, municipal solid waste, 22.9% water, to sanitary landfill/CH S)* Disposal to incineration *(Disposal, raw sewage sludge, to municipal incineration/CH S)* Transport (*Lorry 3.5e7.5t EURO5*), t·km	

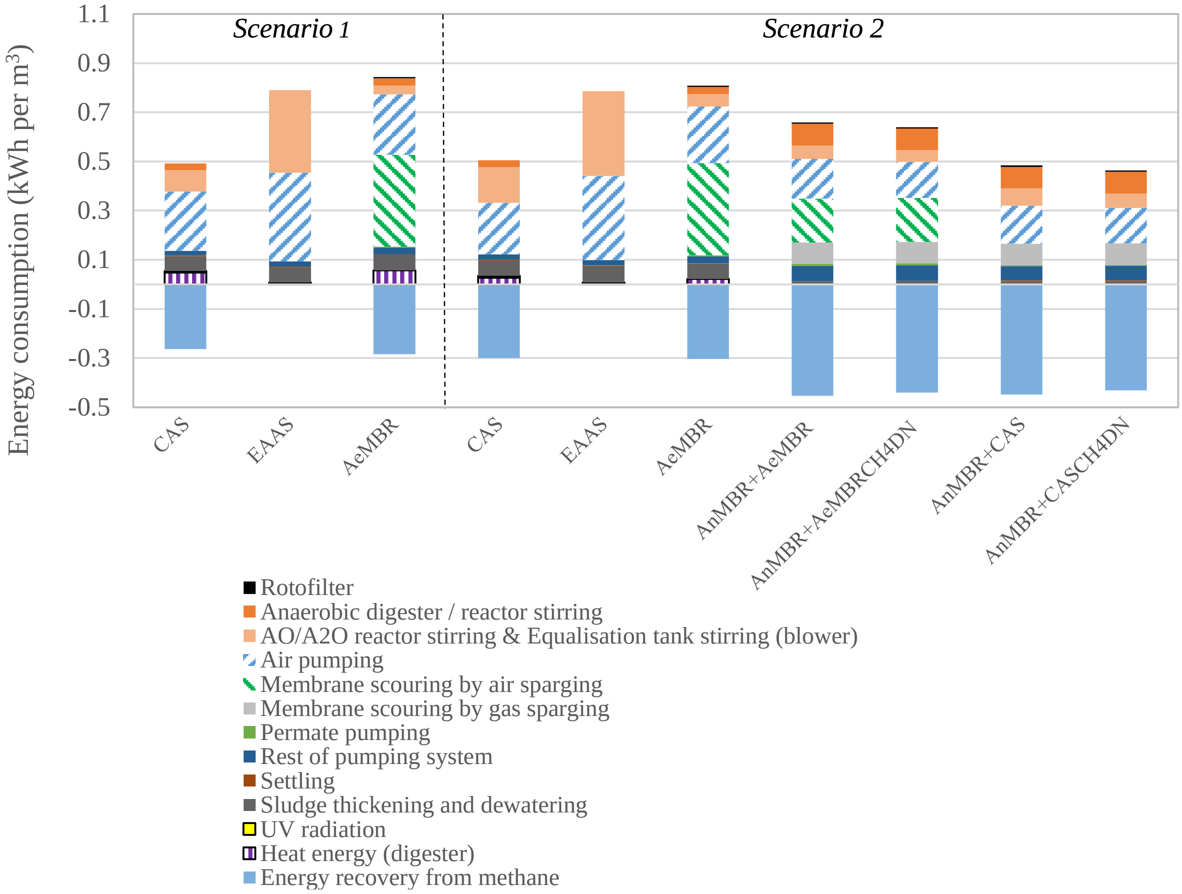

Figure 9.2 Energy balance of CAS, EAAS, AeMBR and AnMBR (AnMBR+AeMBR, AnMBR+AeMBR$_{CH4DN}$, AnMBR+CAS, AnMBR+CAS$_{CH4DN}$) for nitrogen and phosphorous removal. ***Scenario 1**: biological and chemical removal of phosphorus; and **scenario 2**: chemical removal of phosphorus.*

As regards phosphorous removal, Figure 9.2 shows that power requirements for biological and chemical removal of phosphorus (scenario 1) were relatively similar to power requirements for chemical removal (scenario 2). In this respect, although chemical removal of phosphorus produced higher amounts of sludge (increasing therefore energy consumption for sludge thickening and dewatering), biological removal of phosphorus consumed more energy for air pumping and reduced energy recovery potential (a fraction of the organic matter was consumed by polyphosphate-accumulating organisms, reducing therefore the directly-available COD for methanisation). Therefore, higher heat energy demand (lower heat recovery from biogas) was required in scenario 1. On the other hand, power requirements for nitrogen and phosphorus removal were evidently higher than power requirements for nitrogen removal (data not shown). When phosphorus removal was not considered, lower reaction volumes (decreasing energy consumption for stirring) and lower sludge productions (decreasing energy consumption for sludge thickening and dewatering) were obtained.

Nonetheless, it is important to highlight that biological phosphorus removal enables nutrient recovery by applying adequate downstream processes (e.g. struvite crystallization).

Considering energy recovery from methane capture, the highest energy demand corresponded to EAAS since biogas production was null. Indeed, EAAS would not be selected for treating the influent evaluated in this study since this technology is not appropriate for treatment flow rates of 50,000 $m^3 \cdot d^{-1}$. Nonetheless, EAAS was evaluated for comparing AnMBR to current UWW treatment technologies. The highest energy recovery potential (around 0.45 $kWh \cdot m^{-3}$) corresponded to AnMBR+AeMBR and AnMBR+CAS, since the methane dissolved in the effluent was captured for energy production. Nevertheless, although AnMBR+AeMBR$_{CH4DN}$ and AnMBR+CAS$_{CH4DN}$ used the methane dissolved in the AnMBR effluent for denitrification in the AeMBR- and CAS-based post-treatment units, both schemes presented a similar energy recovery potential (0.43 $kWh \cdot m^{-3}$) to AnMBR+AeMBR and AnMBR+CAS. In AnMBR+AeMBR and AnMBR+CAS, it was necessary to bypass a higher fraction of the influent flow to the post-treatment unit for denitrification than when using the dissolved methane for such purpose. Thus, a decrease in methane production was reached in the AnMBR unit due to a reduction in the amount of organic matter directly available for methanisation.

On the other hand, it is important to point out that heat energy input was needed in AeMBR (0.06 and 0.02 $kWh \cdot m^{-3}$ in scenario 1 and 2, respectively) and CAS (0.05 and 0.03 $kWh \cdot m^{-3}$ in scenario 1 and 2, respectively) to maintain a temperature of 35 ºC in the AD unit. This heat energy requirements increased therefore the energy demand in these configurations.

Hence, the net energy demand of the evaluated treatment schemes for nitrogen and phosphorus removal (considering energy recovery from methane) was (see Figure 9.2): 0.79 and 0.78 $kWh \cdot m^{-3}$ for EAAS in scenario 1 and 2, respectively; 0.56 and 0.50 $kWh \cdot m^{-3}$ for AeMBR in scenario 1 and 2, respectively; 0.23 and 0.21 $kWh \cdot m^{-3}$ for CAS in scenario 1 and 2, respectively; 0.20 $kWh \cdot m^{-3}$ for AnMBR+AeMBR and AnMBR+AeMBR$_{CH4DN}$; 0.04 $kWh \cdot m^{-3}$ for AnMBR+CAS; and 0.03 $kWh \cdot m^{-3}$ for AnMBR+CAS$_{CH4DN}$. In this respect, AnMBR technology coupled to a CAS-based post-treatment for nutrient removal at 20 ºC may present nearly null energy demands for the evaluated operating conditions: a theoretical minimum energy consumption of around 0.04 $kWh \cdot m^{-3}$ could be achieved by capturing the methane from both biogas and effluent.

Nevertheless, it is worth to point out that the influent UWW presents a high BOD concentration (715 $mg \cdot L^{-1}$). Therefore, a higher amount of biodegradable organic matter is anaerobically converted into methane than when treating low-loaded UWW. These conditions favour therefore the economic sustainability of AnMBR technology since more energy is generated from methane capture.

9.3.2 Life cycle cost results

Figure 9.3 shows the total cost (divided into capital and operating and maintenance (O&M) costs) of CAS, EAAS, AeMBR and AnMBR (AnMBR+AeMBR, AnMBR+AeMBR$_{CH4DN}$, AnMBR+CAS and AnMBR+CAS$_{CH4DN}$) for nitrogen and phosphorus removal (Figure 9.3a) and for nitrogen removal (Figure 9.3b). Note that bars in Figure 9.3 represent the results obtained (applying a discount rate of 10%) when the fate of the wasted sludge was 80% to farmland, 10% to landfilling, and 10% to incineration. Triangles, rhombus and squares represent the results obtained when the fate of wasted sludge was 100% to farmland, landfilling and incineration, respectively. Moreover, the total cost was also evaluated for the case of applying a discount rate of 5% (represented with a horizontal line in Figure 9.3).

As Figure 9.3a shows, EAAS presented the highest life cycle cost (expressed as total annualised equivalent cost, € per m^3) due to significant operational and capital costs, mainly associated with the electricity cost for aeration and stirring, the null energy recovery from methane and the concrete cost for construction. CAS presented the lowest capital cost since membrane investment cost was null and concrete cost for construction was not significantly important. Nevertheless, in spite of the membrane investment cost, AnMBR+CAS and AnMBR+CAS$_{CH4DN}$ presented both lower life cycle costs than CAS since more energy was recovered from methane capture. AnMBR+AeMBR and AnMBR+AeMBR$_{CH4DN}$ presented higher life cycle costs than CAS since (although energy demand was slightly lower in the formers than in the later) the membrane investment cost in both AeMBR and AnMBR significantly increased total capital costs.

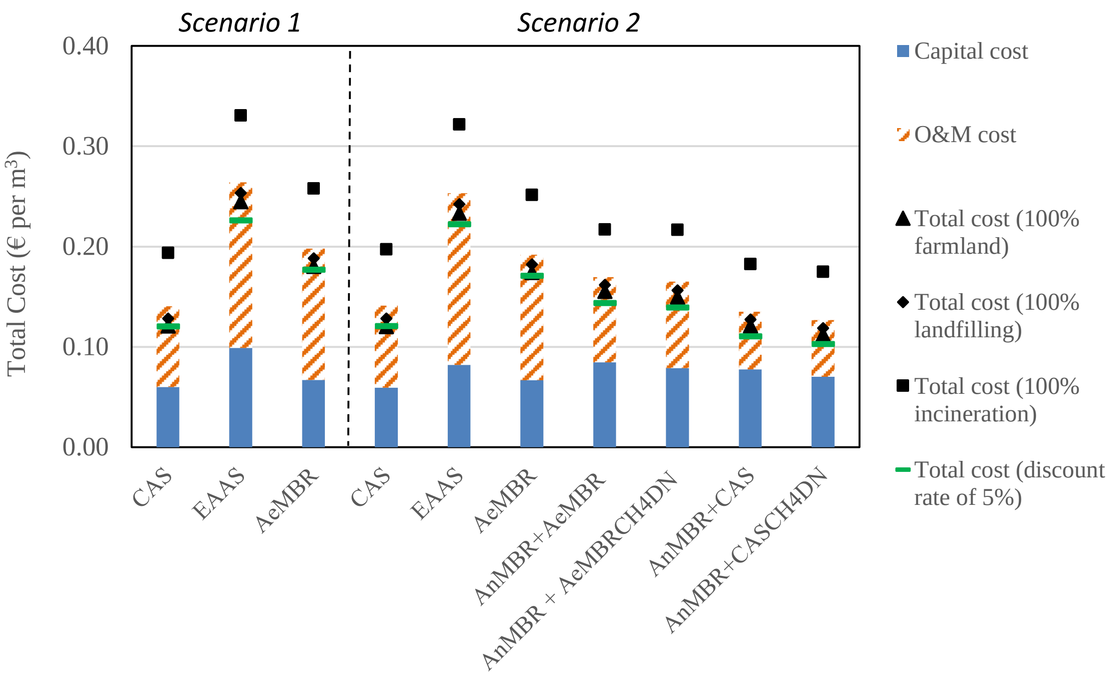

(a)

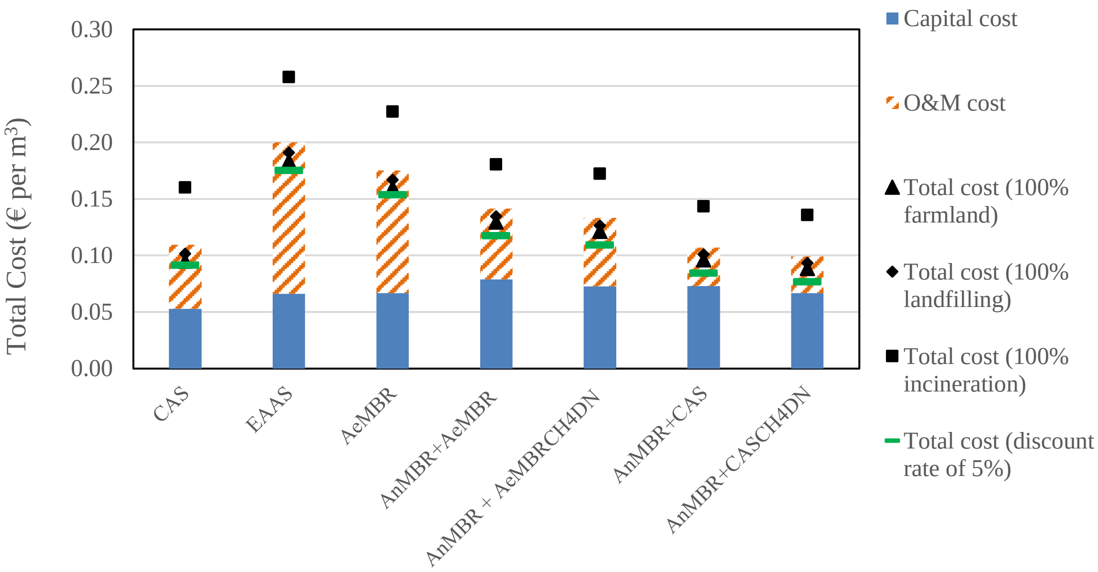

(b)

Figure 9.3 Total cost of CAS, EAAS, AeMBR and AnMBR (AnMBR+AeMBR, AnMBR+AeMBR$_{CH4DN}$, AnMBR+CAS AnMBR+CAS$_{CH4DN}$) for **(a)** nitrogen and phosphorous removal; and **(b)** nitrogen removal. Bars represent a discount rate of 10%. ***Scenario 1****: biological and chemical removal of phosphorus; and* ***scenario 2****: chemical removal of phosphorus.*

The sludge handling and disposal practice was a key factor affecting the life cycle cost of the evaluated UWW treatment schemes. As commented before, total life cycle costs were also calculated assuming 100% of the wasted sludge to be managed with a single method (farmland, landfilling or incineration) (see Figure 9.3). When sludge was used as fertiliser on farmland or landfilled, the life cycle cost was much lower than when the sludge was incinerated. These results were mainly based on the cost assumed for farmland, incineration and landfilling (€4.8, 250.0 and 30.1 per t TSS, respectively) (see Table 9.3). As shown in Figure 9.3, a reduction in total cost of around 30% can be achieved when decreasing the discount rate from 10 to 5%.

As regards phosphorous removal, Figure 9.3a shows that the life cycle costs for biological and chemical removal of phosphorus (scenario 1) were relatively similar to the life cycle costs for chemical removal of phosphorus (scenario 2). In this respect, although lower chemical consumption (decreasing its associated cost), lower sludge production (decreasing sludge handling and disposal cost) and lower energy stirring cost (since the anoxic tank just represented the 10% of the total reaction volume) were obtained in scenario 1, scenario 2 resulted in lower cost related to lower air pumping, higher energy recovery potential (excepting EAAS) and lower reacting volumes (especially in EAAS). On the other hand, life cycle costs for nitrogen and phosphorus removal (see Figure 9.3a) were evidently higher than life cycle costs for nitrogen removal (see Figure 9.3b). In this regard, lower reaction volumes (decreasing power and investment costs) and sludge productions (decreasing sludge handling and disposal cost) were obtained when only nitrogen removal was applied.

Therefore, the life cycle cost of the evaluated treatment schemes for nitrogen and phosphorous removal were (see Figure 9.3a): €0.264 and €0.253 per m^3 for EAAS in scenario 1 and 2, respectively; €0.198 and €0.192 per m^3 for AeMBR in scenario 1 and 2, respectively; €0.169 per m^3 for AnMBR+AeMBR; €0.165 per m^3 for AnMBR+AeMBR$_{CH4DN}$; €0.140 and €0.141 per m^3 for CAS in scenario 1 and 2, respectively; €0.135 per m^3 for AnMBR+CAS; and €0.126 per m^3 for AnMBR+CAS$_{CH4DN}$. On the other hand, the life cycle costs of the evaluated treatment schemes when only nitrogen removal was applied were (see Figure 9.3b): €0.200 per m^3 for EAAS; €0.175 per m^3 for AeMBR; €0.141 per m^3 for AnMBR+AeMBR; €0.133 per m^3 for AnMBR+AeMBR$_{CH4DN}$; €0.110 per m^3 for CAS; €0.107 per m^3 for AnMBR+CAS; and €0.099 per m^3 for AnMBR+CAS$_{CH4DN}$.

Hence, it can be concluded that from an economic perspective, AnMBR+CAS at 20 ºC may be a sustainable approach for moderate-/high-loaded UWW treatment in comparison with other existing technologies. On the other hand, an increase in life cycle costs of up to 17 and 23% are expected in AnMBR+AeMBR when compared to CAS and AnMBR+CAS, respectively. Nonetheless, it is important to highlight that AeMBR-based post-treatments may become an interesting alternative to CAS processes when water reuse is needed (e.g. reclamation for industrial purposes), since a high-quality effluent with nearly complete absence of pathogenic bacteria may be achieved.

On the other hand, different SGD_m and J_{20} values were assessed in AnMBR technology for comparing its economic sustainability to the rest of evaluated systems. In this respect, Figure 9.4 illustrates the effect of decreasing and increasing the operating SGD_m (0.05 and 0.30 $m^3 \cdot m^{-2} \cdot h^{-1}$) and J_{20} (80 and 120% of the critical flux) on the AnMBR total cost. As Figure 9.4 shows, comparing the AnMBR baseline (SGDm of 0.10 $m^3 \cdot m^{-2} \cdot h^{-1}$ and J_{20} of 105% of critical flux) with the scenario operating at J_{20} of 80 and 120% of the critical flux, the life cycle cost of AnMBR technology increases up to 17 and 66%, respectively. On the other hand, when operating at SGD_m of 0.05 and 0.30 $m^3 \cdot m^{-2} \cdot h^{-1}$ the life cycle cost increases up to 10 and 20%, respectively. Hence, current aerobic-based technologies (except EAAS) may become more sustainable than AnMBR if non-optimum values for the different design parameters in AnMBR are applied.

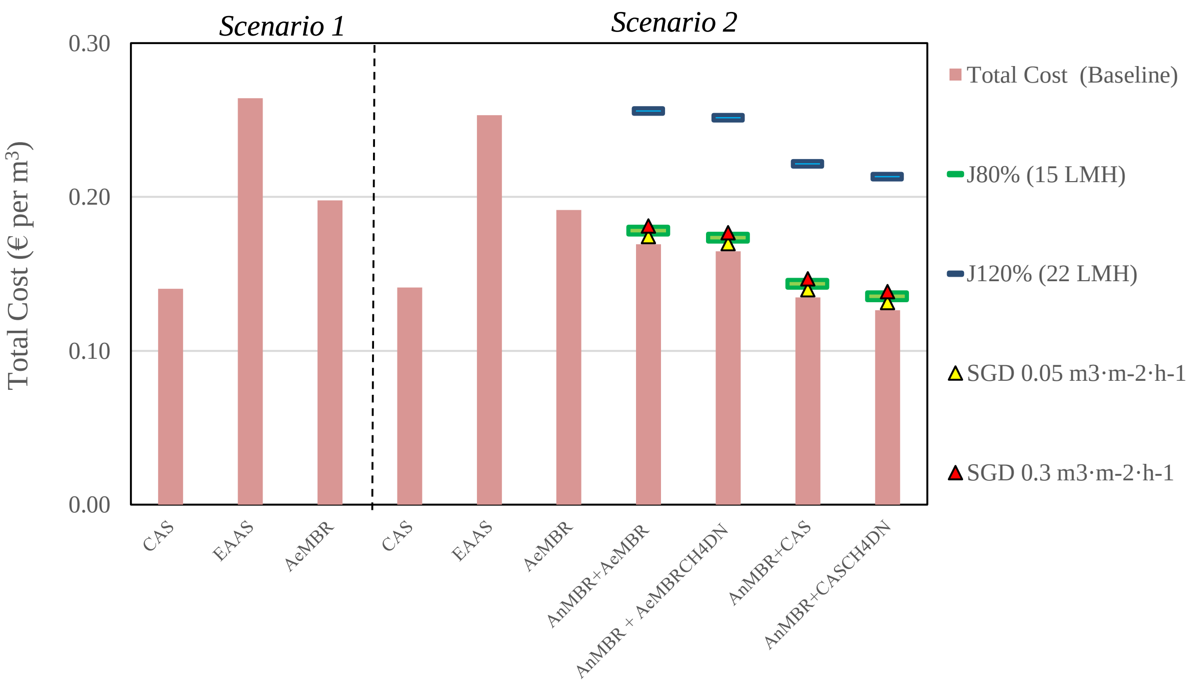

Figure 9.4 Effect of the operational parameters (% of J: 80-120%; and SGD value: 0.05- 0.3 $m^3 \cdot m^{-2} \cdot h^{-1}$) on the AnMBR (AnMBR+AeMBR, AnMBR+$AeMBR_{CH4DN}$, AnMBR+CAS AnMBR+CAS_{CH4DN}) cost and comparison with aerobic-based technologies for UWW treatment: CAS, EAAS and AeMBR for nitrogen and phosphorous removal; Bars represent the baseline (in case of AnMBR: SGD 0.1 $m^3 \cdot m^{-2} \cdot h^{-1}$ and J105%). ***Scenario 1**: biological and chemical removal of phosphorus; and **scenario 2**: chemical removal of phosphorus.*

9.3.3 Life cycle analysis results

As mentioned earlier, the SimaPro software (using Ecoinvent data) was used to assess the potential environmental impacts of the evaluated UWW treatment schemes.

9.3.3.1 Life cycle inventory assessment

The environmental impacts of the factors contemplated in the inventory analysis (see Table 9.4) through the impact categories selected in this study (i.e. marine aquatic ecotoxicity, GWP, abiotic depletion, acidification and eutrophication) are discussed in the following paragraphs. These results are based on the LCA results obtained for the treatment schemes proposed under the different scenarios considered, for both nitrogen and phosphorous removal. Figure 9.5 shows the life cycle inventory assessment for the following impact categories: marine aquatic ecotoxicity, GWP, abiotic depletion and acidification.

Marine aquatic ecotoxicity

As Figure 9.5a shows, the environmental impacts in this impact category were mostly associated with sludge disposal when it is landfilled (with a value of 43 ± 5%; average ± standard deviation) and $FeCl_3$ consumption for chemical phosphorus removal (with a value of 33 ± 6%). This behaviour was similar for all the evaluated schemes. The following in importance (but in a lesser extent) were energy consumption (with a value of 9 ± 6%), sludge disposal (associated with heavy metal emissions to soil) when it is used as fertiliser in farmland (with a value of 12 ± 1%), and employment of materials for construction and equipment (concrete, iron, chromium steel etc…, with a value of 4 ± 1%). Polyelectrolyte and membrane cleaning reagent consumption had barely any environmental impact in comparison with the rest of factors. Note that the fertiliser avoided resulted in a positive environmental impact since the use of synthetic fertiliser on farmland was partially avoided.

GWP

As Figure 9.5b shows, the results in this impact category were mostly associated with energy consumption (with a value of 42 ± 20%), followed to a lesser extent by: emissions to air (e.g. N_2O) when waste sludge was used for landfill or agricultural application (with a value of 35 ± 12%); chemical consumption (mainly $FeCl_3$ for chemical phosphorus removal, with a value of 15 ± 7%); and use of materials for construction and equipment (concrete, iron, chromium steel, etc., with a value of 6 ± 3%).

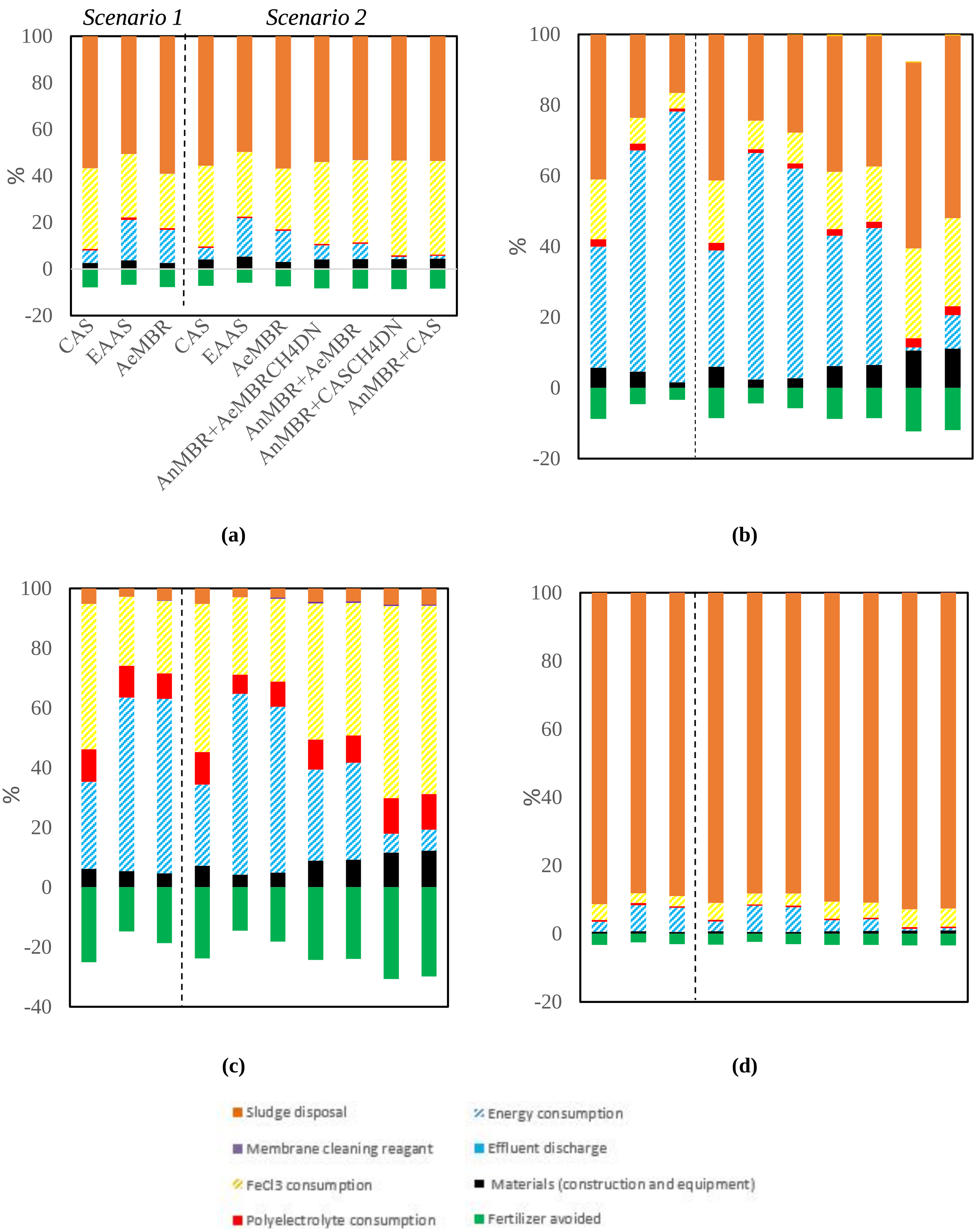

Figure 9.5 Weighted average distribution of the environmental impacts through: **(a)** marine aquatic ecotoxicity; **(b)** GWP; **(c)** abiotic depletion; and **(d)** acidification. ***Scenario 1****: biological and chemical removal of phosphorus; and* ***scenario 2****: chemical removal of phosphorus.*

In EAAS and AeMBR, the environmental impact related to energy consumption was higher than that related to sludge disposal, since considerable energy was required in this treatment scheme, unlike AnMBR and CAS. Also in this case, polyelectrolyte and membrane cleaning reagent consumption had barely any environmental impact as compared to the other factors. Note that the fertiliser avoided gave a positive environmental impact through GWP, since by its use less synthetic fertiliser was needed.

Abiotic depletion

As Figure 9.5c shows, energy consumption (with a value of 37 ± 21%) and chemical consumption ($FeCl_3$ and polyelectrolyte, with a value of 42 ± 16%) were the factors that affected abiotic depletion most. Environmental impacts in EAAS and AeMBR related to energy consumption were higher than the ones related to $FeCl_3$ consumption, contrary to AnMBR and CAS. The following in importance was the employment of materials (concrete, iron, chromium steel etc…, with a value of 7 ± 3%) and the disposal of the wasted sludge (with a value of 4 ± 1%). Consumption of reagents for membrane cleaning had barely any environmental impact through this category compared to the rest factors. Note that fertiliser avoided resulted in a meaningful positive environmental impact in this impact category, even higher than in the rest of impact categories.

Acidification

As Figure 9.5d shows, farmland disposal of the wasted sludge was the main factor affecting environmental impacts through acidification (mainly due to NH_3 emissions). The rest of factors had barely any environmental impact.

Eutrophication

Eutrophication has been considered the most relevant impact category in the majority of published LCAs on WWTPs [9.21]. In this study, effluent discharge (nitrogen, phosphorus and organic matter) was the factor that affected eutrophication most (around 80% in every treatment scheme and scenario), followed to a lesser extent by sludge disposal on farmland (around 20%), mainly due to PO_4^{3-} leakage and NH_3 emissions associated with wasted sludge disposal.

9.3.3.2 Overall inventory results

Figure 9.6 illustrates the LCA results of the impact categories evaluated in this study (i.e. GWP, eutrophication, marine aquatic ecotoxicity, abiotic depletion and acidification). Results in Figure 9.6a have been weighted (based on normalised values per m^3) to assess the magnitude of each impact category over the different treatment schemes and scenarios. Specifically, the results have been weighted applying a value of 100% to the configuration (scheme and scenario) that resulted in the highest environmental impact.

As Figure 9.6a marine aquatic ecotoxicity was considered the most relevant impact category in all the evaluated UWW treatment schemes since the characterised factors in this category (for $Fecl_3$ consumption, sludge production, energy consumption, etc.) are generally higher than the ones from other impact categories. The next in importance but to a lesser extent was eutrophication. It is important to note that although the treatment schemes were designed for meeting the European discharge quality standards, the remaining nutrient and organic matter content in the effluent affected noticeably eutrophication. GWP, abiotic depletion and acidification were not among the most relevant impact categories. However, they are usually regarded as an important environmental issue at least from a political and social point of view. In this respect, the complexity of environmental issues combined with social and political challenges has increased the necessity of better understanding multiple influencing factors that affect categories such as GWP, abiotic depletion and acidification.

As shown in Figure 9.6b, EAAS presented the highest environmental impact in all the impact categories except in eutrophication. As previously commented, it is important to highlight that EAAS resulted in the highest sludge production (and therefore sludge handling and disposal costs) and energy demand, affecting therefore GWP, marine aquatic ecotoxicity, abiotic depletion and acidification considerably. On the other hand, EAAS presented the lowest environmental impact through eutrophication since operating at 20 days of SRT (for complying with the sludge stabilisation criteria) led to significant reductions in the content of nutrients and organic matter in the effluent.

As Figure 9.6b shows, AeMBR presented higher environmental impacts than CAS and AnMBR in all the evaluated impact categories except in eutrophication. As mentioned before, the high sludge production and energy demand of this treatment scheme affected negatively GWP, marine aquatic ecotoxicity, abiotic depletion and acidification considerably.

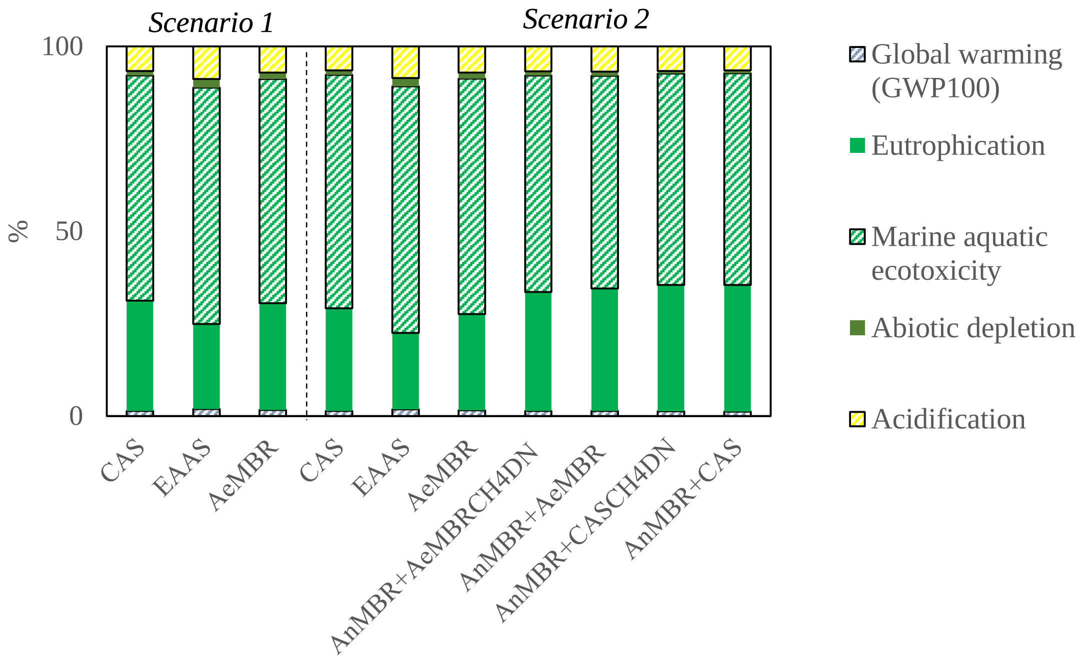

(a)

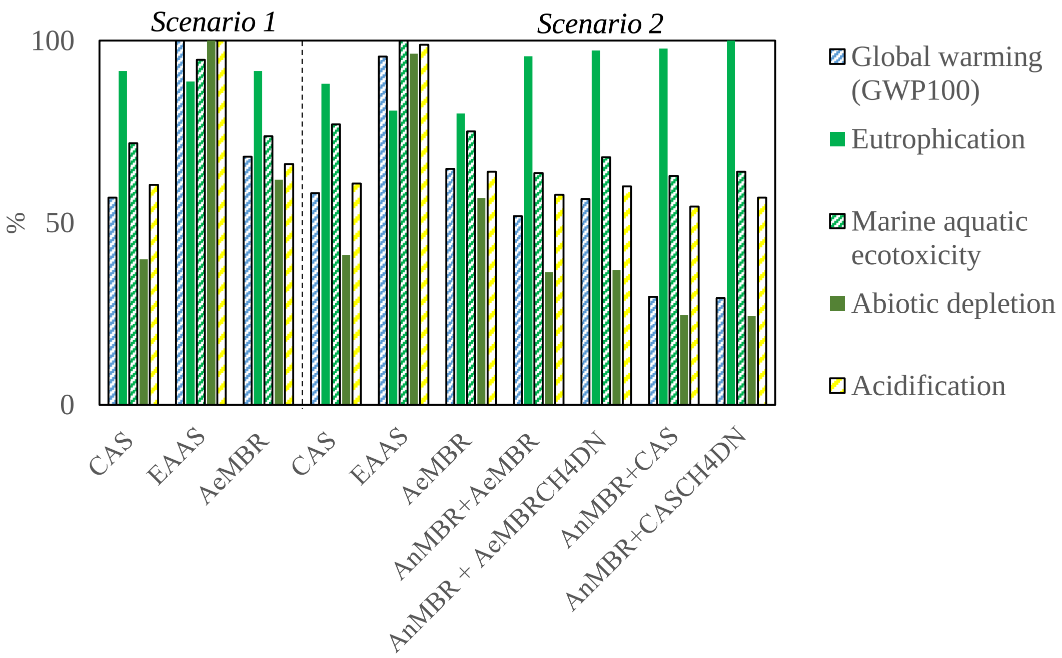

(b)

Figure 9.6 LCA results of the proposed UWW treatment schemes expressed as: **(a)** weighted average distribution, and **(b)** percentage (%). Method: CML 2 baseline 2000 V2.05 / West Europe, 1995 / normalisation / excluding infrastructure processes / excluding long-term emissions**.** ***Scenario 1****: biological and chemical removal of phosphorus; and* ***scenario 2****: chemical removal of phosphorus.*

On the other hand, AnMBR (and CAS to a lesser extent) resulted in the lowest environmental impact in all the evaluated impact categories except in eutrophication. Concerning CAS, the environmental loads of GWP, marine aquatic ecotoxicity, abiotic depletion and acidification were 38, 23, 55 and 38% lower than the ones obtained in EAAS when removing phosphorus chemically, respectively. Regarding AnMBR, this configuration featured the highest environmental impact in eutrophication compared to the rest of evaluated treatment schemes, since the nitrogen content in the discharged effluent was slightly higher than in the rest of configurations (around 9 $mg \cdot L^{-1}$). Nevertheless, the environmental loads of GWP, marine aquatic ecotoxicity, abiotic depletion and acidification of AnMBR were 66, 37, 72 and 44% lower than the ones in EAAS when removing phosphorus chemically, respectively. It is worth to point out that AnMBR presented the lowest sludge production and energy demand. Moreover, AnMBR coupled to a CAS-based post-treatment rather than AeMBR-based post-treatment presented reduced environmental impacts (mainly in GWP and abiotic depletion) mostly because the higher energy demand of the later than the former.

Therefore, the treatment schemes for nitrogen and phosphorus removal contributing eutrophication impact were, in descendent order, the following (see Figure 9.6b): AnMBR+CAS_{CH4DN}, AnMBR+CAS, AnMBR+$AeMBR_{CH4DN}$, AnMBR+AeMBR, CAS, AeMBR, and EAAS. The treatment schemes contributing the rest of impact categories (GWP, marine aquatic ecotoxicity, abiotic depletion and acidification) were, in descendent order, the following (see Figure 9.6b): EAAS, AeMBR, CAS, AnMBR+$AeMBR_{CH4DN}$, AnMBR+AeMBR, AnMBR+CAS_{CH4DN}, and AnMBR+CAS.

Hence, from an environmental perspective, AnMBR could be considered a promising sustainable alternative for moderate-/high-loaded UWW treatment in comparison with other existing technologies. Moreover, it is important to highlight that in AnMBR systems, the nutrients from the treated effluent could be used for fertigation (i.e., irrigation with nutrient-rich water) instead of incorporating an aerobic-based post-treatment for nutrient removal (e.g. CAS-based post-treatment). AnMBR without post-treatment (using the nutrients from the treated effluent for fertigation) may reduce significantly its life cycle cost (savings of up to 42% can be achieved, mostly related to operation costs). Furthermore, this would improve environmental impacts (reduction of up to 53% could be reached in GWP) as a result of: the fertiliser avoided from fertigation, the reduction of energy consumption, and the non-use of $FeCl_3$. By accounting for on-site electricity production, energy offsets of 0.12 kWh per m^3 can be achieved in AnMBR systems (under the scenarios evaluated in this study) when a post-treatment unit for nutrient removal is not required.

Nonetheless, it is important to highlight that the results obtained in this study are strongly dependent on UWW characteristics, operating temperature and methane recovery potential, among others. Specifically, AnMBR technology for UWW treatment increases its sustainability when treating high-loaded UWW at warm/hot temperatures [9.25; 9.5].

9.4 Conclusions

AnMBR technology was compared to aerobic-based UWW treatment technologies by integrating steady-state performance modelling, LCA and LCC approaches. AnMBR using a CAS-based post-treatment for nutrient removal was identified as a sustainable option for moderate-/high-loaded UWW treatment: a minimum energy consumption of 0.04 $kWh \cdot m^{-3}$ could be achieved and low sludge productions could be obtained at given operating conditions. In addition, significant reductions in different environmental impacts (GWP, marine aquatic ecotoxicity, abiotic depletion and acidification) and LCC (minimum LCC value of around €0.135 per m^3) can be achieved in comparison with other existing UWW treatment technologies.

9.5 Acknowledgements

This research work has been supported by the Spanish Ministry of Science and Innovation (MICINN, Project CTM2011-28595-C02-01/02) jointly with the European Regional Development Fund (ERDF) and Generalitat Valenciana (Project GVA-ACOMP2013/203), which are gratefully acknowledged.

9.6 References

9.1 S. Gabarrón, M. Dalmaua, J. Porroa, I. Rodriguez-Rodaa, J. Comasa, Optimization of full-scale membrane bioreactors for wastewater treatment through a model-based approach. Chem. Eng. J. 267 (2015), 34-42.

9.2 S. J. Judd, C. Judd, Principles and Applications of Membrane Bioreactors in Water and Wastewater Treatment. Second Edition, Elsevier, London, UK, 2011.

9.3 A. Fenu, J. Roels, T. Wambecq, K. De Gussem, C. Thoeye, G. De Gueldre, B. Vand De Steene, Energy audit of a full scale MBR system. Desalination 262 (2010), 121-128.

9.4 P. L. McCarty, J. Bae, J. Kim, Domestic wastewater treatment as a net energy producer – can this be achieved? Environ. Sci. Technol. 45 (2011), 7100-7106.

9.5 A. L. Smith, L. B Stadler, L. Cao, N.G. Love, L. Raskin, S. J Skerlos, Navigating Wastewater Energy Recovery 1 Strategies: A Life Cycle Comparison of Anaerobic Membrane Bioreactor and Conventional Treatment Systems with Anaerobic Digestion. Environ. Sci. Technol. 48 (2014), 5972-5981.

9.6 J.B. Giménez, A. Robles, L. Carretero, F. Durán, M.V. Ruano, M.N. Gatti, J. Ribes, J. Ferrer, A. Seco, Experimental study of the anaerobic urban wastewater treatment in a submerged hollow-fibre membrane bioreactor at pilot scale. Bioresour. Technol. 102 (2011) 8799–8806.

9.7 L. Raskin, Anaerobic Membrane Bioreactors for Sustainable Wastewater Treatment. WERF Report U4R08, June 2012.

9.8 A. L. Smith, S. J. Skerlos, L. Raskin, Psychrophilic anaerobic membrane bioreactor treatment of domestic wastewater. Water Res. 47 (2013), 1655-1665.

9.9 H. Ozgun, R. K. Dereli, M. E. Ersahin, C. Kinaci, H. Spanjers, J.B. van Lier, A review of anaerobic membrane bioreactors for municipal wastewater treatment: Integration options, limitations and expectations. Sep. Purif. Technol. 118 (2012), 89-104.

9.10 D. C. Stuckey, Recent developments in anaerobic membrane reactors. Bioresour. Technol. 122 (2013), 137–148.

9.11 H. Lin, J. Chen, F. Wang, L. Ding, H. Hong, Feasibility evaluation of submerged anaerobic membrane bioreactor for municipal secondary wastewater treatment. Desalination 280 (2011) 120–126.

9.12 R. Pretel, A. Robles, M. V. Ruano, A. Seco, J. Ferrer, The operating cost of an anaerobic membrane bioreactor (AnMBR) treating sulphate-rich urban wastewater. Sep. Purif. Technol. 126 (2014), 30-38.

9.13 J. B. Giménez, N. Mart,J. Ferrer, A. Seco, Methane recovery efficiency in a submerged anaerobic membrane bioreactor (SAnMBR) treating sulphate-rich urban wastewater: Evaluation of methane losses with the effluent. Bioresour. Technol. 118 (2012), 67-72.

9.14 C. Visvanathan, R.B Aim, K. Parameshwaran, Membrane separation bioreactors for wastewater treatment. Environ. Sci. Technol. 30 (2000), 1-48.

9.15 J. Ferrer, A. Seco, J. Serralta, J. Ribes, J. Manga, E. Asensi, JJ. Morenilla, F. Llavador, DESASS: A software tool for designing, simulating and optimising WWTPs. Environ. Modell. Softw. 23 (2008), 19-26.

9.16 R. Barat, J. Serralta, M.V. Ruano, E. Jiménez, J. Ribes, A. Seco, J. Ferrer, Biological Nutrient Removal Model Nº 2 (BNRM2): A general model for Wastewater Treatment Plants. Water Sci.Technol. 67 (2013), 1481-1489.

9.17 J. Ferrer, R. Pretel, F. Durán, J.B. Giménez, A. Robles, M.V. Ruano, J. Serralta, J. Ribes, A. Seco, Design methodology for anaerobic membrane bioreactors (AnMBR): A case study. Sep. Purif. Technol. 141 (2015), 378-386.

9.18 R. Pretel, A. Robles, M.V. Ruano, A. Seco, J. Ferrer, Filtration process cost in anaerobic membrane bioreactors (AnMBRs) for urban wastewater treatment. Sent to Sep. Sci. Technol.

9.19 A. Gallego, A. Hospido, M.T. Moreira, G. Feijoo, Environmental performance of wastewater treatment plants for small populations. Resour, Conser. Recy. 52 (2008), 931-940.

9.20 J. Foley, D. de Hass, K. Hartley, P. Lant, Comprehensive life cycle inventories of alternative wastewater treatment systems. Water Res. 44 (2010), 1654-1666.

9.21 G. Rodriguez-Garcia, M. Molinos-Senante, A. Hospido, F. Hernández-Sancho, M.T. Moreira, G. Feijoo, Environmental and economic profile of six typologies of wastewater treatment plants. Water Res. 45 (2011), 5997-6010.

9.22 D. Godin, C. Bouchard, A. Vanrolleghem, Net environmental benefit. Introducing a new LCA approach on wastewater treatment systems. Water Sci. Technol. 65.9 (2012), 1624-1631.

9.23 M. Garrido-Baserba, A. Hospido, R. Reif, M. Molinos-Senante, J. Comas, M. Poch, Including the environmental criteria when selecting a wastewater treatment plant. Environ. Modell. Softw. (2013) 1-9.

9.24 L. Corominas, J. Foley, J.S. Guest, A. Hospido, H.F. Larsen, S. Morera, A. Shaw, Life cycle assessment applied to wastewater treatment: State of the art. Water Res. 47 (2013), 5480-5495.

9.25 R. Pretel, A. Robles, M.V. Ruano, A. Seco, J. Ferrer, Environmental impact of submerged anaerobic MBR (AnMBR) technology used to treat urban wastewater at different temperatures. Bioresour. Technol. 149 (2013), 532 – 540.

9.26 R. Pretel, B.D. Shoener, J. Ferrer, J.S. Guest, Navigating Environmental, Economic, and Technological Trade-Offs in the Design and Operation of Submerged Anaerobic Membrane Bioreactors (AnMBRs). Water Res (2015) In press.

9.27 F. Durán, F, Mathematical modelling of the anaerobic urban wastewater treatment including sulphate-reducing bacteria. Application to an anaerobic membrane bioreactor. Ph.D. thesis. Dept. of Hydraulic Engineering and Environment. Universitat Politècnica de València, Spain, 2013.

9.28 A. Robles, M.V. Ruano, F. García-Usach, J. Ferrer, Sub-critical filtration conditions of commercial hollow-fibre membranes in a submerged anaerobic MBR (HF-SAnMBR) system: The effect of gas sparging intensity. Bioresour. Technol. 114 (2012) 247–254.

9.29 ISO, International Organization for Standardization (ISO) 14040: Environmental Management - Life Cycle Assessment e Principles and Framework (Geneva), 2006.

9.30 MAGRAMA, Official website of the Ministry of Agriculture, Food and Environment. Spanish government, Madrid. Available on: http://www.magrama.gob.es/es/calidad-y-evaluacion-ambiental/temas/prevencion-y-gestion-residuos/flujos/lodos-depuradora/ (Accessed May 21, 2015).

9.31 J. Hobson J, CH4 and N2O emissions from wastewater handling. In: Good practice guidance and uncertainty management in National Greenhouse Gas Inventories. Geneve, Switzerland: Intergovernmental Panel on Climate Change (IPCC) Publications, 2000.

9.32 Bank BEDEC - ITeC database, In Construmatica, Available on http://www.construmatica.com/bedec, (Accessed February 1, 2015).

9.33 Iberdrola S.A., Spanish electricity tariff (Tarifa eléctrica España). In Iberdrola. Available on https://www.iberdrola.es/clientes/empresas/info/mercado-energetico, (Accessed March 5, 2013).

9.34 J.A. Sainz-Lastre, Technologies for sustainability, Processes and unit operations in wastewater treatment (Tecnologías para la sostenibilidad, Procesos y operaciones unitarias en depuración de aguas residuales), Colección EOI Medio Ambiente, Madrid, Spain, 2005.

9.35 Miliarium Aureum, S.L, Approximate cost of WWTP (Coste estimativo EDAR), In Miliarium.com - Ingeniería Civil y Medio Ambiente, Available on http://www.miliarium.com/Proyectos/Depuradoras/introduccion/edar.asp, (Accessed April 20, 2013).

9.36 Bombas Ideal S.A., Distribution Catalogue (Catálogo Distribución), In Bombas Ideal, Available on http://www.bombas-ideal.com/pdf/CAT%20C9%20ES%20%5BD-100512%5D.pdf, (Accessed March 5, 2013).

9.37 SIMEX, Distribution Catalogue in February 2015 (Catálogo Distribución). In *SIMEX "soluciones hidráulicas integrales"* Available on: http://www.simexco.com.mx/productos/precios.pdf, (Accessed February 25, 2015).

9.38 EPA, Environmental Protection Agency. Combined Heat and Power Partnership, Agency of the United States federal government, 2012.

9.39 MAGRAMA. Official website of the Ministry of Agriculture, Food and Environment. Spanish government, Madrid. Survey land prices 2012. Available on http://www.magrama.gob.es/es/estadistica/temas/estadisticas,agrarias/Encuesta_Precios_Tierra_2012_tcm7-298705.pdf (Accessed May 5, 2014).

CHAPTER 10:

Summary and general discussion implementations for full scale implementation and recommendations for future research

10.1 Research work motivation

During the developing period of this Ph.D. thesis several laboratory- and bench-scale studies on submerged anaerobic membrane bioreactor (AnMBR) technology for urban wastewater (UWW) treatment have been published. Literature demonstrates the potentials of AnMBR technology for treating UWW: a high quality effluent can be achieved; whilst also accomplishing meaningful steps toward sustainable wastewater treatment, such as low energy demand stemming from no aeration and energy recovery through methane production. However, recent studies (e.g., [10.1]) have identified the need to focus future research efforts on achieving sustainable operation of AnMBRs treating UWW. Although environmental and economic criteria have been used to evaluate AnMBRs relative to alternative aerobic technologies, a critical barrier to advance on AnMBR development is still the lack of understanding of how detailed design decisions influence system sustainability. Therefore, the objective of this Ph.D. thesis is to further investigate the feasibility of AnMBR as core technology for UWW treatment. Specifically, this thesis focussed on economic and environmental sustainability in AnMBR. The main point of this research work was to operate an AnMBR plant entailing industrial-scale membrane modules. This plant was operated at ambient temperature using wastewater coming from the pre-treatment of a full-scale UWW.

10.2 Implementation of a plant-wide energy model

A detailed and comprehensive plant-wide model for assessing the energy demand of different wastewater treatment systems (beyond the conventional activated sludge (CAS) system) at both steady- and unsteady-state conditions was proposed. The model was coupled to the extended version of the plant-wide mathematical model BNRM2 [10.2] proposed by Durán [10.3], which is implemented in the new version of the simulation software DESASS [10.4]. DESASS allows the design, simulation, upgrading, and optimisation of urban and industrial wastewater treatment plants (WWTPs), including, among others, MBR and AnMBR technologies. Hence, the proposed energy model allows calculating the overall energy demand of different WWTPs, enabling therefore their analysis and improvement from an environmental point of view (e.g. reduction of greenhouse gases (GHG) emissions associated with energy consumption).

Specifically, the model proposed in this Ph.D. thesis enables calculating power and heat energy requirements (W and Q, respectively), and energy recovery (power and heat) from methane and hydrogen capture during the anaerobic treatment of organic matter. The W term (power energy) entailed the main equipment employed in WWTPs (e.g. blowers, pumps, diffusers, stirrers, dewatering systems, etc.). The *Q* term (heat energy) considered heat transfer through pipe and reactor walls, heat transfer due to gas decompression, external heat required when temperature is controlled, and enthalpy of the biological reactions included in the extended version of the plant-wide model BNRM2.

Two case studies were evaluated to assess the model performance: (1) modelling the energy demand of two urban WWTPs based on CAS and submerged AnMBR technologies at steady-state conditions; and (2) modelling the dynamics in reactor temperature and heat energy requirements in an AnMBR plant at unsteady-state conditions.

The experimental and model results indicated that the proposed model is capable to reproduce temperature and/or heat energy requirements versus variations in operating and environmental conditions. In this respect, the results indicated that the proposed model can be used for assessing the energy balance of different wastewater treatment processes, thus being useful for different purposes, e.g. WWTP design or upgrading, or development of new control strategies for energy savings.

10.3 Influence of temperature and SRT in AnMBR sustainability

In this Ph.D. thesis, the environmental impact of an AnMBR system treating UWW was evaluated by applying an energy balance and life cycle assessment (LCA). Since temperature is one of the key operating variables that determine the biological process performance in AnMBR technology, the following three scenarios at three different operating temperatures were evaluated: scenario 1a: AnMBR operating at ambient temperature of 20 ºC (warm climate); scenario 1b: AnMBR operating at ambient temperature of 33 ºC (hot/tropical climate); and scenario 2: AnMBR operating at 33 ºC when the ambient temperature is 20 ºC (controlled temperature requiring energy input). A considerable amount of heat energy was needed to maintain a temperature of 33 ºC when operating at controlled temperature (energy input of 131649 $kJ \cdot m^{-3}$). The energy balance results highlighted the importance of operating at ambient temperature (average 0.19 $kWh \cdot m^{-3}$). Moreover, it must be said that heating the process from 20 to 33 ºC increases the environmental impact caused by electricity consumption considerably (because it affects abiotic depletion, marine aquatic ecotoxicity, global warming potential (GWP) and acidification categories). The environmental loads related to electricity consumption in scenario 1b were slightly lower than in scenario 1a because of the greater volume of biogas produced at higher temperatures. According to the IPCC method, GHG emissions were considerably higher in scenario 2 (10.98 kg CO_2 equivalents) than in scenarios 1a and 1b (0.13 and 0.12 kg CO_2 equivalents, respectively). In this respect, it is important to operate AnMBR at ambient temperature in order to make this technology environmentally feasible, avoiding furthermore the heating impact caused by discharging effluent which is hotter than the temperature of natural water courses. On the other hand, the low energy requirements obtained when operating at ambient temperature (scenario 1a and 1b) makes AnMBR a promising sustainable technology from an energy viewpoint. Besides that, when operating at hot/tropical ambient temperatures (e.g. 33 ºC) more biogas might be captured than at warm ambient temperatures (e.g. 20 ºC), which slightly reduces overall energy consumption (from 0.20 to 0.18 $kWh\cdot m^{-3}$ in this scenario).

Moreover, several experimental and simulation scenarios were evaluated in order to assess the AnMBR performance within a wide range of temperature and sludge retention time (SRT). Methane production increased significantly when operating at both high temperature and high SRT. In particular, the average experimental methane production when operating at 33 ºC and 70 days of SRT was nearly 5 times the one obtained when operating at 17 ºC and 30 days of SRT. It can be considered that an increase in ambient temperature and/or SRT leads to offset the low growth rate of MA [10.5]. Furthermore, simulation results showed adequate effluent COD concentrations and increasing methane productions (achieving significant energy savings) and decreasing sludge productions as temperature and/or SRT increases, within the range of operating conditions evaluated in this study.

10.4 Design and operation of submerged AnMBRs and optimal AnMBR-based configurations

According to Smith *et al.* [10.1], future research efforts should focus on increasing the likelihood of net energy recovery through advancements in fouling control. The key operating challenge in AnMBR technology is to optimise membrane operating in order to minimise any kind of membrane fouling, thus improving energy balance whilst increasing the membrane lifespan [10.6]

In this respect, a methodology was proposed to design an AnMBR WWTP handling UWW with high and low levels of sulphate (5.7 and 57 mg $COD\cdot mg^{-1}$ SO_4-S, respectively) at 15 and 30 ºC. In the proposed methodology, hydraulic retention time (HRT), SRT, r_{rec} (sludge recycling ratio) and mixed liquor suspended solids ($MLSS_{MT}$) were the key operating parameters when designing the biological process in AnMBR technology; and 20 ºC-standardised transmembrane flux (J_{20}), specific gas demand per square metre of membrane area (SGD_m) and $MLSS_{MT}$ were the key operating parameters when designing the corresponding filtration process. With regard to the biological process, the optimum combination of anaerobic reactor volume and sludge recycling flow rate were selected for each SRT and

$MLSS_{MT}$. Regarding the filtration process, different levels combinations of SGD_m, MLSS concentration and J_{20} were assessed in order to determine the lowest filtration cost. The results showed that in winter conditions the optimal *SRT* resulted in 35-41 days at $MLSS_{MT}$ of 15-16 g·L^{-1}, which corresponded to J_{20} of 18 LMH, r_{rec} of 3.2, and HRT of 17 hours. In summer conditions, the optimal *SRT* resulted in 23-27 days at r_{rec} of 1.2, which corresponded to $MLSS_{MT}$ of 12 g·L^{-1} and 21 LMH of J_{20}. On the other hand, the total annual cost of the proposed AnMBR WWTP treating sulphate-rich UWW was €0.101 and €0.097 per m^3 of treated water when (i) no energy was recovered from methane and (ii) energy was recovered from methane (biogas methane and methane dissolved in the effluent), respectively. The total cost when treating low-sulphate UWW resulted in €0.097 and €0.070 per m^3 of treated water for the two aforementioned scenarios, respectively.

Moreover, optimal AnMBR-based configurations for the following operating scenarios were identified: sulphate-rich and low-sulphate UWW treatment at 15 and 30 ºC. Three different AnMBR-based configurations were considered: AnMBR, AnMBR + anaerobic digester (AD), primary settler (PS) + AnMBR + AD. AnMBR without primary settling and further anaerobic digestion of the wasted sludge can be identified as the most feasible option for designing an AnMBR WWTP treating low-sulphate UWW at 30 ºC due to the following: 1) simplicity of the treatment scheme; and 2) reduced total cost (CAPEX plus OPEX). However, the life cycle cost analysis revealed that PS+AnMBR+AD is generally the best option for treating sulphate-rich UWW at 15 and 30 ºC since less COD is consumed by sulphate-reducing bacteria (SRB), in comparison with AnMBR and AnMBR + AD configurations, thus increasing the energy recovery potential of AnMBR technology.

Results of this Ph.D. thesis regarding the effect of the main factors affecting the cost of the filtration process showed that the most important item contributing the mechanical energy consumption of the filtration process in AnMBR systems is the membrane tank biogas recycling blower, which accounts for half of the total mechanical energy requirements. Operating at J_{20} above critical flux (Jc) may reduce both investment (i.e. decreases the required membrane filtration area) and membrane scouring costs (i.e. increases the net permeate flow per membrane area whilst maintaining SGD_m). However, operating at J_{20} above Jc increases chemical cleaning frequency, increasing therefore chemical reagent consumption whilst decreasing membrane lifetime (i.e. increases membrane replacement cost). A considerable increase in total filtration cost was observed when operating at J_{20} above the upper boundary of the critical filtration region (approx. for J_{20} values above 110 % of the Jc). Therefore, since membrane replacement is a key factor affecting the total cost of the filtration process, considerable attention should be paid to the optimisation of membrane lifetime by operating under a sustainable regime. Indeed, the optimal operating J_{20} corresponded to the maximum J_{20} for which membrane replacement was not required (corresponded to a J_{20} value slightly higher than Jc).

The optimal SGD_m value which resulted in minimum total filtration cost was around 0.10 $m^3{\cdot}m^{-2}{\cdot}h^{-1}$ for every MLSS level. The results shown in this Ph.D. thesis revealed that decreasing SGD_m below 0.10 $m^3{\cdot}m^{-2}{\cdot}h^{-1}$ increases total filtration cost due to increasing membrane fouling propensity (i.e. low shear intensities were applied on the membrane surface), which increases membrane chemical cleaning requirements and reduces membrane lifetime. On the other hand, increasing SGD_m above 0.10 $m^3{\cdot}m^{-2}{\cdot}h^{-1}$ allows reducing the costs related to membrane maintenance (i.e. it allows reducing membrane fouling propensity) and/or investment (i.e. it allows increasing optimal J_{20}). Nonetheless, the higher cost related to membrane scouring by gas sparging offsets these possible savings thus resulting in an increase in total filtration cost.

The optimum total filtration cost decreased when decreasing MLSS from 25 to 5 $g{\cdot}L^{-1}$, at SGD_m of 0.10 $m^3{\cdot}m^{-2}{\cdot}h^{-1}$. Thus, it seems to be obvious that the optimum design and operation of the filtration process in AnMBR technology for UWW treatment is achieved when membranes are operated at the lowest allowable MLSS concentration. However, decreasing MLSS means increasing the volume of the anaerobic reactor for a given SRT. Hence, it is required to optimise not only the filtration process but also the biological process (i.e. reactor volume) in order to optimise the cost of AnMBR technology for UWW treatment.

One key point for maximising the long-term economic feasibility of the filtration process in AnMBR technology is decreasing power requirements, whilst maximising membrane lifetime thus limiting membrane replacement cost.

Sensitivity and uncertainty analyses were used to characterise the relative importance of individual design decisions, and to navigate trade-offs across environmental, economic, and technological criteria. The results of the Monte Carlo simulations across the key operating parameters when designing the biological and filtration process in AnMBR showed that MLSS had a high impact on all categories, and was consistently ranked first for all categories except life cycle cost (LCC) operating and maintenance (O&M) (where it ranked second). SRT only had a high impact on LCA Capital (ranked second), which was a result of its effect on tank volume, which in turn determines construction material requirements. r (sludge recycling ratio) was most often ranked second for LCC Capital, which was mainly due to its effect on tank volume when building the plant. SGD_m consistently impacted LCA O&M (ranked second) because of electricity demand from blower operation. J_{20} was ranked first for LCC O&M because of its effect on membrane operation and replacement cost. Thus, the factors driving environmental impacts were tankage and electricity for gas sparging, while costs were driven by tankage and membranes.

Moreover, relationships among decision variables were conducted to identify trade-offs and synergies.Trade-offs exist when adjusting a decision variable produces tension between sustainability metrics and synergies occur when changing a given decision variable moves sustainability metrics in the same direction. The results obtained in this Ph.D. thesis showed that J_{20}, SGD_m, MLSS, and r required the navigation of sustainability trade-offs, but minimising SRT simultaneously improved environmental/economic performance.

10.5 Impact of influent sulphate content in AnMBR sustainability

For UWW, which can easily present low COD/SO_4–S ratio, the competition between Methanogenic Archaea (MA) and SRB can critically affect the amount and quality of the produced biogas [10.7]. Specifically, 2 kg of COD are consumed by SRB in order to reduce 1 kg of influent SO_4-S (see, for instance, [10.8]). Because of this particular significant sulphate content in the influent, an important fraction of COD is consumed by sulphate-reducing bacteria. For instance, in one case study, sulphate content in the influent was approx. 97 mg SO_4-S L^{-1}, almost all of which was reduced to sulphide (approx. 98%). In this respect, 190 mg COD L^{-1} were theoretically consumed by SRB (calculated using the stoichiometric ratio of kg of sulphate reduced to sulphide per kg of COD degraded).

Therefore, considerably far more power and heat could be generated if low/non sulphate-loaded wastewaters are treated in AnMBR. If the sulphate content in the influent is considered to be zero, the amount of influent COD transformed into methane increases significantly (up to 37% of the influent COD) when the sulphate content in the influent is approx. 97 mg SO_4-S L^{-1}. Therefore, the resulting methane generated will increase up to 141 $L_{CH4}\cdot day^{-1}$ (calculated on the basis of the theoretical methane yield under standard temperature and pressure conditions: 350 L_{CH4} kg^{-1}COD). Consequently, in absolute terms, the energy from methane capture (present in biogas and dissolved in the effluent assuming a capture efficiency of 100%) would increase to 0.19 $kWh\cdot m^{-3}$ (power energy) and 592.17 $KJ\cdot m^{-3}$ (heat energy). Mention must also be made of the potential of AnMBR to be net energy producer (surplus electricity that can be exploited in other parts of the WWTP) when treating low-sulphate UWW. Specifically, in mild/warm climates (i.e. tropical or Mediterranean), AnMBR technology is likely to be a net energy producer when treating low/non sulphate-loaded UWW: a theoretical maximum energy production of up to 0.07-0.12 kWh·m^{-3} could be obtained by capturing the methane from both biogas and effluent.

It is worth to point out that AnMBR combined with primary settling and anaerobic digestion of the wasted sludge has also the potential to be a net energy producer not only when treating low-sulphate UWW but also when treating sulphate-rich UWW (maximum theoretical energy production of up to 0.09 kWh per m^3).

10.6 Sustainability of AnMBR compared to other technologies

The economic and environmental sustainability of AnMBR in comparison with aerobic-based technologies for UWW treatment was evaluated. To this aim, steady-state performance modelling, LCA and LCC approaches were integrated. Specifically, AnMBR (coupled to an aerobic-based post-treatment) was compared to aerobic membrane bioreactor (AeMBR), CAS and extended aeration activated sludge (EAAS) technologies, focusing on the removal of organic matter, nitrogen and phosphorus at ambient temperature of 20 ºC.

From an energy, environmental and economic perspective, AnMBR coupled to an aerobic-based post-treatment (especially CAS-based) becomes a promising sustainable technology for UWW treatment in comparison with the rest of evaluated systems. In this respect, for given operating conditions, AnMBR technology coupled to a CAS-based post-treatment for nutrient removal at 20 ºC may present nearly null energy demands: a theoretical minimum energy consumption of around 0.04 kWh·m^{-3} could be achieved by capturing the methane from both biogas and effluent. This energy demand is much lower than other results from full-scale aerobic MBRs for UWW treatment. According to Judd and Judd [10.9], for instance, the full-scale aerobic MBR in Nordkanal (Germany) presented a specific energy demand of 0.9 kWh·m^{-3}, which is low compared to the consumption (approx. 3.9 kWh·m^{-3}) of other full-scale aerobic MBRs (e.g. Immingham Docks MBR WWTP, United Kingdom). On the other hand, CAS in Schilde (Belgium) consumed 0.19 kWh·m^{-3} [10.10].

AnMBR could feature environmental impacts in eutrophication compared to other treatment schemes. Nevertheless, significant reductions in LCC (around €0.135 per m^3) and LCA (reductions in environmental impacts of up to 72, 66, 44 and 37% in abiotic depletion, GWP, acidification and marine aquatic ecotoxicity, respectively) can be achieved by capturing the methane from both biogas and effluent in AnMBR-based treatment schemes. It is worth to point out that AnMBR presented low sludge productions and energy demands. Moreover, AnMBR coupled to a CAS-based post-treatment rather than AeMBR-based post-treatment presented reduced environmental impacts (mainly in GWP and abiotic depletion) mostly because the lower energy recovery potential of the later than the former.

10.7 Energy, nutrient, and sludge management in AnMBR system

Three options were considered when net energy demand was assessed: no methane recovery, only recovering the methane present in the biogas, or total methane capture (recovery of both biogas and methane dissolved in the effluent). LCC results showed that cost savings of up to 16 and 36% (at 15 and 30 ˚C, respectively) are possible compared to no methane recovery. By accounting for energy offsets through on-site production, GHG savings of up to 76-104% (at 15 and 30˚C, respectively) can be achieved. These calculations were made assuming that the methane present in both biogas and effluent streams were recovered and utilised for energy generation. The total cost of the technologies needed for these processes (degassing membrane for dissolved methane and microturbine-based combined heat and power (CHP) for energy generation) were also considered. Based on this analysis, there may exist AnMBR design/operating scenarios that have the potential to generate energy in excess of what is required to run the AnMBR system. It is worth to mention that if methane is released as fugitive emissions, life cycle environmental impacts through GWP would increases up to 99% (from around 0.02 kg CO_2 eq·m^{-3} when methane is completely recovered to around 1.34 kg CO_2 eq·m^{-3} if total methane is released as fugitive emissions).

The framework in this study examined whether or not the treated effluent is used for fertigation (i.e., irrigation with nutrient-rich water) to offset fertiliser needs. Note that calculations of fertiliser offsets from fertigation included assumptions of nitrogen and phosphorus bioavailability (50% and 70%, respectively), consistent with other studies [10.11; 10.12; 10.13]. Based on the LCA data, nutrient recovery reduced eutrophication by approximately 50%, whilst significantly reducing marine toxicity (around -35 kg 1,4-DB·m^{-3}), GWP (-0.06 kg CO_2·m^{-3}) and abiotic depletion (-0.0005 kg Sb eq·m^{-3}) due to the fertiliser avoided.

The main sustainable benefits of AnMBR are that lower volumes of sludge are generated and no further digestion of the wasted sludge would be required to enable its direct disposal on farmland. According to Xing *et al.* [10.14], sludge production in activated sludge processes is generally in the range of 0.3 - 0.5 kg TSS kg^{-1} $COD_{REMOVED}$. The lowest value evaluated in this Ph.D. thesis was 0.21 kg TSS kg^{-1} $COD_{REMOVED}$, which is therefore low compared to other conventional systems. In addition, the evaluated sludge was already stabilised (due to the increase in operating temperature and/or SRT), allowing its directly use as fertiliser on farmland.

Three options were considered in this study for sludge disposal: agricultural application, incineration, or landfilling. Based on the LCC results, savings of up to 50 and 90% can be achieved by selecting agricultural application over landfilling or incineration, respectively. Based on the LCA results, incineration could be a better option over agriculture in terms of GWP100 and eutrophication. In this respect, although agricultural application offsets fertiliser use, it still results in direct emissions to air (e.g., N_2O, NH_3), water (e.g., PO_4), and soil (heavy metals).

Even though the approach used to estimate emissions from land application and fertiliser offsets was consistent with other studies [10.11; 10.12; 10.13], this approach does not account for direct fugitive emissions to air and water that stem from synthetic fertilisers. The negative consequences of land application in terms of GWP100 and eutrophication, therefore, would be reduced if direct emissions from synthetic fertilisers are included in the system boundary since a portion of these emissions would be offset. Beyond GHG and nutrient emissions, agriculture also had the fewest negative impacts in abiotic depletion and marine toxicity.

10.8 The role of AnMBR in carbon neutral wastewater treatment

The main challenge of AnMBR is optimising design and operation in order to improve the sustainability of the technology for treating UWW. AnMBR may be suitable to treat most UWW streams since, as previously commented, it generates a high-quality effluent [10.1; 10.15] whilst achieving meaningful steps toward sustainable UWW treatment: low energy demand stemming from no aeration and energy recovery through methane production. This alternative process is more sustainable than aerobic-based processes because it transforms wastewater into a renewable source of energy [10.16; 10.17], providing therefore a reusable water resource. In this respect, maximising the capture of methane is a key issue in AnMBR technology for achieving energy savings and reducing therefore the overall WWTP carbon footprint.

One great opportunity for simultaneously improve economic and environmental AnMBR performance will consist in reducing energy consumption. It is worth to point out the importance of the development of efficient dissolved methane recovery processes in order to maximise energy recovery and avoid direct GHG emissions. In any case, pursuits aimed to reduce life cycle environmental impacts should not jeopardise effluent quality – the primary responsibility of WWTPs. In this respect, membranes help ensure robust treatment capacity and enable safe nutrient recovery through fertigation, which can have significant economic and environmental benefits through fertiliser and freshwater offsets.

10.9 References

10.1 A.L. Smith, L.B. Stadler, N.G. Love, S.J. Skerlos, L. Raskin, Perspectives on anaerobic membrane bioreactor treatment of domestic wastewater: A critical review, Bioresour. Technol. 122 (2012), 149-159.

10.2 R. Barat, J. Serralta, M.V. Ruano, E. Jiménez, J. Ribes, A. Seco, J. Ferrer, Biological Nutrient Removal Model Nº 2 (BNRM2): A general model for Wastewater Treatment Plants, Water Sci. Technol. 67 (2013), 1481-1489.

10.3 F. Durán, 2013. Mathematical modelling of the anaerobic urban wastewater treatment including sulphate-reducing bacteria. Application to an anaerobic membrane bioreactor (Modelación matemática del tratamiento anaerobio de aguas residuales urbanas incluyendo las bacterias sulfatorreductoras. Aplicación a un biorreactor anaerobio de membranas). Ph.D. thesis. Dept. of Hydraulic Engineering and Environment. Universitat Politècnica de València, Spain.

10.4 J. Ferrer, A. Seco, J. Serralta, J. Ribes, J. Manga, E. Asensi, J.J. Morenilla, F. Llavador, DESASS: a software tool for designing, simulating and optimising WWTPs, Environ. Modell. Softw. 23(2008), 19-26.

10.5 G. Lettinga, S. Rebac and G. Zeeman, Challenge of psychrophilic anaerobic wastewater treatment, Trends Biotechnol. 19 (2001), 363-370.

10.6 A. Robles, M.V. Ruano, J. Ribes, J. Ferrer, Sub-critical long-term operation of industrial scale hollow-fibre membranes in a submerged anaerobic MBR (HF-SAnMBR) system, Sep. Purif. Technol. 100 (2012), 88–96.

10.7 L.W. Hulshoff Pol, Treatment of sulphate-rich wastewaters: microbial and process technological aspects TMR Summer School Programme, The Biological Sulfur Cycle: Environmental Science and Technology, April, Wageningen, The Netherlands, 1998.

10.8 J.B. Giménez, A. Robles, L. Carretero, F. Durán, M.V. Ruano, M.N. Gatti, J. Ribes, J. Ferrer, A. Seco, Experimental study of the anaerobic urban wastewater treatment in a submerged hollow-fibre membrane bioreactor at pilot scale. Bioresour. Technol. 102 (2011) 8799 – 8806.

10.9 S. Judd, C. Judd, The MBR Book: Principles and Applications of Membrane Bioreactors for Water and Wastewater Treatment, 2nd edition, Elsevier, ISBN: 978–0–08–096682–3, 2011.

10.10 A. Fenu, J. Roels, T. Wambecq, K. De Gussem, C. Thoeye, G. De Gueldre, B. Vand De Steene, Energy audit of a full scale MBR system. Desalination 262 (2010), 121-128.

10.11 A. Gallego, A. Hospido, M.T. Moreira, G. Feijoo, Environmental performance of wastewater treatment plants for small populations, Resour. Conser. Recy. 52 (2008) 931–940.

10.12 G. Rodriguez-Garcia, A. Hospido, D.M. Bagley, M.T. Moreira, G. Feijoo. A methodology to estimate greenhouse gases emissions in Life Cycle Inventories of wastewater treatment plants. Environmental Impact Assessment Review 37 (2012) 37–46

10.13 M. Garrido-Baserba, A. Hospido, R. Reif, M. Molinos-Senante, J. Comas, M. Poch, Including the environmental criteria when selecting a wastewater treatment plant. Environ. Modell. Softw. (2013) 1-9.

10.14 C.-H. Xing, W.-Z. Wu, Y. Quian, E. Tardieu, Excess sludge production in membrane bioreactors: a theoretical investigation, J. Environ. Eng. ASCE, 129 (2003) 291–297.

10.15 H. Lin, W. Peng, M. Zhang, J. Chen, H. Huachang, Y. Zhang, A review on anaerobic membrane bioreactors: Applications, membrane fouling and future perspectives, Desalination 314 (2013) 169–188.

10.16 L. Raskin, Anaerobic Membrane Bioreactors for Sustainable Wastewater Treatment. WERF Report U4R08, June 2012.

10.17 A. L, Smith, L.B. Stadler, L. Cao, N.G, Love, L. Raskin, S.J. Skerlos, Navigating Wastewater Energy Recovery 1 Strategies: A Life Cycle Comparison of Anaerobic Membrane Bioreactor and Conventional Treatment Systems with Anaerobic Digestion. Environmental Science & Technology 48 (2014), 5972-5981

CHAPTER 11:

General conclusions

This Ph.D. thesis aimed to investigate the feasibility of submerged anaerobic membrane bioreactors (AnMBRs) as core technology for urban wastewater (UWW) treatment. The main features studied in this Ph.D. thesis focussed on economic and environmental AnMBR sustainability. From this, the following conclusions can be drawn:

A plant-wide energy model for WWTPs: application to AnMBR technology

1. The performance of the proposed plant-wide energy model was assessed by comparing the model results to experimental data obtained from an AnMBR plant that treated effluent from the pre-treatment of a full-scale wastewater treatment plant (WWTP).
2. The proposed model was capable to reproduce temperature and/or heat energy requirements versus variations in operating and environmental conditions.

The operating cost of an anaerobic membrane bioreactor (AnMBR) treating sulphate-rich urban wastewater

3. Operating at high ambient temperature and/or high sludge retention time (SRT) allows achieving significant energy savings even when treating sulphate-rich UWW whenever the methane generated is used as energy resource (minimum value: 0.07 $kWh·m^{-3}$).
4. Low/moderate sludge productions were obtained (minimum value: 0.16 kg $TSS·kg^{-1}$ $COD_{REMOVED}$), which further enhanced the AnMBR operating cost (minimum value: €0.01 per m^3).
5. AnMBR technology is likely to be a net energy producer when treating low/non sulphate-loaded wastewaters in warm/hot climates: theoretical maximum energy productions of up to 0.11 $kWh·m^{-3}$ could be achieved.

Design methodology for submerged anaerobic membrane bioreactors (AnMBR): A case study

6. The optimal SRT in winter conditions tresulted in 35-41 days at mixed liquor suspended solids (MLSS) of 15-16 $g·L^{-1}$, which corresponded to 20 ºC-standardised transmembrane flux (J_{20}) of 18 LMH, sludge recycling ratio (r_{rec}) of 3.2, and hydraulic retention time (HRT) of 17 hours. In summer conditions, the optimal SRT resulted in 23-27 days at r_{rec} of 1.2, which corresponded to MLSS of 12 $g·L^{-1}$ and 21 LMH of J_{20}.
7. The total annual cost of the evaluated AnMBR system treating sulphate-rich UWW was €0.101 and €0.097 per m^3 of treated water when (i) no energy was recovered from methane and (ii) energy was recovered from methane (biogas methane and methane dissolved in the effluent), respectively.

8. The total cost when treating low-sulphate UWW resulted in €0.097 and €0.070 per m^3 of treated water for the two aforementioned scenarios, respectively.

<u>Filtration process cost in submerged anaerobic membrane bioreactors (AnMBRs) for urban wastewater treatment</u>

9. Operating at J_{20} slightly higher than the critical flux (Jc) (around 100-110% of the Jc) and low MLSS (5 $mg \cdot L^{-1}$) resulted in minimum total filtration cost.
10. The optimal specific gas demand per square metre of membrane area (SGD_m) resulted in approx. 0.1 $m^3 \cdot m^{-2} \cdot h^{-1}$ for MLSS ranging from 5 to 25 $g \cdot L^{-1}$ when operating at the corresponding optimal J_{20} (around 100-110% of the Jc).
11. The optimum total filtration cost estimated in this study ranged from €0.03 to €0.12 per m^3 of treated water.

<u>Design of a submerged anaerobic membrane bioreactor (AnMBR) for urban wastewater treatment with and without primary settling</u>

12. AnMBR without primary settling (PS) and further anaerobic digestion (AD) of the wasted sludge was the most feasible option for designing an AnMBR WWTP treating low-sulphate UWW at 30ºC (minimum cost of €0.05 per m^3).
13. The combination PS+AnMBR+AD was the most feasible option when treating sulphate-rich UWW (minimum cost of €0.05 per m^3 at 30ºC): cost savings of up to 40 and 50% can be achieved by including AD and PS+AD to the treatment scheme, respectively.
14. The total cost of the AnMBR WWTP was significantly lower when treating low-sulphate rather than sulphate-rich UWW (cost savings of up to 45% can be met).

<u>Environmental impact of submerged anaerobic MBR (AnMBR) technology used to treat urban wastewater at different temperatures</u>

15. The resulting energy balance highlighted the importance of both operating at ambient temperature and optimising membrane performance (average 0.19 $kWh \cdot m^{-3}$).
16. Maximising the capture of methane from both biogas and effluent streams may enable considerable energy savings in AnMBRs, which enhances the feasibility of this technology technology for UWW treatment
17. Life cycle assessment (LCA) results revealed the importance of both operating at ambient temperature and maximising the recovery of nutrients (eutrophication can be reduced up to 50%) and dissolved methane (positive environmental impact can be achieved) from AnMBR effluent.

Navigating Environmental, Economic, and Technological Trade-Offs in the Design and Operation of Submerged Anaerobic Membrane Bioreactors (AnMBRs)

18. J, SGD_m, MLSS, and r required the navigation of sustainability trade-offs, but minimising SRT simultaneously improved environmental/economic performance.
19. MLSS and J_{20} had the strongest influence over LCA results and capital costs, with J governing operating and maintenance costs.
20. There are design and operational conditions under which submerged AnMBRs could be positive net energy at high operating temperatures, contributing therefore to the pursuit of carbon negative wastewater treatment.

Economic and environmental sustainability of submerged anaerobic MBR (AnMBR) compared to aerobic-based technologies for urban wastewater treatment

21. AnMBR coupled to a post-treatment based on conventional activated sludge (CAS) for nutrient removal was identified as a sustainable option for UWW treatment: a minimum energy consumption of 0.04 $kWh \cdot m^{-3}$ could be achieved and low sludge productions could be obtained under given operating conditions.
22. Although the impact in eutrophication is not reduced in comparison with other aerobic-based technologies, significant reductions in other environmental impacts (global warming potential (GWP), marine aquatic ecotoxicity, abiotic depletion and acidification) and life cycle cost (LCC) (minimum LCC value of around €0.135 per m^3) can be achieved.